Investigating Marine Resources in the Gulf of Mexico at Multiple Spatial and Temporal Scales of Inquiry

by

Joshua Paul Kilborn

A dissertation submitted in partial fulfillment
of the requirements for the degree of
Doctor of Philosophy in Marine Science
with a concentration in Marine Resource Assessment
College of Marine Science
University of South Florida

Co-Major Professor: David F. Naar, Ph.D.
Co-Major Professor: Ernst B. Peebles, Ph.D.
David L. Jones, Ph.D.
Steven A. Murawski, Ph.D.
Theodore S. Switzer, Ph.D.

Date of Approval:
November 8, 2017

Keywords: fisheries, ecosystem management, multivariate statistics, time-series, simulated data

DEDICATION

This dissertation is dedicated to my late father, Paul G. Kilborn and to my mother Nancy B. Woods. My father instilled in me a love and respect for nature that has endured beyond his time on Earth. Our time outdoors together camping, fishing, canoeing, and hiking have been instrumental in defining my character and love for nature. My mother has always supported and encouraged me to be proud of myself and my choices; she is my biggest fan. Thank you to her for showing me how to pick myself up again after I fall down.

ACKNOWLEDGMENTS

First, and foremost, I would like to thank my wife Amanda Kilborn for years of support and understanding while I worked on my Ph.D. I would not have been able to focus on my research so completely without her by my side. Amanda's help has been incalculable, and I will forever be grateful for the stability and comfort she provided to our small family throughout my academic and professional growth.

Secondly, this dissertation would not have been possible without the guidance of my academic advisors. To both of my Co-Major Professors, Dr. David Naar and Dr. Ernst Peebles, thank you for your endless enthusiasm, support, and patience. There were many times when you both helped me by providing new perspectives and insights. I would like to thank Dr. David Jones, in particular, for mentoring me and spending time opening "black boxes" of multivariate statistical theory. I am thoroughly grateful for all of your guidance. Thank you also to my committee members, Dr. Steven Murawski and Dr. Theodore Switzer for your help throughout the process of completing this work. All five of you have been invaluable, and your commitment to quality science has helped refine my understanding of what it means to do "good work".

Third, thank you to the innumerable individuals who have shaped my understanding of the complex and dynamic marine environment (and the World at large). Old and new friends, students, post-doctoral researchers, administrators, staff, and faculty alike have all helped shape me into the scientist I am today. Thank you for pushing the limits of my knowledge and

understanding. Thank you for the support and encouragement to carry on in the difficult times, and for being there to celebrate in the good ones. Particularly, I would like to thank Dr. Orian Tzadik, Dr. Brian Barnes, Michael Drexler, M.S., Dr. Sennai Habtes, Jessica Makowski, M.S., Tasha Snow, M.S., and Dominika Wojcieszek M.S.

This research was made possible, in part, by the NOAA–National Marine Fisheries Service grant NA10NMF4550468, the NOAA–Marine Fisheries Initiative grant NA17NMF4330318, and the USF–College of Marine Science's Anne and Werner Von Rosenstiel Endowed Fellowship. Thank you also to Michael Drexler, M.S. and the Ocean Conservancy for partially supporting the Gulf of Mexico ecosystem modeling work presented in Chapter Five. Travel awards to present portions of this dissertation at international conferences has generously been provided by the USF–College of Marine Science Dean's Office, the USF Student Government, and Woods Hole Oceanographic Institution.

TABLE OF CONTENTS

LIST OF TABLES

LIST OF FIGURES

ABSTRACT

The work in this dissertation represents an attempt to investigate multiple temporal and spatial scales of inquiry relating to the variability of marine resources throughout the Gulf of Mexico large marine ecosystem (Gulf LME). This effort was undertaken over two spatial extents within the greater Gulf LME using two different time-series of fisheries monitoring data. Case studies demonstrating simple frameworks and best practices are presented with the aim of aiding researchers seeking to reduce errors and biases in scientific decision making. Two of the studies focused on three years of groundfish survey data collected across the West Florida Shelf (WFS), an ecosystem that occupies the eastern portion of the Gulf LME and which spans the entire latitudinal extent of the state of Florida. A third study was related to the entire area covered by the Gulf LME, and explored a 30-year dataset containing over 100 long-term monitoring time-series of indicators representing (1) fisheries resource status and structure, (2) human use patterns and resource extractions, and (3) large- and small-scale environmental and climatological characteristics. Finally, a fourth project involved testing the reliability of a popular new clustering algorithm in ecology using data simulation techniques.

The work in Chapter Two, focused on the WFS, describes a quantitatively defensible technique to define daytime and nighttime groundfish assemblages, based on the nautical twilight starting and ending times at a sampling station. It also describes the differences between these two unique diel communities, the indicator species that comprise them, and environmental

drivers that organize them at daily and inter-annual time scales. Finally, the differential responses in the diel, and inter-annual communities were used to provide evidence for a large-scale event that began to show an environmental signal in 2010 and subsided in 2011 and beyond. The event was manifested in the organization of the benthic fishes beginning weakly in 2010, peaking in 2011, and fully dissipating by 2012. The biotic effects of the event appeared to disproportionately affect the nighttime assemblage of fishes sampled on the WFS.

Chapter Three explores the same WFS ecosystem, using the same fisheries-independent dataset, but also includes explicit modeling of the spatial variability captured by the sampling program undertaking the annual monitoring effort. The results also provided evidence of a disturbance that largely affected the nighttime fish community, and which was operating at spatial scales of variability that were larger than the extent of the shelf system itself. Like the previous study, the timing of this event is coincident with the 2010 *Deepwater Horizon* oil spill, the subsequent sub-marine dispersal of pollutants, and the cessation of spillage. Furthermore, the spatial models uncovered the influence of known spatial-abiotic gradients within the Gulf LME related to (1) depth, (2) temperature, and (3) salinity on the organization of daytime groundfish communities. Finally, the models developed also described which non-spatially structured abiotic variables were important to the observed beta-diversity. The ultimate results were the decomposition of the biotic response, within years and divided by diel classification, into the (1) pure-spatial, (2) pure-abiotic, (3) spatial-abiotic, and (4) unexplained fractions of variation. This study, along with that in Chapter Two, also highlighted the relative importance of the nighttime fish community to the assessment of the structure and function of the WFS, and the challenges associated with adequately sampling it, both in space and time.

Because one focus of this dissertation was to develop low-decision frameworks and mathematically defensible alternatives to some common methods in fisheries ecology, Chapter Five employs a clustering technique to identify regime states that relies on hypothesis testing and the use of resemblance profiles as decision criteria. This clustering method avoids some of the arbitrary nature of common clustering solutions seen in ecology, however, it had never been rigorously subjected to numerical data simulation studies. Therefore, a formal investigation of the functional limits of the clustering method was undertaken prior to its use on real fisheries monitoring data, and is presented in Chapter Four. The results of this study are a set of recommendations for researchers seeking to utilize the new method, and the advice is applied in a case study in Chapter Five.

Chapter Five presents the ecosystem-level fisheries indicator selection heuristic (EL-FISH) framework for examining long-term time-series data based on ecological monitoring for resources management. The focus of this study is the Gulf LME, encompassing the period of 1980-2011, and it specifically sought to determine to what extent the natural and anthropogenic induced environmental variability, including fishing extractions, affected the structure, function, and status of marine fisheries resources. The methods encompassed by EL-FISH, and the resulting ecosystem model that accounted for ~73% of the variability in biotic resources, allowed for (1) the identification and description of three fisheries resource regime state phase shifts in time, (2) the determination of the effects of fishing and environmental pressures on resources, and (3) providing context and evidence for trade-offs to be considered by managers and stakeholders when addressing fisheries management concerns. The EL-FISH method is fully transferrable and readily adapts to any set of continuous monitoring data.

CHAPTER ONE:

INTRODUCTION

1.1 DISSERTATION RATIONALE

Scientists make choices. Scientists need to make so many choices that throughout the evolution of scientific discovery a decision making method was derived to ensure unbiased and neutral outcomes (Fisher 1955, Underwood 1997, Quinn and Keough 2002, Popper 2005). It is commonly referred to as the "Scientific Method". In its most basic form (as taught to primary school students) the method exists as a generalized sequence of six steps: (1) observation of an unexplained phenomenon, (2) development of a testable hypothesis to explain the phenomenon, (3) design of an experimental protocol to test the proposed hypothesis, (4) experimentation, along with data collection and analysis (5) assessment of the validity of the hypothesis, and depending on that determination, (6a) report the results to the scientific community and general public (i.e., hypothesis is deemed valid) -or- (6b) develop a new testable hypothesis to explain the observed phenomenon and repeat all steps (i.e., hypothesis is deemed invalid).

A problem with this method is that it contains steps that may be influenced by researcher biases, incorrect assumptions, or arbitrary methodological decisions. In particular, these issues tend to present during steps (3-5) of the generalized method described above. A major focus of this dissertation is on minimizing the uncertainty in ecological analyses that pertain to resources within large marine ecosystems (LMEs). Marine ecosystems are known to be complex and

dynamic, with many connected processes (Mann and Lazier 2006). As a result of these complexities, it is often difficult to determine which temporal and spatial scales are relevant to any resource pool of interest (Hutchinson 1953, Hurlbert 1984, Levin 1992).

1.1.1 Scales of Inquiry in Marine Ecosystems

This work will primarily be considering marine fisheries resources, and the interconnected processes that help to organize them in time and space. When investigating the organizational properties of marine fishes, there are important population-level processes that manifest at large and small scales. For example, many oviparous fish species are broadcast spawners, some utilize more localized approaches to reproduction (e.g., mouth brooding, attaching eggs to benthos), while others are viviparous (e.g., sharks) (Lubzens et al. 2010, McBride et al. 2013). These different reproductive strategies all can be affected at various spatial resolutions, and all contain some component of time to consider. The success of any species that broadcasts large quantities of fertilized eggs, and ultimately larvae, into any LME will surely be dependent on wind, currents, and the appropriateness of the environmental conditions where larvae settle (Hjort 1914, Cushing 1975, 1990). Often these strategies are employed at specific times and/or locations, as dictated by exogenous cues (e.g., moonlight; spawning aggregations) (Helfman et al. 2009). In all fish, throughout the fetal (viviparous) or larval (oviparous) development period, the chemical properties of ambient water (Green 2008) and food availability (Jones 1986, Hutchings 1991) may affect the fitness of any offspring.

The examples presented above represent a small subset of the real-world reproductive strategies that occur in marine species, and the reproductive process is only one piece of what are often complex life-histories that govern these species' ontogenies (Winemiller and Rose 1992,

Helfman et al. 2009). Depending on the stage of a target resource's life cycle, many different spatial and temporal scales may potentially be relevant (Levin 1992). Furthermore, when considering LMEs, the study focus often shifts from a single species to a particular functional group (e.g., plankton), regional assemblage (e.g., sub-tropical fishes, groupers), or management complex (e.g., reef fish). With the growth in modern computing capacity, there have also been more "end-to-end" models developed with the intent to model all of the ecosystem's relevant components from biological, to chemical, to physical, and may also include the human activities as determining factors to model outcomes (Link et al. 2010, Fulton et al. 2011).

1.1.2 Scope and Outline of Dissertation

All of the examples presented in this Introduction are subject inherent biases unwittingly imparted by the researcher via the selection of study designs, data extraction or observation methods, or statistical/analytical techniques. This work seeks to help define best practices and simple frameworks for some common methods utilized in marine ecology, and it provides case studies as examples. Specifically, the dissertation is divided into three main parts: (1) an exploration of the temporal and spatial patterns with respect to an ongoing, large-scale fisheries-independent monitoring program, (2) an exploration of the Gulf of Mexico Large Marine Ecosystem (Gulf LME) from a fisheries resource management perspective over a 30 year time period, and (3) a data-simulation study used to analyze the statistical performance of a popular new method of clustering multivariate and ecological data.

The first area of focus is divided into two separate studies that are both based on an annual, fisheries-independent, summer groundfish trawl-survey, and which was conducted by the Southeast Area Monitoring and Assessment Program (SEAMAP) across a large-scale spatial

feature in the eastern Gulf LME, known as the West Florida Shelf (WFS). The first study, Chapter Two: *SEAMAP Summer Trawl Survey 2010-2012: Groundfish Organization throughout the West Florida Shelf at Diel and Annual Time Scales*, examines temporal patterns in groundfish beta-diversity between daytime and nighttimetime surveys as well as between the first three years of full-scale spatial sampling of the WFS ecosystem. Additionally, concurrent analyses examining patterns in the physical-chemical characteristics of the WFS marine environment were also undertaken at the same temporal resolutions.

In Chapter Three: *SEAMAP Summer Trawl Survey 2010-2012: Spatial and Environmental Control of Groundfishes throughout the West Florida Shelf*, the spatial variability in the SEAMAP sampling design employed on the WFS is explicitly modeled and investigated with respect to the corresponding beta-diversity of groundfishes. Definitions and interactions between the fractions of explained variability in species response corresponding with pure-spatial, mixed-spatial (i.e., spatial-environmental), and pure-environmental are described in this study. The approaches demonstrated in Chapter Two and Chapter Three are transferrable to any comparable system of interest, and together they demonstrate an explicit accounting for multiple temporal and spatial scales of inquiry within data collected by one fisheries-independent monitoring program.

Chapter Four: *Resemblance Profiles as Clustering Decision Criteria: Estimating Statistical Power, Error, and Correspondence for a Hypothesis Test for Multivariate Structure*, examines a promising new multivariate method of cluster detection that has recently emerged, and which is currently undergoing a rise in popularity. The chapter focuses on a numerical simulation study testing the efficacy of this new clustering algorithm using a variety of data complexities, grouping and correlation structures, and probability distributions. In order to minimize inaccurate

clustering results, a set of general guidelines and recommendations were presented for researchers interested in employing these methods. This work was published in the peer-reviewed journal *Ecology and Evolution*, and it has been included in its entirety with permission by the authors Kilborn et al. (2017).

In Chapter Five: *Evidence for the Influence of Basin-scale Climate Dynamics and Fluctuating Fishing Intensity on the Ecosystem-level Organization of Gulf of Mexico Fisheries Resource* presents a framework for elucidating the underlying dynamic interactions between biotic and abiotic indicators of resource and environmental structure and function for the Gulf LME over a 30-year monitoring period. The same multivariate clustering method tested in Chapter Four was used to define time-series data patterns in order to identify ecosystem-level regime states in the Gulf LME. A newly developed, quantitatively defensible method to describe the qualitative differences of the underlying resource structure between any two ecosystem states is demonstrated. Lastly, trade-offs between system states and human use patterns, along with natural environmental variability, are presented, and the entire chapter represents a case study for this readily transferrable analytical framework.

Finally, Chapter Six: *Research Impacts and Concluding Remarks* summarizes the research, results, and conclusions for each study presented in this dissertation. There, the general applicability of the different works are presented, and implications for future considerations and additional studies are also outlined.

1.2 LITERATURE CITED

Cushing, D. H. 1975. Marine Ecology and Fisheries. Cambridge University Press, Cambridge.

Cushing, D. H. 1990. Plankton production and year-class strength in fish populations: An update of the match-mismatch hypothesis. Advances in Marine Biology **26**:249-293.

Fisher, R. 1955. Statistical Methods and Scientific Induction. Journal of the Royal Statistical Society Series B-Statistical Methodology **17**:69-78.

Fulton, E. A., J. S. Link, I. C. Kaplan, M. Savina-Rolland, P. Johnson, C. Ainsworth, P. Horne, R. Gorton, R. J. Gamble, A. D. M. Smith, and D. C. Smith. 2011. Lessons in modelling and management of marine ecosystems: the Atlantis experience. Fish and Fisheries **12**:171-188.

Green, B. S. 2008. Maternal Effects in Fish Populations. Pages 1-105 *in* D. W. Sims, editor. Advances in Marine Biology, Vol 54. Elsevier Academic Press Inc, San Diego.

Helfman, G. S., B. B. Collette, D. E. Facey, and B. W. Bowen. 2009. The diversity of fishes : biology, evolution, and ecology. 2nd edition. Blackwell, Chichester, UK ; Hoboken, NJ.

Hjort, J. 1914. Fluctuations in the great fisheries of northern Europe viewed in the light of biological research, Rapport Process-Verbaux Reunions Conseil International pour l'Explorations de la Mer.

Hurlbert, S. H. 1984. Pseudoreplication and the Design of Ecological Field Experiments. Ecological Monographs **54**:187-211.

Hutchings, J. A. 1991. Fitness consequences of variation in egg size and food abundance in brook trout *Salvelinus fontinalis*. Evolution **45**:1162-1168.

Hutchinson, G. E. 1953. The concept of pattern in ecology. Proc Acad Nat Sci Philadelphia **105**:1-12.

Jones, G. P. 1986. Food availability affects growth in a coral reef fish. Oecologia **70**:136-139.

Kilborn, J. P., D. L. Jones, E. B. Peebles, and D. F. Naar. 2017. Resemblance profiles as clustering decision criteria: Estimating statistical power, error, and correspondence for a hypothesis test for multivariate structure. Ecology and Evolution **7**:2039-2057.

Levin, S. A. 1992. The Problem of Pattern and Scale in Ecology. Ecology **73**:1943-1967.

Link, J. S., E. A. Fulton, and R. J. Gamble. 2010. The northeast US application of ATLANTIS: A full system model exploring marine ecosystem dynamics in a living marine resource management context. Progress in Oceanography **87**:214-234.

Lubzens, E., G. Young, J. Bobe, and J. Cerda. 2010. Oogenesis in teleosts: How fish eggs are formed. General and Comparative Endocrinology **165**:367-389.

Mann, K. H., and J. Lazier. 2006. Dynamics of marine ecosystems: biological-physical interactions in the oceans. Wiley-Blackwell.

McBride, R. S., S. Somarakis, G. R. Fitzhugh, A. Albert, N. A. Yaragina, M. J. Wuenschel, A. Alonso-Fernández, and G. Basilone. 2013. Energy acquisition and allocation to egg production in relation to fish reproductive strategies. Fish and Fisheries:n/a-n/a.

Popper, K. 2005. The logic of scientific discovery. Routledge.

Quinn, G. P., and M. J. Keough. 2002. Experimental design and data analysis for biologists. Cambridge University Press, Cambridge, UK ; New York.

Underwood, A. J. 1997. Experiments in ecology: their logical design and interpretation using analysis of variance. Cambridge University Press.

Winemiller, K. O., and K. A. Rose. 1992. Patterns of life-history diversification in north-american fishes - implications for population regulation. Canadian journal of fisheries and aquatic sciences **49**:2196-2218.

CHAPTER TWO:

SEAMAP SUMMER TRAWL SURVEY 2010-2012: GROUNDFISH ORGANIZATION THROUGHOUT THE WEST FLORIDA SHELF AT DIEL AND ANNUAL TIME SCALES

2.1 INTRODUCTION

Given the particular geology of the Florida peninsula, the marine resources managed by state and federal agencies are typically split between the east and west coasts of the state. Beneath the waters adjacent to Florida's western coastline, and spanning its entire north-south extent, sits a massive carbonate platform called the West Florida Shelf (WFS). The WFS has an areal extent of 170,000 km^2, a gently sloped (< 1°) and negative depth-gradient extending east-to-west, stretches up to 240 km from the shoreline, and is delimited by depth at the 200 meter isobath – beyond which there is a precipitous 1,800 meter drop into the deep Gulf (Bryant et al. 1991, Okey et al. 2004, Hine et al. 2008). The WFS platform dominates the potential fishing area for all anglers based in western Florida, and is essentially the only habitat available to small artisanal and recreational fishers given the distance to, and water depths at, the shelf's boundary edges. The benthic habitat across the WFS is often described as "patchy" and the entire range of possibilities are represented on the platform from flat and low-profile grasses, sands, or hardbottom to high-relief corals, ledges, and canyons. The diversity of WFS habitat morphologies presents a situation where many different gear types (e.g., hook-and-line, trawl, and trap) and fishing operations (e.g.,

large- and small-scale, commercial and recreational) are employed to exploit the living marine resources on the shelf.

The WFS contains areas that have been designated as either marine reserves, sanctuaries, or habitat areas of particular concern (HAPC), including the Florida Middle Grounds HAPC, Madison-Swanson and Steamboat Lumps marine reserves, the North and South Tortugas Ecological Reserves, portions of the Florida Keys National Marine Sanctuary, and the Pulley Ridge special management area (Hine et al. 2008, Simmons et al. 2015). Some of these specially designated areas in the Gulf have fishing restrictions placed upon them, however they are all considered high productivity areas for both commercial and recreational species (Simmons et al. 2015). These high productivity areas, with relatively high-relief morphologies (5-40 m), represent only a fraction of the total area of the WFS, and they are often circumscribed by, or directly adjacent to, the more common lower-relief (≤ 5 m) habitat morphologies of the Gulf (Hine et al. 2008).

Prior to the mid-1960s, WFS fishers mostly worked with gill-net and hook-and-line gear; however, it was shown that (1) there were large areas available for trawl fishing (Juhl 1966) and (2) many relevant species were abundantly distributed across these areas (Juhl 1966, Darcy and Gutherz 1984), and therefore opportunity costs were likely high at the time. In 2012, the total commercial finfish landings for all gear types in west Florida were ~63 million pounds, which accounted for over $60 million in revenue (NMFS 2014). In the same year, approximately 3.9 million recreational anglers took an estimated 14.8 million fishing trips that added over $5 billion in economic impacts to the region (NMFS 2014). Given the enormous economic influence that fishing activities in the Gulf have for the state of FL, and the associated Gulf States region, it is

not surprising that extensive effort has been placed on understanding the complex and dynamic relationships supporting the marine fisheries resources in the Gulf of Mexico's large marine ecosystem (Gulf LME).

2.1.1 Southeast Area Monitoring and Assessment Program

The Southeast Area Monitoring and Assessment Program (SEAMAP) was instituted in 1981 by the National Marine Fisheries Service (NMFS) in conjunction with the Gulf States Marine Fisheries Commission (GSMFC) as a means of collecting fishery independent data for the Gulf of Mexico (Stuntz et al. 1983). One aspect of the SEAMAP implementation was a recurring bottom-trawl survey for groundfishes and shrimp in summer and fall seasons, and which was originally incorporated to measure the effect of Texas shrimp fishing closures (Stuntz et al. 1983) that were enacted in partial fulfillment of a new fishery management plan targeting the Gulf shrimp fisheries (Nichols 1983, 1984, Nichols and Poffenberger 1987). Since 1982, the stated purpose of the SEAMAP bottom-trawl surveys has been to estimate the abundance and distribution of stocks across the northern Gulf of Mexico (Stuntz et al. 1983). The first year that Florida participated in the groundfish and shrimp survey was 2008 (Rester 2011), and full sampling coverage across the entire WFS did not occur until 2010 (Rester 2012). In addition to biological sampling, concurrent environmental observations were made at each survey station in an effort to characterize the abiotic factors that affect the stock dynamics captured by the trawl sampling (Stuntz et al. 1983).

2.1.2 West Florida Shelf Bottom-trawl Survey Sampling Protocol

In the same year that Florida entered the trawl survey effort, the sampling protocol was redefined (Rester 2011, GSMFC 2016) and, for the sake of brevity, only the procedures that applied to those vessels used in this study are detailed here. Full details of all SEAMAP station

selections, gear specifications and calibrations, and standard operating procedures can be found in the GSMFC (2016) operations manual.

Trawl sampling was conducted on a 24-hour schedule using 30 minute standard tows at the recommended vessel speed of 2.5-3.0 knots. The time spent between trawls was dictated by the time required to move the research vessel to the next sampling station. The WFS sampling was undertaken in NMFS Gulf shrimp landing statistical zones (SZ) 1-10, and the probability of selection for any potential trawl station was defined by the proportional areal contribution of the station's SZ to the entire sampling universe. The HAPCs and marine protected areas were removed from the potential pool prior to site selection, and any stations selected within a known sponge, coral, artificial-reef, or special habitat were either dropped from the station list or moved to nearby, alternate sites (see GSMFC 2016 for details). Within each SZ, the stations were additionally stratified by depth, and selection probabilities were once again proportionally allocated based on the areal contribution to the SZ for the depth ranges: 2-20 fathoms (3.7-36.6 m) and 21-60 fathoms (38.4-109.7 m).

Bottom trawls were conducted using a 12.8 meter (42 feet) semi-balloon trawl with 4.1 cm (1 5/8 inches) stretched mesh. For each trawl sample, all biological specimens were sorted and identified to the species level, and the total number of individuals and the batch weight were recorded. Additional size, age, and sex distribution subsampling protocols were in place, as detailed in the operations manual (GSMFC 2016), however only the species composition and abundance data were used for this study. After the recovery of the trawl net, a comprehensive set of concurrent environmental observations were made for each station including weather conditions, sea state, and physical-chemical properties of the seawater.

2.1.3 Study Aims

Given the importance of the WFS to Gulf fisheries, the prominence of the physical feature for western Florida fishers, and the new implementation of fisheries-independent trawl-survey sampling for the full extent of the WFS, this study aims to characterize the first three years of benthic-trawl catches surveyed via the SEAMAP effort. These catches often contain many species that are not commercially or recreationally targeted. However, these species may still potentially be influential to those species of interest, especially given that the Gulf LME has been shown to have a large diversity of trophic connections and pathways that influence the organization of species shelf-wide (Okey and Mahmoudi 2002, Chagaris et al. 2015, Gruss et al. 2015, Sagarese et al. 2017). It is also noteworthy that there are several important target species that *are* regularly sampled in the SEAMAP surveys, including at least four epinephelids, four lutjanids, eight sparids, six carangids, and one scombrid.

The primary purpose of this study is to examine the SEAMAP groundfish survey data on first-order principles, and to compile and prepare the database for future, in-depth analyses. Two principle questions are to be answered by this work, namely: (1) should the biological samples be divided into daytime and nighttime sampling events, and if so, how; and (2) should the biological and/or environmental samples for each year be examined individually, or is the inter-annual variation such that combining all three years' datasets together is sufficient?

2.2 METHODS

2.2.1 Organization of Selected WFS Data

For this study, I used data from the first three years of the summer groundfish and shrimp surveys conducted at the full extent of the WFS (2010-2012). Data were collected on the R/V

Tommy Munro in the summer season for all three years; survey cruise identifiers and sampling dates are listed in Table 2.1. Data were acquired from the online, public-access SEAMAP database that is compiled and validated by the GSMFC (seamap.gsfmc.org; accessed Feb. 2015). Only the biological census data (i.e., species identification and abundance) and concurrent environmental observations for each station were extracted from the SEAMAP database for analysis. The data used for this study were subdivided into two broad categories – *responses* and *predictors*. Variables contained in the response category were biotic data comprised of composition and abundance for all vertebrate fish species collected via trawl-fishing. The predictor variables characterized the physical-chemical environmental conditions at the time of fishing, and they were subdivided into (1) SEAMAP data collected in situ, and (2) data derived from satellite observations post hoc, based on the SEAMAP samples' spatiotemporal locations.

2.2.1.1 Response data. Catch data were retained for all vertebrate fish samples that were able to be identified to the species level. Using the starting and ending geographic coordinates for each trawl sample, the great-circle distance was calculated between points to determine the total linear distance trawled at each station. For all species enumerated in any sample, the abundance values were converted to "catch per km^2 swept" by dividing by the product of the trawl net width (0.0094 km; GSMFC 2016) and the total distance traveled for each trawl tow. Standardizing the data in this way allowed for all tows to be comparable, even though the total area swept at each trawl station varied slightly.

2.2.1.2 Predictor data. The standard SEAMAP protocol includes observations of the properties of the seawater at each station's endpoint for (1) the surface, (2) maximum depth, and (3) one-half the maximum depth (GSMFC 2016). The variables retained for this study that were

measured in this way were: temperature (°C), dissolved oxygen (ppm), salinity (ppt, ‰), and chlorophyll concentration (mg m^{-3}). The depth at the end of each station and the range for the depths covered from start to finish for each station (meters) were also included as predictors.

Table 2.1 – Metadata for SEAMAP sampling cruises. The research vessel and cruise identifier for SEAMAP summer shrimp and groundfish trawl sampling cruises for the West Florida Shelf. Fishing operations were undertaken 24-hours a day during the dates listed for sampling legs.

Research Vessel	Cruise ID	Leg 1	Leg 2
Tommy Munro	765	June 26 - July 05, 2010	July 8 - July 14, 2010
Tommy Munro	836	June 8 - June 24, 2011	July 29 - July 31, 2011
Tommy Munro	857	June 7 - June 20, 2012	June 28 - July 4, 2012

Seven satellite data products were used to augment the in situ dataset to potentially improve the explanatory power of subsequent models and analyses; see Table 2.2 for the complete list of all 21 abiotic predictor variables utilized. Since all sampling events were referenced in both space and time, the extraction of any georeferenced satellite-datum consisted of the following steps: (A) identify the image pixel that contained the ending coordinates for the station, (B) identify the temporal bin that contained the sampling event's date, and (C) cross-reference (A) and (B) to retrieve the unique, spatiotemporally-referenced, and remote-sensed observation. Steps (A-C) were repeated for all sampling events within each summer survey. Four level-3 data products, binned over 8-days and with 4 km resolution, from the MODIS-Aqua satellite were included for analysis. They were (1) the absorption coefficient of light at 443 nm (m^{-1}) that is due to detritus and gelbstoff (Franz and Werdell 2010, Werdell et al. 2013, NASA Goddard Space Flight Center 2014b), (2) the diffuse attenuation coefficient for visible light at 490 nm (m^{-1}) (Lee et al. 2005a, Lee et al. 2005b, NASA Goddard Space Flight Center 2014a), (3) the photosynthetically available radiation (Einsteins m^{-1} day^{-1}) based on the Frouin model (Frouin and Pinker 1995,

Frouin et al. 2002, NASA Goddard Space Flight Center 2014d), and (4) the concentration of particulate organic carbon (mg m^{-3}) in the water (Stramski 2008, Stramski et al. 2008).

Three additional remote sensed variables were developed at the University of South Florida's Institute for Marine Remote Sensing and incorporated in this study with their permission. Two metrics for primary productivity with 1 km resolution were included: (1) the monthly rate of change for chlorophyll-*a* (chl-*a*) concentrations (100 * mg m^{-1} day^{-1}), with chl-*a* defined by O'Reilly et al. (2000), and with respect to the previous month (Habtes 2014, NASA Goddard Space Flight Center 2014c), and (2) the estimated net primary production rate (mg m^{-2} day^{-1}), derived from the chl-*a* data, defined by the Behrenfeld and Falkowski (1997) algorithm, and averaged over 7-days. The final physical-environmental predictor included was the average, daily estimated depth for the mixed layer (m) for each unique sampling event (Kara et al. 2000, Habtes 2014), and it was derived from the NASA JPL ECCO2 model with 0.25° resolution (http://ecco2.jpl.nasa.gov/products/).

2.2.2 Data Pretreatment

Response data were compiled into a site-by-species matrix ($\mathbf{Y}_z$) for each survey year (z), and the predictor data were concatenated into site-by-descriptor matrices ($\mathbf{X}_z$). When reconciling the $\mathbf{Y}_z$ and $\mathbf{X}_z$ data for all z, any response samples that did not have a full set of comparable predictor data to consider were removed from the dataset (and vice versa). All data were organized both by individual years ($\mathbf{Y}_z$ and $\mathbf{X}_z$), and also as one combined dataset for all three years of survey data considered ($\mathbf{Y}$ and $\mathbf{X}$). The predictor matrices were standardized via the z-scores translation to account for varying units of measure among descriptors (Legendre and Legendre 2012).

Table 2.2 – Predictor variables. A full list of all predictor variables contained in **X** with a description for each data series, its temporal and geographic scale, and SI units of measure.

Predictor	Description	Temporal Scale	Resolution	Units
CHLORSURF	Chlorophyll concentration at water surface	in situ	point	mg m^{-3}
CHLORMID	Chlorophyll concentration at 1/2 maximum depth	in situ	point	mg m^{-3}
CHLORMAX	Chlorophyll concentration at maximum depth	in situ	point	mg m^{-3}
CHLa_ROC	Chlorophyll-*a* concentration rate of change	30-day composite	1 km	100 * mg m^{-1} day^{-1}
DEPTH_EMAX	Maximum depth of sampling station	in situ	point	m
DEPTH_MXLD	Mixed layer depth	in situ	1/4°	m
DEPTH_RNG	Sampling station depth range	in situ	point	m
NPP	Net primary production	7-day composite	1 km	mg m^{-2} day^{-1}
OXYSURF	Oxygen concentration at water surface	in situ	point	ppm
OXYMID	Oxygen concentration at 1/2 maximum depth	in situ	point	ppm
OXYMAX	Oxygen concentration at maximum depth	in situ	point	ppm
SALSURF	Salinity at water surface	in situ	point	ppt (‰)
SALMID	Salinity at 1/2 maximum depth	in situ	point	ppt (‰)
SALMAX	Salinity at maximum depth	in situ	point	ppt (‰)
TEMPSURF	Water temperature at the surface	in situ	point	°C
TEMPMID	Water temperature at 1/2 maximum depth	in situ	point	°C
TEMPMAX	Water temperature at maximum depth	in situ	point	°C
KD490	Diffuse attenuation coefficient (490 nm) K2 algorithm	8-day composite	4 km	m^{-1}
ABS_GELB	Absorption coefficient (443 nm) due to detritus and gelbstoff	8-day composite	4 km	m^{-1}
PAR	Photosynthetically available radiation Frouin model	8-day composite	4 km	Einsteins m^{-1} day^{-1}
POC	Particulate organic carbon	8-day composite	4 km	mg m^{-3}

Prior to reconciliation of the response and predictor matrices, the biological descriptors were parsed for each year such that only the species that were present in at least 5% of the samples for that year were retained. When combining all $\mathbf{Y}_z$ into a global response dataset ($\mathbf{Y}$) only the species that were present in all three years' surveys were retained. All $\mathbf{Y}_z$ and $\mathbf{Y}$ were square-root transformed to balance the effects of both rare and highly abundant species (Legendre and Legendre 2012). For each trawl represented in the untransformed $\mathbf{Y}$, the species richness (S), Pielou's evenness (J') (Pielou 1966), and Shannon's diversity index (H') (Legendre and Legendre 2012) were calculated. Additionally, *daytime* and *nighttime* assignments were made based on the ending time and location for each tow. For each sampling station's endpoint, the time of day when nautical twilight began in the morning and ended in the evening was calculated for the date that sampling occurred. Nautical twilight (NT) begins and ends when the sun is 12° below the horizon, and marks the point in time when the visible light environment changes such that distinguishing the outlines of objects becomes easier (NT_{start}) or more challenging (NT_{end}). Bottom trawls that ended within the range of NT were deemed "daytime", and those outside the range "nighttime".

2.2.3 Statistical Analyses

All statistical analyses were implemented in MATLAB R2014b using the statistics package and the Fathom (Jones 2017) and Darkside (Kilborn 2017) toolboxes for MATLAB. To justify the stratification of samples into day or nighttime events, and to determine if the fish communities represented by this stratification were different from one another, all three diversity indices were individually tested against the diurnal classifier using one-way analysis of variance (ANOVA). Fisher's F-statistic was used to assess the ANOVA models (Fisher 1921, Quinn and Keough 2002)

and statistical significance for all hypothesis tests (including those described below) was determined using distribution-free permutation methods (Anderson 2001b) with α = 0.05 and 1,000 permutations (Manly 2006).

When examining the multivariate datasets, Bray-Curtis dissimilarity matrices, (Bray and Curtis 1957) for the zero-inflated, transformed abundance data ($\mathbf{Y}_{BC}$), and Euclidean distance matrices (Legendre and Legendre 2012) for the standardized environmental, abiotic data ($\mathbf{X}_{Euc}$), were derived. To determine if it was appropriate to combine all years' data together, permutation based (non-parametric) ANOVA (np-MANOVA; Anderson 2001a, McArdle and Anderson 2001) was employed. The multivariate equivalent of Fisher's *F*-statistic was used to test the null hypothesis (H_o) of no difference among groups' mean values (Anderson 2001a), and significance was assessed using 1,000 permutations (α = 0.05) of the observations in either **Y** or **X** (Anderson 2001a, b). The np-MANOVA results were verified and visualized using canonical analysis of principle coordinates (CAP; Anderson and Willis 2003, Legendre and Legendre 2012). Leave-one-out (LOO) cross validation was used to assess the effectiveness of using the CAP models as unknown sample classifiers. Where homogeneity of multivariate dispersions among groups was assumed (i.e., CAP and np-MANOVA), it was verified using the multivariate equivalent of Levene's test (Anderson 2006, Anderson et al. 2006, Anderson and Walsh 2013). Finally, to identify the species in the multivariate response data that were significantly indicative of each group in a classifier (i.e., day/night, or year), the indicator value method (IndVal; Dufrene and Legendre 1997) was employed.

Table 2.3 – Daytime vs. nighttime trawl diversity indices. The descriptive statistics for all diversity indices calculated from the three-year response dataset **Y**. All values based on $N = 390$ samples, where S = species richness, H' = Shannon's diversity, and J' = Pielou's evenness.

	Daytime Trawls			Nighttime Trawls		
	S	H'	J'	S	H'	J'
Minimum	2	0.37	0.07	10	0.51	0.10
Mean	17	1.82	0.36	29	2.31	0.46
Median	16	1.89	0.38	29	2.38	0.47
Mode	10	1.04	0.21	31	0.51	0.10
Maximum	43	2.81	0.56	56	3.15	0.62
Variance	65.5	0.30	0.01	83.2	0.21	0.01
Stnd. Deviation	8.1	0.55	0.11	9.1	0.45	0.09
Stnd. Error	0.5	0.03	0.01	0.8	0.04	0.01

2.3 RESULTS

After combining all three years' data, there were $N = 390$ trawl samples and a total $S = 154$ vertebrate fish species captured, from 54 different families (Appendix A, Table A.1). The maximum richness for any single trawl was 56 species, and the minimum was two; recall that samples with no species in them were excluded from all $\mathbf{Y}_z$. The theoretical maximum value for Shannon's H' index was $H'_{max} = \ln(S) = 5.037$, however for all N, $0.37 \leq H'_n \leq 3.15$. Pielou's J' has a potential range of 0-1, and for all N observations, $0.07 \leq J'_n \leq 0.67$. See Table 2.3 for more details.

2.3.1 Daytime vs. Nighttime Sampling

The ANOVA results in Table 2.4 support the decision to use a NT-based, knife-edge cutoff between daytime and nighttime trawl stations (Figure 2.1). All three diversity indices had significantly different mean values for day ($N_{day} = 258$) and night ($N_{night} = 132$) trawls (Table 2.3, Table 2.4). The mean S for nighttime trawls was 71% higher than those in the daytime, and the most common number of species encountered at night was three times higher than during the

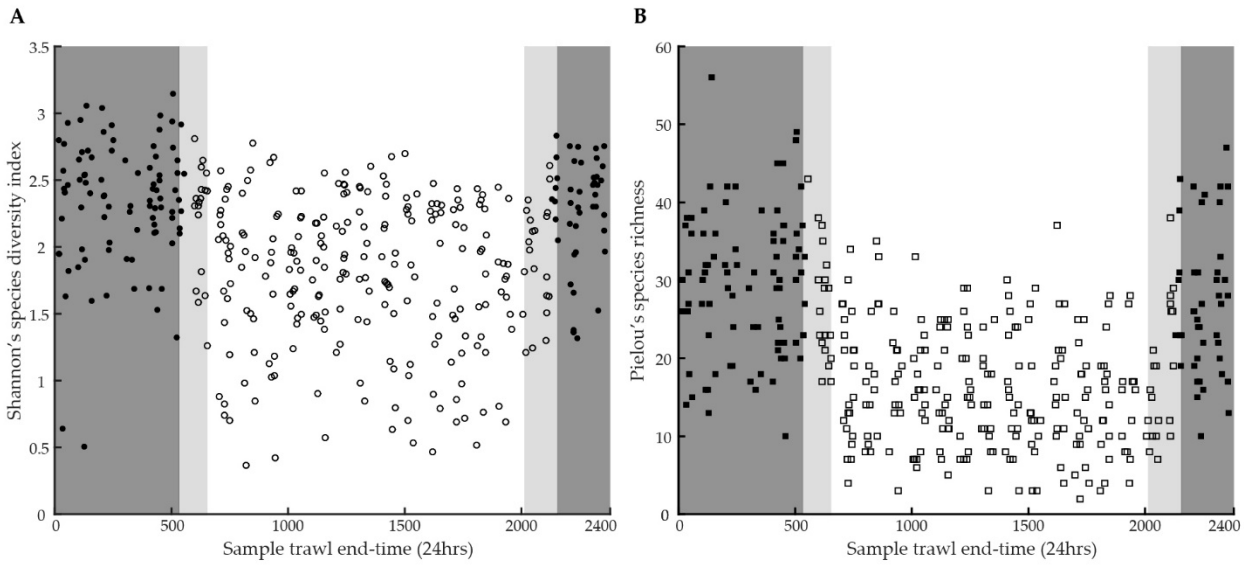

Figure 2.1 – SEAMAP trawl richness and diversity vs. sampling time of day. Plot of Shannon's diversity index (A) and the species richness (B), versus the time of day when the trawl was completed. Trawl data are drawn from summer SEAMAP sampling in 2010-2012 on the West Florida Shelf (N = 390 total samples). Daytime (N_{day} = 258; open symbols) and nighttime (N_{night} = 132; filled symbols) samples were classified using the nautical twilight boundaries at the actual time place that trawl sampling was completed. Dark gray shaded areas represent nighttime and light gray areas correspond to the range of all possible times that marked the start or end of nautical twilight.

day (31 and 10, respectively). Pielou's J' increased by 27% from daytime to nighttime, and with increases in both species richness and evenness from day to night, the observed 27% increase in Shannon's H' was expected. It should be noted that J' is calculated directly from H' (Pielou 1966), and therefore the dynamics of the two indices should be identical.

Trawl samples collected during daytime sampling operations tended to be more likely to contain 10 or less species, while nighttime samples never captured less than 10 different species in any trawl over the entire three year period of the study. Only six species were identified as significant indicator species for daytime sampling events using IndVal analysis (Table 2.5), however there were 69 different species indicative of the nighttime trawls. Indicator values (I)

Table 2.4 – Results for univariate and multivariate ANOVA tests. A table of results for one-way analysis of variance (ANOVA) to test for differences between daytime and nighttime trawl samples with respect to species richness (*S*), Shannon's diversity (*H*′), and Pielou's evenness (*J*′). Also presented are the results of multivariate ANOVA for all **X** (MANOVA), and the non-parametric version for all **Y** (np-MANOVA), tested against reduced and full temporal models. All *p*-values were calculated using 1,000 permutations and significance was assessed with α = 0.05. *F* = Fisher's *F*-statistic (or its multivariate equivalent), *SS* = sum of squares, *MS* = mean square, and *df* = degrees of freedom. All values in parentheses refer to the residual model.

	Factor	*F*	*p*-value	*SS*	*MS*	*df*
S	Day v. Night	173.66	0.001	12,417.36 (27,743.41)	12,417.356 (71.50)	1 (388)
H′	Day v. Night	76.30	0.001	20.68 (105.15)	20.68 (0.27)	1 (388)
J′	Day v. Night	76.30	0.001	0.82 (4.14)	0.82 (0.01)	1 (388)
Y	2010, 2012	5.20	0.001	1.67 (82.21)	1.67 (0.32)	1 (256)
	2010, 2011, 2012	4.91	0.001	3.04 (119.91)	1.52 (0.31)	2 (387)
X	2011, 2012	23.14	0.001	371.05 (4,473.00)	371.05 (16.03)	1 (279)
	2010, 2011, 2012	27.75	0.001	1,024.50 (7,144.50)	512.27 (18.46)	2 (387)

range from 0 to 100 and are considered a percentage; for example, any species that is present in all samples within group 'A' and not in any other groups' samples would be considered a 100% indicator for group 'A' (Dufrene and Legendre 1997). It is noteworthy that the largest *I* recorded for the daytime samples was 24.8 (*D. punctatus*), while those samples collected in darkness had 27 different species with $I > 25.0$ (Table 2.5), and three species with $I \geq 70.0$ (*S. papillosum*, *S. hispidus*, and *S. calcarata*).

2.3.2 Year Effect on Trawl Sampling

Both **Y** and **X** were examined independently to determine if it were appropriate to study all years lumped together ($N = 390$), or if each year should be analyzed separately ($N_{2010} = 109$, $N_{2011} = 132$, $N_{2012} = 149$). Since a MANOVA approach was employed, each years' dataset's multivariate dispersion was measured and they were checked for homogeneity. For the response data in **Y**, the data dispersion for 2011 was different from 2010 ($F = 4.34$, $p = 0.033$) and 2012 ($F =$

11.98, $p = 0.001$), and the multivariate spread of the abiotic data in **X** for the year 2010 was different than both 2011 ($F = 25.66$, $p = 0.001$) and 2012 ($F = 15.48$, $p = 0.001$). In both cases this was used as justification to further reduce the combined dataset to only the two years with homogenous dispersions for additional testing via MANOVA.

2.3.2.1 Biotic Response by Year. The results of the np-MANOVA for the years 2010 and 2012 indicated that there was a significant difference in the WFS groundfish beta-diversity observed between the two years (Table 2.4). An additional np-MANOVA for all three years of data together confirmed that there was a year effect (Table 2.4), and pairwise np-MANOVA confirmed that all years were significantly different from one another (Appendix A, Table A.2). The CAP analysis using all $m = 38$ canonical axes corroborated the results of the full np-MANOVA model (Trace statistic = 0.7049, $p = 0.001$, $m = 38$, variability of $\mathbf{Y}_{BC}$ expl. = 99.6%), and the associated ordination diagram clearly shows that the three years' objects are plotted in discrete clusters, with minor data cloud overlap (Figure 2.2).

The IndVal analysis of the **Y** data showed that each year had a different set of species best suited to describing that year's trawl catches. Both 2010 and 2012 had similar IndVal species lists in both quantity and magnitude of indicator species, as well as associated I values. The years 2010 and 2012 each had six indicator species (Table 2.6) with both having only one with $I > 20$ (*S. poeyi* and *N. usta*, respectively). The low maximum values for I imply that no species were excellent indicators for these two years, but the six listed for each year were marginally more abundant in, and specific to, the years that they were identified as significant by IndVal. The trawl samples collected in 2011 had 27 species identified with significant I's, and nine of those 27 had $I > 20$.

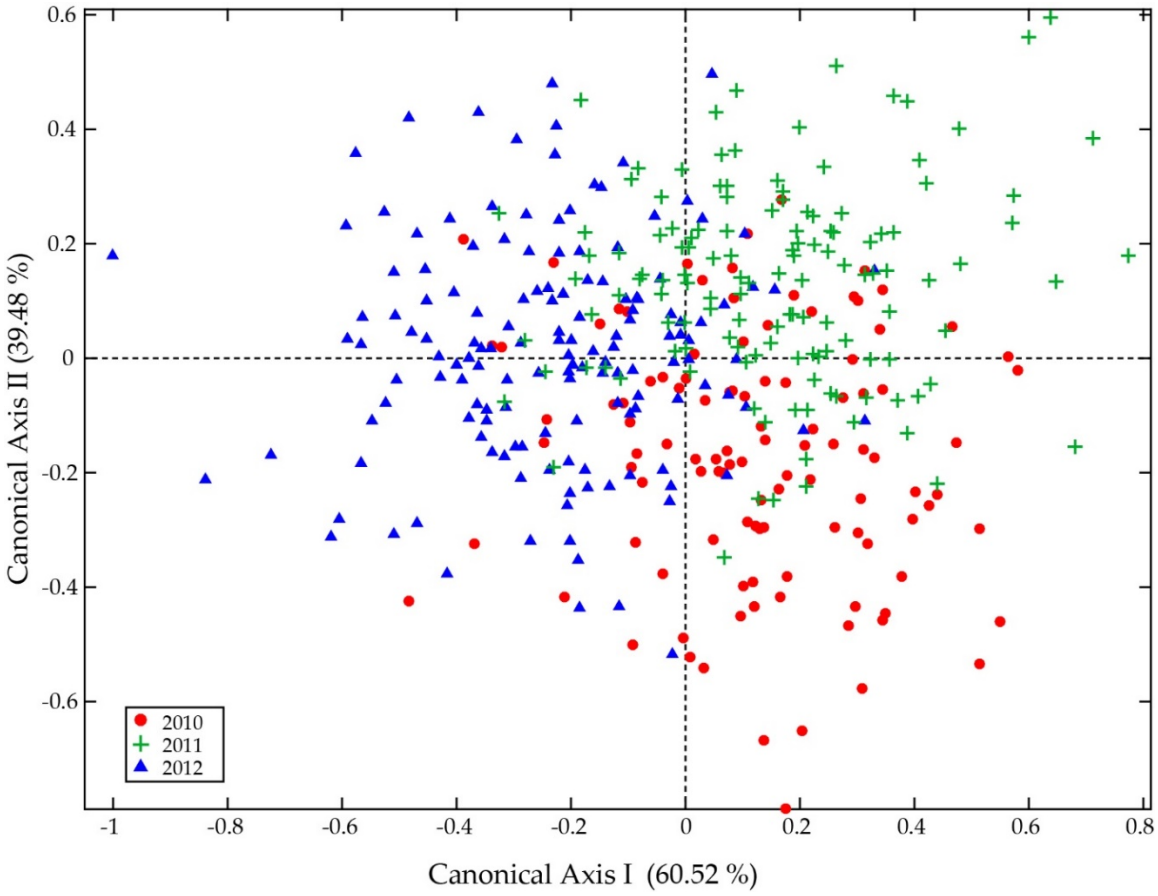

Figure 2.2 – CAP ordination diagram for SEAMAP trawl beta-diversity 2010-2012. The ordination diagram associated with the canonical analysis of principle coordinates (CAP) for all three years of groundfish trawl survey data collected across the West Florida Shelf during the summer season in the years 2010-2011. Each canonical axis can be used to describe (or explain) the total variability between each year's group of objects; where axes I and II account for 62.52% and 39.48%, respectively. Any two objects' (i.e., trawl samples') proximity to one another can be interpreted as likeness, and objects close together are more similar than those farther apart. See inset legend for symbol details.

2.3.2.2 Environmental Predictors by Year. The results of the MANOVA for $\mathbf{X}_{2011}$ and $\mathbf{X}_{2012}$ indicated that there was a significant difference between the two years with respect to the environmental conditions on the WFS at the time SEAMAP summer groundfish surveys were conducted (Table 2.4). The results of the full model also showed that there was a difference among years (F = 27.75, p = 0.001), and pairwise MANOVA confirmed that all years had uniquely different physical-chemical characteristics (Appendix A, Table A.2).

Table 2.5 – Results of daytime vs. nighttime IndVal analysis. A comprehensive list of all representative daytime and nighttime vertebrate fish species identified by the indicator value (IndVal) method for SEAMAP summer operations on the West Florida Shelf during the years 2010-2012. Only the significant IndVal species are represented (1,000 iterations, $\alpha = 0.05$), and their strength as an indicator (I) is also listed. All names were taken from the American Fisheries Society (AFS) naming guide (Page et al. 2013); parenthetical family names are the accepted AFS common families.

	Family	**Scientific Name**	**Common Name**	***I***	***p*-value**
Daytime	Carangidae (jacks)	*Decapterus punctatus*	Round Scad	24.8	0.029
	Labridae (wrasses and parrotfishes)	*Xyrichtys novacula*	Pearly Razorfish	15.3	0.001
	Carangidae (jacks)	*Chloroscombrus chrysurus*	Atlantic Bumper	12.7	0.011
	Synodontidae (lizardfishes)	*Saurida brasiliensis*	Largescale Lizardfish	11.5	0.027
	Rhinobatidae (guitarfishes)	*Rhinobatos lentiginosus*	Atlantic Guitarfish	5.4	0.027
	Gobiesocidae (clingfishes)	*Gobiesox strumosus*	Skilletfish	4.2	0.045
Nighttime	Paralichthyidae (sand flounders)	*Syacium papillosum*	Dusky Flounder	78.1	0.001
	Monacanthidae (filefishes)	*Stephanolepis hispidus*	Planehead Filefish	71.0	0.001
	Scorpaenidae (scorpionfishes)	*Scorpaena calcarata*	Smoothhead Scorpionfish	70.0	0.001
	Scorpaenidae (scorpionfishes)	*Scorpaena brasiliensis*	Barbfish	60.9	0.001
	Ophidiidae (cusk-eels)	*Ophidion holbrooki*	Bank Cusk-eel	54.9	0.001
	Serranidae (sea basses)	*Diplectrum formosum*	Highfin Sandperch	54.8	0.001
	Synodontidae (lizardfishes)	*Trachinocephalus myops*	Snakefish	54.0	0.001
	Synodontidae (lizardfishes)	*Synodus intermedius*	Sand Diver	54.0	0.001
	Synodontidae (lizardfishes)	*Synodus foetens*	Inshore Lizardfish	53.2	0.001
	Haemulidae (grunts)	*Haemulon aurolineatum*	Tomtate	53.0	0.001
	Tetraodontidae (puffers)	*Sphoeroides dorsalis*	Marbled Puffer	47.4	0.001
	Serranidae (sea basses)	*Centropristis ocyurus*	Bank Sea Bass	43.3	0.001
	Triglidae (searobins)	*Prionotus ophryas*	Bandtail Searobin	42.4	0.001
	Ostraciidae (boxfishes)	*Acanthostracion quadricornis*	Scrawled Cowfish	41.9	0.002

Table 2.5 (Continued)

Monacanthidae (filefishes)	*Monacanthus ciliatus*	Fringed Filefish	41.6	0.001
Bothidae (lefteye flounders)	*Bothus robinsi*	Twospot Flounder	41.5	0.001
Ophidiidae (cusk-eels)	*Lepophidium jeannae*	Mottled Cusk-eel	39.9	0.001
Tetraodontidae (puffers)	*Sphoeroides spengleri*	Bandtail Puffer	37.0	0.001
Ophidiidae (cusk-eels)	*Ophidion antipholus*	Longnose Cusk-eel	36.6	0.001
Triglidae (searobins)	*Bellator militaris*	Horned Searobin	35.8	0.001
Triglidae (searobins)	*Prionotus roseus*	Bluespotted Searobin	35.5	0.001
Ogcocephalidae (batfishes)	*Halieutichthys aculeatus*	Pancake Batfish	35.4	0.001
Haemulidae (grunts)	*Orthopristis chrysoptera*	Pigfish	33.4	0.001
Batrachoididae (toadfishes)	*Porichthys plectrodon*	Atlantic Midshipman	30.8	0.001
Triglidae (searobins)	*Prionotus martis*	Barred Searobin	27.0	0.001
Cynoglossidae (tonguefishes)	*Symphurus diomedeanus*	Spottedfin Tonguefish	26.6	0.001
Apogonidae (cardinalfishes)	*Apogon pseudomaculatus*	Twospot Cardinalfish	26.0	0.001
Paralichthyidae (sand flounders)	*Etropus rimosus*	Gray Flounder	22.6	0.001
Muraenidae (morays)	*Gymnothorax saxicola*	Honeycomb Moray	21.4	0.001
Paralichthyidae (sand flounders)	*Paralichthys albigutta*	Gulf Flounder	21.0	0.001
Sciaenidae (drums & croakers)	*Pareques umbrosus*	Cubbyu	20.8	0.001
Ogcocephalidae (batfishes)	*Ogcocephalus parvus*	Roughback Batfish	19.2	0.004
Paralichthyidae (sand flounders)	*Cyclopsetta fimbriata*	Spotfin Flounder	18.3	0.001
Rajidae (skates)	*Raja eglanteria*	Clearnose Skate	15.8	0.001
Serranidae (sea basses)	*Serranus phoebe*	Tattler	15.7	0.017
Triglidae (searobins)	*Prionotus rubio*	Blackfin Searobin	14.5	0.001
Triglidae (searobins)	*Prionotus alatus*	Spiny Searobin	14.2	0.007
Cynoglossidae (tonguefishes)	*Symphurus urospilus*	Spottail Tonguefish	13.3	0.001
Paralichthyidae (sand flounders)	*Citharichthys macrops*	Spotted Whiff	12.3	0.001
Scorpaenidae (scorpionfishes)	*Scorpaena agassizii*	Longfin Scorpionfish	12.2	0.004

Table 2.5 (Continued)

Ophidiidae (cusk-eels)	*Otophidium omostigma*	Polka-dot Cusk-eel	12.1	0.001
Ophichthidae (snake eels)	*Echiophis intertinctus*	Spotted Spoon-nose Eel	12.1	0.001
Rajidae (skates)	*Raja texana*	Roundel Skate	11.4	0.001
Ophidiidae (cusk-eels)	*Ophidion selenops*	Mooneye Cusk-eel	11.4	0.001
Gerreidae (mojarras)	*Eucinostomus harengulus*	Tidewater Mojarra	11.2	0.043
Sparidae (porgies)	*Calamus nodosus*	Knobbed Porgy	11.2	0.016
Paralichthyidae (sand flounders)	*Gastropsetta frontalis*	Shrimp Flounder	10.5	0.009
Priacanthidae (bigeyes)	*Pristigenys alta*	Short Bigeye	10.3	0.002
Phycidae (phycid hakes)	*Urophycis regia*	Spotted Codling	10.1	0.001
Synodontidae (lizardfishes)	*Saurida normani*	Shortjaw Lizardfish	9.6	0.006
Uranoscopidae (stargazers)	*Kathetostoma albigutta*	Lancer Stargazer	9.5	0.001
Ogcocephalidae (batfishes)	*Ogcocephalus corniger*	Longnose Batfish	9.1	0.004
Cynoglossidae (tonguefishes)	*Symphurus plagiusa*	Blackcheek Tonguefish	8.6	0.001
Apogonidae (cardinalfishes)	*Phaeoptyx xenus*	Sponge Cardinalfish	8.0	0.001
Triglidae (searobins)	*Prionotus scitulus*	Leopard Searobin	7.9	0.023
Nettastomatidae (duckbill eels)	*Hoplunnis diomediana*	Blacktail Pikeconger	6.8	0.001
Tetraodontidae (puffers)	*Sphoeroides nephelus*	Southern Puffer	6.8	0.002
Mullidae (goatfishes)	*Upeneus parvus*	Dwarf Goatfish	6.7	0.001
Paralichthyidae (sand flounders)	*Etropus cyclosquamus*	Shelf Flounder	6.1	0.007
Ophichthidae (snake eels)	*Ophichthus puncticeps*	Palespotted Eel	6.1	0.002
Serranidae (sea basses)	*Serraniculus pumilio*	Pygmy Sea Bass	5.1	0.001
Apogonidae (cardinalfishes)	*Apogon aurolineatus*	Bridle Cardinalfish	4.7	0.016
Phycidae (phycid hakes)	*Urophycis earllii*	Carolina Hake	4.5	0.015
Apogonidae (cardinalfishes)	*Apogon affinis*	Bigtooth Cardinalfish	4.3	0.028
Triglidae (searobins)	*Prionotus tribulus*	Bighead Searobin	4.2	0.006
Serranidae (sea basses)	*Centropristis philadelphica*	Rock Sea Bass	3.8	0.006

Table 2.5 (Continued)

	Triglidae (searobins)	*Prionotus longispinosus*	Bigeye Searobin	3.8	0.004
	Apogonidae (cardinalfishes)	*Phaeoptyx pigmentaria*	Dusky Cardinalfish	3.4	0.014
	Congridae (conger eels)	*Paraconger caudilimbatus*	Margintail Conger	2.3	0.025

Table 2.6 – Results of annual IndVal analysis. A comprehensive list of each years' representative vertebrate fish species identified by the indicator value (IndVal) method for SEAMAP summer operations on the West Florida Shelf during the years 2010-2012. See Table 2.5 caption for additional table details and naming information.

	Family	**Scientific Name**	**Common Name**	***I***	***p*-value**
2010	Synodontidae (lizardfishes)	*Synodus poeyi*	Offshore Lizardfish	21.0	0.009
	Clupeidae (herrings)	*Sardinella aurita*	Spanish Sardine	14.4	0.001
	Synodontidae (lizardfishes)	*Saurida brasiliensis*	Largescale Lizardfish	13.2	0.002
	Phycidae (phycid hakes)	*Urophycis regia*	Spotted Codling	10.8	0.001
	Synodontidae (lizardfishes)	*Saurida normani*	Shortjaw Lizardfish	7.5	0.024
	Pomacanthidae (angelfishes)	*Pomacanthus arcuatus*	Gray Angelfish	6.4	0.014
2011	Paralichthyidae (sand flounders)	*Syacium papillosum*	Dusky Flounder	36.5	0.001
	Synodontidae (lizardfishes)	*Synodus foetens*	Inshore Lizardfish	32.4	0.005
	Monacanthidae (filefishes)	*Monacanthus ciliatus*	Fringed Filefish	29.9	0.001
	Serranidae (sea basses)	*Centropristis ocyurus*	Bank Sea Bass	28.5	0.001
	Ostraciidae (boxfishes)	*Acanthostracion quadricornis*	Scrawled Cowfish	26.4	0.014
	Scorpaenidae (scorpionfishes)	*Scorpaena brasiliensis*	Barbfish	24.4	0.003
	Carangidae (jacks)	*Trachurus lathami*	Rough Scad	24.1	0.001
	Tetraodontidae (puffers)	*Sphoeroides dorsalis*	Marbled Puffer	23.9	0.002
	Sciaenidae (drums & croakers)	*Equetus lanceolatus*	Jackknife-fish	21.5	0.042
	Tetraodontidae (puffers)	*Sphoeroides spengleri*	Bandtail Puffer	18.5	0.005

Table 2.6 (Continued)

	Triglidae (searobins)	*Prionotus ophryas*	Bandtail Searobin	17.7	0.002
	Muraenidae (morays)	*Gymnothorax saxicola*	Honeycomb Moray	17.1	0.001
	Ogcocephalidae (batfishes)	*Halieutichthys aculeatus*	Pancake Batfish	15.8	0.018
	Paralichthyidae (sand flounders)	*Etropus rimosus*	Gray Flounder	13.6	0.002
	Rajidae (skates)	*Raja eglanteria*	Clearnose Skate	11.1	0.001
	Ophidiidae (cusk-eels)	*Ophidion antipholus*	Longnose Cusk-eel	10.8	0.007
	Syngnathidae (pipefishes & seahorses)	*Hippocampus erectus*	Lined Seahorse	10.6	0.007
	Ogcocephalidae (batfishes)	*Ogcocephalus cubifrons*	Polka-dot Batfish	10.2	0.002
	Cynoglossidae (tonguefishes)	*Symphurus diomedeanus*	Spottedfin Tonguefish	10.0	0.003
	Labridae (wrasses and parrotfishes)	*Xyrichtys novacula*	Pearly Razorfish	9.4	0.007
	Sciaenidae (drums & croakers)	*Pareques umbrosus*	Cubbyu	9.0	0.042
	Apogonidae (cardinalfishes)	*Apogon pseudomaculatus*	Twospot Cardinalfish	8.6	0.039
	Monacanthidae (filefishes)	*Aluterus heudelotii*	Dotterel Filefish	8.0	0.006
	Sparidae (porgies)	*Stenotomus caprinus*	Longspine Porgy	8.0	0.002
	Triglidae (searobins)	*Prionotus rubio*	Blackwing Searobin	6.8	0.026
	Ophichthidae (snake eels)	*Echiophis intertinctus*	Spotted Spoon-nose Eel	6.7	0.003
	Priacanthidae (bigeyes)	*Pristigenys alta*	Short Bigeye	6.5	0.034
2012	Labridae (wrasses and parrotfishes)	*Nicholsina usta*	Emerald Parrotfish	20.5	0.001
	Haemulidae (grunts)	*Orthopristis chrysoptera*	Pigfish	15.9	0.011
	Haemulidae (grunts)	*Haemulon plumieri*	White Grunt	15.7	0.002
	Sparidae (porgies)	*Calamus arctifrons*	Grass Porgy	8.3	0.031
	Ephippidae (spadefishes)	*Chaetodipterus faber*	Atlantic Spadefish	7.4	0.027
	Clupeidae (herrings)	*Opisthonema oglinum*	Atlantic Thread Herring	7.4	0.003

Table 2.7 – Leave-one-out cross-validation confusion matrix. The sample reclassification success rates for each year. The values on the matrix diagonal represent the percentage of correct classifications for a year and its own observations. The off-diagonal values represent the misclassification rates; this is the percentage of the time in which samples from the year represented in the row are reclassified as samples from the year in the column header. The values in each row sum to 100%.

	2010	2011	2012
2010	86.2%	13.8%	0.0%
2011	10.6%	84.1%	5.3%
2012	0.7%	4.0%	95.3%

Further support for the difference between years was provided by the CAP procedure (Trace statistic = 1.0318 $p = 0.001$, $m = 14$, variability of $\mathbf{X}_{Euc}$ expl. = 95.3%). The choice of m for this CAP model was made to maximize the LOO classification success rate (88.97%) and the proportion of the variability in $\mathbf{X}_{Euc}$ explained by the retained axes, while simultaneously minimizing the residual sums-of-squares and total number of canonical axes used. Samples held out from 2012 and reclassified, based on the observations within them, were done so correctly 95.3% of the time, whereas both 2010 and 2011 were slightly less likely to have their samples correctly reclassified (86.2% and 84.1%, respectively). The confusion matrix resultant from the LOO cross-validation (Table 2.7) showed that 2012 was the least likely to be misrepresented (i.e., was the most unique) while the remaining two years appeared to be somewhat more similar to each other.

The ordination diagram from the CAP for **X** (Figure 2.3) displayed a greater degree of overlap in the multivariate data clouds for 2010 and 2011 than there was for either year with 2012. In fact, 2012 is mostly independent of the other two years and only a handful of its observations existed within another year's multivariate hyperspace. Axis-I represents 75.09% of the

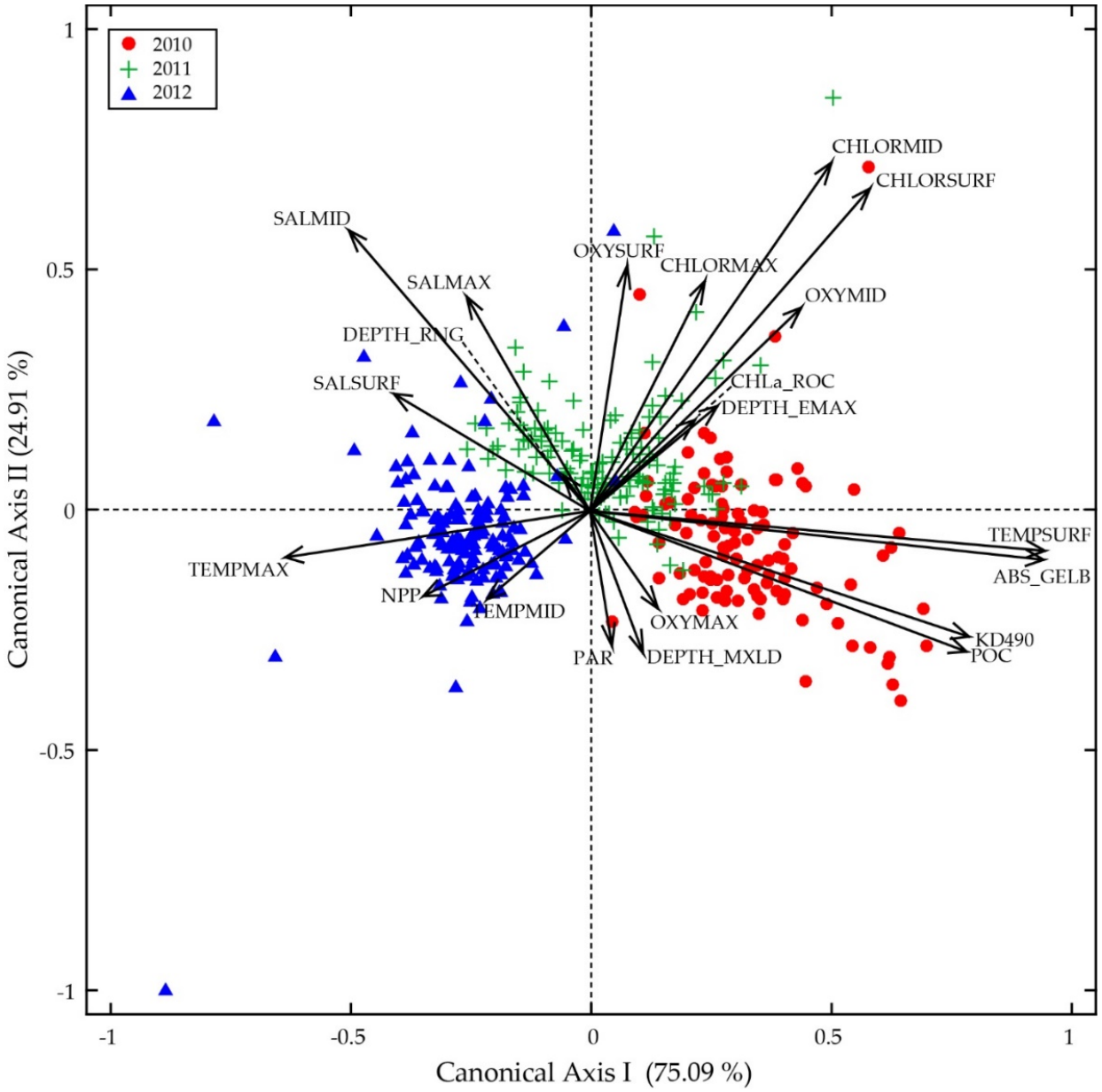

Figure 2.3 – CAP ordination diagram for SEAMAP trawl marine environment in 2010-2012. The ordination diagram for the canonical analysis of principle coordinates (CAP) based on marine environmental data collected across the West Florida Shelf while conducting SEAMAP summer groundfish trawl surveys during 2010-2011. Objects (i.e., trawl samples) are ordinated with respect to the abiotic variables used to describe the physical-chemical conditions at the end of a trawling station (see Table 2.2 for names and descriptions); samples close together are considered similar marine environments. Vectors are interpreted as relative gradients with only the positive ends visualized. The intersection of any object's orthogonal projection with any environmental gradient is equivalent to that object's modelled estimate for that descriptor. Separation between groups is interpreted as described in the caption for Figure 2.2, and in this case the CAP axes I and II account for 75.09% and 24.91%, respectively. See inset legend for symbol details.

explained difference between years, and the greatest amount of separation between the years' data clouds was also mostly along this axis; meanwhile, axis-II explained less variability (24.91%) and accounted for less separation between years' objects (Figure 2.3).

2.4 DISCUSSION

2.4.1 Nautical Twilight and the Influence of Ambient Light on the WFS

It is widely accepted both anecdotally and scientifically that the composition of representative species for daytime and nighttime communities are often considerably different (Clark and Levy 1988, Neilson and Perry 1990, Bennett et al. 2002, Reebs 2002, Helfman et al. 2009, Orbesen et al. 2017). What is not widely agreed upon is a standard definition of how to delineate these two community types for all marine environments, especially given the dynamic and highly variable nature of the submarine light environment. Aside from the northwestern portion, a majority of the WFS is generally considered to be oligotrophic with nutrient loads transported onto the shelf from riverine and deepwater inputs via winds, currents, and upwelling events associated with loop current dynamics (Hurlburt and Thompson 1980, Kumpf et al. 1999, Muller-Karger 2000, Rabalais 2002, He and Weisberg 2003, Vargo et al. 2008). The entire shelf system supports significant amounts of benthic primary production (Kumpf et al. 1999, Okey et al. 2004, Vargo et al. 2008), implying that light is readily available at most depths represented in this study. Therefore, it is reasonable to assume that, even with widely varying optical properties for seawater on very short timescales, the groundfish species of the WFS are not typically immersed in continuous darkness due to physical shading in the water column, and that they are very likely responsive to light cues based on diel cycles.

The most noticeable contrast between the daytime and nighttime samples was the vastly increased species richness (*S*) and diversity (*H'*) of the nighttime trawl catches when compared to those from the daytime. The species identified in Table 2.5 represent which species were significant indicators for each sample typology (i.e., day or night), and the magnitude of *I* represents species' capacity to serve as an indicator. As previously noted, a strong indicator species is one that is specific to one group, and also exhibits high fidelity within that group (Dufrene and Legendre 1997). The lack of strength for daytime indicator species' *I* values implies that either they have (1) low group specificity, whereby they are also found in several nighttime samples, (2) low site fidelity, where they are infrequently encountered in daytime samples, or (3) a combination of both.

The nighttime samples, on the other hand, had several strong indicator species with high *I*, and over 65 species identified by IndVal as significant (Table 2.5). The implication of the stark difference in both the quantity and quality of indicators for nighttime versus daytime trawl samples is that the communities observed in the darkness are substantially more unique and diverse than those from the daytime net tows. Nocturnal species are well represented in the trawl samples, but also on the indicator list provided by IndVal. Of the four families of eels observed (Ophidiidae, Nettastomatidae, Ophichthidae, Congridae, in order of abundance), all nine species observed were significant indicators, exhibited extremely high specificity, and in some cases high fidelity as well (Figure 2.4). Furthermore, several other families with notable nocturnal species showed the same patterns as the eels, such as: (1) Paralichthyidae, (2) Monacanthidae, (3) Scorpaenidae, (5) Synodontidae, and (6) Triglidae.

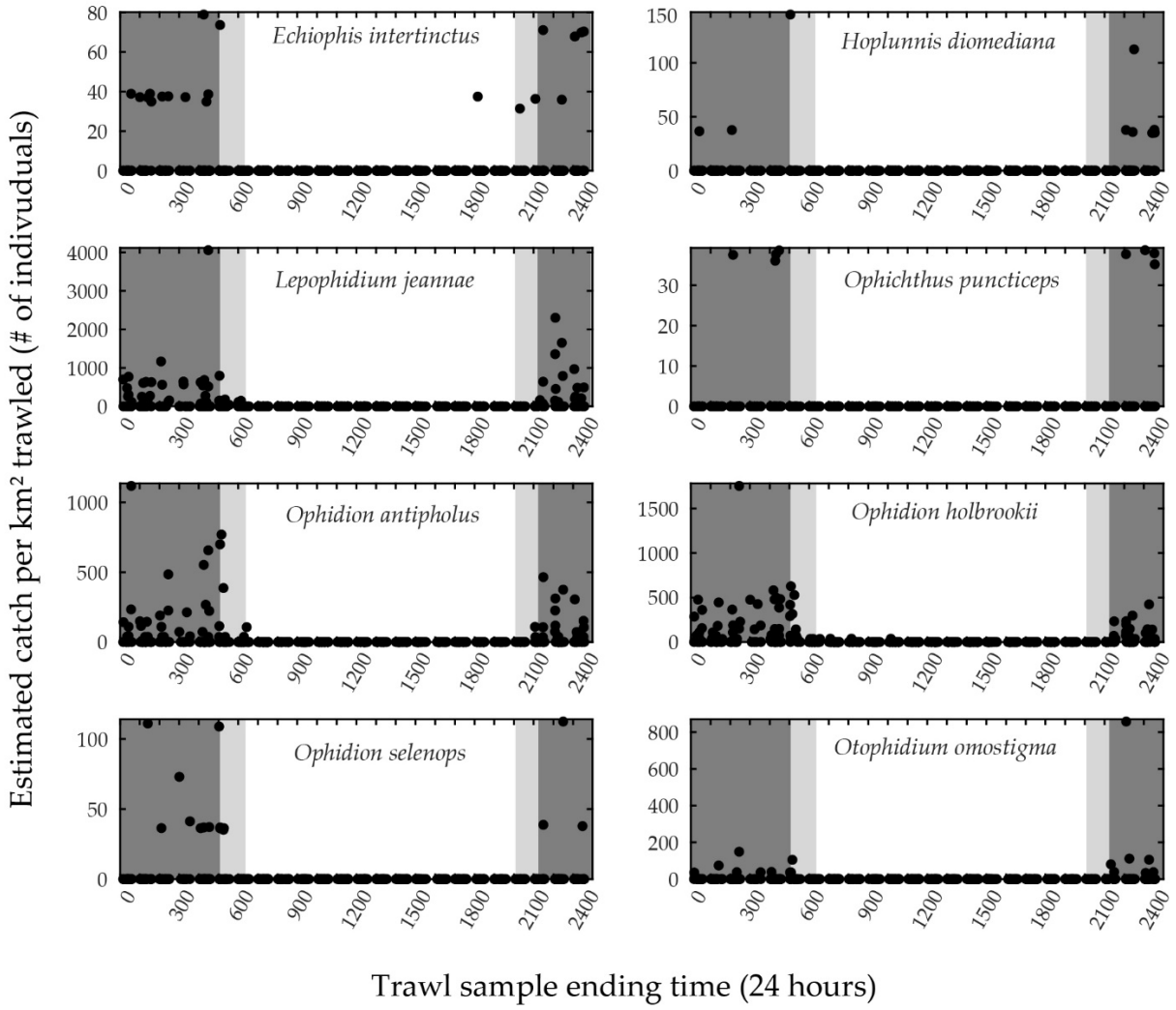

Figure 2.4 –Estimated catch for all eels versus sampling time of day. The estimated abundance per km² trawled (black circles) for eight different species of eels observed during the summer SEAMAP groundfish trawl surveys for the West Florida Shelf during 2010-2012. The horizontal axis represent the time of day when each sampling station was completed, and the light environment (i.e., daytime or nighttime) is noted by the gray shaded areas (see Figure 2.1 caption for more details).

Given the significant differences in *S*, *J'*, and *H'*, as well as the stark contrasts in the actual representative species assemblages for daytime versus nighttime samples, the diurnal stratification of samples was justified. Additionally, using the nautical twilight boundaries to define the light environment for bottom-trawl samples was also reasonable. The NT-based, knife-

edge cutoff is preferential to defining some other crepuscular time period because it not only reduces the number of total analyses required due to dataset stratification, but it also allows the researcher to retain as many samples as possible that are representative of daytime and nighttime groundfish communities.

2.4.2 Annual Variation in Environmental Predictors and Biological Responses

The statistical examination of the annually stratified response and predictor matrices revealed that there were distinct differences between all years from 2010 to 2012 with respect to both the beta-diversity of groundfish catches and the physical-chemical state of the sampling universe. The tests for homogenous dispersions exposed the fact that 2010 was a much more variable year in terms of the environmental conditions observed when compared to the rest of the years in the study, and likewise, the year 2011 was more variable in terms of beta-diversity. These results support some level of environmental control of groundfish organization in the Gulf LME, as well as a potential lag in the system's biological response. In the independent analyses of **Y** and **X**, both the reduced and full MANOVA models were corroborated by pairwise MANOVA and CAP, and visualized via canonical ordination of the CAP results. The statistical justifications for the stratification of the datasets according to sampling year for future analyses to define relationships between environmental status and fish community organization are clear (Table 2.4, Table 2.7; Table A.2). The first-order qualitative differences among years are described below.

2.4.2.1 Environmental predictors. When compared to the other two years, 2010 had much higher concentrations of particulate organic carbon (POC), light attenuation values, light absorption due to gelbstoff and detritus, and sea surface temperatures. The same year was

observed to have relatively lower seawater temperatures at maximum and mid-water depths, net primary production (NPP), and salinity (all depths). Because 2010 and 2012 were ordinated on opposite ends of axis-I, and they did not differ greatly along the vertical axis, their qualitative characteristics were more-or-less mirror images of one another, although the spread of the 2010 data cloud was greater than all other years (Figure 2.3). The sampling in 2010 was undertaken just two months after the *Deepwater Horizon* oil spill, and the abnormal variability observed in the environmental predictors for that year could be biased by any sample's proximity to the oil spill and the timing of subsurface oil particulate dispersal and sedimentation (Murawski et al. 2014, Romero et al. 2017). Furthermore, with the exception of salinity, the characteristics that were used to qualitatively describe the marine environment in 2010 could be partially explained by physical shading in the water column due to increased particulate matter, which would be consistent with a catastrophic event like an oil spill. The fact that only two years later the physical-chemical environment is a mirror image of the 2010 sampling season also supports the idea that the observed state in the Gulf LME in 2010 was transient, and likely due to the rapid onset of a major event whose effects were dispersed relatively quickly.

Samples from 2011 were plotted in between 2010 and 2012, along axis-I, and can therefore be thought of as having qualitative characteristics that are transitional between the two extremes noted for the endpoint years. The transition year's objects were also positioned higher along axis-II than the other two years, which implies 2011 had unique characteristics of its own. In particular, 2011 differed due to higher chlorophyll concentrations and associated rates of change, higher dissolved oxygen (DO) concentrations at the surface and mid-water depths, and lower DO at maximum depths. Other prominent physical characteristics unique to 2011 included overall

lower photosynthetically available radiation (PAR) levels and shallower mixed layer depths during trawl sampling (Figure 2.3). Lastly, both the LOO cross-validation and the CAP ordination diagram for **X** strongly supported the notion that 2010 and 2011 were more alike to one another than 2012 was to either of those years. Taken in total, the CAP results also strengthen the claim that 2011 was a transitional year between the environmental regime observed in 2010 and the alternate state exhibited in 2012.

2.4.2.2 Biological responses. The organization of beta-diversity throughout the WFS exhibited a somewhat lagged response to the dynamic environmental conditions described above. In terms of the composition and abundance of species sampled, 2011 observations were significantly more variable than either of the other two years in the study, while all years were shown to have different representative communities (Figure 2.2). In a semi-enclosed basin, such as the Gulf LME, it is reasonable to assume that, in general, the overall list of species present in the system would not change substantially on annual time scales. Therefore, it could be argued that much of the variability observed would likely be due to shifts in (1) species' distributions or (2) population demographics based on environmental control. Other explanations include (3) chance encounters with different rare, cryptic, or non-target species in trawl samples or (4) some other unaccounted for error or sampling bias. In a "stable" system (i.e., *lower* variability in beta-diversity), the short-term annual differences for trawl community indicator species would likely be controlled more by options (3) and (4), rather than by some major environmental intervention. The results presented here more generally support the environmental control hypothesis and a highly connected trophic structure across the WFS (i.e., options (1) and (2) above).

For all years studied, the strength of IndVal species' *I* values were generally poor (all $I \leq 36.5$), but 2011 had nine *I* values that were larger than the maximum *I* for either 2010 or 2012. Additionally, if only those nine species with stronger indicators were interpreted, it would still be > 30% more IndVal representatives than were identified for either 2010 or 2012. These results suggest that these species were much better indicators for 2011 than those IndVal species identified for 2010 and 2012 were for their respective years; this also bolsters the case for the biological assemblage represented in 2011 being anomalous compared to the other years.

When examined in temporal order, a pattern emerges that describes a changing biological response for the WFS groundfish from 2010-2012. The initial year of sampling was characterized by species from primarily the Synodontidae family and one species from the Phycidae family, and in both cases these fishes are thought to prefer soft-bottom, sediment-dominated habitats (Helfman et al. 2009). The set of indicator species identified for 2011 was much larger and much more diverse than 2010. However, like 2010, most of the IndVal species identified for 2011 were representatives of families that were shown to have strong associations with nighttime samples, as discussed in section 2.4.1, (Table 2.5 and Table 2.6). Because most nocturnal species either prefer darkness or have a need to avoid predation during the daylight hours, and in a system like the WFS where deep water refuges are typically not proximal, it is most likely that these species are either taking cover within rugose benthic structure (e.g., reefs or rubble) or in soft sediments (e.g., sand or mud). Therefore, the increased prevalence of normally cryptic, nocturnal species as indicators for the entire sampled community, which was primarily sampled in the daylight hours, may be interpreted as evidence for some physical perturbation of the preferred habitats. The perturbation would have had to either (1) increase the catchability of these species, or (2)

somehow confer a competitive advantage to the now more dominant species that resulted in a demographic change.

Of the two options presented to explain the increases of nocturnal, benthic species as indicators for 2010-2011, the former is more likely, especially considering the contrast in indicator species identified for the final year in the study. The most consequential species represented in the assemblage of indicator species for 2012 were from the Labridae and Haemulidae families, with additional representatives from Sparidae, Ephippidae, and Clupeidae as well. This indicator assemblage (1) contained no known nocturnal species and (2) was comprised of species that mostly prefer seagrasses (*N. usta*, *O. chrysoptera*, *H. plumieri*, and *C. arctifrons*). It is conceivable that the sampling efforts in 2012 were biased toward seagrass habitats due to the random selection process, however, this was not assessed in this study. The change in indicator species could also be explained by a cessation, or shifting, of the environmental conditions that lead to the assemblages observed in 2010 and 2012 but, once again, further analysis would be required to determine the efficacy of this, or any other, proposition.

2.5 CONCLUSIONS

2.5.1 Summary Discussion

The main purposes of this study were to (1) determine the timing and significance of any diel changes in groundfish communities on the West Florida Shelf, and (2) assess the efficacy of aggregating multiple years of SEAMAP biological and/or environmental data for use in multivariate statistical analyses. In both cases, strong support was found for not only dividing the SEAMAP database into daytime and nighttime samples, but also for analyzing each year of data independently.

Daytime and nighttime groundfish trawl samples were shown to have different characteristic fish communities present. Species richness and diversity were significantly greater in nighttime samples, and the indicator species for samples collected in darkness were much stronger than those from the daytime due to frequent encounters with obligate nocturnal species. The timing of the observed community shifts were well predicted by using the local nautical twilight boundaries to define the submarine light regime for the unique combinations of sampling date, time, and location.

With respect to both the fish communities and the marine environment, each year in this study was statistically different from the other years. This gives strong weight to the contention that each year should be analyzed independently when assessing questions related to beta-diversity or environmental dynamics on the WFS or, at the very least, statistical control for a year effect must employed. The timing of the shifts in the system's environmental variability and composition, along with the apparent lagged response in the changes observed in beta-diversity, suggest strong environmental control over the groundfish organization on the WFS. The environmental states on the WFS displayed a gradient of disturbance through time, starting with a rapidly perturbed state in 2010, that transitioned away from that state during 2011, and settled into a less-variable state in 2012. The biological response manifested as changes in groundfish community composition, and was such that species that were shown to be members of the nighttime communities in the diel study were more likely to be selected as an indicator species for the first two years in the annual study, even though the number of nighttime samples in both years was fewer than daytime samples. This implies a disturbance to the benthic habitat that was substantial enough that these supposed nocturnal species were more representative in all

summer trawls over the time period 2010-2011 than they were in 2012, regardless of the time of day for the sampling haul. The lagged biological response was characterized by a highly anomalous composition of indicator species for 2011, and once again, a more normalized assemblage observed in 2012.

2.5.2 Future Work

Detailed cause-and-effect relationships are difficult to determine based on multivariate statistical modeling. Implicative lines were drawn from the rapid and catastrophic changes to the marine environment in the spring and summer of 2010 from the *Deepwater Horizon* oil spill to the subsequent changes in groundfish beta-diversity observed. These implications, however, are only speculative at this time. Significant, directed, and focused scientific studies will need to be undertaken to test the hypothesis that an oil spill was the true mechanism behind the observed changes, but the results presented here are compelling enough to justify further investigation into several compelling lines of scientific inquiry.

Additionally, future efforts to characterize environmental control over biological resource organization on the WFS should be undertaken with the assumption that heterogeneity exists among years and light environments, and independent analyses among these stratifications are preferable. Furthermore, given the scale of the physical feature of the WFS, future work should also take into consideration spatial factors that may contribute to the organization of the environmental and biological resources of the shelf ecosystem.

2.6 LITERATURE CITED

Anderson, M. J. 2001a. A new method for non-parametric multivariate analysis of variance. Austral Ecology **26**:32-46.

Anderson, M. J. 2001b. Permutation tests for univariate or multivariate analysis of variance and regression. Canadian journal of fisheries and aquatic sciences **58**:626-639.

Anderson, M. J. 2006. Distance-based tests for homogeneity of multivariate dispersions. Biometrics **62**:245-253.

Anderson, M. J., K. E. Ellingsen, and B. H. McArdle. 2006. Multivariate dispersion as a measure of beta diversity. Ecology Letters **9**:683-693.

Anderson, M. J., and D. C. I. Walsh. 2013. PERMANOVA, ANOSIM, and the Mantel test in the face of heterogeneous dispersions: What null hypothesis are you testing? Ecological Monographs **83**:557-574.

Anderson, M. J., and T. J. Willis. 2003. Canonical analysis of principal coordinates: A useful method of constrained ordination for ecology. Ecology **84**:511-525.

Behrenfeld, M. J., and P. G. Falkowski. 1997. Photosynthetic rates derived from satellite-based chlorophyll concentration. Limnology and Oceanography **42**:1-20.

Bennett, W. A., W. J. Kimmerer, and J. R. Burau. 2002. Plasticity in vertical migration by native and exotic estuarine fishes in a dynamic low-salinity zone. Limnology and Oceanography **47**:1496-1507.

Bray, J. R., and J. T. Curtis. 1957. An odination of the upland forest communities of souther Wisconsin. Ecological Monographs **27**:326-349.

Bryant, W. R., J. Lugo, C. Cordova, and A. Salvador. 1991. Physiography and bathymetry. The Gulf of Mexico Basin: Boulder, Geological Society of America, Decade of North American Geology, v. J:13-30.

Chagaris, D. D., B. Mahmoudi, C. J. Walters, and M. S. Allen. 2015. Simulating the Trophic Impacts of Fishery Policy Options on the West Florida Shelf Using Ecopath with Ecosim. Marine and Coastal Fisheries **7**:44-58.

Clark, C. W., and D. A. Levy. 1988. Diel Verticle Migrations by Juvenile Sockeye Salmon and the Antipredation Window. American Naturalist **131**:271-290.

Darcy, G. H., and E. J. Gutherz. 1984. Abundance and density of demersal fishes on the west Florida shelf, January 1978. Bulletin of Marine Science **34**:81-105.

Dufrene, M., and P. Legendre. 1997. Species assemblages and indicator species: The need for a flexible asymmetrical approach. Ecological Monographs **67**:345-366.

Fisher, R. A. 1921. Studies in crop variation I An examination of the yield of dressed grain from Broadbalk. Journal of Agricultural Science **11**:107-135.

Franz, B. A., and P. J. Werdell. 2010. A generalized framework for modeling of inherent optical properties in ocean remote sensing applications. Proceedings of Ocean Optics, Anchorage, Alaska **27**.

Frouin, R., B. A. Franz, and P. J. Werdell. 2002. The SeaWiFS PAR product. In: Hooker, S.B. and Firestone, E.R., Algorithm Updates for the Fourth SeaWiFS Data Reprocessing, NASA Tech Memo, 2003-206892. NASA Goddard Space Flight Center, Greenbelt, MD.

Frouin, R., and R. T. Pinker. 1995. Estimating photosynthecially active radiation (PAR) at the Earth's surface from satellite observations. Remote Sensing of Environment **51**:98-107.

Gruss, A., M. J. Schirripa, D. Chagaris, M. Drexler, J. Simons, P. Verley, Y. J. Shin, M. Karnauskas, R. Oliveros-Ramos, and C. H. Ainsworth. 2015. Evaluation of the trophic structure of the West Florida Shelf in the 2000s using the ecosystem model OSMOSE. Journal of Marine Systems **144**:30-47.

GSMFC. 2016. SEAMAP Operations Manual for Trawl and Plankton Surveys. Pages 1-117, Gulf States Marine Fisheries Commission, Ocean Springs, MS.

Habtes, S. Y. 2014. Variability in the Spatial and Temporal Patterns of Larval Scombrid Abundance in the Gulf of Mexico.

He, R. Y., and R. H. Weisberg. 2003. A loop current intrusion case study on the West Florida shelf. Journal of Physical Oceanography **33**:465-477.

Helfman, G. S., B. B. Collette, D. E. Facey, and B. W. Bowen. 2009. The diversity of fishes : biology, evolution, and ecology. 2nd edition. Blackwell, Chichester, UK ; Hoboken, NJ.

Hine, A. C., R. B. Halley, S. D. Locker, B. D. Jarrett, W. C. Jaap, D. J. Mallinson, K. T. Ciembronowicz, N. B. Ogden, B. T. Donahue, and D. F. Naar. 2008. Coral reefs, present and past, on the west Florida shelf and platform margin. Coral Reefs of the USA:127-173.

Hurlburt, H. E., and J. D. Thompson. 1980. A numerical study of loop current intrusion and eddy shedding. Journal of Physical Oceanography **10**:1611-1651.

Jones, D. L. 2017. The Fathom Toolbox for MATLAB. University of South Florida, College of Marine Science, St. Petersburg, FL.

Juhl, R. 1966. Experimental fish trawling survey along the Florida west coast. Commercial Fisheries Revue **28**:1-5.

Kara, A. B., P. A. Rochford, and H. E. Hurlburt. 2000. An optimal definition for ocean mixed layer depth. Journal of Geophysical Research-Oceans **105**:16803-16821.

Kilborn, J. P. 2017. The Darkside Toolbox for Matlab. University of South Florida, College of Marine Science, St. Petersburg, FL.

Kumpf, H., K. A. Steidinger, and K. Sherman. 1999. The Gulf of Mexico large marine ecosystem : assessment, sustainability, and management. Blackwell Science, Malden, Mass., USA.

Lee, Z. P., M. Darecki, K. L. Carder, C. O. Davis, D. Stramski, and W. J. Rhea. 2005a. Diffuse attenuation coefficient of downwelling irradiance: An evaluation of remote sensing methods. Journal of Geophysical Research-Oceans **110**.

Lee, Z. P., K. P. Du, and R. Arnone. 2005b. A model for the diffuse attenuation coefficient of downwelling irradiance. Journal of Geophysical Research: Oceans **110**.

Legendre, P., and L. Legendre. 2012. Numerical Ecology. Third English edition edition. Elsevier, Amsterdam, The Netherlands.

Manly, B. F. 2006. Randomization, bootstrap and Monte Carlo methods in biology. Chapman & Hall/CRC Press, Boca Raton.

Matlab. R2014. The MathWorks, Inc., Natick, Massachusetts, United States.

McArdle, B. H., and M. J. Anderson. 2001. Fitting multivariate models to community data: A comment on distance-based redundancy analysis. Ecology **82**:290-297.

Muller-Karger, F. E. 2000. The spring 1998 northeastern Gulf of Mexico (NEGOM) cold water event: Remote sensing evidence for upwelling and for eastward advection of Mississippi water (or: How an errant loop current anticyclone took the NEGOM for a spin). Gulf of Mexico Science **18**:55-67.

Murawski, S. A., W. T. Hogarth, E. B. Peebles, and L. Barbeiri. 2014. Prevalence of External Skin Lesions and Polycyclic Aromatic Hydrocarbon Concentrations in Gulf of Mexico Fishes, Post-Deepwater Horizon. Transactions of the American Fisheries Society **143**:1084-1097.

NASA Goddard Space Flight Center, O. E. L., Ocean Biology Processing Group. 2014a. Moderate-resolution Imaging Spectroradiometer (MODIS) Aqua Downwelling Diffuse Attenuation Coefficient Data; 2014 Reprocessing. NASA OB.DAAC, Greenbelt, MD, USA.

NASA Goddard Space Flight Center, O. E. L., Ocean Biology Processing Group. 2014b. Moderate-resolution Imaging Spectroradiometer (MODIS) Aqua Inherenet Optical Properties Data; 2014 Reprocessing. NASA OB.DAAC, Greenbelt, MD, USA.

NASA Goddard Space Flight Center, O. E. L., Ocean Biology Processing Group. 2014c. Moderate-resolution Imaging Spectroradiometer (MODIS) Aqua Ocean Color Data; 2014 Reprocessing. NASA OB.DAAC, Greenbelt, MD, USA.

NASA Goddard Space Flight Center, O. E. L., Ocean Biology Processing Group. 2014d. Moderate-resolution Imaging Spectroradiometer (MODIS) Aqua Photosynthetically Available Radiation Data; 2014 Reprocessing. NASA OB.DAAC, Greenbelt, MD, USA.

Neilson, J. D., and R. I. Perry. 1990. Diel vertical migrations of marine fishes: An obligate or facultative process? Advances in Marine Biology **26**:115-168.

Nichols, S. 1983. Impacts of the 1981 and 1982 Texas closure on brown shrimp yields. US Department of Commerce, National Oceanic and Atmospheric Administration, National Marine Fisheries Service, Southeast Fisheries Center.

Nichols, S. 1984. Impacts of the 1982 and 1983 closure of the Texas FCZ on brown shrimp yields. Southeast Fisheries Center, Miami Laboratory.

Nichols, S., and J. Poffenberger. 1987. Analysis of alternative closures for improving brown shrimp yield in the Gulf of Mexico. Report to the Gulf of Mexico Fishery Management Council.

NMFS. 2014. Fisheries Economics of the United States, 2012. Pages 1-175 *in* T. M. NMFS-F/SPO-137, editor., U.S. Department of Commerce, NOAA.

O'Reilly, J. E., S. Maritorena, D. A. Siegel, M. C. O'Brien, D. Toole, B. G. Mitchell, M. Kahru, F. P. Chavez, P. Strutton, G. F. Cota, K. L. Carder, F. Muller-Karger, L. Harding, A. Magnuson, D. Phinney, G. F. Moore, J. Aiken, K. R. Arrigo, R. Letelier, and M. Culver. 2000. Ocean color chlorophyll a algorithms for SeaWiFS, OC2, and OC4: Version 4. NASA Tech. Memo. 206892. National Aeronautics and Space Administration, Goddard Space Flight Center, Greenbelt, MD.

Okey, T. A., and B. A. Mahmoudi. 2002. An Ecosystem Model of the West Florida Shelf for use in Fisheries Management and Ecological Research: Vol II. Model Construction. Pages 1-154. Florida Marine Research Institute, St. Petersburg, Florida.

Okey, T. A., G. A. Vargo, S. Mackinson, M. Vasconcellos, B. Mahmoudi, and C. A. Meyer. 2004. Simulating community effects of sea floor shading by plankton blooms over the West Florida Shelf. Ecological Modelling **172**:339-359.

Orbesen, E. S., D. Snodgrass, G. S. Shideler, C. A. Brown, and J. F. Walter. 2017. Diurnal patterns in Gulf of Mexico epipelagic predator interactions with pelagic longline gear: implications for target species catch rates and bycatch mitigation. Bulletin of Marine Science **93**:573-589.

Page, L. M., H. Espinosa-Pérez, L. T. Findley, C. R. Gilbert, R. N. Lea, N. E. Mandrak, R. L. Mayden, and J. S. Nelson. 2013. Common and Scientific Names of Fishes From the United States, Canada, and Mexico. 7th edition. American Fisheries Society, Bethesda, Maryland.

Pielou, E. C. 1966. The measurement of diversity in different types of biological collections. Journal of Theoretical Biology **13**:131-144.

Quinn, G. P., and M. J. Keough. 2002. Experimental design and data analysis for biologists. Cambridge University Press, Cambridge, UK ; New York.

Rabalais, N. N. 2002. Nitrogen in aquatic ecosystems. Ambio **31**:102-112.

Reebs, S. G. 2002. Plasticity of diel and circadian activity rhythms in fishes. Reviews in Fish Biology and Fisheries **12**:349-371.

Rester, J. K. 2011. SEAMAP Environmental and Biological Atlas of the Gulf of Mexico, 2008. Gulf States Marine Fisheries Commission, Ocean Springs, MS.

Rester, J. K. 2012. SEAMAP Environmental and Biological Atlas of the Gulf of Mexico, 2010. Gulf States Marine Fisheries Commission, Ocean Springs, MS.

Romero, I. C., G. Toro-Farmer, A.-R. Diercks, P. Schwing, F. Muller-Karger, S. Murawski, and D. J. Hollander. 2017. Large-scale deposition of weathered oil in the Gulf of Mexico following a deep-water oil spill. Environmental Pollution **228**:179-189.

Sagarese, S. R., M. V. Lauretta, and J. F. Walter. 2017. Progress towards a next-generation fisheries ecosystem model for the northern Gulf of Mexico. Ecological Modelling **345**:75-98.

Simmons, C. M., A. B. Collins, and R. Ruzicka. 2015. Distribution and diversity of coral habitat, fishes, and associated fisheries in US waters of the Gulf of Mexico. Pages 19-37 *in* S. A. Bortone, editor. Interrelationships between Corals and Fisheries. Crc Press-Taylor & Francis Group, Boca Raton.

Stramski, D. 2008. Corrigendum to "Relationships between the surface concentration of particulate organic carbon and optical properties in the eastern South Pacific and eastern Atlantic Oceans" published in Biogeosciences, 5, 171–201, 2008. Biogeosciences **5**:595-595.

Stramski, D., R. A. Reynolds, M. Babin, S. Kaczmarek, M. R. Lewis, R. Röttgers, A. Sciandra, M. Stramska, M. S. Twardowski, B. A. Franz, and H. Claustre. 2008. Relationships between the surface concentration of particulate organic carbon and optical properties in the eastern South Pacific and eastern Atlantic Oceans. Biogeosciences **5**:171-201.

Stuntz, W. E., C. E. Bryan, K. Savastano, R. S. Waller, and P. A. Thompson. 1983. SEAMAP Environmental and Biological Atlas of the Gulf of Mexico, 1982. Gulf States Marine Fisheries Commission, Ocean Springs, MS.

Vargo, G. A., C. A. Heila, K. A. Fanning, L. K. Dixon, M. B. Neely, K. Lester, D. Ault, S. Murasko, J. Havens, J. Walsh, and S. Bell. 2008. Nutrient availability in support of Karenia brevis blooms on the central West Florida Shelf: What keeps Karenia blooming? Continental Shelf Research **28**:73-98.

Werdell, P. J., B. A. Franz, S. W. Bailey, G. C. Feldman, E. Boss, V. E. Brando, M. Dowell, T. Hirata, S. J. Lavender, Z. P. Lee, H. Loisel, S. Maritorena, F. Melin, T. S. Moore, T. J. Smyth, D. Antoine, E. Devred, O. H. F. d'Andon, and A. Mangin. 2013. Generalized ocean color inversion model for retrieving marine inherent optical properties. Applied Optics **52**:2019-2037.

CHAPTER THREE:

SEAMAP SUMMER TRAWL SURVEY 2010-2012: SPATIAL AND ENVIRONMENTAL CONTROL OF GROUNDFISHES THROUGHOUT THE WEST FLORIDA SHELF

3.1 INTRODUCTION

The identification and description of patterns in biological systems is a longstanding challenge in ecology (Hutchinson 1953). Often, some level of attention must be paid to the spatial scale of the observation-universe, and it can be critical to the meaningful interpretation of observed biological responses (Borcard et al. 1992, Levin 1992, Leibold et al. 2004). Spatial considerations are problematic to marine fisheries management due to the ever-changing distributions of living marine resources, and the dynamic nature of the relationships that underlie mechanisms that apparently control their organization. In theory, one controlling factor could cede organizational power to another factor over time, and then subsequently regain dominance when the system conditions return to a favorable state (Holling 1973, Mollmann and Diekmann 2012).

When considering fisheries metacommunities (Leibold et al. 2004), proper consideration should be given to important factors associated with biological thresholds (e.g., temperature, salinity), habitat preferences (e.g., depth, bottom type), and spatial connectivity between populations, resources, and the environment. Nevertheless, spatial scales of inquiry are often singular in nature (e.g., large or small, local or regional), indirect, or absent altogether, implying

a disregard for the connectivity of processes across the multiple spatial scales that necessarily exist within any physical system (Leibold et al. 2004). For example, a fish species that prefers deep, cold, high-salinity water *and* high-relief, bottom structure may be more likely to aggregate in high densities on isolated, vertical, submarine structures than on protracted, shelf-edge walls (where populations may be more diffuse due to the increased habitable space in the appropriate depth zone). In this example, it would be important to consider any potential spatial distributions for adequate, high-relief structures, along with the distributions physical-chemical conditions among them, when examining any organizational preferences of this living marine resource.

Furthermore, many known fisheries-relevant abiotic factors exhibit large-scale, directional gradients [e.g., temperature (Locarnini et al. 2013), salinity (Zweng et al. 2013)], or may present with more dynamic patterns across a range of possible spatial extents [e.g., water currents (He and Weisberg 2003), nutrient fluxes (Weisberg et al. 2005, Garcia et al. 2014), habitat patchiness (Levin 1992)]. Finally, density-dependent biotic effects surrounding competition and predation, within and among species, can be prominent organizing forces of fish resources (Hixon and Carr 1997, Holbrook and Schmitt 2002). Given that the limitation of resources, habitat-type, or shelter are primarily expressed as functions of spatial availability (i.e., density), then ecological density-dependence is a spatial consideration, and the mechanisms that support it may exist at multiple, relevant scales.

3.1.1 West Florida Shelf Spatial Challenges

The West Florida Shelf (WFS) spans 170,000km^2, with its northern edge extending just above the 30th northern parallel, persisting south almost all the way to the 24th parallel (Bryant et al. 1991), and covering 6.5° of latitude (700 km) (Hine et al. 2008). Along its east-to-west axis, the

WFS reaches up to 240 km from the Florida shoreline, and exhibits a gently sloping, negative depth gradient (<1°) that terminates at the 200 meter isobath (Bryant et al. 1991, Okey et al. 2004, Hine et al. 2008) (Figure 3.1). Direct riverine and submarine groundwater inputs into the WFS are present along the entire latitudinal extent of the system, and are marked by large/medium-sized estuaries such as Pensacola Bay, Apalachicola Bay, Waccasassa Bay, Tampa Bay, Charlotte Bay, and Florida Bay (Kumpf et al. 1999, Hu et al. 2006, Conmy et al. 2009). Additionally, the WFS system is also indirectly influenced by the Mississippi, Atchafalaya, and Mobile River outflows to the northwest, as they, too, deliver large quantities of dissolved organic and inorganic particulates, freshwater, and other dissolved constituents to the seawater, all of which may potentially be advected onto the WFS via wind and currents (Kumpf et al. 1999, Del Castillo et al. 2001, Weisberg et al. 2005).

Accompanying the dynamic physical-chemical properties of the water mass above the WFS are complex patterns among the diversity of seabed morphologies and bottom types along the seafloor. The large platform that underlies the WFS was formed over time by shallow water carbonate upbuilding and the accumulation of evaporates (Bryant et al. 1991). The resultant present-day, topological features include low-relief formations parallel to coastlines, and which are associated with rising sea levels in the Gulf of Mexico following the Pleistocene glacial maximum (Locker et al. 1996, Kumpf et al. 1999, Hine et al. 2008, Hine and Locker 2011). Other sand-ridge features observed on the WFS are thought to be the result of more localized physical processes present in the inner shelf (Davis et al. 1993). Mesophotic reefs, paleoshorelines, sand ridges, and other high- and low-relief structures are distributed throughout the WFS (Bryant et al. 1991, Jarrett et al. 2005, Hine et al. 2008), and the remaining area of the platform consists

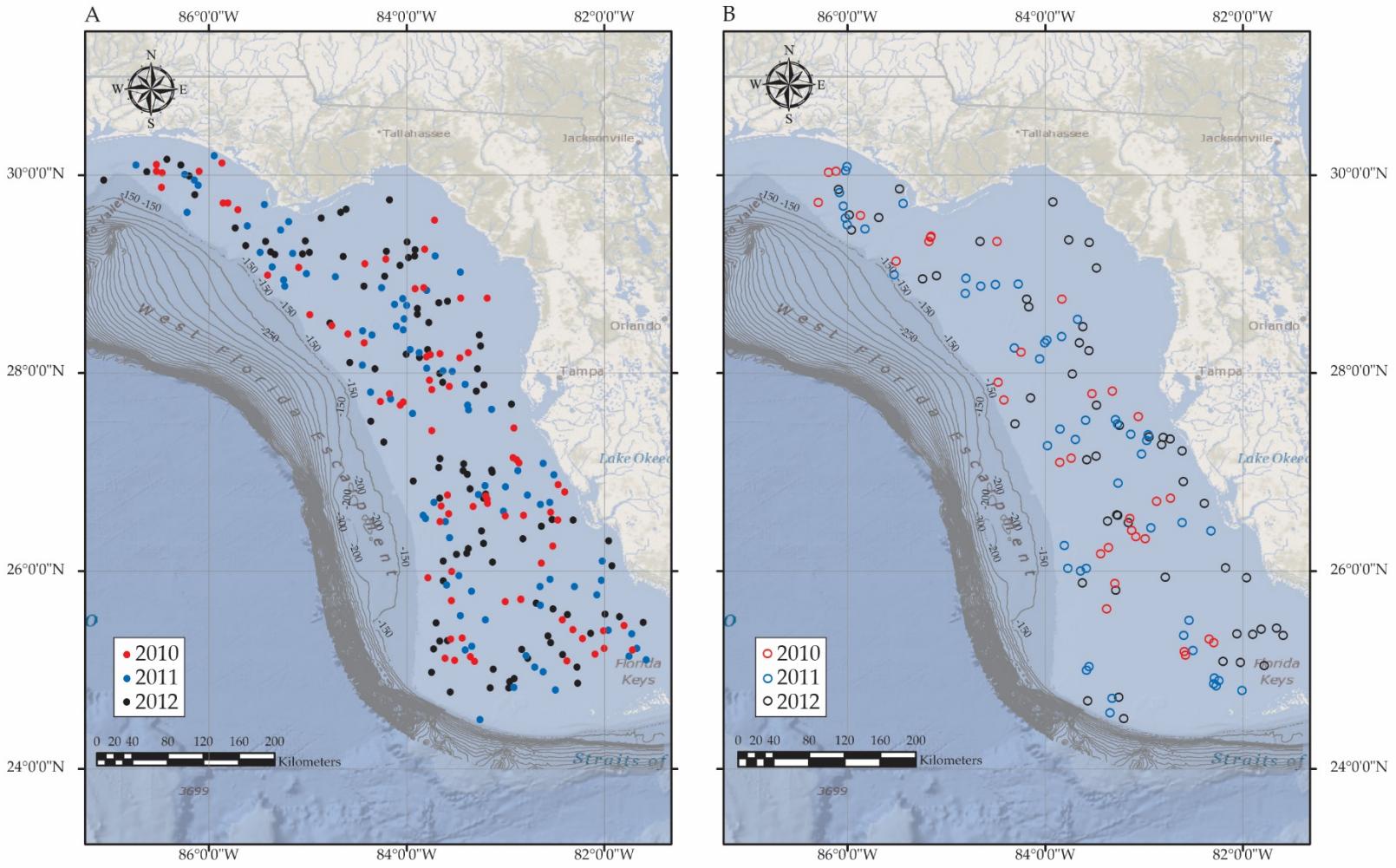

Figure 3.1 – West Florida Shelf SEAMAP sampling area. Map of the 2010-2012 SEAMAP summer groundfish survey sampling stations during daytime (A) and nighttime (B) fishing operations. Bathymetric contours are listed in meters (GEMS 2017).

mostly of silt, sand, clay, and mud (Bryant et al. 1991, Locker et al. 1999). Because the WFS resides within the euphotic zone (Okey et al. 2004), large amounts of seagrasses are also found in this environment (Okey and Mahmoudi 2002), and in general large portions of the WFS are appropriate for resource exploitation using trawl-net fishing gear (Juhl 1966).

3.1.2 West Florida Shelf Scales of Inquiry

Marine fisheries resources maintain complex life histories due to shifting biological requirements, abilities, and physical thresholds throughout their ontogenies (Helfman et al. 2009). As such, if any of those limiting factors are themselves organized by some unknown processes, then the challenge of disentangling potential cause-and-effect relationships between habitat preferences, stock strength, or resource distributions, and the dynamic physical-chemical environment, must also include relevant scales of inquiry in both the spatial and temporal dimensions. In Chapter Two, the temporal scales relevant to the WFS groundfish communities were examined with respect to diel- and annual-scale temporal patterns. Those study results support the temporal scales of inquiry that will be used in the following work, and are summarized as follows: (1) The WFS groundfish communities exhibited significant differences in both daytime versus nighttime species assemblages in all years; (2) Each year was statistically distinct and should be considered independently of one another with respect to the beta-diversity of fishes and the physical-chemical environment, regardless of time of day.

3.1.3 Study Objectives

The purpose of this study was to determine the extent of spatial control over the biological response in fishes sampled across the WFS by the Southeast Area Monitoring and Assessment Program (SEAMAP) during the summer groundfish surveys of 2010-2012. Attention was also

given to exposing potential physical-chemical mechanisms that may characterize any observed spatial organization of groundfish communities. By partitioning the explained variability of the biotic resources' response into spatially and non-spatially controlled portions, the relevant scales of inquiry may be elucidated for abiotic indices that are pertinent to commercially or recreationally important fishes.

Specifically, this work sought to: (1) Determine if there was any spatial control of the beta-diversity of groundfishes sampled on the WFS; (2) Describe the abiotic variables that contributed to the spatially structured portion of biotic variability; (3) Identify the non-spatially structured abiotic indicators that influenced the organization of beta-diversity; and (4) Make recommendations regarding appropriate scales of inquiry for WFS living marine resources, and any relevant factors to consider at those scales.

3.2 METHODS

3.2.1 Organization of Selected Data

Fisheries independent data were collected for SEAMAP during the 2010-2012 summer sampling seasons along the WFS (Figure 3.1). Data were extracted from the public-access SEAMAP database (seamap.gsfmc.org; accessed Feb. 2015), and details of the cruise and vessel identifiers, along with sampling dates, are listed in Table 2.1. As described in §2.2.1, for each sampling cruise, the biological census data were compiled into a *response* matrix, **Y**, and the set of variables representing the physical-chemical environment were assembled in an abiotic *predictor* matrix, **X**. An expansion of the traditional response-predictor framework was made to accommodate the spatial characteristics of the SEAMAP sampling universe, thus an additional *spatial-predictor* matrix (**S**) was included for analyses, and which contained the geographic

coordinates (decimal degrees) for each trawl sampling event's endpoint. For all z = {2010, 2011, 2012}, the N total observations contained in the matrices $\mathbf{Y}_z$, $\mathbf{X}_z$, and $\mathbf{S}_z$, were matched such that $\mathbf{Y}_z(n)$, $\mathbf{X}_z(n)$, and $\mathbf{S}_z(n)$ all contained information about the same spatiotemporal sampling event (n). Within each year, samples were stratified as daytime and nighttime events using the methods described in §2.2.2 utilizing the local nautical twilight period as a knife-edge criterion.

3.2.1.1 Non-spatial data. Non-spatial data consisted of the biotic and abiotic observations contained in $\mathbf{Y}_z$ and $\mathbf{X}_z$, for all z, respectively. Biotic response data in $\mathbf{Y}_z$ consisted of species composition and abundance for all vertebrate fish, identified to the species level, that were captured in each trawl sample (i.e., benthic and demersal fishes). These count data were standardized by the area trawled (km^2) for each sampling station, and only species present in at least 5% of all samples were retained for analyses. If any sample $\mathbf{Y}_z(n)$ was removed or missing, for any reason (e.g., incomplete sample due to net failure, no vertebrates collected), the corresponding sample was also removed from $\mathbf{X}_z$, and $\mathbf{S}_z$.

The abiotic predictor data in $\mathbf{X}_z$ were collected for each station at the end of the trawl fishing, or they were derived from satellite observations extracted from NASA archives, as detailed in §2.2.1. See Table 2.2 for a full list of predictor variables, descriptions, and units of measure. All $\mathbf{X}_z$ were stratified and organized to correspond with the daytime and nighttime groundfish survey observations in $\mathbf{Y}_z$ described above. For each stratification of $\mathbf{X}_z$, the data were standardized using a z-scores translation (Legendre and Legendre 2012).

3.2.1.2 Spatial data. The sampling events in any $\mathbf{Y}_z$ and $\mathbf{X}_z$ pair had a corresponding matrix, $\mathbf{S}_z$, containing the geographic coordinates for the endpoint of each trawl sample in year z. Prior to analysis, all polar coordinates reported in the SEAMAP database were converted from

decimal degrees to Universal Transverse Mercator (UTM) units ($\mathbf{W}_z$) in two-dimensional, Cartesian space (Legendre and Legendre 2012). Euclidean distance matrices ($\mathbf{EUC}_z$) for each $\mathbf{W}_z$ were decomposed into eigenvector maps using the principle coordinates of neighbor matrices (PCNM) technique (Borcard and Legendre 2002, Borcard et al. 2004) in conjunction with minimum spanning trees (MST; Rohlf 1973). This form of PCNM is a special case of the more general Moran's Eigenvector Maps (Dray et al. 2006, Dray et al. 2012), and so the matrices of spatial variables returned from this implementation will be referred to as **MEM**s hereafter.

PCNM enlists principle coordinates analysis (PCoA; Gower 1966) to decompose a truncated distance matrix, $\mathbf{D}_\Delta$, based on any set of two-dimensional coordinates (Borcard and Legendre 2002, Borcard et al. 2004). The matrix $\mathbf{D}_\Delta$ for any $\mathbf{W}_z$, was created by (A) calculating $\mathbf{EUC}_z$, (B) creating a MST for $\mathbf{EUC}_z$, (C) finding the length of the longest link in the MST solution and setting this value as the truncation distance, Δ, and (D) replacing all of the values along the diagonal of $\mathbf{EUC}_z$, and where $\geq \Delta$, with the value 4Δ (Borcard and Legendre 2002, Dray et al. 2006). The eigenvectors returned by the PCoA orthogonalization of $\mathbf{D}_\Delta$ were not scaled using the corresponding eigenvalues (Dray et al. 2006), and then only the positive eigenvectors ($\mathbf{MEM}^+_z$) were retained as for use as spatial variables in subsequent statistical analyses. The $\mathbf{MEM}^+_z$ were used to describe all observable spatial scales within the sampling universe (Figure 3.2), ranging from full sampling extent down to the truncation distance Δ (Borcard et al. 2004). It should be noted that the decomposition of spatial scales is directly related to the sampling effort for the set of observations (N), and fewer samples, no matter how widely dispersed, will result in fewer observable spatial scales to test against for relationships (Borcard and Legendre 2002).

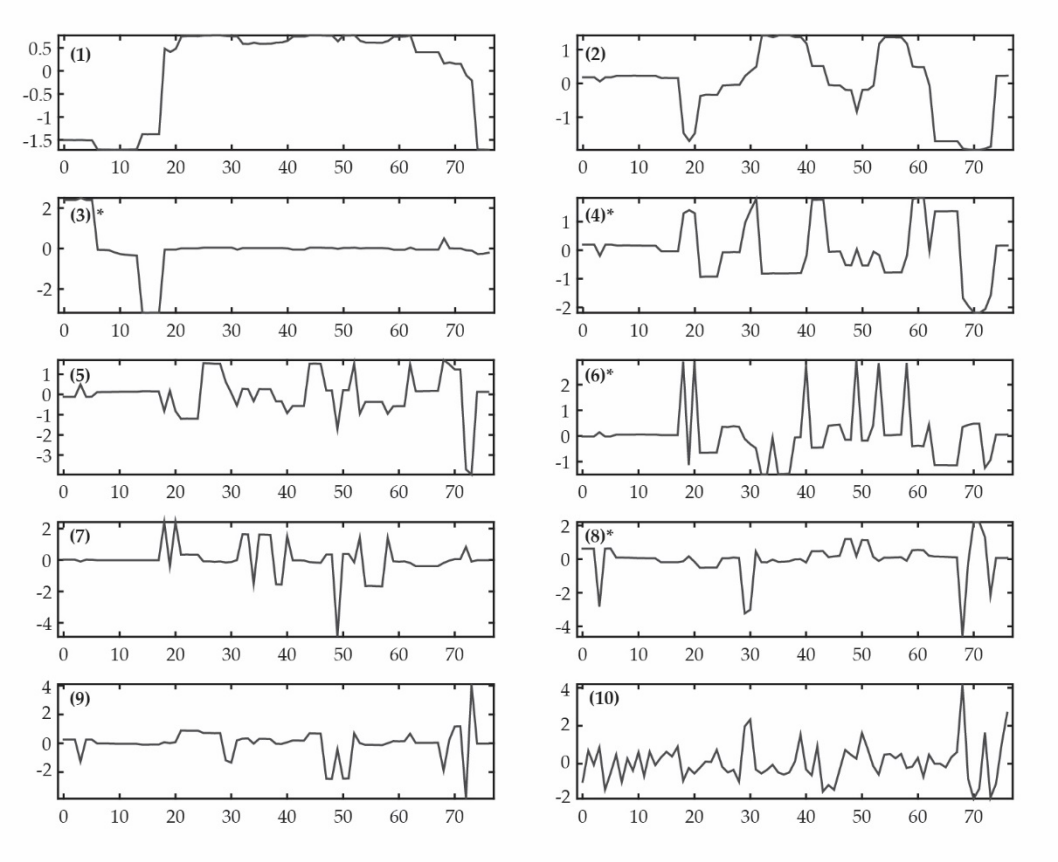

Figure 3.2 – A representative selection of positive spatial eigenfunctions. Line plots representing the spatial decomposition of the sampling universe defined via PCNM for the daytime summer SEAMAP trawl survey in 2010. The eigenfunction values along the ordinate axis are standardized to have mean of zero, and standard deviation of one. The abscissa represents station sampling order ($N = 77$). The parenthetical value corresponds with the spatial scale of the eigenvector, and as these values increase, the spatial scale represented by the **MEM**$^{+}$ decreases (**MEM**$^{+}_{[1]}$ >> **MEM**$^{+}_{[10]}$). Those **MEM**$^{+}$ that were forward-selected for the 2010 **MEM**$^{+}_{SEL}$ model are noted (*).

3.2.2 Statistical Analyses

3.2.2.1 Data pretreatment. All data organization, pretreatment, and statistical analyses were performed in MATLAB 2014b utilizing both the Fathom (Jones 2017) and Darkside (Kilborn 2017) toolboxes for MATLAB. All data tables were organized where rows corresponded with objects (trawl stations), and columns with descriptors (independent and dependent variables). Analyses were performed separately for each stratification of the light environment and the year

(i.e., 2010 was independent of 2011 and 2012, and 2010 daytime was independent of 2010 nighttime, etc.).

To select the best data transformation and dissimilarity metric for the response data, several options were considered (Appendix B, Table B.1), and the combination with the greatest, significant R^2_{adj} value was selected for each stratification of $\mathbf{Y}_z$ (Table 3.1). With the exception of the 2011 daytime samples, $\mathbf{Y}_z$ data were square-root transformed, in order to reduce the influence of overly abundant or rare species (Legendre and Legendre 2012). All zero-inflated, response data were subjected to the Morisita-Horn dissimilarity (Chao et al. 2005, 2006, Legendre and Legendre 2012) to determine resemblance among samples with respect to the groundfish species composition and abundance (i.e., beta-diversity).

Table 3.1 – SEAMAP summer groundfish trawl survey metadata for 2010-2012. Metadata for each SEAMAP summer trawl survey undertaken between the years 2010-2012, and divided into daytime and nighttime fishing operations. For each year, and subcategory, the number of samples (*N*), total species richness, raw data transformation, multivariate dissimilarity measure, number of positive spatial eigenvectors ($\mathbf{MEM}^+$) identified by PCNM, and number of eigenvectors retained for the optimal spatial model ($\mathbf{MEM}^+_{SEL}$) are listed. MorH = the Morisita-Horn dissimilarity, and **Y** = the raw species and composition and abundance data scaled to trawl area.

	Daytime			**Nighttime**		
	2010	*2011*	*2012*	*2010*	*2011*	*2012*
Trawl Samples (*N*)	77	82	99	31	50	51
Species Richness	80	76	79	102	116	112
Y Transformation	$\mathbf{Y}^{1/2}$	$\log_{10}(\mathbf{Y}+1)$	$\mathbf{Y}^{1/2}$	$\mathbf{Y}^{1/2}$	$\mathbf{Y}^{1/2}$	$\mathbf{Y}^{1/2}$
Dissimilarity	MorH	MorH	MorH	MorH	MorH	MorH
$\mathbf{MEM}^+$	10	10	13	3	3	4
$\mathbf{MEM}^+_{SEL}$	4	2	2	0	0	0

3.2.2.2 Hypothesis testing. All hypothesis tests were conducted using a redundancy analysis framework employing either distance-based (db-RDA; Legendre and Anderson (1999),

McArdle and Anderson (2001)) or classical canonical analysis (RDA, Rao (1964)). These one-way, constrained analyses are commonly used in ecology to account for linear influences of predictors (**X** or **W**) on an observed response (**Y**). They specifically seek to measure the amount of predictor variability that explains (or accounts for) the variation contained within the response data (Rao 1964, Legendre and Anderson 1999). The canonical coefficient of determination (R^2; Miller and Farr) was calculated, and its adjusted form (R^2_{adj}; Ezekiel 1930) was used as an unbiased estimator for the fraction of **Y**'s variation explained by **X** (or **W**) (Ohtani 2000). The pseudo *F*-statistic (McArdle and Anderson 2001) was used to assess the null hypothesis (H_o) of no explanatory power for a set of predictors with respect to a set of responses in db-RDA, and the traditional *F*-statistic (Miller 1975) was used for RDA. Statistical significance was determined via 1,000 permutations of the residuals (Anderson 2001, Manly 2006), and with *p*-value interpretations based on $\alpha = 0.05$.

3.2.2.3 Forward selection of variables. Due to the high number of both abiotic and spatial predictors utilized in this study, forward-selection techniques were employed along with redundancy analyses, as described by Blanchet et al. (2008), and referred hereafter as db-RDA$_{SW}$ or RDA$_{SW}$. To reduce type-I error rates, a global test for significance of the full model (e.g., db-RDA$_{Y|X}$) was assessed, and forward-selection procedures were only applied when the global model was significant (Blanchet et al. 2008). During forward selection, any potential new variable ($\mathbf{x}_i$), the one with the greatest *F*-statistic out of all marginal tests, was conditionally added to the parsimonious model (**Q**), and then retained if, (1) the *p*-value < α for the db-RDA of **Y** and $\mathbf{x}_i$ (db-RDA$_{Y|x_i|Q}$; where any previously selected variables in **Q** are used as a covariables), and (2) the R^2_{adj} for the new model of db-RDA$_{Y|Q}$ is ≤ R^2_{adj} for the global db-RDA$_{Y|X}$ test (Blanchet et al. 2008). By

adhering to these stopping rules, no variable that explains a negligible amount of the total variability in **Y** should be retained in the optimal model **Q**.

The db-RDA$_{SW}$ approach was used to reduce the sets of $\mathbf{MEM}^{+}$ and **X** to create the optimal models ($\mathbf{MEM}^{+}{}_{SEL}$ and $\mathbf{X}_{SEL}$, respectively) to account for any explained variation in SEAMAP biological trawl samples due to positive spatial autocorrelation ($\mathbf{MEM}^{+}$), or non-spatially structured abiotic predictors. Variable selection via RDA$_{SW}$ was used to create optimal subsets of abiotic predictors ($\mathbf{Q}^{I}$ and $\mathbf{Q}^{II}$) to explain the canonical axes I and II (respectively) for any $\mathbf{MEM}^{+}{}_{SEL}$.

3.2.2.4 Variation partitioning. Distance-based techniques, like db-RDA$_{Y|X}$ for example, utilize Gower's centered matrix **G**, that has the following advantageous properties: (1) it can be produced from any distance matrix, (2) it retains all of the variation contained in the pairwise resemblance matrix from which it was derived, and (3) that variation can be partitioned directly (Gower 1966, McArdle and Anderson 2001). Another desirable quality of the db-RDA approach is the ability to directly calculate Gower's residual matrix ($\mathbf{G}_{RES}$), associated with the unexplained variability in the solution, using only **G** and the "hat matrix", **H**, where $\mathbf{H} = \mathbf{X}(\mathbf{X'X})^{-1}\mathbf{X'}$ (McArdle and Anderson 2001). Exploiting these properties allowed for the retention of the unexplained portion of the variability after conducting db-RDA, to be used in further analyses (McArdle and Anderson 2001); this is essentially a distance-based extension of partial-RDA (Borcard et al. 1992, Legendre and Legendre 2012).

Spatial trends in **Y** that were larger than the sampling universe were explored and then removed by conducting db-RDA $_{Y|W}$ and retaining the detrended response data ($\mathbf{Y}_{DT} = \mathbf{G}_{RES}$) for analysis. Redundancy analyses related to $\mathbf{Y}_{DT}$, were used to explore the SEAMAP groundfish response with respect to (1) the spatial variability explained by $\mathbf{MEM}^{+}{}_{SEL}$, and (2) for the

remaining unexplained variability (i.e., the non-spatially explicit response). The spatially explicit variability explained by the solution to db-RDA$_{\mathbf{Y}_{DT}|\mathbf{MEM}^{+}_{SEL}}$ was also examined at the level of the first two canonical axes ($\mathbf{CA}^{I}$ & $\mathbf{CA}^{II}$), which together represent the greatest amount of explained variability of all of the solution's orthogonal axes.

After all optimal models were selected, variation partitioning (VPA; Borcard et al. 1992, Peres-Neto et al. 2006, Legendre 2008) was used to verify the manual, partial-RDA exercises described above. This technique decomposed the variation in response data, in this case $\mathbf{Y}_{DT}$, among multiple sets of predictors. Here, one set of predictors corresponded to either the $\mathbf{X}_{SEL}$ model, or $\mathbf{X}_{SEL}$ concatenated with the unique predictors in $\mathbf{Q}^{I}$ and $\mathbf{Q}^{II}$. This model matrix represented the hypothesized, relevant abiotic components to the biological response. The second set of predictors considered were the positive spatial eigenvectors that best described the biotic response, $\mathbf{MEM}^{+}_{SEL}$. By employing a series of partial-RDAs, the variability in $\mathbf{Y}_{DT}$ was reduced into the unique and combined fractions explained by the spatial- and non-spatial abiotic predictors considered. The results described the fractions of the explained variability where [a] = non-spatially structured abiotic, [b] = spatially structured abiotic, [c] = pure-spatial, and [d] = error fractions. Venn diagrams were then created to illustrate the varying levels of spatial and abiotic control over the biological response. This allowed for the comparison of the VPA results across years, and for direct interpretation of annual changes to explained variability.

3.3 RESULTS

Reconciling $\mathbf{Y}_{z}$, $\mathbf{X}_{z}$, and $\mathbf{W}_{z}$ for all z = {2010, 2011, 2012} produced a total of N = {108, 132, 150} trawl samples, respectively, during the summer SEAMAP surveys. After stratification by the ambient light environment, the average annual composition of trawls were such that

approximately 66% were collected during the daytime, and ~33% at night (Table 3.1). The mean species richness during daylight hours was 79 species, whereas the nighttime samples averaged 110 unique species; richness ranged from 22-40% higher for samples collected at night.

The PCNM for each $\mathbf{W}_z$ yielded no less than 10 spatial $\mathbf{MEM}^+$s for the daytime (max = 13), and no more than four for the nighttime samples (mode = 3) (Table 3.1). Preliminary db-RDA tests showed that for all *z*, daytime and nighttime beta-diversity was significantly related to the entire set of $\mathbf{MEM}^+_z$ spatial variables (Table 3.2). The daytime years' db-RDA results had median R^2_{adj} = 0.0771, nighttime years had a median R^2_{adj} = 0.1506, and, with the exception of the 2012 nighttime test, all years' R^2_{adj} were within 1σ of the mean (Table 3.2). These results indicated a linear spatial trend at a scale greater than the extent of the sampling universe, and the residuals ($\mathbf{G}_{RES}$) from each years' analysis were used as the linearly detrended data ($\mathbf{Y}_{DT}$) for all subsequent analyses (Legendre and Legendre 2012).

3.3.1 West Florida Shelf Daytime Sampling

3.3.1.1 Spatial eigenvector model selection. Forward selection via db-RDA$_{SW}$ for $\mathbf{MEM}^+$s successfully produced optimal spatial models to describe the variability in trawl sample beta-diversity (Table 3.3). In all three cases, the global tests revealed that the spatial eigenvectors accounted for at least 5.7% of the variability in any $\mathbf{Y}_{DT}$. In 2010, there were four significant $\mathbf{MEM}^+$s identified, whereas only two were selected for the remaining years in the study. The total variability in beta-diversity explained by $\mathbf{MEM}^+_{SEL}$ ranged from lows of R^2_{adj} = {0.0481, 0.0452} in 2011 and 2012, respectively, to a high value in 2010, where R^2_{adj} = 0.1048.

In 2010, the $\mathbf{MEM}^+_{SEL}$ model explained 10.48% (R^2_{adj}) of the total variability in the groundfish survey data. Ten percent of R^2 = 0.1519 was accounted for by $\mathbf{CA}^{I}_{2010}$ and 4% by $\mathbf{CA}^{II}_{2010}$,

while the remaining canonical axes accounted for < 1% of the total unadjusted, explained variability (Table 3.3). In 2011, $\mathbf{CA}^{I}_{2011}$ accounted for virtually all of the explained variability (6.2%), and in 2012, $\mathbf{CA}^{I}_{2012}$ and $\mathbf{CA}^{II}_{2012}$ described 4.0% and 2.5%, respectively. As in 2010, all remaining canonical axes for 2011 and 2012 were responsible for negligible amounts of explained variability and they were not considered further. After each db-RDA$_{SW}$ model run, the new $\mathbf{G}_{RES}$, containing the remaining unexplained variability, was retained for further analyses.

3.3.1.2 Spatially structured abiotic predictors. The $\mathbf{CA}^{I}$ and $\mathbf{CA}^{II}$ scores for each year's spatially-explicit, daytime model were used to determine which abiotic predictors might influence the spatially structured variability in groundfish beta-diversity. The residual results from this set of tests were also retained in $\mathbf{G}_{RES}$ matrices to assess which abiotic variables were independent of spatial control, yet were still influential to the observed organization of fishes. The 2011 RDA$_{SW}$ global tests for the both $\mathbf{CA}^{I}$ and $\mathbf{CA}^{II}$ against the standardized $\mathbf{X}$ were both statistically insignificant (Table 3.4) at the level of the global test, and therefore only 2010 and 2012 were subjected to forward selection of abiotic predictors against their canonical axes.

Four unique abiotic predictors were selected to describe the canonical axes in 2010 spatial model (station depth and temperature at maximum depth, surface salinity, and mixed layer depth), and five were chosen for 2012 (chlorophyll-a rate of change, maximum depth, mixed layer depth, and temperature at maximum depth and the surface) (Table 3.4). Approximately 40% of the explanatory power of $\mathbf{CA}^{I}_{2010}$ was described by the optimal abiotic model selected for that axis ($\mathbf{Q}^{I}_{2010}$), while 30% of $\mathbf{CA}^{II}_{2010}$ was explained by its corresponding $\mathbf{Q}^{II}_{2010}$. In 2012, only one abiotic variable was selected to model $\mathbf{CA}^{I}_{2012}$ (maximum depth), and its explanatory power was relatively weak (~3%), whereas 33% of $\mathbf{CA}^{II}_{2012}$ could be explained by $\mathbf{Q}^{II}_{2012}$.

Table 3.2 – Results for db-RDA of MEM⁺ against ΔY. Results of detrending the SEAMAP summer trawl fishing response data using the positive spatial eigenvectors (**MEM⁺**) identified via PCNM for 2010-2012 daytime and nighttime sampling. Permutation testing of the *F*-statistic was completed with 1,000 iterations, and *p*-value significance was determined using $\alpha = 0.05$. R^2 and R^2_{adj}, are the unadjusted and adjusted coefficients of determination, respectively. λ_{CA} are the canonical eigenvalues for axes I and II, where the value in parentheses corresponds with axis II. CA^I and CA^{II} represent the fractions of the total explained variance (CA_{all}) in the response described by canonical axes I and II, respectively, and ε represents the unexplained fraction.

									Fraction of Variance Explained		
	Year	Response	Predictor	*F*	*p*-value	R^2	R^2_{adj}	λ_{CA}	CA^I	CA^{II}	CA_{all}	ε
Daytime	2010	**ΔY**	**MEM⁺**	4.175	0.001	0.1014	0.0771	1.61 (0.69)	0.0709	0.0305	0.1014	0.8986
	2011	**ΔY**	**MEM⁺**	4.196	0.001	0.0960	0.0731	1.34 (0.36)	0.0757	0.0203	0.0960	0.9040
	2012	**ΔY**	**MEM⁺**	5.692	0.001	0.1060	0.0874	2.44 (0.89)	0.0778	0.0282	0.1060	0.8940
Nighttime	2010	**ΔY**	**MEM⁺**	4.171	0.001	0.2296	0.1745	0.82 (0.43)	0.1504	0.0791	0.2296	0.7704
	2011	**ΔY**	**MEM⁺**	5.345	0.001	0.1853	0.1506	1.47 (0.35)	0.1497	0.0356	0.1853	0.8147
	2012	**ΔY**	**MEM⁺**	2.129	0.045	0.0815	0.0432	0.57 (0.34)	0.0511	0.0304	0.0815	0.9185

Table 3.3 – Results from forward selection of MEM⁺ against $\mathbf{Y}_{DT}$ using db-RDA$_{SW}$. Comprehensive table of results for the stepwise, forward selection of positive spatial eigenvectors (**MEM⁺**) against the detrended biological response data ($\mathbf{Y}_{DT}$). *Global Tests* examine the full set of **MEM⁺**s against $\mathbf{Y}_{DT}$, and conditional testing is not permitted if the global test results are not deemed significant (1,000 permutations; $\alpha = 0.05$). *Conditional Test* results were tabulated, if deemed appropriate by global testing. Final models are based on adding the individual **MEM⁺**s one-by-one and measuring the partial db-RDA statistics (marked with δ) for the new model, as well as the cumulative adjusted coefficient of determination for the new model, $\Sigma(R^2_{adj})$. The final *Spatial Model* db-RDA results for the optimal model selected are also presented. All RDA table header information is the same as presented for Table 3.2.

Global Tests	Year	Response	Predictor	*F*	*p*-value	R^2	R^2_{adj}
Daytime	2010	$\mathbf{Y}_{DT}$	**MEM⁺**	1.893	0.002	0.2229	0.1052
	2011	$\mathbf{Y}_{DT}$	**MEM⁺**	1.529	0.007	0.1772	0.0613
	2012	$\mathbf{Y}_{DT}$	**MEM⁺**	1.457	0.007	0.1822	0.0571

Table 3.3 (Continued)

Global Tests		Year	Response	Predictor	F	p-value	R^2
Nighttime	2010	$\mathbf{Y}_{DT}$	$\mathbf{MEM}^{+}$	0.267	0.997	0.0288	-0.0792
	2011	$\mathbf{Y}_{DT}$	$\mathbf{MEM}^{+}$	1.471	0.132	0.0875	0.0280
	2012	$\mathbf{Y}_{DT}$	$\mathbf{MEM}^{+}$	1.285	0.206	0.1005	0.0223

Conditional Tests	Year	Response	Predictor	δF	p-value	δR^2	δR^2_{adj}	$\Sigma(R^2_{adj})$
Daytime	2010	$\mathbf{Y}_{DT}$	$\mathbf{MEM}^{+}_{3}$	3.921	0.001	0.0497	0.0370	0.0370
		"	$\mathbf{MEM}^{+}_{6}$	3.284	0.006	0.0404	0.0276	0.0655
		"	$\mathbf{MEM}^{+}_{4}$	2.790	0.014	0.0335	0.0206	0.0875
		"	$\mathbf{MEM}^{+}_{8}$	2.403	0.029	0.0283	0.0154	0.1048
	2011	$\mathbf{Y}_{DT}$	$\mathbf{MEM}^{+}_{7}$	3.622	0.001	0.0433	0.0313	0.0313
			$\mathbf{MEM}^{+}_{10}$	2.404	0.027	0.0283	0.0161	0.0481
	2012		$\mathbf{MEM}^{+}_{3}$	3.393	0.002	0.0338	0.0238	0.0238
			$\mathbf{MEM}^{+}_{9}$	3.170	0.005	0.0309	0.0209	0.0452

									Fraction of Variance Explained			
Spatial Models	Year	Response	Predictor	F	p-value	R^2	R^2_{adj}	λ_{CA}	CA^{I}	CA^{II}	CA_{all}	ε
Daytime	2010	$\mathbf{Y}_{DT}$	$\mathbf{MEM}^{+}_{[3, 4, 6, 8]}$	3.223	0.001	0.1519	0.1048	2.10 (0.84)	0.1030	0.0401	0.1519	0.8481
	2011	$\mathbf{Y}_{DT}$	$\mathbf{MEM}^{+}_{[7, 10]}$	3.045	0.001	0.0716	0.0481	0.99 (0.16)	0.0619	0.0097	0.0716	0.9284
	2012	$\mathbf{Y}_{DT}$	$\mathbf{MEM}^{+}_{[3, 9]}$	3.319	0.001	0.0647	0.0452	1.12 (0.69)	0.0400	0.0247	0.0647	0.9353

3.3.1.3 Non-spatially structured abiotic predictors. The unexplained variability remaining in the response after spatial analysis was examined using the db-RDA$_{SW}$ procedure against all **X**. The stepwise, forward-selection procedure identified parsimonious models ($\mathbf{X}_{SEL}$) for all three years in the study, indicating organizational control of groundfish beta-diversity by non-spatially structured abiotic predictors. The $\mathbf{X}_{SEL}$ models contained five, eight, and six unique predictors, for 2010, 2011, and 2012, respectively (Table 3.5). The explained variability was the lowest in 2010 (R^2_{adj} = 0.2396), peaked in 2011 (R^2_{adj} = 0.3231), and returned to the three-year mean in 2012 (R^2_{adj} = 0.2749).

3.3.1.4 Variation partitioning. The results of the daytime VPA tests were largely consistent with the detailed analyses for each set of detrended data, and their subsequent sets of residual data. Since no variables were selected to explain the $\mathbf{MEM}^{+}{}_{SEL}$ model in 2011, only 2010 and 2012 were tested in VPA using expanded subsets of **X** (i.e., [$\mathbf{Q}^{I}\mathbf{Q}^{II}\mathbf{X}_{SEL}$]), and the 2011 analysis was based only on $\mathbf{X}_{SEL}$. In all cases, fraction [a], which was associated with non-spatial, abiotic predictors, accounted for the greatest amount of explained variability in $\mathbf{Y}_{DT}$ (Figure 3.3). When [a] was considered together with fraction [b] (i.e., spatially-structured, abiotic predictors), all abiotic predictors selected in stepwise procedures explained up to 37.5% of the variability in beta-diversity in any year, and averaged 35.5% explained for the three years in the study (Appendix B, Table B.2). The pure-spatial component identified by VPA (i.e., fraction [c]) was only statistically significant in 2011 and 2012, and averaged only 1.7% explained, whereas fraction [b] accounted for ~3% in both years (Figure 3.3). The 2010 samples displayed the greatest spatial control over environmental predictors, with that year's [b] = 10.1%. The average unexplained variability for all $\mathbf{Y}_{DT}$ was ~63%.

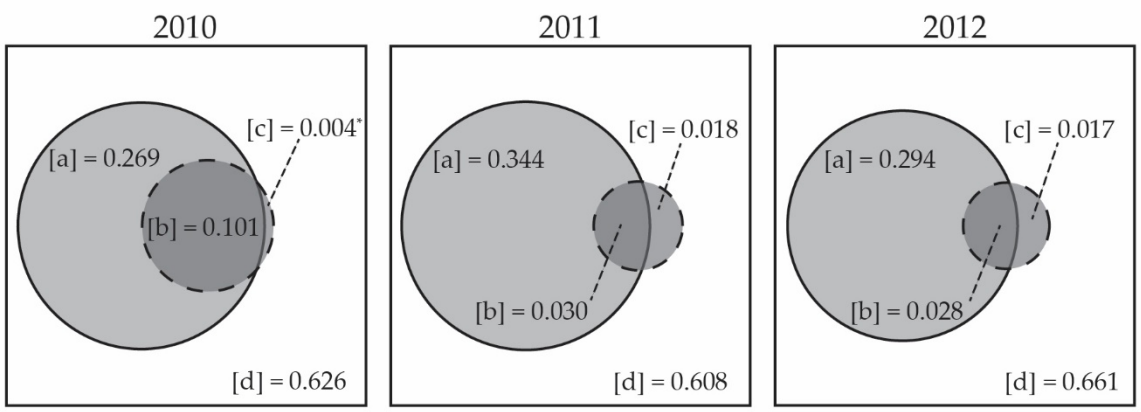

Figure 3.3 – Variation partitioning Venn diagrams. The results from the variation partitioning from the SEAMAP daytime trawl-surveys in the summers of 2010-2012 are presented as proportional Venn diagrams. Each square represents the total variation in the set of response data ($\mathbf{Y}_{DT}$), solid-lined circles represent the fractions of the total variation contributed by abiotic predictors ($\mathbf{X}_{SEL}$, $\mathbf{Q}^{I}$, and $\mathbf{Q}^{II}$) and dashed-lined circles are the spatial predictors ($\mathbf{MEM}^{+}{}_{SEL}$). The fractions illustrated are associated with the non-spatially ([a]) and spatially ([b]) structured predictors, as well as the pure-spatial component ([c]). Any remaining space within the square represents the unexplained fraction of the variation ([d]). Each fraction's area is scaled proportionally by the amount of the variation explained by predictor set. All values were determined to be statistically significant via permutation testing (1,000 iteration, $\alpha = 0.05$), except where otherwise noted (*).

3.3.2 West Florida Shelf Nighttime Sampling

3.3.2.1 Spatial eigenvectors and variation partitioning. Forward selection via db-RDA$_{SW}$ for $\mathbf{MEM}^{+}$s against each year's $\mathbf{Y}_{DT}$ was halted at the level of the global test, and therefore failed to produce optimal spatial models to describe the observed beta-diversity for any year's nighttime trawl samples (Table 3.3). The maximum R^2_{adj} for any year was in 2011 ($R^2_{adj} = 0.0280$), however none of the *F*-statistics were determined to be significant. Since no $\mathbf{MEM}^{+}$s were selected to explain any fraction of the variability in $\mathbf{Y}_{DT}$, there was no opportunity to identify any spatially structured abiotic predictors in the observed datasets from 2010-2012. In addition, the VPA procedure was rendered moot in the nighttime setting, as there were only two relevant datasets

to analyze – one of each, biological responses and abiotic predictors (non-spatial). Therefore, the relevant variation partitioning was undertaken via traditional db-RDA.

3.3.2.2 Non-spatially structured abiotic predictors. Using db-RDA$_{SW}$, the forward-selection procedure identified parsimonious $\mathbf{X}_{SEL}$ for all three years of nighttime trawl data (Table 3.6). The explained variability for any $\mathbf{X}_{SEL}$ was highest in 2010 and 2011, where the two-year mean $R^2_{adj} = 0.4617$, and was lowest in 2012 ($R^2_{adj} = 0.3787$). The increase in R^2_{adj} for the first two years in the study came with the cost of having almost three times as many explanatory predictors than were selected in 2012 (six, five, and two, respectively; see Table 3.6 for $\mathbf{X}_{SEL}$ details).

3.4 DISCUSSION

Recall that the purpose of this study was to review the 2010-2012 SEAMAP summer WFS groundfish trawl-survey data to discover and describe any spatial control of beta-diversity via predictors representing pure-spatial, or spatially organized, abiotic predictors. Additionally, this work attempted to identify which non-spatially structured, abiotic predictors were relevant to the organization of fishes along the WFS.

3.4.1 Spatial Control of Groundfishes on the WFS

The organization of groundfish communities along the WFS exhibited some degree of spatial control at multiple scales of inquiry. Relevant spatial scales ranged from greater than the sampling universe (Table 3.2), to sub-shelf extent, and presented with varying degrees of granularity (Figure 3.2). Furthermore, these spatial controls manifest differently from year to year, and from daytime to nighttime samples.

Table 3.4 – Results from forward selection of X against CA^{I} and CA^{II} using RDA$_{SW}$. Comprehensive table of results for the stepwise, forward selection of abiotic predictors (**X**) to describe canonical axes I and II (**CA^{I}** and **CA^{II}**, respectively) from the spatial models described in Table 3.3. The values in the square-bracketed subscripts denote the eigenvectors that make up the **MEM^{+}_{SEL}** model. The weighting factor in the conditional table describes the numerical weight for each selected variable in the optimal model retained along the listed axis. **Q^{I}** and **Q^{II}** represent the optimal, mixed-spatial models selected for each axis considered. All other table and header information are the same as presented in Table 3.2 and Table 3.3.

Global Tests	Year	Response	Predictor	F	p-value	R^2	R^2_{adj}
Daytime	2010	$\mathbf{CA}^{I}_{[3, 4, 6, 8]}$	**X**	3.595	0.001	0.5785	0.4176
		$\mathbf{CA}^{II}_{[3, 4, 6, 8]}$	"	2.928	0.002	0.5278	0.3475
	2011	$\mathbf{CA}^{I}_{[7, 10]}$	**X**	1.660	0.062	0.3674	0.1460
		$\mathbf{CA}^{II}_{[7, 10]}$	"	1.530	0.126	0.3488	0.1208
	2012	$\mathbf{CA}^{I}_{[3, 9]}$	**X**	2.189	0.012	0.3738	0.2030
		$\mathbf{CA}^{II}_{[3, 9]}$	"	3.490	0.001	0.4876	0.3479

Conditional Tests	Year	Response	Predictor	δF	p-value	δR^2	δR^2_{adj}	$\Sigma(R^2_{adj})$	Weight
Daytime	2010	$\mathbf{CA}^{I}_{[3, 4, 6, 8]}$	DEPTH_EMAX	20.704	0.001	0.2163	0.2059	0.2059	-0.0640
		"	TEMPMAX	6.832	0.008	0.0662	0.0538	0.2632	0.1786
		"	SALSURF	18.320	0.001	0.1439	0.1325	0.4029	-0.1472
		$\mathbf{CA}^{II}_{[3, 4, 6, 8]}$	SALSURF	22.004	0.002	0.2268	0.2165	0.2165	0.0626
		"	DEPTH_MXLD	9.875	0.002	0.0910	0.0789	0.2994	-0.0337
	2012	$\mathbf{CA}^{I}_{[3, 9]}$	CHLa_ROC	3.935	0.059	0.0390	0.0291	0.0291	0.0236
		$\mathbf{CA}^{II}_{[3, 9]}$	DEPTH_EMAX	22.048	0.001	0.1852	0.1768	0.1768	0.0686
		"	DEPTH_MXLD	12.532	0.002	0.0941	0.0847	0.2643	0.0075
		"	TEMPMAX	5.109	0.023	0.0368	0.0269	0.2945	0.0511
		"	TEMPSURF	6.148	0.012	0.0420	0.0322	0.3308	-0.0143

Table 3.4 (Continued)

Mixed-Spatial Models	Year	Response	Predictor	*F*	*p*-value	R^2	R^2_{adj}
Daytime	2010	$\mathbf{CA}^{I}_{[3, 4, 6, 8]}$	$\mathbf{Q}^{I}$	18.096	0.001	0.4265	0.4029
	2010	$\mathbf{CA}^{II}_{[3, 4, 6, 8]}$	$\mathbf{Q}^{II}$	17.242	0.001	0.3179	0.2994
	2012	$\mathbf{CA}^{I}_{[3, 9]}$	$\mathbf{Q}^{I}$	3.935	0.072	0.0390	0.0291
	2012	$\mathbf{CA}^{II}_{[3, 9]}$	$\mathbf{Q}^{II}$	13.111	0.001	0.3581	0.3308

Table 3.5 – Results from forward selection of X against daytime $\mathbf{G}_{RES}$, using db-RDA$_{SW}$. Comprehensive table of results for the stepwise, forward selection of abiotic predictors (**X**) against the residual Gower's centered matrix ($\mathbf{G}_{RES}$) retained after the db-RDA of the $\mathbf{MEM}^{+}_{SEL}$ spatial models, for the SEAMAP daytime, summer surveys. Each $\mathbf{X}_{SEL}$ represents the optimal, non-spatial, abiotic model selected for the corresponding set of biological response residuals considered. All other table and header information are the same as presented in Table 3.2 and Table 3.3.

Global Tests	Year	Response	Predictor	*F*	*p*-value	R^2	R^2_{adj}
Daytime	2010	$\mathbf{G}_{RES, [3, 4, 6, 8]}$	**X**	2.313	0.001	0.4689	0.2661
	2011	$\mathbf{G}_{RES, [7, 10]}$	**X**	2.874	0.001	0.5014	0.3269
	2012	$\mathbf{G}_{RES, [3, 9]}$	**X**	3.055	0.001	0.4545	0.3057

Conditional Tests	Year	Response	Predictor	δF	*p*-value	δR^2	δR^2_{adj}	$\Sigma(R^2_{adj})$
Daytime	2010	$\mathbf{G}_{RES, [3, 4, 6, 8]}$	DEPTH_EMAX	15.217	0.001	0.1687	0.1576	0.1576
		"	TEMPMAX	3.116	0.004	0.0336	0.0207	0.1807
		"	OXYMAX	3.412	0.001	0.0356	0.0228	0.2066
		"	CHLORMID	3.067	0.006	0.0311	0.0182	0.2284
		"	DEPTH_MXLD	2.061	0.047	0.0206	0.0076	0.2396
	2011	$\mathbf{G}_{RES, [7, 10]}$	DEPTH_EMAX	21.041	0.001	0.2082	0.1983	0.1983
		"	NPP	4.099	0.001	0.0391	0.0270	0.2282
		"	SALSURF	3.506	0.001	0.0324	0.0203	0.2520

Table 3.5 (Continued)

Conditional Tests	Year	Response	Predictor	δF	*p*-value	δR^2	δR^2_{adj}	$\Sigma(R^2_{adj})$
	2011	$\mathbf{G}_{RES, [7, 10]}$						
		"	TEMPMAX	2.585	0.010	0.0234	0.0112	0.2669
		"	TEMPMID	2.866	0.005	0.0253	0.0131	0.2842
		"	SALMID	2.548	0.007	0.0221	0.0098	0.2985
		"	DEPTH_MXLD	2.553	0.018	0.0217	0.0094	0.3127
		"	OXYMID	2.135	0.035	0.0178	0.0056	0.3231
	2012	$\mathbf{G}_{RES, [3, 9]}$	TEMPMAX	19.590	0.001	0.1680	0.1594	0.1594
		"	NPP	9.059	0.001	0.0717	0.0622	0.2239
		"	OXYMAX	2.513	0.008	0.0196	0.0095	0.2360
		"	ABS_GELB	2.789	0.004	0.0213	0.0113	0.2501
		"	SALMAX	2.576	0.012	0.0194	0.0093	0.2624
		"	SALMID	2.596	0.014	0.0192	0.0091	0.2749

									Fraction of Variance Explained			
Non-Spatial Models	Year	Response	Predictor	*F*	*p*-value	R^2	R^2_{adj}	λ_{CA}	CA^{I}	CA^{II}	CA_{all}	ε
Daytime	2010	$\mathbf{G}_{RES, [3, 4, 6, 8]}$	$\mathbf{X}_{SEL}$	5.790	0.001	0.2896	0.2396	3.36 (0.83)	0.1943	0.0481	0.2896	0.7104
	2011	$\mathbf{G}_{RES, [7, 10]}$	$\mathbf{X}_{SEL}$	5.833	0.001	0.3900	0.3231	3.22 (0.86)	0.2169	0.0575	0.3900	0.6100
	2012	$\mathbf{G}_{RES, [3, 9]}$	$\mathbf{X}_{SEL}$	7.192	0.001	0.3193	0.2749	4.82 (2.28)	0.1838	0.0869	0.3193	0.6807

Table 3.6 – Results from forward selection of X against nighttime $\mathbf{Y}_{DT}$ using db-RDA$_{sw}$. Comprehensive table of results for the stepwise, forward selection of abiotic predictors (**X**) against the detrended biological response data ($\mathbf{Y}_{DT}$) for the SEAMAP nighttime summer trawl surveys. Each $\mathbf{X}_{SEL}$ represents the optimal, non-spatial, abiotic model selected for the corresponding set of biological response data. All other table and header information are the same as presented in Table 3.2 and Table 3.3.

Global Tests	Year	Response	Predictor	F	p-value	R^2	R^2_{adj}
Nighttime	2010	$\mathbf{Y}_{DT}$	**X**	3.111	0.008	0.8789	0.5964
	2011	$\mathbf{Y}_{DT}$	**X**	3.019	0.001	0.6937	0.4639
	2012	$\mathbf{Y}_{DT}$	**X**	3.477	0.001	0.7157	0.5099

Conditional Tests	Year	Response	Predictor	δF	p-value	δR^2	δR^2_{adj}	$\Sigma(R^2_{adj})$
Nighttime	2010	$\mathbf{Y}_{DT}$	DEPTH_EMAX	10.816	0.001	0.2716	0.2465	0.2465
		"	PAR	3.235	0.011	0.0754	0.0436	0.3004
		"	CHLORMAX	2.979	0.015	0.0649	0.0326	0.3466
		"	SALMAX	3.264	0.013	0.0656	0.0334	0.3972
		"	TEMPSURF	2.859	0.021	0.0536	0.0210	0.4374
		"	CHLORMID	2.667	0.023	0.0469	0.0140	0.4726
	2011	$\mathbf{Y}_{DT}$	DEPTH_EMAX	19.520	0.001	0.2891	0.2743	0.2743
		"	SALSURF	4.938	0.003	0.0676	0.0482	0.3293
		"	TEMPMAX	6.988	0.001	0.0848	0.0658	0.4051
		"	SALMAX	3.180	0.015	0.0369	0.0168	0.4320
		"	POC	2.535	0.037	0.0284	0.0082	0.4508
	2012	$\mathbf{Y}_{DT}$	TEMPMAX	27.767	0.001	0.3617	0.3487	0.3487
		"	DEPTH_MXLD	3.366	0.012	0.0418	0.0223	0.3787

Table 3.6 (Continued)

									Fraction of Variance Explained			
Non-Spatial Models	Year	Response	Predictor	*F*	*p*-value	R^2	R^2_{adj}	λ_{CA}	CA^{I}	CA^{II}	CA_{all}	ε
Nighttime	2010	$\mathbf{Y}_{DT}$	$\mathbf{X}_{SEL}$	5.480	0.001	0.5781	0.4726	1.18 (0.56)	0.2824	0.1339	0.5781	0.4219
	2011	$\mathbf{Y}_{DT}$	$\mathbf{X}_{SEL}$	9.043	0.001	0.5068	0.4508	2.42 (1.18)	0.3011	0.1480	0.5068	0.4932
	2012	$\mathbf{Y}_{DT}$	$\mathbf{X}_{SEL}$	16.237	0.001	0.4035	0.3787	3.77 (0.34)	0.3704	0.0331	0.4035	0.5965

3.4.1.1 Pure-spatial control. During the detrending of the biological datasets with **MEM**$^{+}$s, it became apparent that there was large-scale spatial control of beta-diversity beyond the extent captured by the current SEAMAP sampling protocol. This makes sense, given that the WFS represents only a portion of the Gulf of Mexico's large marine ecosystem, and that the system has very dynamic physical-chemical properties that are influenced from beyond the shelf's spatial boundaries (He and Weisberg 2003, Weisberg et al. 2005). What was notable, however, was the fact that the daytime versus nighttime dichotomy was immediately present, even at scales larger than the sampling universe. Not only was the variability in the daytime and nighttime samples differentially explained by the pure-spatial variables, but the magnitude of explanatory power was less variable for daytime species than for those at night. Over the three years of the study, the explanatory power from the spatial effects acting at scales larger than the size of the sampling area for the daytime surveys ranged from 7.3-8.7%, and averaged ~8%.

Alternatively, for nighttime samples at this scale, the first two years of the study showed much greater pure-spatial control with R^2_{adj} = {17.5%, 15.1%}, and that control dropped precipitously to 4.3% in 2012. These results are consistent with those from Chapter Two, where nighttime groundfish assemblages were particularly susceptible to a large-scale event that perturbed the normal activity of these species in 2010 and 2011, and which then returned to a less chaotic state in 2012. If a disturbance scenario were assumed to be true, then it may be possible that the greater large-scale spatial control observed in 2010 and 2011 for nighttime groundfish communities was anomalous, and that the 2012 regime is indicative of a more normal spatial control paradigm.

Forward selection of **MEM**$^{+SEL}$ spatial models was successful only for the daytime samples. One explanation for this pattern may be the sparsity of samples collected during nighttime surveys, as they only account for about 1/3 of any year's *N*. While nighttime sampling did achieve complete spatial coverage on the WFS, the greater mean distances between nighttime samples than those for daytime samples (Figure 3.1) contributed to coarser spatial decompositions via PCNM, and to fewer **MEM**$^{+}$s for the nighttime surveys (Table 3.1). Due to the resolution deficiencies in the **MEM**$^{+}$s used to describe the SEAMAP nighttime sampling space, no spatial control of beta-diversity (pure- or spatial-abiotic) was detectable at sub-shelf scales for this unique assemblage of species.

All three daytime **MEM**$^{+SEL}$ models' VPA results indicated some degree of both pure-spatial and mixed-spatial abiotic control of the groundfish assemblages (Figure 3.3). The pure-spatial fraction of explained variability, [c], in the 2010 model was not only < 0.5%, but also statistically insignificant, and therefore it was considered random, thus leaving only mixed-spatial control of the beta-diversity to consider in that year. The mixed-spatial fraction was greater than that of the pure-spatial fraction in all three study years, and in 2011 and 2012, pure-spatial control never accounted for more than 1.8% of the explained variability in fishes. Based on this analysis, with the SEAMAP survey in its current form on the WFS, the pure-spatial fraction of the explained variation in groundfish beta-diversity either (1) cannot be described, or (2) has negligible effects.

3.4.1.2 Spatially structured abiotic predictors. The total fraction of the variability explained by pure- and mixed-spatial predictors was greatest in 2010, and was less than one-half of that maximum value in the two subsequent years. The 2010 mixed fraction, [b], accounted for

96% of all spatially-explained variability ([b] + [c]), and in 2011 and 2012, [b] contributed around 60% to the total spatial component (Figure 3.3). Unfortunately, the total spatially explained variability in beta-diversity for 2011 and 2012 averaged 4.7%, and to account for 60% of that (~2.8%) was not a great increase in understanding of the organizational dynamics for groundfishes on the WFS. On the other hand, in 2010, when 96% of all spatially-explained variability (10.5%) was accounted for by the mixed fraction, this represented a reasonable increase in knowledge of the influence of spatially structured abiotic predictors for that year.

Forward selection of abiotic predictors against the canonical axes via RDA_{SW} produced significant solutions for only 2010 and 2012 (Table 3.4). Recall that the $\mathbf{CA}^{I}_{2010}$ for 2010's $\mathbf{MEM}^{+}_{SEL}$ model explained twice as much variability as $\mathbf{CA}^{II}_{2010}$, and a similar pattern was displayed in the canonical axes of the 2012 solution. In both years, the spatially structured abiotic predictors selected were typically depth or temperature related. This came as no surprise given the spatial variability of the geology of the WFS, and the fact that the latitudinal extent of the shelf system is so large. The $\mathbf{CA}^{I}_{2012}$ axis was best explained by the rate of change of chlorophyll-a concentrations (30-day composite), but the corresponding $\mathbf{Q}^{I}_{2012}$ model was deemed insignificant ($p = 0.072$) and had a particularly low $R^2_{adj} = 0.0291$ (Table 3.4). Axis-II in 2012 was best explained by depths at the end of the trawl station and of the mixed layer (MXLD), and by temperatures at both maximum depth and the surface. However, the 2012 solutions are largely negligible in their explanatory power; for example, consider that the $\mathbf{Q}^{II}_{2012}$ model explains 33% of $\mathbf{CA}^{II}_{2012}$'s 2.5% fraction of the explained variability from the 2012 db-$RDA_{Ydt|MEM+SEL}$ solution. Thus, further interpretation will only be given to the 2010 solution, and the spatially-structured abiotic manifestations in that year.

In 2010, the total unadjusted explained variability (R^2) in beta-diversity was 15.2%; $\mathbf{CA}^{I}_{2010}$ accounted for ~10% of that, while $\mathbf{CA}^{II}_{2010}$ captured ~4%. The final $\mathbf{Q}^{I}_{2010}$ model explained ~40% of the original 10%, and the $\mathbf{Q}^{II}_{2010}$ model explained ~30% of $\mathbf{CA}^{II}_{2010}$'s corresponding 4%. The first canonical axis was best described by the sampling stations' depth, water temperature at the maximum depth, and the surface salinity. The second axis highlighted the spatial character of the MXLD during the time of sampling, and also implicated surface salinity as important (Table 3.4, Figure 3.4).

Salinity and depth gradients trended more saline and deeper as distance from shore increased, while temperature values tended to decline. Low-salinity stations were more likely to be inshore and relatively close to the same latitude as riverine inputs; however, a southerly, increasing gradient of surface salinity was detected along the outer-shelf stations, presumably resulting from increasing distance to the Mississippi River. Below ~27.5° of latitude, the depth profile of the WFS trends shallower, and these stations' salinity values remained relatively high with low temperatures, until just north of the Florida Keys. There, the freshwater discharge from the Everglades begins to become evident, and the very shallow maximum depths are more favorable for increased temperatures (Figure 3.4a).

The spatial dynamics of the MXLD and salinity are illustrated in Figure 3.4b, and the patterns in salinity are similar to those modeled for $\mathbf{CA}^{I}_{2010}$. Beginning at the northern end of the WFS, stations exhibited relatively low salinity values and deeper MXLD, then transitioned to higher salinity and shallower MXLD around 27.5°, and ultimately to deeper MXLD and lower salinity stations extending into the FL Keys. These trends may be explained by one or more of (1) the location of the Loop Current, (2) underwater morphology, or (3) something not considered.

3.4.2 Non-spatially Structured Abiotic Control of WFS Groundfishes

The results presented here indicate that, across all years, for both the daytime and at night, there was significant organizational control over groundfish beta-diversity on the WFS due to non-spatially structured, abiotic drivers. The amount of control and the predominant controlling predictors were variable at both diel and annual time scales. Over the three years studied, the average degree of control described by $\mathbf{X}_{SEL}$ was greater for nighttime assemblages (43.4%) than for daytime communities (27.9%), and the nighttime optimal models were slightly more parsimonious overall.

3.4.2.1 Daytime abiotic control. Interestingly, the majority of the explanatory power for any one year was typically dominated by one predictor – the maximum depth at the end of the trawl station (partial-R^2_{adj} = 16% and 20% in 2010 and 2011) or the temperature at that depth (16% in 2012) (Table 3.5). The median partial-R^2_{adj} for the remaining predictors in $\mathbf{X}_{SEL}$ was 2% in 2010 and 1% for both 2011 and 2012, with minimum values all < 1%, maximums < 6.2%, and altogether accounting for 7-10% of the explained biotic variability in any year. Also of note were, (1) the absence of the ending depth in $\mathbf{X}_{SEL}$ for 2012, (2) the presence of the MXLD as an important factor in only 2010 and 2011, and (3) at least one temperature and (4) one oxygen concentration factor was selected for all three years' $\mathbf{X}_{SEL}$. Other notable predictors included net primary production and salinity (2011 and 2012), chlorophyll-a concentration at mid water depth (2010) and the absorption of light due to gelbstoff (2012).

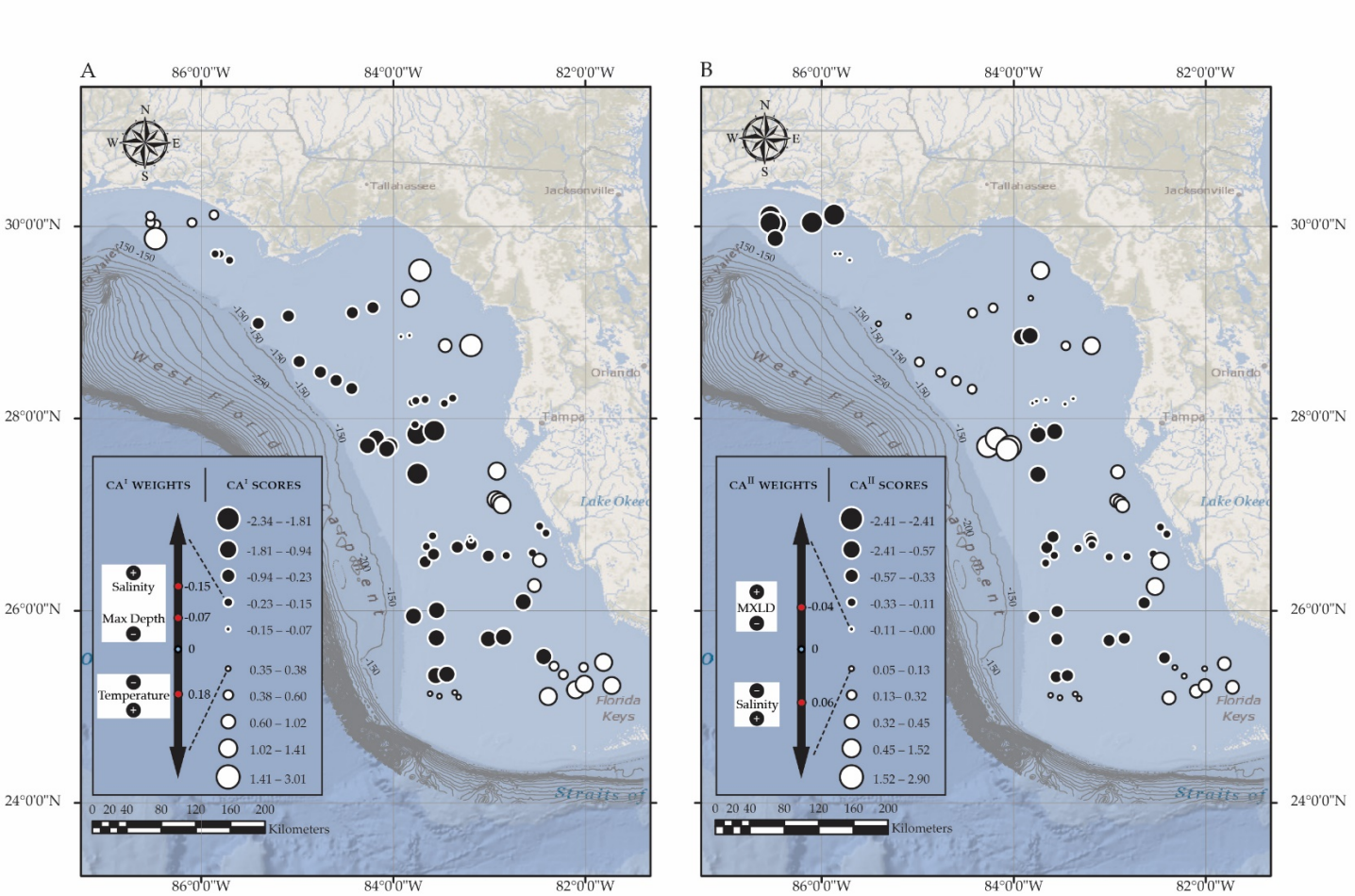

Figure 3.4 – Map of 2010 spatial model canonical axis scores with predictor weights. The 2010 spatial model results mapped for CA^{I} (A) and CA^{II} (B), where the circle sizes are proportional to the score on that axis, and color denotes positive (white) and negative (black) scores. Spatially structured abiotic predictors ($\mathbf{Q}^{I}_{2010}$ and $\mathbf{Q}^{II}_{2010}$, respectively), and their numerical weighting along each axis, are noted. The +/- signs at the top and bottom of the white boxes indicate which end of the scores gradient the boxed predictors have relatively elevated (+) or relatively depleted (-) absolute values. MXLD = mixed layer depth.

3.4.2.2 Nighttime abiotic control. Similar trends as were noted in the daytime samples were also observed in the nighttime trawls, whereby (1) a single predictor numerically dominated the model's explanatory power in each year, (2) that predictor was the maximum depth at the end of a trawl station in 2010 and 2011 (25% and 27%, respectively), (3) it switched to the temperature at that maximum depth in 2012 (35%), and (4) all three years' $\mathbf{X}_{SEL}$ models contained at least one water temperature factor (Table 3.6). Of the remaining predictors in 2010 and 2011, the partial-R^2_{adj} minimums were < 1.5%, the maximums were < 6.6%, the median was 3.3%, and altogether they accounted for an additional 14.5% and 14% of the observed response, respectively. The 2012 $\mathbf{X}_{SEL}$ model was the simplest, with only the MXLD adding any additional explanatory power to the model, albeit to a low degree (2.2%). Both models in 2010 and 2011 contained salinity and temperature factors, while each was primarily driven by maximum depth. The 2010 model was additionally characterized by chlorophyll-a concentrations and photosynthetically available radiation, whereas the 2011 model was better defined by adding consideration of the particulate organic carbon in the water.

3.5 CONCLUSION

3.5.1 Appropriate Scales of Inquiry for the WFS Biological Resources

The West Florida Shelf's benthic ecosystem is subject to spatial control for its groundfish resources and a portion of the abiotic variables that affect their organization. Control was identified at larger-than-shelf and sub-shelf scales, and within the WFS it ranged from relatively large to small scales, and was defined by the distances between sampling stations as a result of the survey design. Due to the relative sparsity of stations sampled under nighttime fishing conditions, it is unlikely that the current SEAMAP groundfish survey sampling design will be

able to capture any sub-shelf scale, spatial effects. This was not the case, however, when investigating larger-than-shelf scales.

Spatially structured organization of biological resources beyond the scale of the sampling universe was evident in both daytime and nighttime samples, but displayed interesting variability over time. The results in Chapter Two exposed a dynamic response in the nighttime groundfish communities that appeared to have been associated with a large-scale depositional event like an oil spill. The timing of the disturbance was coincident with that of the *Deepwater Horizon* oil spill that began in 2010, and the effects were shown to persist for approximately one year after the cessation of the spill (Chapter Two); however, the true nature of the observed patterns is still unknown. Here, a biological response was observed that was primarily affecting the nighttime assemblages, and which began in 2010, persisted through 2011, and declined significantly in 2012. Therefore, however inefficient the SEAMAP sampling survey design may be at detecting sub-shelf scale, spatial effects (particularly at night), the design is sufficient enough to capture effects from processes operating at very large spatial-scales beyond that of the WFS's full extent.

Only the daytime SEAMAP groundfish sampling design was sufficient for detecting sub-shelf scale, spatial dependence of the biological resources. However, there may be room to improve, since the only well-described effects of spatially-structured, abiotic predictors tended to fall into the already rigorously studied categories of depth, temperature, and salinity gradients on the WFS. Indeed, the influence of the mixed-layer depth and the rate of change of chlorophyll-a concentrations appeared in the modeled results, but not with enough significance or explanatory power to warrant excitement. While the patterns deduced from the interactions of

depth, salinity, and temperature described in 2010 provide an example of the power of **MEMs** to model complex spatial processes acting upon a large ecosystem's biological response, PCNM is limited by the sampling resolution, and less dominant patterns may be difficult to discern.

The sampling resolution issue is no small challenge, given the extreme cost and physical effort required to undertake a continuous sampling program such as SEAMAP. The benefits might outweigh the cost, however. As illustrated in Figure 3.3, the pure-spatial component was not adequately captured in any of the modeling exercises. The likely reason is that the fraction of the variability, in ecological terms, would be equivalent to that which is the result of density-dependent species interactions (i.e., competition, predation), and more specifically, positive spatial autocorrelation. Finer sampling resolution may help to elucidate intra- or interspecies behavioral dynamics that may otherwise be undetected.

3.5.2 Recommendations and Future Directions

The purpose of the SEAMAP groundfish survey is to provide fisheries-independent data to aid the description of the abundance and distribution of stocks in the Gulf of Mexico (Stuntz et al. 1983). Chapter Two highlighted the facts that this sampling effort annually surveys two different species assemblages (i.e., daytime and nighttime), both with the potential to rapidly reorganize due to external pressures. Here, the abilities of the program to capture both pure- and mixed-spatial control over those same resources is elucidated.

It is clear that the daytime SEAMAP survey design is adequate to capture mixed-spatial effects of well-known abiotic gradients in the Gulf, particularly depth, temperature, and salinity. These factors, if not the explicit focus of any study effort, should be controlled for as covariates in numerical models. In order to capture lesser-known mixed-spatial effects, an increase in

sampling resolution is required. Furthermore, the failure of the daytime 2011 spatial model bolsters the point that, even for known mixed-spatial effects, the current sampling resolution may still be inadequate in some cases.

Because of the inability of the nighttime survey to capture sub-shelf scale spatial effects, additional sampling effort for this portion of the survey would improve its ability to detect trends. Two-thirds of the current sampling effort favors the daytime sampling, likely due to the length of daylight hours and increased handling time of trawls at night, and the result is loss of power to detect any spatial organization of the nighttime resources. One potential solution could be to shorten the standard trawl time for each station. The effects of this would be twofold; it would (1) immediately increase the resolution of the survey and potentially reduce handling time of catches, and (2) reduce the potential for trawling through multiple habitat types (e.g., seagrass, sand, sponge) within a single station.

The work presented here illustrates the capacity for differential responses in the two species assemblages surveyed by SEAMAP, as well as the potential importance of studying the nighttime community in earnest. The actual details of the biological responses, whose drivers were discussed here, were omitted from this study. In part, this is due to the extensive attention given to the organizing forces and the effects of space, but it is also because a more focused approach would be preferential. As briefly mentioned above, to determine the fine-scale control of species organizational patterns, even within the current sampling protocols, careful statistical consideration must be given to the covariates of space, depth, temperature, and salinity. Finally, additional focus on the negative spatial eigenvectors resultant from PCNM may be warranted in this context. These spatial components can be used to model the negative spatial autocorrelation

among response variables, and could elucidate other density dependent effects such as avoidance.

In general, the SEAMAP summer groundfish survey program is a successful implementation of a fisheries-independent monitoring program. The concurrent abiotic sampling is very informative, and together with the biological samples, the volume and quality of biotic and abiotic data produced are exceptional and valuable. Augmentation of these datasets by adding remote-sensed satellite data adds to the utility of the program, and allows for a larger array of questions that could be explored with the outputs of this sampling effort

3.6 LITERATURE CITED

Anderson, M. J. 2001. Permutation tests for univariate or multivariate analysis of variance and regression. Canadian journal of fisheries and aquatic sciences **58**:626-639.

Blanchet, F. G., P. Legendre, and D. Borcard. 2008. Forward selection of explanatory variables. Ecology **89**:2623-2632.

Borcard, D., and P. Legendre. 2002. All-scale spatial analysis of ecological data by means of principal coordinates of neighbour matrices. Ecological Modelling **153**:51-68.

Borcard, D., P. Legendre, C. Avois-Jacquet, and H. Tuomisto. 2004. Dissecting the spatial structure of ecological data at multiple scales. Ecology **85**:1826-1832.

Borcard, D., P. Legendre, and P. Drapeau. 1992. Partialling out the spatial component of ecological variation. Ecology **73**:1045-1055.

Bryant, W. R., J. Lugo, C. Cordova, and A. Salvador. 1991. Physiography and bathymetry. The Gulf of Mexico Basin: Boulder, Geological Society of America, Decade of North American Geology, v. J:13-30.

Chao, A., R. L. Chazdon, R. K. Colwell, and T. J. Shen. 2005. A new statistical approach for assessing similarity of species composition with incidence and abundance data. Ecology Letters **8**:148-159.

Chao, A., R. L. Chazdon, R. K. Colwell, and T. J. Shen. 2006. Abundance-based similarity indices and their estimation when there are unseen species in samples. Biometrics **62**:361-371.

Conmy, R. N., P. G. Coble, J. P. Cannizzaro, and C. A. Heil. 2009. Influence of extreme storm events on West Florida Shelf CDOM distributions. Journal of Geophysical Research-Biogeosciences **114**:17.

Davis, R. A., J. Klay, and P. Jewell. 1993. Sedimentology and Stratigraphy of Tidal Sand Ridges Southwest Florida Inner Shelf. Journal of Sedimentary Petrology **63**:91-104.

Del Castillo, C. E., P. G. Coble, R. N. Conmy, F. E. Muller-Karger, L. Vanderbloemen, and G. A. Vargo. 2001. Multispectral in situ measurements of organic matter and chlorophyll fluorescence in seawater: Documenting the intrusion of the Mississippi River plume in the West Florida Shelf. Limnology and Oceanography **46**:1836-1843.

Dray, S., P. Legendre, and P. R. Peres-Neto. 2006. Spatial modelling: a comprehensive framework for principal coordinate analysis of neighbour matrices (PCNM). Ecological Modelling **196**:483-493.

Dray, S., R. Pelissier, P. Couteron, M. J. Fortin, P. Legendre, P. R. Peres-Neto, E. Bellier, R. Bivand, F. G. Blanchet, M. De Caceres, A. B. Dufour, E. Heegaard, T. Jombart, F. Munoz, J. Oksanen, J. Thioulouse, and H. H. Wagner. 2012. Community ecology in the age of multivariate multiscale spatial analysis. Ecological Monographs **82**:257-275.

Ezekiel, M. 1930. Methods of Ccorrelation Analysis. John Wiley and Sons, New York.

Garcia, H., R. Locarnini, T. Boyer, J. Antonov, O. Baranova, M. Zweng, J. Reagan, and D. Johnson. 2014. World Ocean Atlas 2013, Volume 4: Dissolved Inorganic Nutrients (Phosphate, Nitrate, Silicate), S. Levitus, Ed., A. Moshonov, Technical Ed.; NOAA Atlas NESDIS, vol. 76, 25 pp.

GEMS. 2017. Bathymetry Contours for West Florida Shelf with 50m divisions. Texas Sea Grant College Program, Texas A & M University, Geoscience Earth & Marine Services, Inc.

Gower, J. C. 1966. Some distance properties of latent root and vector methods used in multivariate analysis. Biometrika **53**:325-338.

He, R. Y., and R. H. Weisberg. 2003. A loop current intrusion case study on the West Florida shelf. Journal of Physical Oceanography **33**:465-477.

Helfman, G. S., B. B. Collette, D. E. Facey, and B. W. Bowen. 2009. The diversity of fishes : biology, evolution, and ecology. 2nd edition. Blackwell, Chichester, UK ; Hoboken, NJ.

Hine, A., and S. Locker. 2011. The Florida Gulf of Mexico Continental Shelf – Great Contrasts and Significant Transitions. The Gulf of Mexico: Origin, Water, and Biotia, Geology, Texas A&M University Press **3**:101-127.

Hine, A. C., R. B. Halley, S. D. Locker, B. D. Jarrett, W. C. Jaap, D. J. Mallinson, K. T. Ciembronowicz, N. B. Ogden, B. T. Donahue, and D. F. Naar. 2008. Coral reefs, present and past, on the west Florida shelf and platform margin. Coral Reefs of the USA:127-173.

Hixon, M. A., and M. H. Carr. 1997. Synergistic predation, density dependence, and population regulation in marine fish. Science **277**:946-949.

Holbrook, S. J., and R. J. Schmitt. 2002. Competition for shelter space causes density-dependent predation mortality in damselfishes. Ecology **83**:2855-2868.

Holling, C. S. 1973. Resilience and stability of ecological systems. Annual Rev Ecol Syst **4**:1-23.

Hu, C. M., F. E. Muller-Karger, and P. W. Swarzenski. 2006. Hurricanes, submarine groundwater discharge, and Florida's red tides. Geophysical Research Letters **33**:5.

Hutchinson, G. E. 1953. The concept of pattern in ecology. Proc Acad Nat Sci Philadelphia **105**:1-12.

Jarrett, B. D., A. C. Hine, R. B. Halley, D. F. Naar, S. D. Locker, A. C. Neumann, D. Twichell, C. Hu, B. T. Donahue, W. C. Jaap, D. Palandro, and K. Ciembronowicz. 2005. Strange bedfellows - a deep-water hermatypic coral reef superimposed on a drowned barrier island; southern Pulley Ridge, SW Florida platform margin. Marine Geology **214**:295-307.

Jones, D. L. 2017. The Fathom Toolbox for MATLAB. University of South Florida, College of Marine Science, St. Petersburg, FL.

Juhl, R. 1966. Experimental fish trawling survey along the Florida west coast. Commercial Fisheries Revue **28**:1-5.

Kilborn, J. P. 2017. The Darkside Toolbox for Matlab. University of South Florida, College of Marine Science, St. Petersburg, FL.

Kumpf, H., K. A. Steidinger, and K. Sherman. 1999. The Gulf of Mexico large marine ecosystem : assessment, sustainability, and management. Blackwell Science, Malden, Mass., USA.

Legendre, P. 2008. Studying beta diversity: ecological variation partitioning by multiple regression and canonical analysis. Journal of Plant Ecology **1**:3-8.

Legendre, P., and M. J. Anderson. 1999. Distance-based redundancy analysis: Testing multispecies responses in multifactorial ecological experiments. Ecological Monographs **69**:1-24.

Legendre, P., and L. Legendre. 2012. Numerical Ecology. Third English edition edition. Elsevier, Amsterdam, The Netherlands.

Leibold, M. A., M. Holyoak, N. Mouquet, P. Amarasekare, J. M. Chase, M. F. Hoopes, R. D. Holt, J. B. Shurin, R. Law, D. Tilman, M. Loreau, and A. Gonzalez. 2004. The metacommunity concept: a framework for multi-scale community ecology. Ecology Letters **7**:601-613.

Levin, S. A. 1992. The Problem of Pattern and Scale in Ecology. Ecology **73**:1943-1967.

Locarnini, R., A. Mishonov, J. Antonov, T. Boyer, H. Garcia, O. Baranova, M. Zweng, C. Paver, J. Reagan, D. Johnson, M. Hamilton, and D. Seidov. 2013. World Ocean Atlas 2013, Volume 1: Temperature. S. Levitus, Ed., A. Moshonov, Technical Ed.; NOAA Atlas NESDIS 73, 40 pp.

Locker, S. D., L. J. Doyle, T. T. Logue, and P. B. County. 1999. Surface Sediments of the NW Florida Inner Continental Shelf: A Review of Previous Results, Assessment and Recommendations. Pages 49-62 *in* Physical/Biological Oceanographic Integration Workshop for the.

Locker, S. D., A. C. Hine, L. P. Tedesco, and E. A. Shinn. 1996. Magnitude and timing of episodic sea-level rise during the last deglaciation. Geology **24**:827-830.

Manly, B. F. 2006. Randomization, bootstrap and Monte Carlo methods in biology. Chapman & Hall/CRC Press, Boca Raton.

Matlab. R2014. The MathWorks, Inc., Natick, Massachusetts, United States.

McArdle, B. H., and M. J. Anderson. 2001. Fitting multivariate models to community data: A comment on distance-based redundancy analysis. Ecology **82**:290-297.

Miller, J. K. 1975. The sampling distribution and a test for the significance of the bimultivariate redundancy statistic: a Monte Carlo study. Multivariate Behavioral Research **10**:233-244.

Miller, J. K., and S. D. Farr. 1971. Bimultivariate redundancy: a comprehensive measure of interbattery relationship. Multivariate Behavioral Research **6**:313-324.

Mollmann, C., and R. Diekmann. 2012. Marine ecosystem regime shifts induced by climate and overfishing: a review for the northern hemisphere. Pages 303-347 *in* G. Woodward, U. Jacob, and E. J. Ogorman, editors. Advances in Ecological Research, Vol 47: Global Change in Multispecies Systems, Pt 2. Elsevier Academic Press Inc, San Diego.

Ohtani, K. 2000. Bootstrapping R-2 and adjusted R-2 in regression analysis. Economic Modelling **17**:473-483.

Okey, T. A., and B. A. Mahmoudi. 2002. An Ecosystem Model of the West Florida Shelf for use in Fisheries Management and Ecological Research: Vol II. Model Construction. Pages 1-154. Florida Marine Research Institute, St. Petersburg, Florida.

Okey, T. A., G. A. Vargo, S. Mackinson, M. Vasconcellos, B. Mahmoudi, and C. A. Meyer. 2004. Simulating community effects of sea floor shading by plankton blooms over the West Florida Shelf. Ecological Modelling **172**:339-359.

Peres-Neto, P. R., P. Legendre, S. Dray, and D. Borcard. 2006. Variation partitioning of species data matrices: Estimation and comparison of fractions. Ecology **87**:2614-2625.

Rao, C. R. 1964. The use and interpretation of principal component analysis in applied research. Sankhyā: The Indian Journal of Statistics, Series A:329-358.

Rohlf, F. J. 1973. Hierarchical clustering using minimum spanning tree. The Computer Journal **16**:93-95.

Stuntz, W. E., C. E. Bryan, K. Savastano, R. S. Waller, and P. A. Thompson. 1983. SEAMAP Environmental and Biological Atlas of the Gulf of Mexico, 1982. Gulf States Marine Fisheries Commission, Ocean Springs, MS.

Weisberg, R. H., R. He, Y. Liu, and J. I. Virmani. 2005. West Florida shelf circulation on synoptic, seasonal, and interannual time scales. Circulation in the Gulf of Mexico: Observations and models:325-347.

Zweng, M., J. Reagan, J. Antonov, R. Locarnini, A. Mishonov, T. Boyer, H. Garcia, O. Baranova, D. Johnson, D. Seidov, and M. Biddle. 2013. World Ocean Atlas 2013, Volume 2: Salinity. S. Levitus, Ed., A. Moshonov, Technical Ed.; NOAA Atlas NESDIS 74, 39 pp.

CHAPTER FOUR:

RESEMBLANCE PROFILES AS CLUSTERING DECISION CRITERIA: ESTIMATING STATISTICAL POWER, ERROR, AND CORRESPONDENCE FOR A HYPOTHESIS TEST FOR MULTIVARIATE STRUCTURE

4.1 COPYRIGHT CLEARANCE

Appendix C: *Resemblance profiles as clustering decision criteria: Estimating statistical power, error, and correspondence for a hypothesis test for multivariate structure*, presents work previously published in the journal *Ecology and Evolution*, published by John Wiley & Sons, Ltd. DOI: 10.1002/ece3.2760 (http://onlinelibrary.wiley.com/doi/10.1002/ece3.2760/epdf). A complete reprint is provided with the authors' permission in Appendix C. © 2017 JP Kilborn; Jones, DL; Peebles, EB; Naar, DF.

4.2 RESEARCH OVERVIEW

The original work in Appendix C represents a data-simulation study to test the performance capabilities of clustering multivariate datasets using resemblance profiles as decision criteria. This new clustering technique was developed upon sound logical statistical principles, and has gained popularity in recent years, but was untested from a rigorous data-simulation standpoint. By simulating data with known structural properties such as (1) the probability distribution of the underlying data, (2) the number of groups, (3) the amount of group overlap in multivariate space, (4) the within group dispersions, and (5) the within group

correlation structures among descriptors, we were able to develop a set of guidelines for researchers to consider. These recommendations emphasize the following points: (1) In the presence of high group overlap, these clustering techniques may be unreliable; (2) Medium-to-high correlation structures among descriptors should be avoided and, therefore, clustering multispecies composition and abundance data may be difficult to interpret; (3) Multivariate datasets subjected to these clustering techniques should contain at least 25 descriptors for maximum efficiency; and (4) Slightly less reliable, but still acceptable, clustering results may be achieved using a minimum of 10 descriptors.

4.3 AUTHOR CONTRIBUTIONS

All authors contributed equally to the conception of this work. The numerical data simulation scenarios were designed by JPK and DLJ. Simulated data were produced by JPK using MATLAB code developed by both JPK and DLJ. JPK analyzed the data and all authors discussed the results and their implications. JPK wrote the manuscript and compiled all tables, figures, and supplemental information. All authors commented on the manuscript throughout the preparation process.

CHAPTER FIVE:

EVIDENCE FOR THE INFLUENCE OF BASIN-SCALE CLIMATE DYNAMICS AND FLUCTUATING FISHING INTENSITY ON THE ECOSYSTEM-LEVEL ORGANIZATION OF GULF OF MEXICO FISHERIES RESOURCES

5.1 INTRODUCTION

5.1.1 Marine Fisheries Ecosystem Management

Ecosystem-based fisheries management (EBFM) is a flexible process that considers the associations among species inhabiting an ecosystem, and their responses to the diverse suite of varying environmental and anthropogenic influences that limit and control their populations. An invigorated focus by government and regulatory agencies on this type of management process has exposed the underlying complexity of the issue of implementation. While the overarching tenets of ecosystem based management (EBM) advocate a more holistic approach, EBFM lacked formal definitions for objectives, reference points, and methodologies (Larkin 1996, Leggett and Frank 2008). Initially, EBFM in marine systems was defined as a set of three essential goals: (1) sustainable yield of products for human consumption and animal foods, (2) maintenance of biodiversity, and (3) protection from the effects of pollution and habitat degradation (Larkin 1996). The Ecological Society of America viewed EBM in broader terms, and while sustainability and biodiversity were still among their goals, they advocated for inclusion of: (1) measurable goals to achieve sustainability, (2) ecological models to improve understanding of the system, (3)

an emphasis on connectivity among constituents of the ecosystem, (4) recognition of the dynamic nature of the system, (5) a consideration of context and scale when applying management needs to a specific system, (6) humans as components of the ecosystem, (7) adaptability over time in management efforts, and (8) accountability to ensure progress (Christensen et al. 1996).

In U.S. fisheries, the incorporation of EBFM into the decision-making process is strongly advocated, with the aim of improving the ability to protect, restore, and sustain living marine resources, while balancing the competing interests of multiple stakeholders (Link 2016). Since the emergence of this working definition for EBFM, the focus for researchers, managers, and stakeholders has shifted towards its implementation (Link 2005).

5.1.2 Integrated Ecosystem Assessment and Ecosystem Status Reports

Integrated ecosystem assessment (IEA) provides a practical framework for implementing EBFM while balancing socioeconomic and ecological management objectives (Levin et al. 2009). Significant challenges remain, including: (1) identification of ecosystem-level leading indicators for monitoring and management (Link 2005, Link et al. 2012), (2) describing chronological system states and shifts in ecosystem-response regimes (Mollmann and Diekmann 2012, Levin and Mollmann 2015), (3) quantitatively defining historical fishery ecosystem state changes related to dynamic environmental and human use patterns (Hilborn 2011, Hilborn 2012, Mollmann and Diekmann 2012, Levin and Mollmann 2015), and (4) assessing trade-offs within ecosystems to inform the evaluation of various management strategies.

An advantage of the IEA framework is that the scope of an ecosystem assessment is defined relative to the needs of the particular system and its management focus (Levin et al. 2009). When scoping management challenges, it is important to define the goals of the program and to

obtain the best available data and indices that pertain to the particular set of challenges being considered – importantly, these data and indices must be relevant to the scale of the marine ecosystem of interest. An ecosystem status report (ESR) serves as a critical piece of the IEA framework for a large marine ecosystem (LME) during both the scoping and implementation processes. To produce an ESR, full sets of indicators are developed such that each is representative of a relevant component of the target LME (NOAA 2009, Andrews et al. 2013, Karnauskas et al. 2013). Each indicator time series should chronicle the status of a LME's living marine resource, the physical environment, or the associated natural and anthropogenic factors that affect them (Bowen and Riley 2003, Tscherning et al. 2012, Kelble et al. 2013). Indicators are often divided using a conceptual model which represents drivers, pressures, states, impacts/services, and responses of the ecosystem independently (DPSER; Bowen and Riley 2003, Tsherning et al. 2012, Kelble et al. 2013). However, this framework imposes a hierarchal structure among categories that: (1) may not actually exist in the ecosystem, or (2) fails to consider complex interrelationships that occur among indicators (Tscherning et al. 2012). In the context of management, a more appropriate analytical approach would employ functional sets of response and predictor indicators to reveal potential cause-and-effect relationships within the ecosystem (Niemeijer and de Groot 2008, Tscherning et al. 2012).

The sheer number of indicators supplied by an ESR provide a vast wealth of information describing the complex interplay among key biotic, abiotic, and anthropogenic elements of an LME. Interpreting the dynamic interactions between multiple indicators of ecosystem state, which themselves vary in response to internal driving mechanisms and external influences, can be an overwhelming challenge. Temporal patterns in predictors and responses can be used to

identify the suites of indicators that represent relative indicator-regime states. The exposition of indicator-regime status in an EBFM context can be thought of as the consideration of changes in food web and system dynamics, represented by changing community compositions and structures (Mollmann and Diekmann 2012), across the entire study area. Rapid changes in LME regime state, called *phase shifts*, can have large-scale effects on both the natural ecology of a system, and the human economies that rely on it (Mollmann and Diekmann 2012, Levin and Mollmann 2015, Wernberg et al. 2016). It is becoming increasingly important to account for and describe potential regime stable states, phase shifts, and alternate stable states when implementing fisheries management policy (Levin et al. 2009, Mollmann and Diekmann 2012, Levin and Mollmann 2015).

5.1.3 Study Aims

This study presents a new, ecosystem-level, fisheries indicator selection heuristic (EL-FISH) (Figure 5.1), that leverages the scientific method in order to perform hypothesis-based tests by applying state-of-the-art analytical tools specifically designed to model multivariate ecological data sets. As a case study, a subset of ESR data (Table 5.1) from the Gulf of Mexico large marine ecosystem (Gulf LME) that was explored by Karnauskas et al. (2015) was re-examined. Canonical ordination methods (ter Braak 1994, Legendre and Legendre 2012), were used to directly test null hypotheses (H_o) concerning the functional relationships among sets of response and predictor indicators that describe the state of the Gulf LME. Using the scientifically valid response-predictor paradigm in place of an organizational structure dictated by DPSER, EL-FISH was used to: (1) test H_o and determine statistical significance for an effect of predictors on the responses of the Gulf LME, (2) describe the most influential response and predictor indicators for the ecosystem,

(3) determine the magnitude and direction of the gradients of influence on and within the observed ecosystem response, (4) identify regime stable states, and (5) identify indicator trade-offs and patterns that should be targeted for long-term monitoring, further study, and/or management action/policy updates.

5.2 METHODS

5.2.1 Gulf of Mexico Large Marine Ecosystem

The Gulf of Mexico qualifies as a large marine ecosystem with an areal extent of just over 1.5 million km^2, and an average depth of ~1600 meters (Kumpf et al. 1999). Living marine resources within the Gulf LME support valuable commercial and recreational fisheries. In 2012, the Gulf's commercial fisheries landings contributed $763 million in revenue to the economies of the five Gulf States (Texas, Louisiana, Mississippi, Alabama, and Florida). Additional estimated sales impacts ranged from a low of $17 million in Florida to $2.5 billion in Texas, with a total sales impact of $5.26 billion in 2012. Also in 2012, approximately 3.1 million recreational anglers took an estimated 23 million fishing trips into Gulf waters. These recreational fishing activities contributed, either directly or indirectly, $10 billion to their respective regional economies (NMFS 2014). However, recent studies indicate that many exploited species are currently experiencing overfishing, due in part to increasing fishing effort during recent decades. Overfishing of exploited stocks may be manifested in a variety of population-level responses, including declining abundances, reduced sizes, and skewed sex ratios (Coleman et al. 1996, Ault et al. 2005a, Ault et al. 2005b).

Table 5.1 – Indicator list for Gulf of Mexico EL-FISH. Details of all $i = 49$ response (**Y**) and $j = 30$ predictor (**X**) indicators used for the EL-FISH analysis of the Gulf of Mexico. Full details for all indicators, and their origins, are contained in the 2013 Gulf ESR (Karnauskas et al. 2013, Karnauskas et al. 2015). Descriptor categories, as assigned for this study (EL-FISH) and by the original authors (DPSER), are included here.

i	Y	Description	EL-FISH	DPSER
1	MENHADEN	Abundance of N Gulf menhaden (*Brevoortia patronus*)	Population state - LT	State - LT
2	N SHRMP	Abundance of all commercial Shrimp spp. in N Gulf	Population state - LT	State - LT
3	S SHR 1	Abundance of Redspotted Shrimp (*Farfantepenaeus brasiliensis)* in S Gulf	Population state - LT	State - LT
4	S SHR 5	Abundance of Crystal Shrimp (*Sicyonia brevirostris)* in S Gulf	Population state - LT	State - LT
5	BRD BP BBS	Abundance of Brown Pelican (*Pelecanus occidentalis carolinensis*) BBS survey	Population state - UT	State - UT
6	BRD BP CBC	Abundance of Brown Pelican (*Pelecanus occidentalis carolinensis*) CBC survey	Population state - UT	State - UT
7	BRD RS BBS	Abundance of Roseate Spoonbill (*Platalea ajaja*) BBS survey	Population state - UT	State - UT
8	BRD RS CBC	Abundance of Roseate Spoonbill (*Platalea ajaja*) CBC survey	Population state - UT	State - UT
9	N BN SHARK	Abundance of Blacknose Shark (*Carcharhinus acronotus*) in N Gulf	Population state - UT	State - UT
10	N BT SHARK	Abundance of Blacktip Shark (*Carcharhinus limbatus*) in N Gulf	Population state - UT	State - UT
11	N COBIA	Abundance of Cobia (*Rachycentron canadum*) in N Gulf	Population state - UT	State - UT
12	N GAG GR	Abundance of Gag (*Mycteroperca microlepis*) in N Gulf	Population state - UT	State - UT
13	N KING MAC	Abundance of King Mackerel (*Scomberomorus cavalla*) in N Gulf	Population state - UT	State - UT
14	N MUTTON	Abundance of Mutton Snapper (*Lutjanus analis*) in N Gulf	Population state - UT	State – UT
15	N SPAN MAC	Abundance of Spanish Mackerel (*Scomberomorus maculatus*) in N Gulf	Population state - UT	State - UT

Table 5.1 (Continued)

i	Y	Description	EL-FISH	DPSER
16	N TILE E	Abundance of Tilefish (*Caulolatilus spp.* & *Lopholatilus chamaeleonticeps*) in NE Gulf	Population state - UT	State - UT
17	N TILE W	Abundance of Tilefish (*Caulolatilus spp.* & *Lopholatilus chamaeleonticeps*) in NW Gulf	Population state - UT	State - UT
18	N TRIGGER	Abundance of Gray Triggerfish (*Balistes capriscus*) in N Gulf	Population state - UT	State - UT
19	N YE GR E	Abundance of Yellowedge Grouper (*Epinephelus flavolimbatus*) in NE Gulf	Population state - UT	State - UT
20	N YE GR W	Abundance of Yellowedge Grouper (*Epinephelus flavolimbatus*) in NW Gulf	Population state - UT	State - UT
21	REV MEX	Total revenue for Mexican commercial fishing	Revenue - Commercial fishing	Socioeconomic
22	REV US	Total revenue for U.S. commercial fishing	Revenue - Commercial fishing	Socioeconomic
23	DIV LA	Shannon-Weiner diversity off Louisiana in fall	Structure/Function - All fishes	Impact
24	DIV TX	Shannon-Weiner diversity off Texas in fall	Structure/Function - All fishes	Impact
25	EVEN LA	Species evenness off Louisiana in fall	Structure/Function - All fishes	Impact
26	EVEN TX	Species evenness off Texas in fall	Structure/Function - All fishes	Impact
33	MTL SURV	Mean trophic-level in N Gulf	Structure/Function - All fishes	Impact
27	PD RATIO	Ratio of pelagic to demersal fish in catches in N Gulf	Structure/Function - All fishes	Impact
28	RICH LA	Species richness off Louisiana in fall	Structure/Function - All fishes	Impact

Table 5.1 (Continued)

i	Y	Description	EL-FISH	DPSER
29	RICH TX	Species richness off Texas in fall	Structure/Function - All fishes	Impact
30	MTL COM	Mean trophic-level of U.S. commercial catch	Structure/Function - Commercial fishes	Impact
31	MTL COM2	Mean trophic-level of U.S. commercial catch (excl. Gulf menhaden)	Structure/Function - Commercial fishes	Impact
32	MTL MEX	Mean trophic-level of Mexican commercial catch	Structure/Function - Commercial fishes	Impact
34	PRED COM	Proportion of predatory fishes in U.S. commercial catch	Structure/Function - Commercial fishes	Impact
35	PRED COM2	Proportion of predatory fishes in U.S. commercial catch (excl. Gulf menhaden)	Structure/Function - Commercial fishes	Impact
36	PRED MEX	Proportion of predatory fishes in Mexican commercial catch	Structure/Function - Commercial fishes	Impact
37	MTL REC	Mean trophic-level of U.S. recreational catch	Structure/Function - Recreational fishes	Impact
38	PRED REC	Proportion of predatory fishes in U.S. recreational catch	Structure/Function - Recreational fishes	Impact
39	ATL CROK	Mean fork-length of Atlantic Croaker (*Micropogonias undulatus*) in U.S. recreational catch	Structure/Function - Stock specific	Impact
40	GROW GRA	Growth rate of Gray Snapper (*Lutjanus griseus*) in N Gulf	Structure/Function - Stock specific	Impact
41	KINGFSH	Mean fork-length of Southern Kingfish (*Menticirrhus americanus*) in U.S. recreational catch	Structure/Function - Stock specific	Impact
42	MAMM STR	Mammal stranding events in N Gulf	Structure/Function - Stock specific	State - UT
43	RED DRUM	Mean fork-length of Red Drum (*Sciaenops ocellatus*) in U.S. recreational catch	Structure/Function - Stock specific	Impact

Table 5.1 (Continued)

i	Y	Description	EL-FISH	DPSER
44	RED SNAP	Mean fork-length of Red Snapper (*Lutjanus campechanus*) in U.S. recreational catch	Structure/Function - Stock specific	Impact
45	S FLOUND	Mean fork-length of Southern Flounder (*Paralichthys lethostigma*) in U.S. recreational catch	Structure/Function - Stock specific	Impact
46	SEATRT	Mean fork-length of Spotted Seatrout (*Cynoscion nebulosus*) in U.S. recreational catch	Structure/Function - Stock specific	Impact
47	SHEEPHD	Mean fork-length of Sheepshead (*Archosargus probatocephalus*) in U.S. recreational catch	Structure/Function - Stock specific	Impact
48	SPAN MAC	Mean fork-length of Spanish Mackerel (*Scomberomorus maculatus*) in U.S. recreational catch	Structure/Function - Stock specific	Impact
49	TUR NEST	Nesting rates for Kemp's Ridley Turtle (*Lepidochelys kempii*) in Tamaulipas, Mexico	Structure/Function - Stock specific	State - UT

j	X	Description	EL-FISH	DPSER
1	AMO MEAN	Annual mean value of Atlantic Multidecadal Oscillation	Climatology - Basin	Climate
2	AWP DOY	Atlantic Warm Pool maximum, day of year	Climatology - Basin	Climate
3	AWP MEAN	Atlantic Warm Pool annual mean	Climatology - Basin	Climate
4	MAR FLD	Marsh flooding rate in Barataria Bay, LA	Climatology - Local	Physical
5	HURR ACT	ACE index of hurricane activity	Climatology - Regional	Physical
6	PRECIP	Total precipitation for Mississippi River watershed	Climatology - Regional	Physical
7	LAND FIS	Total landings U.S., finfish (excluding Gulf menhaden)	Fisheries extraction - Commercial	Climate
8	LAND INV	Total landings U.S., invertebrates	Fisheries extraction - Commercial	Climate
9	LAND MEN	Total landings U.S., Gulf menhaden (*Brevoortia patronus*)	Fisheries extraction - Commercial	State - LT
10	MEX FISH	Total landings Mexico, all finfish	Fisheries extraction - Commercial	Impact

Table 5.1 (Continued)

j	X	Description	EL-FISH	DPSER
11	MEX INV	Total landings Mexico, invertebrates	Fisheries extraction - Commercial	Impact
12	LAND REC	Total landings U.S., recreational fishes	Fisheries extraction - Recreational	Impact
13	EFF MEN	U.S. Gulf menhaden (*Brevoortia patronus*) fishing effort	Fishing effort - Commercial	Impact
14	EFF MEX	Number of Mexican registered fishing boats	Fishing effort - Commercial	Socioeconomic
15	REC DAYS	Number of U.S. recreational fishing days	Fishing effort - Recreational	Impact
16	REC TRIP	Number of U.S. recreational angler trips	Fishing effort - Recreational	Impact
17	DO LA F	Annual mean dissolved O_2 off Louisiana in fall	Physical environment - Local	Physical
18	DO LA S	Annual mean dissolved O_2 off Louisiana in summer	Physical environment - Local	Physical
19	DO TX F	Annual mean dissolved O_2 off Texas in fall	Physical environment - Local	Physical
20	DO TX S	Annual mean dissolved O_2 off Texas in summer	Physical environment - Local	Physical
21	SED CONC	Total suspended sediment discharge for the Mississippi River	Physical environment - Local	Physical
22	STR FLOW	Mean streamflow for Mississippi River	Physical environment - Local	Physical
23	AREA HYP	Area of hypoxic zone in N Gulf	Physical environment - Regional	Physical
24	FERT USE	Index of fertilizer consumption for Mississippi River watershed	Physical environment - Regional	Physical
25	NO3 LOAD	Mississippi River total basin load of NO_3	Physical environment - Regional	Physical
26	SST MAX	Max monthly mean sea surface temperature	Physical environment - Regional	Climate

Table 5.1 (Continued)

j	X	Description	EL-FISH	DPSER
27	SST MEAN	Mean offshore sea surface temperature	Physical environment - Regional	Climate
28	ZOO SPR	Mean biomass of zooplankton offshore U.S. in spring	Physical environment - Regional	Climate
29	OIL RIGS	Number of U.S. Gulf oil rigs installed	Resource extraction - Commercial	Physical
30	OIL SPL	Number of U.S. Gulf oil spills	Resource extraction - Commercial	Physical

5.2.2 EL-FISH in the Gulf of Mexico Large Marine Ecosystem

The EL-FISH protocol was defined as five steps that can be used to inform all phases of the IEA loop (Figure 5.1), and it can complement long-term monitoring programs by providing a comprehensive assessment of the historical dynamics of all elements undertaken by the monitoring effort. The analyses described here were conducted using the Fathom (Jones 2017) and Darkside (Kilborn 2017) toolboxes for MATLAB and were implemented in version R2014b (Matlab R2014). The steps of EL-FISH are described below within the terms of the Gulf case study, but they are transferrable to any similar collections of continuous, time-series data.

5.2.2.1 Step 1: Define scope of inquiry within the response-predictor framework. Understanding the response in the structure and function of Gulf fisheries resources, due to changes in anthropogenic pressures and natural ecosystem variability, can help to refine the decision framework used to set and achieve management goals (Jennings 2005, Link 2005, Levin et al. 2009, Mollmann and Diekmann 2012). The EL-FISH approach allows great flexibility when parameterizing models, and this particular analysis was framed to answer the specific question: "What influence does human activity and uncontrollable climate and environmental forcing (predictors) have on the overall status, structure, and function of the Gulf LME's associated fishery resources (responses)?" By defining the scope of inquiry in this way, a statistical H_o is generated, and a useful logical framework presents itself for parameterizing the ecosystem model and organizing the indicators. For this case study, H_{o1} = "The variability in predictor indicator time-series of anthropogenic and environmental pressures cannot be used to explain the variability in indicators of ecosystem resources and socio-economic responses over the same time period."

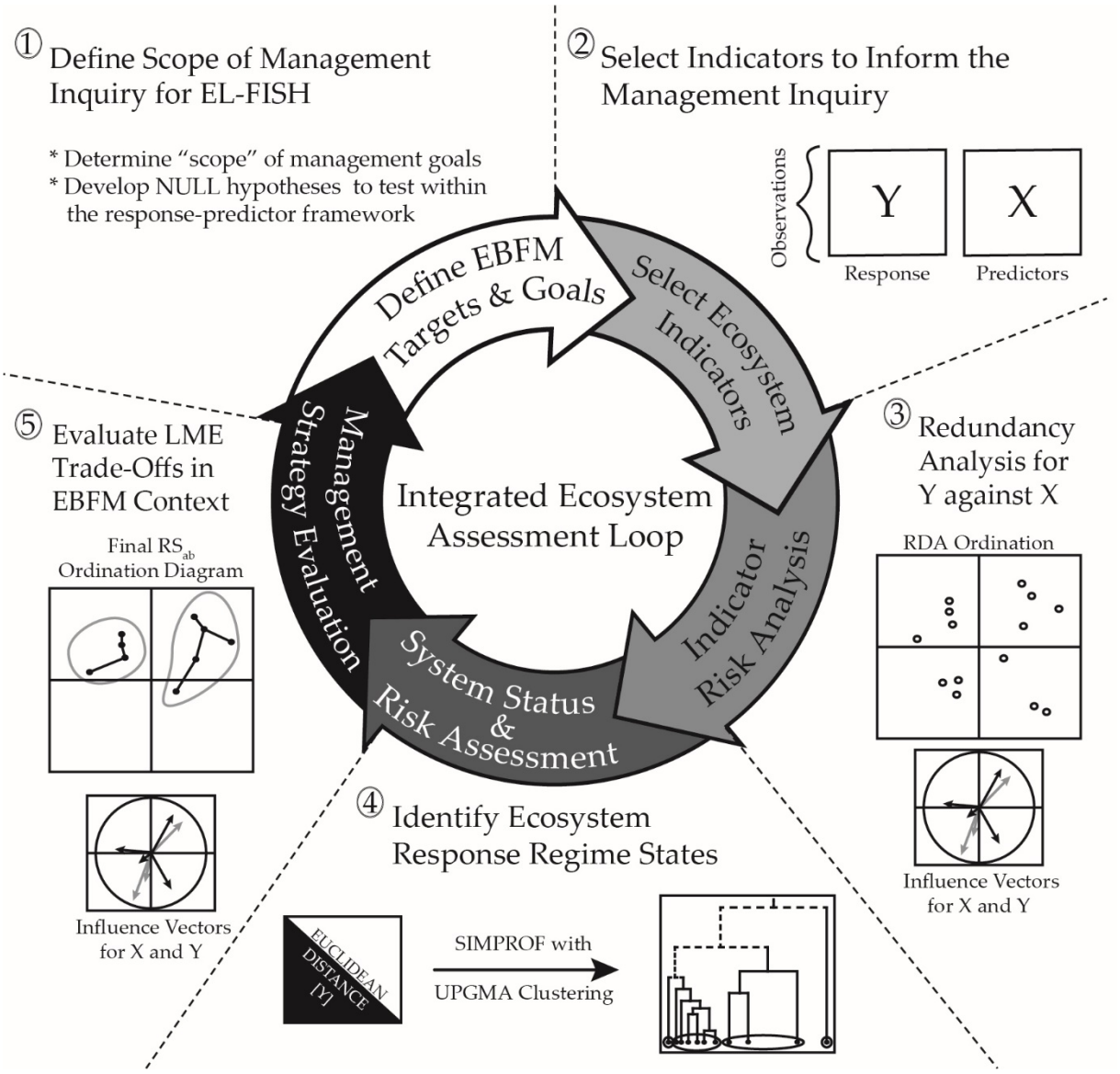

Figure 5.1 – Conceptual framework for EL-FISH. The inner loop represents the IEA assessment protocol (Levin et al. 2009) and its five steps (marked by dashed lines and increasing grayscale gradient). The numbered text outside of the IEA loop marks Steps 1-5 for the complementary EL-FISH protocol, and indicates how the IEA steps can be enhanced by employing the listed techniques.

5.2.2.2 Step 2: Select indicators to inform objectives. An ecosystem status report for the Gulf LME was published in 2013, providing full details of more than 100 indicators developed to reflect the dynamic nature of the ecosystem, its associated resources, and its dependent

communities, for the period 1950–2011 (Karnauskas et al. 2013). In many cases, consistent annual records were not available until the 1960's or 1980's, while other indicators were reliably recorded or modeled throughout the entire period of the ESR (Figure 5.2). Following the DPSER approach, the report's authors arranged the indicators as: (1) *drivers* describing climate and physical measures of the environment, (2) *states* providing abundance measures of upper and lower trophic-levels of living marine resources, and corresponding diversity indices, and (3) *responses* capturing impacts relevant to fishery resource structure (e.g., mean trophic-level) and socioeconomic change (e.g., fishery revenues).

For the present study, the DPSER datasets were reconfigured into one pair of data matrices –comprised of response and predictor indicators– such that the resultant ecosystem model was related to the scope and H_{o1} previously defined. To assess the impacts of human activity and climate/ecosystem variability on the structure and function of fisheries resources, as well as the economic benefits derived from them, a subset of 79 total indicators from the 2013 Gulf ESR were used (Table 5.1). Here, $i = 49$ response and $j = 30$ predictor indicators were compiled into continuous time-series data matrices (**Y** and **X**, respectively) for the period 1980-2011. For cases where an indicator's observation was missing for any year, the time series mean was imputed (Karnauskas et al. 2015). Both matrices were standardized via z-score translation due to differences in units of measure between indicators (Legendre and Legendre 2012).

Response indicators in **Y** were chosen to represent the set of descriptors that account for (1) the population status of relevant upper and lower trophic-level species, (2) the structure and function of the Gulf LME's commercial and recreational fisheries resource complexes and stocks, and (3) the socioeconomic value of both the U.S. and Mexican commercial fishing fleets

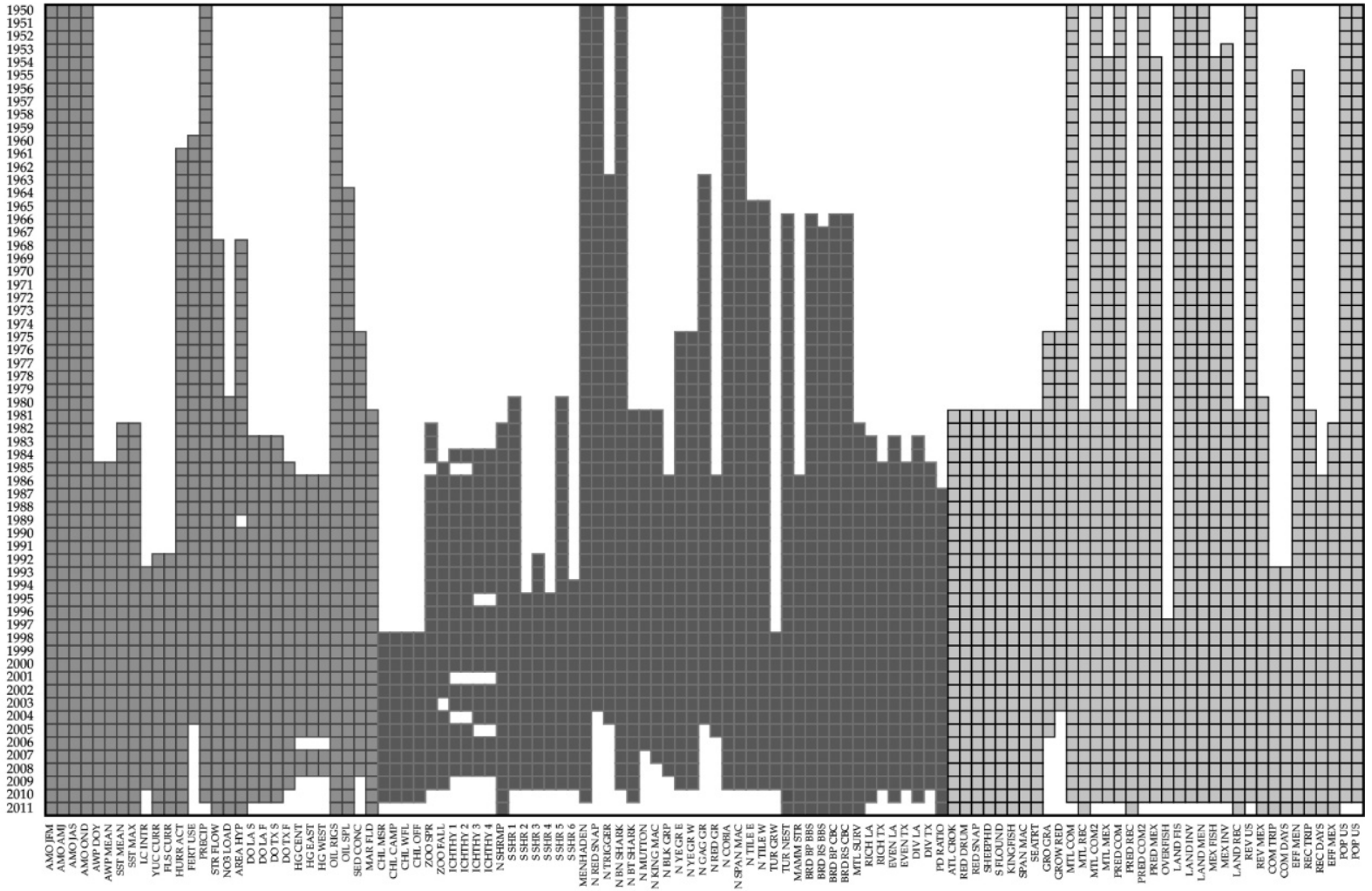

Figure 5.2 – Heatmap of Gulf LME ecosystem status report indicators. Heatmap representation of time series data for the period 1950-2011 contained in the 2013 ESR for the Gulf of Mexico (Karnauskas et al. 2013). For all indicators, solid squares represent years where data were available and whitespace indicates missing values. Indicators were categorized using the DPSER framework as either *responses*, *drivers*, or *states* and are shaded light, medium, or dark gray, respectively.

(Table 5.1). Predictor indicators in **X** included descriptors of (1) large-scale climatological features, (2) fishing extractions and (3) effort, both commercial and recreational, (4) the natural physical-chemical environment, and (5) oil industry activity (Table 5.1).

5.2.2.3 Step 3: Conduct canonical analysis of the response-predictor model. To assess H_{o1}, canonical redundancy analysis (RDA; Rao 1964) was conducted. RDA is widely used in ecology and employs a matrix of predictor indicators (**X)** to account for the variation in a matrix of response indicators (**Y**). Multivariate multiple regression of **Y** against **X** was performed and m canonical axes were generated as linear combinations of the indicators in **X**; their corresponding eigenvalues represent the variance in **Y** accounted for by each axis. The canonical coefficient of determination (R^2; Miller and Farr 1971) measured the success the predictors had in explaining the responses, while the adjusted form of this measure (R^2_{adj}; Ezekiel 1930) provided an unbiased estimate of the fraction of variation in **Y** explained by **X** (Ohtani 2000). Statistical significance in RDA was determined using distribution-free tests based on 1,000 permutations of the residuals of the model (Anderson 2001, Manly 2006), and all p-value interpretations were based on $\alpha = 0.05$. A reduced-space ordination diagram of **Y** constrained by **X** was produced via RDA scaling type-1, allowing objects (years) and the associated indicators underlying both **X** and **Y** to be depicted in the multivariate space defined by the two most important canonical axes (Legendre and Legendre 2012).

5.2.2.4 Step 4: Identify regime states in the response observations. To determine if multivariate structure existed among years with respect to **Y**, clustering via the unweighted pair group method with arithmetic mean (UPGMA; Rohlf 1963) coupled with resemblance profiles as decision criterion (SIMPROF; Clarke et al. 2008, Kilborn et al. 2017) was employed. This form of

clustering, referred to as SIMPROF clustering hereafter, assesses the H_{o2} = "there is no multivariate structure among objects (years) with respect to a set of descriptors (**Y**)". This assessment is made at all possible levels of resemblance identified by an UPGMA clustering-solution produced from an appropriate resemblance matrix. This method was developed as a form of constrained clustering via hypothesis testing (Clarke et al. 2008), and is well suited for high-dimensional continuous datasets with relatively large sample sizes (Kilborn et al. 2017). Here, **Y** was converted into a square, symmetric, Euclidean-distance matrix ($\mathbf{Y}_{Euc}$; Legendre and Legendre 2012) and subjected it to SIMPROF clustering in order to obtain multivariate clusters of years with similar underlying fisheries ecosystem properties. To account for multiple tests of significance within a single dendrogram, the progressive Bonferoni *p*-value correction method (Clarke et al. 2008, Legendre and Legendre 2012) was employed (1,000 iterations; $\alpha = 0.05$). Only clusters of years with more than three members were considered long-term regime states (*RS*s) and were retained for further analysis.

To qualitatively describe the structure and function of the LME resources within each *RS* identified, the results of the RDA analysis were revisited. Using RDA (scaling type-1), the ordination of years was represented visually along with the response indicators in **Y** to quantitatively determine the relatively prominent (or absent) characteristics that describe the differences between pairs of *RS*s identified. This was accomplished by examining the orthogonal vector projections from each SIMPROF group's centroid to the set of indicator gradients underlying **Y**. However, prior to examination, all *m* sets of canonical-axes coordinates, for the response's objects and indicator biplot vectors, were multiplicatively weighted by the proportion of the variability in **Y** explained their respective canonical axis (CA^m).

The orthogonal projection of any group of year's centroid onto an indicator gradient (Figure 5.3) represents an approximation of that *RS*s fitted value along that gradient (Legendre and Legendre 2012). To determine the prominence of response indicators within *RS*s, the orthogonal projections were obtained for all gradients represented in **Y,** and the distance from the origin to each point of orthogonal intersection was calculated. The sign of the value is used to represent either the "relatively high" (positive) or "relatively low" (negative) end of the indicator gradient and was based on the location of the vector's "head". Group centroid projections intersecting a gradient in the same quadrant as the head or tail were given a positive or negative sign, respectively. The difference in any *RS*'s signed centroid projection value from that of the previous *RS* along an indicator gradient [$\Delta_{ab}(\mathbf{y}_i)$, where *a* and *b* denote the centroids being compared along gradient $\mathbf{y}_i$], was used to add detail to the nature of the temporal relationship between any two regime states. The sign and magnitude of $\Delta_{ab}(\mathbf{y}_i)$ was interpreted as being reflective of the relative changes, for any indicator, over the time period between the two regime states selected (i.e., positive values reflect positive relative changes over time, and vice versa).

For each pairwise comparison of *RS*s, *a* and *b* (RS_{ab}), the list of response indicators was reduced from the full set of 49, by examining the proportional contribution of each response indicator ($\mathbf{y}_i$) to the total dissimilarity between any two group centroids' projections along all response-indicator gradients [$\lambda_{ab}(\mathbf{y}_i)$, where *a*, *b*, and $\mathbf{y}_i$ are defined above]. A matrix of Euclidean distances between all 28 possible pairs of centroid projection-coordinates, along all 49 indicators, was assembled and all $\lambda_{ab}(\mathbf{Y})$ were calculated. Here, only indicators whose $\lambda_{ab}(\mathbf{y}_i) \geq$ the lower bound of the 75th percentile of all indicators' proportions, for any pair of *a* and *b*, were retained. These indicators were interpreted as being sufficiently indicative of the drivers underlying the

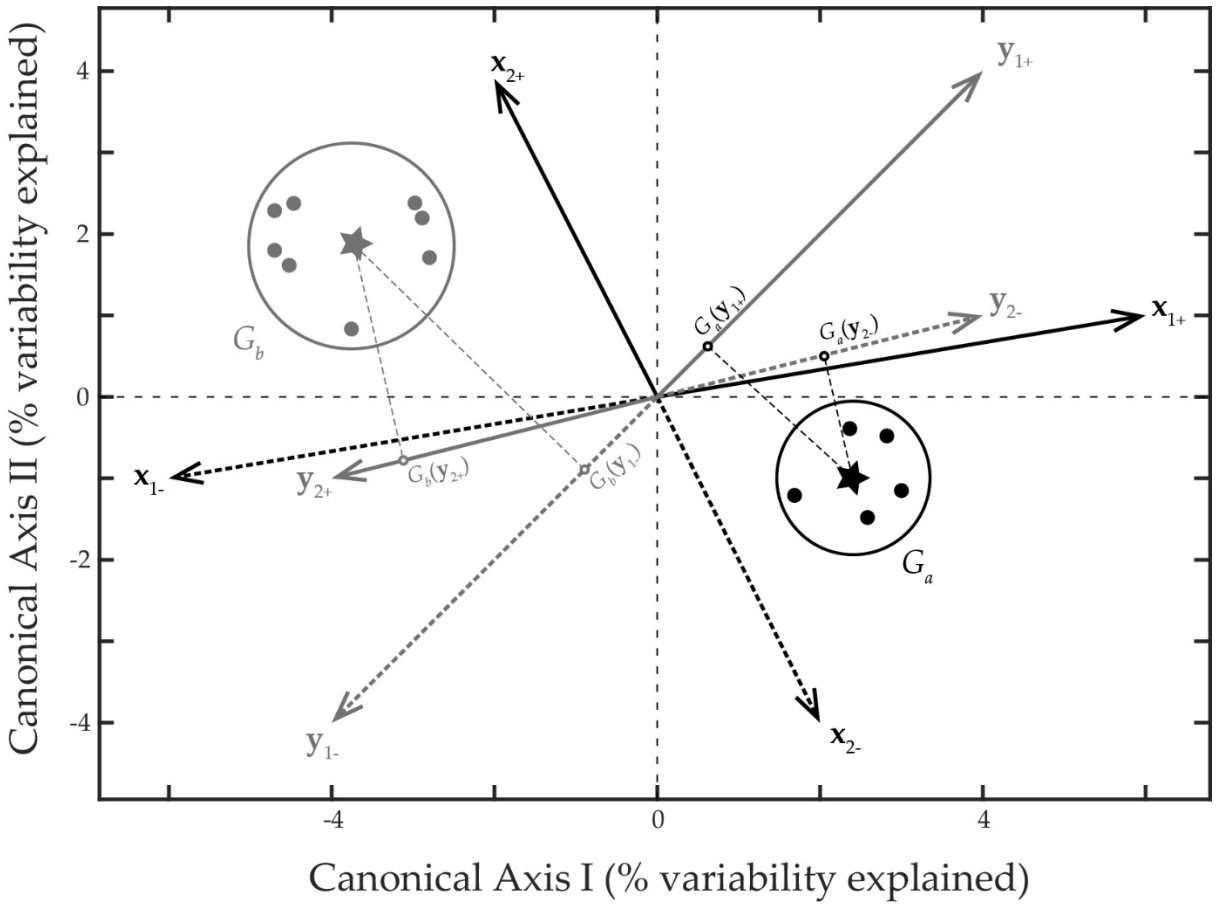

Figure 5.3 – RDA scaling type-1 primer. Cartoon depicting the major components of a redundancy analysis scaling type-1 distance triplot. The first two canonical axes are drawn and the proportion of explained variability represented by each CA^m is displayed along each axis. Small filled circles represent objects; the colors black and gray represent groups *a* and *b*, respectively, and the colored stars represent each group's centroid. Objects' site scores are representative of their dissimilarity, and two objects in close proximity are considered to have low dissimilarity and are more alike with respect to the underlying gradients of **Y**. Both **Y** and **X** (gray and black vectors, respectively) are typically visualized with only the positive ends (+; solid vectors), and the negative ends of the gradients are only implied (–; dotted vectors). Orthogonal projections from each group centroid are drawn and noted with group and vector identifiers. For example, the projection from G_a onto $\mathbf{y}_1$ is marked with a perpendicular line mapped to the positive end of vector $\mathbf{y}_i$ to point $G_a(\mathbf{y}_{1+})$. The Euclidean distance from this point to the origin represents the fitted value for group *a* onto vector $\mathbf{y}_1$. The difference in two projections represents the relative difference between the two groups with respect to the chosen indicator and is defined by $\Delta_{ab}(\mathbf{y}_i) = G_b(\mathbf{y}_i) - G_a(\mathbf{y}_i)$. Gradients from **X** must be interpreted with respect to the variability explained by each CA^m and their corresponding axis coordinates are representative of the correlation between the underlying indicators and the object site scores obtained along each axis.

difference between any two regime states identified. The choice of threshold value is left to the discretion of the researcher, and could be replaced by other equally defensible techniques [e.g., the inclusion of the fewest indicators whose $\lambda_{ab}(\mathbf{y}_i)$ sum to a predetermined threshold proportion].

5.2.2.5 Step 5: Evaluate trade-offs between long-term regime states and predictors. Trade-offs between regime states described in Step 4 and the predictors that influence them were elucidated by synthesizing all of the information obtained from the RDA and its ordination diagram, the SIMPROF clustering analysis, and the indicator reduction methods described above. To determine which predictor indicators in **X** were most influential to the ordination of *RS*s obtained, and to reduce the list to a more manageable number, the Pearson correlation coefficient (r_{jm}; Legendre and Legendre 2012) was calculated between each descriptor in **X** and all of the m canonical axes (CA^m) defined by the RDA model. Significance was assessed for all r_{jm} using permutation testing (5,000 iterations, $\alpha = 0.05$), and only the significantly correlated predictor indicators were retained for CA^m where $m = \{1, 2\}$. The influence of the predictors to the final ordination of years was determined by extracting the canonical weighting-coefficients (**C**) for all **X** along CA^I and CA^{II}. Canonical weightings were defined by the formula $\mathbf{C} = \mathbf{BU}$, and can be interpreted in the same manner as regression coefficients (Legendre and Legendre 2012). Matrix **B** is defined as $\mathbf{B} = (\mathbf{X'X})^{-1}\mathbf{X'Y}$, and represents the ordinary least squares approximation of the solution to regression of **Y** against **X**. Matrix **U** is the result of eigenanalysis of the fitted **Y** values where, $\mathbf{Y}_{fit} = \mathbf{XB}$, and it is the projection matrix used to represent the canonical RDA solution in Euclidean space (Legendre and Legendre 2012).

Final ordination diagrams were created that contained (1) the identification of LME regime states through time, (2) the response indicators in **Y** that best represented differences

between the states observed, and (3) the predictor indicators in **X** that were most likely to influence the assemblage of prominent **Y** indicators within *RS*s. Many management scenarios involve the objective of managing resources or environments from one state (usually an undesirable present state) to another (a more productive or more pristine state), or to sustainably maintain some other preferred state. Visualizations of the final RDA solution for pairs of *RS*s were used to highlight the trade-offs between critical regime stable states, the response indicators that qualitatively describe them, and the underlying human and natural drivers that influence which *RS* qualities become manifest.

5.3 RESULTS

5.3.1 EL-FISH Steps 1-3

5.3.1.1 Scoping, parameterization, and RDA modeling. The results of EL-FISH Steps 1 and 2 were straightforward, and were part of the planning process described in §5.2 above. The outcome of Step 1 was the testable H_{o1} defined by the study's scoping decision to focus on the impacts of human activities and environmental forcing events on the structure and function of the Gulf LME's fisheries resources. In Step 2, the response and predictor indicators were compiled into datasets **Y** and **X** (Table 5.1), and one square-symmetric distance matrix was calculated for use in SIMPROF clustering ($\mathbf{Y}_{Euc}$ only, Step 4).

The canonical redundancy analysis in Step 3 yielded statistically significant results (F = 3.780, R^2 = 0.991, R^2_{adj} = 0.729, df_{model} = 30, df_{error} = 1, p-value = 0.003); therefore, the H_{o1} of no explanatory power for the predictor indicators on fisheries ecosystem response, was rejected. Of the total variability in **Y** explained by the model, 31.96% and 16.18% of that variability was described by the first two canonical axes (CA^{I} and CA^{II}, respectively). The other CA^{m} orthogonal

axes (m = {3-28}) accounted for 50.96% of the remaining explained variability, with only the m = {3, 4, 5} axes individually accounting for more than 5-8% (see Appendix D, Table D.1 for full RDA table outputs). The RDA ordination diagram (Figure 5.4) was used as a two-dimensional representation of the final 30-dimensional RDA solution, and to visualize 48.14% of the variability in **Y** explained by **X**. The annual coordinates on the plot were ordinated with respect to $\mathbf{Y}_{\text{Euc}}$, and any two years that were plotted close to one another were considered more alike than those that were relatively far apart in Euclidean space. Vector biplots for all $\mathbf{y}_i$ and $\mathbf{x}_j$ were used to represent the indicators' gradients that underlie (1) the ordination of years ($\mathbf{Y}_{\text{Euc}}$; Figure 5.4a), and (2) the predictors (**X**) capacity to explain the response (**Y**; Figure 5.4b).

5.3.2 EL-FISH Step 4

5.3.2.1 Identification of long-term regime states. The results of the SIMPROF clustering for $\mathbf{Y}_{\text{Euc}}$ (Appendix D, Table D.2) identified eight statistically significant groups of years in multivariate space (Figure 5.4b). Of the eight groups identified, four were comprised of no more than three years (RS_2, RS_4, RS_5, and RS_8), and were (arbitrarily) not considered as long-term regime states. The remaining four (RS_1, RS_3, RS_6, and RS_7) had at least five member years, with the two largest RSs situated at either end of the time series (RS_1: 1980-1986; RS_7: 2003-2009, 2011); all were considered long-term regime states. The pairs RS_{17} and RS_{36} were separated in canonical space primarily along CA^{I} (Figure 5.4b), and CA^{II} best described the differences between RS_{13} and RS_{67}.

The minimum proportional contribution to the difference between RSs for any response indicator was $\lambda_{ab}(\mathbf{y}_i) = 0.01\%$ and the maximum $\lambda_{ab}(\mathbf{y}_i)$ was 4.2% (Appendix D, Table D.3). After

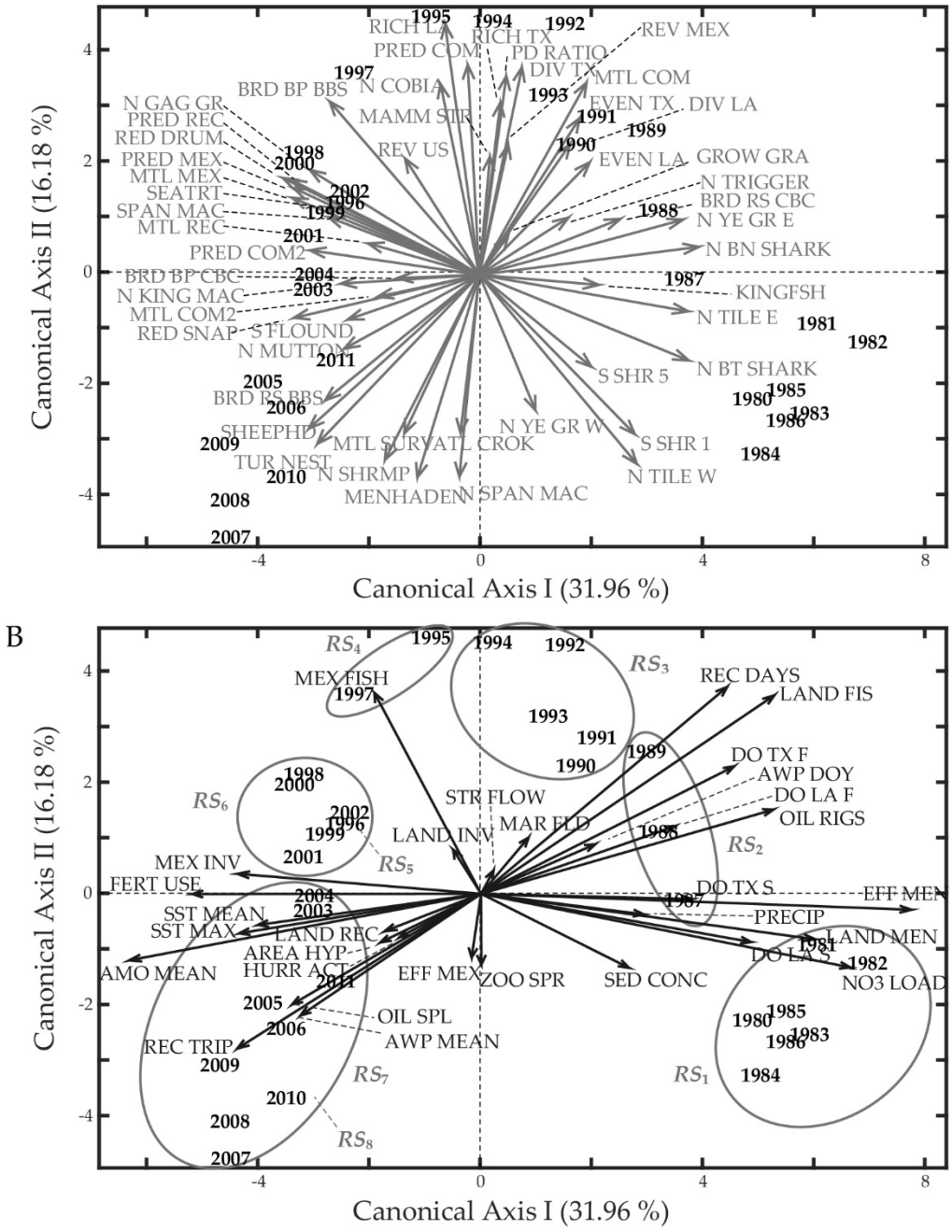

Figure 5.4 – Gulf EL-FISH full RDA solution. RDA ordination diagram of the first two CA^{m} of the Gulf of Mexico RDA solution for **X** and **Y**. CA^{I} (31.96%) is depicted on the abscissa and CA^{II} (16.18%) on the ordinate axis. (A) The distance biplot annual scores (years) and the underlying **Y** gradients (gray vectors) describing the dissimilarities (proximity) between them. (B) The distance biplot of years and the underlying **X** gradients (black vectors) describing the dynamic ecosystem-pressures. The ordination of years in both panels are identical, and the gray circles are drawn around the *RS*s identified by SIMPROF clustering (B). Both sets of indicators have been scaled by a factor of 15 for interpretability. See Figure 5.3 for additional details of RDA scaling type-1 distance triplots.

application of the indicator retention-threshold requirement [$\lambda_{ab}(\mathbf{y}_i) \geq 75^{th}$ percentile], no more than 13 indicators were retained for any pairwise comparison of states (RS_{ab}), and of those retained, the total proportion of the difference accounted for was within the range {3.8-4.8%} (see Appendix D, Table D.3). The frequency distribution of all $\lambda_{ab}(\mathbf{Y})$ tended to become more skewed toward the right tail as the states became more separated along CA^{I} (Appendix D, Figure D.1). The signed differences between centroid projections along all indicators, $\Delta_{ab}(\mathbf{Y})$, displayed skewness patterns similar to those of the distributions of $\lambda_{ab}(\mathbf{Y})$. In most cases, the $\Delta_{ab}(\mathbf{y}_i)$ values tended to either increase or decrease with time and as the separation between the regime states increased (Table 5.2). The values of $\Delta_{ab}(\mathbf{Y})$ for any RS_{ab} pair typically ranged between relatively similar absolute values due to the placement of the regime states' centroids.

5.3.3 EL-FISH Step 5

5.3.3.1 Evaluation of regime state and predictor trade-offs. The ordination of years (i.e., the regime states) was produced by projecting the standardized **Y** data into the canonical space defined via RDA. The post-hoc check for indicators' correlations (r_{jm}) with each CA^{m} revealed significant correlations between 19 of 30 indicators from **X** with CA^{I}, and six with CA^{II}. Only one predictor identified for CA^{II} was not also retained for CA^{I} (Mexican finfish landings); all other CA^{II} indicators were also significantly correlated with CA^{I} (Table 5.3). The canonical regression coefficients for the predictor indicators from **C** ranged from -1.36 (dissolved oxygen offshore Louisiana in fall) to 2.74 (total U.S. finfish landings, excluding Gulf menhaden) along CA^{I}, and from -1.47 (U.S. recreational fishing days) to 3.21 (total U.S. finfish landings, excluding Gulf menhaden) along CA^{II}. The minimum absolute value for all significant coefficients (i.e., the lowest

magnitude of influence) for CA^{I} was 0.01 (mean sea surface temperature), and 0.16 (number of U.S. Gulf oil spills) for CA^{II} (Table 5.3).

Table 5.2 (Part 1) – Table of all $\Delta_{ab}(Y)$. Table of all differences between centroid projections for each response indicator in **Y** (rows) between all possible RS_{ab} pairs' centroids (columns). Indicators are organized according to the subcategories assigned in Table 5.1. All table cells are color coded where warm colors represent negative $\Delta_{ab}(\mathbf{y}_i)$ and cool colors are for positive values; the indicators that passed the threshold requirement set in EL-FISH Step 4 are presented in boldface. Each column's colors are scaled to the global minimum and maximum $\Delta_{ab}(\mathbf{y}_i)$ values, and the color white represents zero. All summary statistics are provided in the last five rows.

		RS_1 v RS_2	RS_1 v RS_3	RS_1 v RS_4	RS_1 v RS_5	RS_1 v RS_6	RS_1 v RS_7	RS_1 v RS_8	RS_2 v RS_3	RS_2 v RS4	RS_2 v RS_5	RS_2 v RS_6	RS_2 v RS_7	RS_2 v RS_8
Lower - TL	MENHADEN	-0.06	-0.06	0.34	0.90	0.96	1.62	1.78	0.00	0.41	0.96	1.02	1.69	1.85
	N SHRMP	0.17	0.36	0.96	1.50	1.60	2.22	2.33	0.18	0.79	1.33	1.43	2.04	2.16
	S SHR 1	**-0.96**	**-1.70**	**-2.61**	-2.64	-2.81	-2.74	-2.57	**-0.74**	**-1.65**	-1.68	-1.85	-1.78	-1.61
	S SHR 5	**-0.95**	**-1.68**	**-2.62**	-2.69	-2.87	-2.85	-2.70	**-0.73**	**-1.67**	-1.75	-1.92	-1.91	-1.75
Upper - TL	BRD BP BBS	**0.97**	**1.71**	**2.60**	2.60	2.77	2.66	2.48	**0.74**	1.63	1.63	1.80	1.70	1.52
	BRD BP CBC	0.78	1.41	2.38	2.67	2.84	**3.10**	**3.03**	0.63	1.59	**1.88**	**2.06**	**2.32**	2.25
	BRD RS BBS	0.52	0.97	1.82	2.26	2.41	2.88	2.90	0.44	1.29	1.74	1.89	**2.35**	**2.37**
	BRD RS CBC	-0.67	-1.22	-2.15	-2.52	-2.68	**-3.04**	**-3.02**	-0.55	-1.47	-1.85	-2.01	**-2.37**	**-2.35**
	N BN SHARK	-0.76	-1.37	-2.33	-2.64	-2.81	**-3.10**	**-3.04**	-0.61	-1.57	**-1.88**	**-2.05**	**-2.34**	-2.28
	N BT SHARK	-0.89	-1.59	**-2.56**	**-2.74**	**-2.92**	-3.03	-2.92	**-0.70**	**-1.67**	-1.85	**-2.03**	-2.14	-2.02
	N COBIA	0.81	1.40	1.86	1.52	1.62	1.13	0.89	0.59	1.05	0.71	0.81	0.32	0.08
	N GAG GR	**0.93**	**1.64**	**2.60**	**2.73**	**2.91**	2.95	2.81	**0.72**	**1.68**	1.80	1.98	2.03	1.89
	N KING MAC	0.78	1.40	2.36	2.66	2.84	**3.10**	**3.04**	0.62	1.58	**1.88**	**2.06**	**2.32**	2.26
	N MUTTON	0.62	1.13	2.03	2.43	2.59	2.99	**2.99**	0.51	1.41	1.81	1.97	**2.37**	**2.37**
	N SPAN MAC	-0.39	-0.64	-0.57	-0.04	-0.05	0.62	0.83	-0.25	-0.17	0.35	0.35	1.01	1.22
	N TILE E	-0.84	-1.51	-2.48	**-2.72**	**-2.90**	**-3.09**	**-3.00**	-0.67	**-1.64**	**-1.88**	**-2.06**	-2.24	-2.15
	N TILE W	**-0.97**	**-1.71**	**-2.59**	-2.59	-2.76	-2.64	-2.46	**-0.74**	-1.62	-1.62	-1.79	-1.67	-1.49
	N TRIGGER	-0.59	-1.07	-1.96	-2.38	-2.53	-2.96	-2.96	-0.49	-1.37	-1.79	-1.94	**-2.37**	**-2.37**
	N YE GR E	-0.71	-1.29	-2.23	-2.58	-2.75	**-3.07**	**-3.04**	-0.58	-1.52	**-1.87**	**-2.03**	**-2.36**	**-2.32**
	N YE GR W	**-0.93**	**-1.63**	-2.33	-2.14	-2.28	-1.95	-1.72	-0.70	-1.39	-1.20	-1.34	-1.01	-0.79
Rev.	REV MEX	0.19	0.28	-0.01	-0.56	-0.60	-1.27	-1.45	0.09	-0.20	-0.75	-0.78	-1.46	-1.64
	REV US	**0.97**	**1.70**	2.53	2.45	2.61	2.41	2.21	**0.73**	1.56	1.48	1.64	1.45	1.25

Table 5.2 – Part 1 (Continued)

		RS_1 v RS_2	RS_1 v RS_3	RS_1 v RS_4	RS_1 v RS_5	RS_1 v RS_6	RS_1 v RS_7	RS_1 v RS_8	RS_2 v RS_3	RS_2 v RS_4	RS_2 v RS_5	RS_2 v RS_6	RS_2 v RS_7	RS_2 v RS_8
Structure & Function	DIV LA	-0.32	-0.61	-1.32	-1.83	-1.95	-2.52	-2.60	-0.29	-1.01	-1.52	-1.64	-2.20	-2.28
	DIV TX	0.35	0.57	0.45	-0.08	-0.08	-0.75	-0.96	0.22	0.10	-0.43	-0.44	-1.10	-1.31
	EVEN LA	-0.45	-0.84	-1.65	-2.12	-2.26	-2.77	-2.81	-0.39	-1.20	-1.67	-1.81	-2.31	**-2.36**
	EVEN TX	-0.28	-0.54	-1.23	-1.75	-1.87	-2.45	-2.54	-0.26	-0.95	-1.47	-1.59	-2.17	-2.26
	MTL SURV	0.14	0.29	0.87	1.42	1.51	2.13	2.26	0.16	0.74	1.28	1.37	2.00	2.12
	PD RATIO	0.22	0.33	0.07	-0.48	-0.51	-1.19	-1.38	0.11	-0.15	-0.70	-0.73	-1.40	-1.59
	RICH LA	0.74	1.28	1.64	1.25	1.33	0.79	0.54	0.53	0.89	0.50	0.58	0.04	-0.20
	RICH TX	0.33	0.53	0.39	-0.15	-0.16	-0.82	-1.03	0.20	0.06	-0.48	-0.49	-1.15	-1.36
	MTL COM	-0.22	-0.43	-1.07	-1.60	-1.71	-2.31	-2.41	-0.21	-0.86	-1.39	-1.49	-2.09	-2.20
	MTL COM2	0.73	1.32	2.27	2.60	2.77	**3.08**	**3.04**	0.59	1.54	**1.87**	**2.04**	**2.35**	**2.31**
	MTL MEX	**0.89**	**1.59**	**2.56**	**2.74**	**2.92**	3.03	2.91	**0.70**	**1.67**	1.85	2.03	2.14	2.02
	PRED COM	0.64	1.08	1.30	0.85	0.91	0.31	0.07	0.45	0.66	0.22	0.27	-0.33	-0.56
	PRED COM2	0.83	1.50	2.47	**2.72**	**2.89**	**3.09**	**3.00**	0.66	1.63	**1.88**	**2.06**	2.26	2.17
	PRED MEX	**0.90**	**1.61**	**2.57**	**2.74**	**2.92**	3.01	2.89	**0.70**	**1.67**	1.84	2.02	2.11	1.99
	MTL REC	0.87	1.55	2.52	**2.73**	**2.91**	**3.07**	2.96	0.68	**1.65**	**1.87**	**2.05**	2.20	2.10
	PRED REC	**0.91**	**1.62**	**2.58**	**2.74**	**2.92**	3.00	2.87	**0.71**	**1.67**	1.83	2.01	2.09	1.96
	ATL CROK	-0.36	-0.58	-0.47	0.06	0.07	0.73	0.94	-0.22	-0.11	0.42	0.42	1.09	1.30
	GROW GRA	-0.34	-0.65	-1.39	-1.90	-2.02	-2.57	-2.65	-0.31	-1.05	-1.55	-1.67	-2.23	**-2.30**
	KINGFSH	-0.82	-1.47	-2.44	**-2.70**	**-2.88**	**-3.10**	**-3.02**	-0.65	-1.62	**-1.88**	**-2.06**	-2.28	-2.20
	MAMM STR	0.41	0.67	0.61	0.09	0.09	-0.57	-0.78	0.26	0.20	-0.32	-0.31	-0.97	-1.19
	RED DRUM	**0.91**	**1.61**	**2.58**	**2.74**	**2.92**	3.00	2.88	**0.71**	**1.67**	1.83	2.01	2.10	1.97
	RED SNAP	0.73	1.31	2.26	2.60	2.77	**3.08**	**3.04**	0.59	1.53	**1.87**	**2.04**	**2.36**	**2.31**
	S FLOUND	0.69	1.25	2.19	2.55	2.71	**3.06**	**3.03**	0.56	1.50	**1.86**	2.02	**2.37**	**2.34**
	SEATRT	**0.90**	**1.60**	**2.57**	**2.74**	**2.92**	3.02	2.90	**0.70**	**1.67**	1.84	2.02	2.12	2.00
	SHEEPHD	0.49	0.91	1.75	2.20	2.35	2.83	2.86	0.42	1.25	1.71	1.85	**2.34**	**2.37**
	SPAN MAC	0.89	1.58	**2.55**	**2.74**	**2.92**	3.04	2.93	0.69	**1.67**	**1.85**	**2.03**	2.15	2.04
	TUR NEST	0.44	0.83	1.63	2.11	2.24	2.75	2.80	0.38	1.19	1.66	1.80	2.31	**2.35**
	Minimum	-0.97	-1.71	-2.62	-2.74	-2.92	-3.10	-3.04	-0.74	-1.67	-1.88	-2.06	-2.37	-2.37
	Mean	0.17	0.29	0.43	0.42	0.45	0.41	0.37	0.13	0.27	0.25	0.28	0.24	0.20
	Maximum	0.97	1.71	2.60	2.74	2.92	3.10	3.04	0.74	1.68	1.88	2.06	2.37	2.37
	Stnd Dev	0.68	1.21	1.97	2.17	2.32	2.54	2.51	0.53	1.30	1.54	1.69	1.97	1.95
	Stnd Err	0.10	0.17	0.28	0.31	0.33	0.36	0.36	0.08	0.19	0.22	0.24	0.28	0.28

Table 5.2 (Part 2) – Table of all $\Delta_{ab}(Y)$. See Table 5.2 (Part 1) for full description of details of this continuation of that table.

		RS_3 v RS_4	RS_3 v RS_5	RS_3 v RS_6	RS_3 v RS_7	RS_3 v RS_8	RS_4 v RS_5	RS_4 v RS_6	RS_4 v RS_7	RS_4 v RS_8	RS_5 v RS_6	RS_5 v RS_6	RS_5 v RS_8	RS_6 v RS_7	RS_6 v RS_8	RS_7 v RS_8
Lower - TL	MENHADEN	0.41	0.96	1.02	1.68	1.85	**0.56**	**0.62**	**1.28**	**1.44**	0.06	**0.72**	**0.88**	**0.66**	**0.83**	0.16
	N SHRMP	0.61	1.15	1.24	**1.86**	**1.97**	**0.54**	**0.64**	**1.25**	**1.37**	0.10	**0.71**	**0.83**	**0.61**	0.73	0.11
	S SHR 1	-0.91	-0.94	-1.11	-1.04	-0.87	-0.03	-0.20	-0.13	0.04	-0.17	-0.10	0.07	0.07	0.24	0.17
	S SHR 5	-0.94	-1.01	-1.19	-1.17	-1.02	-0.08	-0.25	-0.24	-0.08	-0.18	-0.16	-0.01	0.02	0.17	0.15
Upper - TL	BRD BP BBS	0.89	0.89	1.06	0.96	0.78	0.00	0.17	0.07	-0.11	0.17	0.06	-0.12	-0.11	-0.29	-0.18
	BRD BP CBC	**0.96**	1.26	**1.43**	1.69	1.62	0.29	0.47	0.72	0.66	0.17	0.43	0.37	0.26	0.19	-0.07
	BRD RS BBS	0.85	**1.30**	**1.44**	**1.91**	**1.93**	0.44	**0.59**	1.06	1.08	0.15	0.61	0.64	0.46	0.49	0.02
	BRD RS CBC	-0.93	**-1.30**	**-1.46**	-1.83	-1.80	-0.37	-0.54	-0.90	-0.88	-0.16	-0.53	-0.50	-0.36	-0.34	0.02
	N BN SHARK	-0.96	**-1.27**	**-1.44**	-1.73	-1.67	-0.31	-0.49	-0.77	-0.71	-0.17	-0.46	-0.40	-0.28	-0.23	0.06
	N BT SHARK	**-0.97**	-1.15	-1.33	-1.44	-1.32	-0.18	-0.36	-0.47	-0.35	**-0.18**	-0.29	-0.17	-0.11	0.00	0.12
	N COBIA	0.46	0.12	0.22	-0.27	-0.51	-0.34	-0.24	-0.73	-0.97	0.10	-0.39	-0.63	-0.49	**-0.73**	**-0.24**
	N GAG GR	0.96	1.08	1.26	1.31	1.17	0.13	0.31	0.35	0.21	**0.18**	0.22	0.09	0.05	-0.09	-0.14
	N KING MAC	0.96	1.26	**1.44**	1.70	1.64	0.30	0.47	0.74	0.67	0.17	0.44	0.37	0.26	0.20	-0.06
	N MUTTON	0.90	**1.30**	**1.46**	**1.86**	**1.86**	0.40	0.56	0.96	0.96	0.16	0.56	0.56	0.40	0.40	-0.01
	N SPAN MAC	0.08	0.60	0.60	1.26	1.47	**0.52**	0.52	**1.18**	**1.40**	0.00	0.66	**0.87**	**0.66**	**0.88**	**0.21**
	N TILE E	**-0.97**	-1.21	-1.39	-1.58	-1.49	-0.24	-0.42	-0.61	-0.51	**-0.18**	-0.37	-0.27	-0.19	-0.10	0.09
	N TILE W	-0.88	-0.88	-1.05	-0.93	-0.75	0.01	-0.16	-0.05	0.14	-0.17	-0.05	0.13	0.12	0.30	0.18
	N TRIGGER	-0.89	**-1.30**	**-1.46**	**-1.88**	**-1.89**	-0.42	-0.57	-1.00	-1.00	-0.16	-0.58	-0.59	-0.43	-0.43	0.00
	N YE GR E	-0.94	**-1.29**	**-1.46**	-1.78	-1.75	-0.35	-0.51	-0.84	-0.80	-0.17	-0.50	-0.46	-0.33	-0.29	0.04
	N YE GR W	-0.70	-0.51	-0.65	-0.32	-0.09	0.19	0.05	0.38	0.61	-0.14	0.19	0.42	0.33	0.56	**0.22**

Table 5.2 – Part 2 (Continued)

		RS3 v RS4	RS3 v RS5	RS3 v RS6	RS3 v RS7	RS3 v RS8	RS4 v RS5	RS4 v RS6	RS4 v RS7	RS4 v RS8	RS5 v RS6	RS5 v RS6	RS5 v RS8	RS6 v RS7	RS6 v RS8	RS7 v RS8
Rev.	REV MEX	-0.29	-0.84	-0.88	-1.55	**-1.73**	**-0.55**	**-0.59**	**-1.26**	-1.45	**-0.04**	**-0.71**	**-0.89**	**-0.67**	**-0.86**	-0.18
	REV US	0.83	0.75	0.91	0.71	0.51	-0.08	0.08	-0.11	-0.31	0.16	-0.04	-0.24	-0.20	-0.40	**-0.20**
Structure & Function	DIV LA	-0.72	-1.23	-1.35	**-1.91**	**-1.99**	-0.51	**-0.63**	**-1.20**	-1.28	-0.12	**-0.69**	-0.77	-0.57	-0.65	-0.08
	DIV TX	-0.12	-0.65	-0.66	-1.32	-1.53	**-0.53**	-0.54	**-1.20**	**-1.41**	0.00	**-0.67**	**-0.88**	**-0.67**	**-0.88**	**-0.21**
	EVEN LA	-0.81	**-1.28**	-1.42	**-1.92**	**-1.97**	-0.47	**-0.61**	-1.11	-1.16	-0.14	-0.64	-0.69	-0.50	-0.55	-0.04
	EVEN TX	-0.69	-1.21	-1.32	**-1.90**	**-1.99**	**-0.52**	**-0.63**	**-1.21**	**-1.30**	-0.11	**-0.69**	**-0.78**	-0.58	-0.67	-0.09
	MTL SURV	0.58	1.12	1.22	**1.84**	**1.96**	**0.54**	**0.64**	**1.26**	**1.38**	0.09	**0.72**	**0.84**	**0.62**	**0.75**	0.12
	PD RATIO	-0.26	-0.81	-0.84	-1.52	-1.70	**-0.55**	-0.58	**-1.25**	**-1.44**	-0.03	**-0.70**	**-0.89**	**-0.67**	**-0.86**	**-0.19**
	RICH LA	0.36	-0.03	0.05	-0.49	-0.73	-0.39	-0.31	-0.85	-1.09	0.08	-0.46	-0.70	-0.54	**-0.78**	**-0.24**
	RICH TX	-0.14	-0.68	-0.69	-1.36	-1.56	**-0.54**	-0.55	**-1.21**	**-1.42**	-0.01	**-0.68**	**-0.88**	**-0.67**	**-0.87**	**-0.21**
	MTL COM	-0.64	-1.17	-1.28	**-1.88**	**-1.98**	**-0.53**	**-0.64**	**-1.24**	**-1.34**	-0.10	**-0.71**	**-0.81**	**-0.60**	-0.71	-0.10
	MTL COM2	0.95	**1.28**	**1.45**	1.76	1.72	0.33	0.50	0.81	0.77	0.17	0.48	0.44	0.31	0.27	-0.04
	MTL MEX	**0.97**	1.15	1.33	1.44	1.32	0.18	0.36	0.47	0.35	**0.18**	0.29	0.17	0.11	-0.01	-0.12
	PRED COM	0.21	-0.23	-0.17	-0.77	-1.01	-0.45	-0.39	-0.99	-1.23	0.06	-0.54	-0.78	**-0.60**	**-0.84**	**-0.24**
	PRED COM2	**0.97**	1.22	1.40	1.60	1.51	0.25	0.43	0.62	0.54	**0.18**	0.37	0.29	0.20	0.11	-0.09
	PRED MEX	**0.97**	1.13	1.31	1.40	1.28	0.17	0.34	0.44	0.32	**0.18**	0.27	0.15	0.09	-0.03	-0.12
	MTL REC	**0.97**	1.19	1.36	1.52	1.41	0.21	0.39	0.54	0.44	**0.18**	0.33	0.23	0.15	0.05	-0.10
	PRED REC	**0.96**	1.12	1.30	1.38	1.26	0.16	0.34	0.42	0.29	**0.18**	0.26	0.13	0.08	-0.04	-0.13
	ATL CROK	0.11	0.64	0.65	1.31	1.52	**0.53**	0.54	**1.20**	**1.41**	0.00	**0.67**	**0.88**	**0.67**	**0.88**	**0.21**
	GROW GRA	-0.74	-1.24	-1.36	**-1.92**	**-1.99**	-0.50	**-0.63**	-1.18	-1.26	-0.12	**-0.68**	-0.75	-0.55	-0.63	-0.07
	KINGFSH	**-0.97**	-1.23	-1.41	-1.63	-1.55	-0.26	-0.44	-0.66	-0.58	**-0.18**	-0.39	-0.31	-0.22	-0.14	0.08
	MAMM STR	-0.06	-0.58	-0.58	-1.24	-1.45	**-0.52**	-0.52	-1.18	**-1.39**	0.01	-0.65	**-0.87**	**-0.66**	**-0.88**	**-0.22**
	RED DRUM	**0.97**	1.12	1.30	1.39	1.26	0.16	0.34	0.42	0.30	**0.18**	0.26	0.14	0.08	-0.04	-0.12

Table 5.2 – Part 2 (Continued)

		RS_3 v RS_4	RS_3 v RS_5	RS_3 v RS_6	RS_3 v RS_7	RS_3 v RS_8	RS_4 v RS_5	RS_4 v RS_6	RS_4 v RS_7	RS_4 v RS_8	RS_5 v RS_6	RS_5 v RS_6	RS_5 v RS_8	RS_6 v RS_7	RS_6 v RS_8	RS_7 v RS_8
Structure & Function	RED SNAP	0.95	**1.29**	**1.45**	1.77	1.73	0.34	0.51	0.82	0.78	0.17	0.48	0.44	0.32	0.27	-0.04
	S FLOUND	0.93	**1.30**	**1.46**	1.81	1.78	0.36	0.53	0.87	0.84	0.17	0.51	0.48	0.35	0.32	-0.03
	SEATRT	**0.97**	1.14	1.32	1.42	1.30	0.17	0.35	0.45	0.33	**0.18**	0.28	0.16	0.10	-0.02	-0.12
	SHEEPHD	0.83	**1.29**	**1.43**	**1.92**	**1.95**	0.46	**0.60**	1.08	1.12	0.14	0.63	0.66	0.48	0.51	0.03
	SPAN MAC	**0.97**	1.16	1.34	1.46	1.34	0.19	0.37	0.49	0.37	**0.18**	0.30	0.19	0.12	0.01	-0.11
	TUR NEST	0.80	**1.28**	1.42	**1.92**	**1.97**	0.47	**0.61**	1.12	1.17	0.14	0.65	0.69	0.51	0.55	0.05
	Minimum	-0.97	-1.30	-1.46	-1.92	-1.99	-0.55	-0.64	-1.26	-1.45	-0.18	-0.71	-0.89	-0.67	-0.88	-0.24
	Mean	0.14	0.12	0.15	0.11	0.08	-0.02	0.01	-0.03	-0.06	0.03	-0.01	-0.05	-0.04	-0.07	-0.04
	Maximum	0.97	1.30	1.46	1.92	1.97	0.56	0.64	1.28	1.44	0.18	0.72	0.88	0.67	0.88	0.22
	Stnd Dev	0.79	1.08	1.21	1.55	1.56	0.38	0.48	0.89	0.96	0.14	0.51	0.58	0.43	0.52	0.13
	Stnd Err	0.11	0.15	0.17	0.22	0.22	0.05	0.07	0.13	0.14	0.02	0.07	0.08	0.06	0.07	0.02

After identifying the RS_{ab} pairs of interest and refining the list of response indicators that describe the differences between them, the final ordination diagrams were created. These visualization tools incorporated all of the retained response and predictor indicators that best highlighted the differences between selected RS_{ab} pairs and the pressures that affect them. In this case study, visualizations were created for (1) the three phase shifts between all four long-term *RS*s, as they appeared in the time series, and (2) the terminal states identified for the study period (RS_1 and RS_7) (Figure 5.5). The two panels on the right side of Figure 5.5 illustrate the effect of CA^{I} on the Gulf LME fisheries resource responses, while the two panels on the left highlight the effects of CA^{II} on fisheries regime state.

5.4 DISCUSSION

The utility of EL-FISH is the distillation of large amounts of interconnected data in a way that can be useful for informing fisheries managers and stakeholders undertaking resource management at the ecosystem scale. Specifically, EL-FISH was designed to fit within the IEA process (Figure 5.1), and to utilize time-series data compiled in regional ecosystem status reports (or any other long-term monitoring effort). It is critical that the arrangement of the model's indicator sets are consistent with the scope of a particular management concern if it is to be an effective tool. The Gulf LME example shown here was parameterized to test for impacts of human fishing activities and environmental variability on the overall structure, function, and productivity of the LME's resources. The Gulf LME model's predictors accounted for 72.9% (R^2_{adj}) of the total variability in the ecosystem's fishery resources, and here it was shown that the functional response of the LME has undergone significant reorganizations due to natural and anthropogenic pressures. Fisheries resources reorganized into at least four different long-term

regime states between 1980 and 2011. Relevant fisheries management trade-offs in the Gulf were elucidated by examining the chronological trends in **X** while considering the differences between RS_{ab} pairs during phase shifts (i.e., the time in between the noted chronology of *RS*s). These observations are discussed in more detail below.

Table 5.3 – Correlated predictors and canonical axis weights. Table of predictor indicators ($\mathbf{x}_j$) that were significantly correlated with the first two canonical axes (5,000 iterations; $\alpha = 0.05$). Axis weights from **C**, *p*-values, and subcategory assignments are also given; indicators are sorted by descending $|\mathbf{c}_{jm}|$.

Axis	$\mathbf{x}_j$	$\mathbf{c}_{jm}$	*p*-value	Predictor category
CA^{I}	LAND FIS	2.74	0.0004	Fisheries extraction - Commercial
	NO3 LOAD	2.06	0.0002	Physical environment - Regional
	EFF MEN	1.46	0.0002	Fishing effort - Commercial
	DO LA F	-1.36	0.0138	Physical environment - Local
	AMO MEAN	1.11	0.0002	Climatology - Basin
	REC DAYS	-0.97	0.0020	Fishing effort - Recreational
	OIL SPL	-0.95	0.0092	Resource extraction - Commercial
	MEX INV	-0.86	0.0024	Fisheries extraction - Commercial
	FERT USE	-0.82	0.0006	Physical environment - Regional
	PRECIP	0.81	0.0428	Climatology - Regional
	SST MAX	-0.60	0.0030	Physical environment - Regional
	LAND MEN	-0.56	0.0002	Fisheries extraction - Commercial
	DO TX S	0.45	0.0086	Physical environment - Local
	DO LA S	0.30	0.0004	Physical environment - Local
	DO TX F	-0.26	0.0010	Physical environment - Local
	AWP MEAN	0.20	0.0240	Climatology - Basin
	REC TRIP	0.10	0.0020	Fishing effort - Recreational
	OIL RIGS	-0.09	0.0002	Resource extraction - Commercial
	SST MEAN	-0.01	0.0066	Physical environment - Regional
CA^{II}	LAND FIS	3.21	0.0004	Fisheries extraction - Commercial
	REC DAYS	-1.47	0.0002	Fishing effort - Recreational
	MEX FISH	1.20	0.0002	Fisheries extraction - Commercial
	REC TRIP	-0.71	0.0068	Fishing effort - Recreational
	AWP MEAN	-0.21	0.0368	Climatology - Basin
	OIL SPL	-0.16	0.0488	Resource extraction - Commercial

5.4.1 Gulf LME – Predictor Trends through Time (1980-2011)

Examination of the predictor gradients alongside the ordination of years (Figure 5.4b) allowed the construction of a narrative encapsulating the dynamics of the pressures exerted upon the Gulf LME since 1980. The RDA results indicated the majority of the explained variability in the model was described by CA^{I} (31.96%) with a lesser amount described by CA^{II} (16.18%). Recall that the indicator weightings contained in **C** (Table 5.3) are interpreted as regression coefficients for each predictor along any CA^{m}. The top five numerical influences ($|\mathbf{c}_{jm}| > 1$) along CA^{I} were (1) the total U.S. commercial finfish landings (excluding Gulf menhaden, *Brevoortia patronus*), (2) the total basin load of dissolved inorganic nitrate (NO_3) for the Mississippi river outflow, (3) the U.S. Gulf menhaden fishing effort, (4) the fraction of dissolved oxygen in waters offshore Louisiana during fall, and (5) the annual mean value of the Atlantic Multidecadal Oscillation index (AMO). For CA^{II}, only three of six significantly correlated indicators had $|\mathbf{c}_{j2}| > 1$: (1) total U.S. commercial finfish landings (excl. Gulf menhaden), (2) total number of U.S. recreational fishing days, and (3) total Mexican finfish landings.

While it is notable that both canonical axes were most influenced by U.S. commercial fishing pressure in the Gulf, the indicators influencing CA^{I} were generally from three categories of predictors: (1) fishing pressures, (2) large-scale climatological forcing, and (3) physical-chemical environmental changes (e.g., nutrient loads). Fisheries extractions and effort accounted for 31.5% of all CA^{I} indicators, with an additional 10.5% being representative of oil extraction and pollution. The remaining 58% of influential predictors were indicative of climate dynamics and

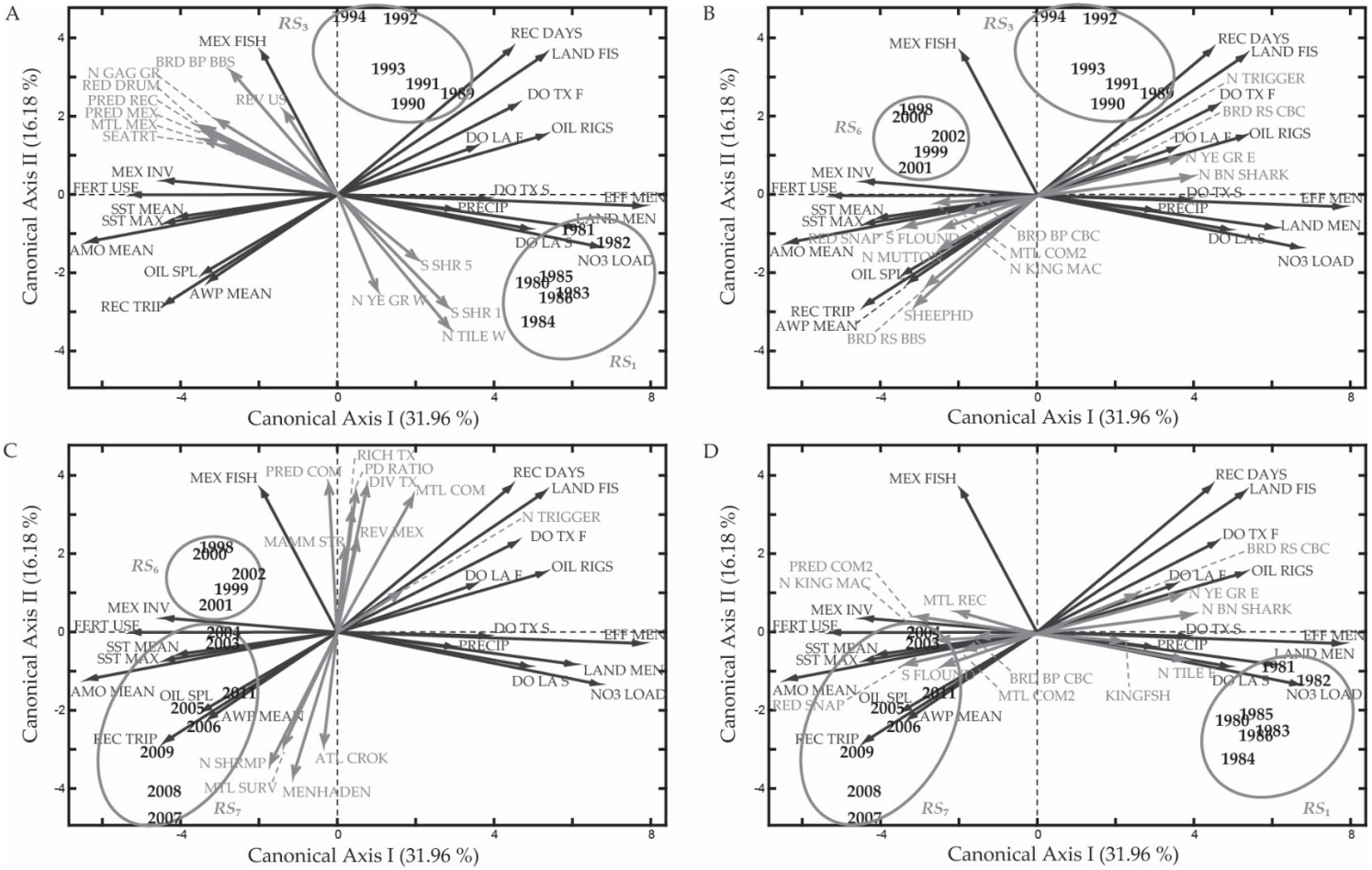

Figure 5.5 – EL-FISH final ordination diagrams for RS_{ab} pairs in the Gulf LME. RDA distance triplots combining all relevant EL-FISH results into reduced ordination plots specific to describing the differences between the regime states noted. Panels describe the chronological order of the Gulf LME's phase shifts from RS_1 to RS_3 (A), then from RS_3 to RS_6 (B), and finally from RS_6 to RS_7 (C). The final panel (D) describes the differences between the two terminal system states in the study period. In all final visualizations, only the $\mathbf{y}_i$ whose $\lambda_{ab} \geq 75^{th}$ percentile and the $\mathbf{x}_j$ that were significantly correlated with CA^I or CA^{II}, were drawn. Indicator gradient vectors were overlain with the ordination of years for only the RS_{ab} pairs of interest; all other years were removed for clarity. Figure symbols and colors are identical to Figure 5.4; see Figure 5.3 for additional details of RDA scaling type-1 distance triplots.

changes in the Gulf's physical-chemical environment that can largely be attributed to the complex teleconnections between the Gulf LME's regional/local dynamics and basin-scale climatological changes (Enfield et al. 2001, Ting et al. 2011, Zhang et al. 2012, Karnauskas et al. 2013, Nye et al. 2014, Karnauskas et al. 2015).

The EL-FISH model results indicated that a primary, large-scale climatic factor organizing Gulf LME fisheries resources was the Atlantic Multidecadal Oscillation, and it captured the generally agreed upon AMO phase shift from a cold (negative) to warm (positive) regime between 1994-1995 (Nye et al. 2014). The AMO index is primarily a measure of sea surface temperature (SST) across the North Atlantic basin, and is hypothesized to have far-reaching teleconnections including those related to ocean circulation (Nye et al. 2014), ocean stratification (Zhang et al. 2012), precipitation patterns (Enfield et al. 2001), and cyclone activity (Vimont and Kossin 2007). Since the phenomenon was only first described around the 1994/1995 phase shift (Schlesinger and Ramankutty 1994), only the dynamics of the change from cold-to-warm phases have been directly observed, and the frequency of the AMO is unknown. The effects attributed to the AMO vary by locale (Nye et al. 2014), and here the contention is that the following physical changes in the Gulf LME were coincident with the 1994/1995 transition of the AMO: (1) increasing Gulf-wide SST mean and maximum values, (2) decreasing regional precipitation, (3) decreasing NO_3 loading from the Mississippi watershed, and (4) decreasing dissolved O_2 concentrations in continental-shelf waters of LA and TX (spring and fall). The Atlantic Warm Pool (AWP) is also a metric for SST, and it tracks closely with the AMO (Appendix D, Figure D.2), but was found to be less influential in the EL-FISH model (Table 5.3). These results agree with Karnauskas et al. (2015) and implicate the AMO index as the climate indicator with the best explanatory power for

the Gulf LME. The AWP is not without merit as an explanatory index, and this is illustrated along both CA^{I} and CA^{II}, where it has a low, but significant influence; however, the numerical effect in both cases is overwhelmed by more prominent indicators (i.e., AMO climate influence and fishing effort and extractions).

It would be misleading to ignore fishing activities and characterize CA^{I} as only the axis of climate forcing and ecosystem change. Indeed, fisheries extractions and pressures underwent great shifts during the period of this study for a multitude of reasons, not the least of which being legislative actions and evolutions in resource management foci and methods (Adams et al. 2000, Smith et al. 2003, Coleman et al. 2004, Karnauskas et al. 2015). The size of the commercial fishing fleet increased throughout the 1980s as a result of federal development programs and the American Fisheries Promotion Act of 1980 (National Research NRC 1994, Hsu and Wilen 1997, Karnauskas et al. 2015), and these increases coincided with peaks in landings of all finfish and fishing effort for Gulf menhaden. Menhaden dominated fish catches in the Gulf throughout the period of this study (Karnauskas et al. 2013), and they continue to be the largest component of modern commercial catches in the Gulf LME (NMFS 2014). While decreasing U.S. commercial extractions of shrimp species are not negligible, the steadily rising Mexican invertebrate extractions had a larger explanatory influence on CA^{I} (Figure 5.4b).

Recreational fishing activity also played an organizing role in the Gulf LME (Coleman et al. 2004, Karnauskas et al. 2015), with both the annual numbers of total individual trips taken by anglers and total fishing days (standardized to a 12-hour fishing day) influencing CA^{I}. The 1980s and early- to mid-1990s were indicative of higher numbers of fishing days and lower individual trips taken, while the late 1990s through the 2010s displayed the opposite trend. Interpretation of

the dynamics in recreational effort are particularly difficult to untangle since there are many potential scenarios that can be constructed to explain them, including changes in seasonal closures, variable operating costs for fishing, fluctuating customer demand, increasing international competition, and weather-related concerns (Adams et al. 2004, McCluskey and Lewison 2008, Carter and Letson 2009, Karnauskas et al. 2013).

Along CA^{II}, the $|\mathbf{c}_{j2}|$ of U.S. finfish landings (excl. Gulf menhaden) was more than double the next ranked weighting, and four of the top five $|\mathbf{c}_{j2}|$ were explicitly related to either commercial or recreational fishing activities (Table 5.3). The dominance of fishing indicators for CA^{II} implies that the vertical variability between *RS*s in Figure 5.4 is largely driven by anthropogenic pressures surrounding resource extraction. Further evidence for human activity being the primary agent of separation along CA^{II} is given by the small, but significant, impact of the annual number of oil spills recorded in the U.S. on CA^{II}. The changes in the oil industry are visualized in Figure 5.4b, where the time periods on the right-hand side of the plot are associated with higher numbers of U.S. oil rigs being installed on an annual basis, and those on the left are more indicative of having fewer new installations. During the period of declining installations, however, there appears to be an increase in oil spills in the Gulf LME.

5.4.2 Gulf LME – Regime States through Time (1980-2011)

For the period 1980-2011, Karnauskas et al. (2015) described one ecosystem-wide phase shift in resource states for the Gulf LME that occurred during the mid-1990s, and they argued that the AMO was a fundamental factor in that shift. The results produced by EL-FISH for the Gulf agree with their assessment that the AMO, and its indirect effects, were major organizing forces in the LME, however, the presence of at least two more ecosystem-wide phase shifts from

1980-2011 were also noted. The relatively orderly chronological progression of the LME's system states leads to the discussion of *RS* phase shifts that follows. However, it is important to note that the order of the *RS* manifestations may or may not be relevant to managers, since it is theoretically possible for an ecosystem's *RS* to change from one observed state to another, while only progressing through new response states not previously considered (or observed). For this reason, EL-FISH results should be interpreted with caution, as they may merely provide justification for additional studies, to determine the validity or mechanism of a cause-and-effect relationship pattern detected, rather than advocating for the implementation of a particular management action.

Four regime states with durations of at least five years were identified by the EL-FISH protocol, and they were accompanied by three chronological phase-shifts. The same major phase-shift demarcated by the end of RS_3 in 1994, as noted by Karnauskas et al. (2015), was captured and described for the Gulf LME marine resources. Additionally, one transitional phase-shift before the onset of RS_3, and a second transitional shift between 2002/2003, were identified by the procedure. The Gulf LME's major response phase-shift was described by examining the $\lambda_{ab}(\mathbf{y}_i)$ for RS_{36} and RS_{17} (Figure 5.5b and Figure 5.5d). Recall that these two RS_{ab} pairs were primarily separated along CA^I, and that this axis described the majority of the variation in $\mathbf{Y}$. Also recall that CA^I was largely explained by changes in the AMO and its teleconnected effects, but also by fishing pressures and regulatory changes. The phrase "major phase-shift" refers to the fact that this phase change is not only represented by the temporally-contiguous state change noted between RS_{36}, but also that this shift in resources was well represented in the comparison of the two endpoint regime states in the time series (RS_{17}), and that the LME's responses revealed by

both comparisons are notably similar. Therefore, this major shift represents the predominant change in the Gulf LME over the 30 year period examined in this study. The two transitional shifts were best described by the differences between RS_{13} and RS_{67}, and were most influenced by CA^{II} (Figure 5.5a and Figure 5.5c), which was almost exclusively characterized by anthropogenic pressures, primarily fishing.

5.4.2.1 Gulf LME major phase-shift. The CA^{I} major phase-shift that occurred in the Gulf LME fisheries response coincides with the change in AMO to a warm water regime in the mid-1990s. The relative stability of the ecosystem state from 1990-1994 (RS_3) abruptly ended, and it was not until 1998 that some apparent system stability returned (RS_6: 1998-2002). The notable differences between RS_{36} were surprisingly consistent with those from RS_{17}, with seven overlapping indicators (Figure 5.5b and Figure 5.5d). The members of RS_{17} represent the two beginning and ending long-term regime states in the time series and are also the two largest subsets of years identified. Therefore, it is safe to postulate that these two *RS*s are more or less the two equilibrium positions for the Gulf LME from 1980-2011, one general resource regime state before the major phase-shift, and one after. The shared ecosystem responses between RS_{36} and RS_{17} were evident in the population statuses of key upper trophic-level species such as abundance decreases in Blacknose Sharks (*Carcharhinus acronotus*) Gray Triggerfish (*Balistes capriscus*) in the northern Gulf, tilefishes (*Caulolatilus spp*. and *Lopholatilus chamaeleonticeps*) and Yellowedge Grouper (*Epinephelus flavolimbatus*) in the northeast, and, according to one survey, Roseate Spoonbills (*Platalea ajaja*). Increases in upper trophic-level abundances were observed for King Mackerel (*Scomberomorus cavalla*) and Mutton Snapper (*Lutjanus analis*), Eastern Brown Pelicans (*Pelecanus occidentalis carolinensis*), and in a second survey for Roseate Spoonbills.

Indicators of resource structure and function, for both mixed species and individual fish stocks, all showed signs of improvement after the transition to a warm AMO phase, and potentially also in response to changing fishing regulatory and capitalization strategies. Individual stock changes included mean fork-length increases for Red Snapper (*Lutjanus campechanus*), Southern Flounder (*Paralichthys lethostigma*), and Sheepshead (*Archosargus probatocephalus*), and also decreasing mean fork-lengths for Southern Kingfish (*Menticirrhus americanus*). Other signs of shifting structure and function included increasing mean trophic-level (MTL) and proportions of predatory fishes in U.S. commercial catches (excl. Gulf menhaden), along with MTLs for recreational catches.

5.4.2.2 Gulf LME transitional phase-shifts. By examining RS_{13}, it was determined which characteristics of the LME first responded to the changing pressures described by CA^{I}, and were then exacerbated by the pressures controlling CA^{II}. Likewise, the RS_{67} transition displayed which fisheries ecosystem qualities began stabilization first after the major phase-shift, and before a more equilibrium-like state was achieved. Even though the RS_{13} and RS_{67} transitions occurred primarily along CA^{II}, which was best described by human fishing activity (Figure 5.5a and Figure 5.5c), the observed responses for the two shifts were wholly different. These differential responses to changing fishing efforts and extractions highlighted the dramatic effect that human activity, particularly in the northern Gulf, had on specific stocks and LME resources. In both cases there was a mix of (1) upper and lower trophic-level responses, (2) structural changes to the resource communities, and (3) fluctuations in revenue patterns for both U.S. and Mexican fishers.

The RS_{13} shift represents the intermediate change between the relatively stable period of the 1980s and the time period just before the major reorganization of the LME. This regime shift

was characterized by decreases in the abundances of two lower trophic-level species in the southern Gulf, Redspotted Shrimp (*Farfantepenaeus brasiliensis*) and Crystal Shrimp (*Sicyonia brevirostris*), and of two upper trophic-level species, Tilefish and Yellowedge Grouper, in the northwestern Gulf. Other notable trends include increasing abundances of Brown Pelicans and Gag (*Mycteroperca microlepis*) in the northern Gulf. Also increasing were the mean fork-lengths of Spotted Seatrout (*Cynoscion nebulosus*) and Red Drum (*Sciaenops ocellatus*), along with the proportion of predatory fishes caught in U.S. recreational catches. Finally, Mexican commercial fisheries responded with increasing MTL and proportion of predatory fishes for catches, and U.S. total commercial revenues rose over this time period.

The second transitional shift, RS_{67}, completes the LME's state trajectory from the major shift in the mid-1990s through a stabilizing period (RS_6) and into a more equilibrium-like system status (RS_7). Unlike the other regime shifts described, the changes in the ecosystem's response between RS_{67} were largely manifest in indicators of individual stocks' or multispecies complexes' structural attributes, with a much less pronounced effect in population-state indices. The response changes during this shift include increases in two lower trophic-level indicators of abundance, Gulf menhaden and all commercial shrimp species, and with decreasing abundances of Gray Triggerfish in the upper trophic food web. Changes to commercial fish stocks were evidenced by decreasing MTL (incl. Gulf menhaden) and proportions of predators in the U.S. catches, also by declining revenues for Mexican fisheries. Fisheries-independent indicators also exhibited declining species richness and diversity values offshore TX (fall only), along with community demographic shifts favoring demersal species over pelagics in the northern Gulf, and with MTL increasing simultaneously. Indicators of positive changes included less frequent

mammal stranding events and increasing mean fork-lengths for Atlantic Croaker (*Micropogonias undulatus*).

5.4.2.3 Gulf LME indicator rates of change. When examined in chronological order, the regime states of the Gulf LME's fisheries resources transitioned in the late 1980s, mostly induced by fishing pressures, before the major state change that is marked by the 1994-1995 AMO phase-shift, and coincident with fisheries regulatory changes (e.g., the Florida net ban initiated in 1995, Adams et al. 2000). After which, another transitional phase change in fisheries resource states was noted between the mid-1990s and early 2000s, and which was once again exacerbated by changing fishing activities. If only RS_{17} were examined, it would appear as though great gains have been made in the overall state of the Gulf LME's fisheries composition and structure, and this result is consistent with others' findings (Karnauskas et al. 2013, Karnauskas et al. 2015). However, these results indicate that for MTL and the proportion of predators in the catches (recreational and commercial, excluding Gulf menhaden, both U.S. and Mexican), $\Delta_{67}(\mathbf{y}_i) << \Delta_{36}(\mathbf{y}_i) < \Delta_{13}(\mathbf{y}_i)$ (Table 5.2). This pattern implies a slowing over time of the gains in MTL and rising numbers of predators in catches, and this result is consistent with analyses of the Gulf fisheries with menhaden and shrimp trends removed (de Mutsert et al. 2008). This slowing-growth trend was also present in the generally improving mean fork-lengths of commercially and recreationally important species such as Red Drum, Spotted Seatrout, and Spanish Mackerel (*Scomberomorus maculatus*).

Other notable indicators displayed this slowing activity only during the major ecosystem transition in the mid-1990s, through the stabilization period lasting until 2002, and into the final long-term regime state in the time series ($\Delta_{67}(\mathbf{y}_i) << \Delta_{36}(\mathbf{y}_i)$). Many generally declining indicators

also showed signs of slowing as the turbulent regime shift captured by CA^{I} passed, and more stability was conferred to the resource pool with increasing time from the disturbance period. However, declines seemed to be overrepresented in indicators of upper trophic-level species abundance, with a notable exceptions being decreasing richness, diversity, and evenness in key fisheries regions of the northern Gulf LME.

5.5 IMPLICATIONS AND FUTURE WORK

Employing the EL-FISH framework allowed the distillation of the large amount information contained in the Gulf of Mexico ESR, and allowed for testing the hypothesis that fisheries resources' structure, function, and status in the Gulf are being affected by anthropogenic pressures and natural ecosystem variability. The interpretation of the EL-FISH results have shown (1) that this relationship does exist in the Gulf LME, (2) that the differential responses in the marine resources can be characterized as long-term regime states, and (3) that phase shifts between RS_{ab} pairs have characteristic dynamics that can be used to describe the trade-offs between ecosystem pressures and resource responses.

The Gulf LME's fisheries resources are sensitive to the basin-scale warming of the North Atlantic Ocean and the teleconnected processes associated with it. These changes induced a long-term major phase-shift in the living marine resources of the Gulf, but they were not the only factors driving the patterns observed. Recreational and commercial fishing activity played large roles in all of the phase shifts described here. Perhaps, the changing pressure from significant fisheries expansions in the 1980s tested the limits of the resources' resilience, conferred by the previous equilibrium period's stability, and eventually pushed the system past a threshold point. Another proposition is that the environment of increasing regulatory restrictions on fishing

activity might have changed the dynamics and structure of the resources by virtue of the changing human usage-patterns directly or indirectly induced by new legislative measures. There is no question that fishing regulatory changes had profound effects on the function and stability of fisheries resources in the Gulf LME; however, there is much to be learned regarding the effects of individual management decisions. Direct testing and evidence are required to say with certainty that any management action had a quantifiable and direct effect on the outcome of any marine resource, and the use of empirical simulation studies or marine strategy evaluations (Sainsbury et al. 2000, Levin et al. 2009, Wayte 2009) to examine any trade-offs uncovered here is strongly encouraged.

The causal implications elucidated by EL-FISH between predictor trajectories and the dynamics of any regime shift should be interpreted as justification for more detailed studies, or as support for continued long-term monitoring efforts and research. Several important commercial and recreational Gulf species displayed marked changes over the period of this study, and potential improvements to predictive and/or assessment models could be made immediately by adding considerations of (1) large-scale climate effects, (2) other species with analogous or cascading responses, as determined by EL-FISH, or (3) trends in rates of change for specific subsets of indicators at well-defined intervals (i.e., defensible regime state periods).

Finally, among the greatest advantages of the IEA assessment loop are its iterative and adaptive qualities. EL-FISH fits into the IEA loop at all five critical components, and can be used to narrow the focus during complex management evaluations while taking competing pressures and responses into account. This is especially useful in management systems covering large areal extents, containing many management stakeholders and interest groups, and/or having

diverse aquatic resources and coastal communities reliant upon them. Even within the context of this Gulf of Mexico large marine ecosystem case study, additional configurations of the 100+ indicators contained within the ESR could be used to investigate other management inquiries. The EL-FISH protocol is a transferrable and powerful tool that can be used to distill large and complex, ecosystem-level indicator datasets, and to provide subsets of relevant indicators for future consideration or implementation in ecosystem-based management efforts.

5.6 LITERATURE CITED

Adams, C., S. Jacob, and S. Smith. 2000. What happened after the net ban? FE 123. University of Florida IFAS Extension, Gainesville.

Adams, C. M., E. Hernandez, and J. C. Cato. 2004. The economic significance of the Gulf of Mexico related to population, income, employment, minerals, fisheries and shipping. Ocean & Coastal Management **47**:565-580.

Anderson, M. J. 2001. Permutation tests for univariate or multivariate analysis of variance and regression. Canadian journal of fisheries and aquatic sciences **58**:626-639.

Andrews, K., G. Williams, and V. Gertseva. 2013. Anthropogenic Drivers and Pressures. California Current Integrated Ecosystem Assessment: Phase II Report 2012, PS Levin, BK Wells, and MB Sheer, eds.

Ault, J. S., J. A. Bohnsack, S. G. Smith, and J. G. Luo. 2005a. Towards sustainable multispecies fisheries in the Florida, USA, coral reef ecosystem. Bulletin of Marine Science **76**:595-622.

Ault, J. S., S. G. Smith, and J. A. Bohnsack. 2005b. Evaluation of average length as an estimator of exploitation status for the Florida coral-reef fish community. Ices Journal of Marine Science **62**:417-423.

Bowen, R. E., and C. Riley. 2003. Socio-economic indicators and integrated coastal management. Ocean & Coastal Management **46**:299-312.

Carter, D. W., and D. Letson. 2009. Structural Vector Error Correction Modeling of Integrated Sportfishery Data. Marine Resource Economics **24**:19-41.

Christensen, N. L., A. M. Bartuska, J. H. Brown, S. Carpenter, C. D'Antonio, R. Francis, J. F. Franklin, J. A. MacMahon, R. F. Noss, D. J. Parsons, C. H. Peterson, M. G. Turner, and R.

G. Woodmansee. 1996. The Report of the Ecological Society of America Committee on the Scientific Basis for Ecosystem Management. Ecological Applications **6**:665-691.

Clarke, K. R., P. J. Somerfield, and R. N. Gorley. 2008. Testing of null hypotheses in exploratory community analyses: similarity profiles and biota-environment linkage. Journal of Experimental Marine Biology and Ecology **366**:56-69.

Coleman, F. C., W. F. Figueira, J. S. Ueland, and L. B. Crowder. 2004. The impact of United States recreational fisheries on marine fish populations. Science **305**:1958-1960.

Coleman, F. C., C. C. Koenig, and L. A. Collins. 1996. Reproductive styles of shallow-water groupers (Pisces: Serranidae) in the eastern Gulf of Mexico and the consequences of fishing spawning aggregations. Environmental Biology of Fishes **47**:129-141.

de Mutsert, K., J. H. Cowan, T. E. Essington, and R. Hilborn. 2008. Reanalyses of Gulf of Mexico fisheries data: Landings can be misleading in assessments of fisheries and fisheries ecosystems. Proceedings of the National Academy of Sciences of the United States of America **105**:2740-2744.

Enfield, D. B., A. M. Mestas-Nunez, and P. J. Trimble. 2001. The Atlantic multidecadal oscillation and its relation to rainfall and river flows in the continental US. Geophysical Research Letters **28**:2077-2080.

Ezekiel, M. 1930. Methods of Ccorrelation Analysis. John Wiley and Sons, New York

Hilborn, R. 2011. Future directions in ecosystem based fisheries management: A personal perspective. Fisheries Research **108**:235-239.

Hilborn, R. 2012. The evolution of quantitative marine fisheries management 1985-2010. Natural Resource Modeling **25**:122-144.

Hsu, S. L., and J. E. Wilen. 1997. Ecosystem management and the 1996 Sustainable Fisheries Act. Ecology Law Quarterly **24**:799-811.

Jennings, S. 2005. Indicators to support an ecosystem approach to fisheries. Fish and Fisheries **6**:212-232.

Jones, D. L. 2017. The Fathom Toolbox for MATLAB. University of South Florida, College of Marine Science, St. Petersburg, FL.

Karnauskas, M., M. J. Schirripa, J. K. Craig, G. S. Cook, C. R. Kelble, J. J. Agar, B. A. Black, D. B. Enfield, D. Lindo-Atichati, B. A. Muhling, K. M. Purcell, P. M. Richards, and C. Z. Wang. 2015. Evidence of climate-driven ecosystem reorganization in the Gulf of Mexico. Global Change Biology **21**:2554-2568.

Karnauskas, M., M. J. Schirripa, C. R. Kelble, G. S. Cook, and J. K. Craig. 2013. Ecosystem status report for the Gulf of Mexico. Pages 1-52 *in* N. U.S. Department of Commerce, editor.

Kelble, C. R., D. K. Loomis, S. Lovelace, W. K. Nuttle, P. B. Ortner, P. Fletcher, G. S. Cook, J. J. Lorenz, and J. N. Boyer. 2013. The EBM-DPSER Conceptual Model: Integrating Ecosystem Services into the DPSIR Framework. Plos One **8**.

Kilborn, J. P. 2017. The Darkside Toolbox for Matlab. University of South Florida, College of Marine Science, St. Petersburg, FL.

Kilborn, J. P., D. L. Jones, E. B. Peebles, and D. F. Naar. 2017. Resemblance profiles as clustering decision criteria: Estimating statistical power, error, and correspondence for a hypothesis test for multivariate structure. Ecology and Evolution **7**:2039-2057.

Kumpf, H., K. A. Steidinger, and K. Sherman. 1999. The Gulf of Mexico large marine ecosystem: assessment, sustainability, and management. Blackwell Science, Malden, Mass., USA.

Larkin, P. A. 1996. Concepts and issues in marine ecosystem management. Reviews in Fish Biology and Fisheries **6**:139-164.

Legendre, P., and L. Legendre. 2012. Numerical Ecology. Third English edition edition. Elsevier, Amsterdam, The Netherlands.

Leggett, W. C., and K. T. Frank. 2008. Paradigms in fisheries oceanography. Pages 331-+ *in* R. N. Gibson, R. J. A. Atkinson, and J. D. M. Gordon, editors. Oceanography and Marine Biology: An Annual Review, Vol 46. Crc Press-Taylor & Francis Group, Boca Raton.

Levin, P. S., M. J. Fogarty, S. A. Murawski, and D. Fluharty. 2009. Integrated Ecosystem Assessments: Developing the Scientific Basis for Ecosystem-Based Management of the Ocean. PLoS Biol **7**:e1000014.

Levin, P. S., and C. Mollmann. 2015. Marine ecosystem regime shifts: challenges and opportunities for ecosystem-based management. Philosophical Transactions of the Royal Society B-Biological Sciences **370**:8.

Link, J. 2016. Ecosystem-Based Fisheries Management Policy. Pages 1-8. U.S. Department of Commerce, NOAA, National Marine Fisheries Service, Washington, DC.

Link, J. S. 2005. Translating ecosystem indicators into decision criteria. Ices Journal of Marine Science **62**:569-576.

Link, J. S., S. Gaichas, T. J. Miller, T. Essington, A. Bundy, J. Boldt, K. F. Drinkwater, and E. Moksness. 2012. Synthesizing lessons learned from comparing fisheries production in 13

northern hemisphere ecosystems: emergent fundamental features. Marine Ecology Progress Series **459**:293-302.

Manly, B. F. 2006. Randomization, bootstrap and Monte Carlo methods in biology. Chapman & Hall/CRC Press, Boca Raton.

Matlab. R2014. The MathWorks, Inc., Natick, Massachusetts, United States.

McCluskey, S. M., and R. L. Lewison. 2008. Quantifying fishing effort: a synthesis of current methods and their applications. Fish and Fisheries **9**:188-200.

Miller, J. K., and S. D. Farr. 1971. Bimultivariate redundancy: a comprehensive measure of interbattery relationship. Multivariate Behavioral Research **6**:313-324.

Mollmann, C., and R. Diekmann. 2012. Marine ecosystem regime shifts induced by climate and overfishing: a review for the northern hemisphere. Pages 303-347 *in* G. Woodward, U. Jacob, and E. J. Ogorman, editors. Advances in Ecological Research, Vol 47: Global Change in Multispecies Systems, Pt 2. Elsevier Academic Press Inc, San Diego.

Niemeijer, D., and R. S. de Groot. 2008. Framing environmental indicators: moving from causal chains to causal networks. Environment, Development and Sustainability **10**:89-106.

NMFS. 2014. Fisheries Economics of the United States, 2012. Pages 1-175 *in* T. M. NMFS-F/SPO-137, editor., U.S. Department of Commerce, NOAA.

NOAA. 2009. Ecosystem Assessment Report for the Northeast U.S. Continental Shelf Large Marine Ecosystem. Page 34 *in* T. M. Ref Doc. 09-11, editor. U.S. Department of Commerce, Northeast Fish Sci Cent.

NRC. 1994. Improving the management of US marine fisheries. National Acadamies Press, National Research Council, Washington, DC.

Nye, J. A., M. R. Baker, R. Bell, A. Kenny, K. H. Kilbourne, K. D. Friedland, E. Martino, M. M. Stachura, K. S. Van Houtan, and R. Wood. 2014. Ecosystem effects of the Atlantic Multidecadal Oscillation. Journal of Marine Systems **133**:103-116.

Ohtani, K. 2000. Bootstrapping R-2 and adjusted R-2 in regression analysis. Economic Modelling **17**:473-483.

Rao, C. R. 1964. The use and interpretation of principal component analysis in applied research. Sankhyā: The Indian Journal of Statistics, Series A:329-358.

Rohlf, F. J. 1963. Classification of Aedes by numerical taxonomic methods (Diptera: Culicidae). Annals of the Entomological Society of America **56**:798-804.

Sainsbury, K. J., A. E. Punt, and A. D. M. Smith. 2000. Design of operational management strategies for achieving fishery ecosystem objectives. Ices Journal of Marine Science **57**:731-741.

Schlesinger, M. E., and N. Ramankutty. 1994. An oscillation in the global climate system of period 65-70 years. Nature **367**:723-726.

Smith, S., S. Jacob, M. Jepson, and G. Israel. 2003. After the Florida net ban: The impacts on commercial fishing families. Society & Natural Resources **16**:39-59.

ter Braak, C. J. F. 1994. Canonical community ordination. Part I: Basic theory and linear methods. Écoscience **1**:127-140.

Ting, M. F., Y. Kushnir, R. Seager, and C. H. Li. 2011. Robust features of Atlantic multi-decadal variability and its climate impacts. Geophysical Research Letters **38**:6.

Tscherning, K., K. Helming, B. Krippner, S. Sieber, and S. G. Y. Paloma. 2012. Does research applying the DPSIR framework support decision making? Land Use Policy **29**:102-110.

Vimont, D. J., and J. P. Kossin. 2007. The Atlantic meridional mode and hurricane activity. Geophysical Research Letters **34**.

Wayte, S. 2009. Evaluation of new harvest strategies for SESSF species. Australian Fisheries Management Authority and CSIRO Marine and Atmospheric Research, Hobart. 137p.

Wernberg, T., S. Bennett, R. C. Babcock, T. de Bettignies, K. Cure, M. Depczynski, F. Dufois, J. Fromont, C. J. Fulton, R. K. Hovey, E. S. Harvey, T. H. Holmes, G. A. Kendrick, B. Radford, J. Santana-Garcon, B. J. Saunders, D. A. Smale, M. S. Thomsen, C. A. Tuckett, F. Tuya, M. A. Vanderklift, and S. Wilson. 2016. Climate-driven regime shift of a temperate marine ecosystem. Science **353**:169-172.

Zhang, L. P., C. Z. Wang, and L. X. Wu. 2012. Low-frequency modulation of the Atlantic warm pool by the Atlantic multidecadal oscillation. Climate Dynamics **39**:1661-1671.

CHAPTER SIX:

RESEARCH IMPACTS AND CONCLUDING REMARKS

6.1 RESEARCH OVERVIEW

The stated purpose of this dissertation was to develop frameworks to help researchers avoid inherent biases specifically associated with temporal and spatial factors in marine fisheries ecology. To that end, I presented three case studies and one data simulation study, all focused on those stated goals. Recall that in Chapter Two and Chapter Three, I explored the groundfish survey data collected throughout the West Florida Shelf (WFS) during the summers of 2010-2012, in the eastern Gulf of Mexico. In Chapter Four, I tested the statistical limits of a popular new clustering algorithm using data simulation techniques, and the resulting recommendations were applied to real-world ecosystem monitoring data in the work presented in Chapter Five. In that chapter, I focused on a large-scale time-series study of the Gulf of Mexico large marine ecosystem (Gulf LME) from 1980-2011, and I described a new conceptual framework, called the ecosystem-level fisheries indicator selection heuristic (EL-FISH), that I developed to distill complex sets of ecosystem indicators representing resource and system structure and function.

6.1.1 Chapter Two Summary

Chapter Two focused on the groundfish trawl data collected by the Southeast Area Monitoring and Assessment Program (SEAMAP) in the summer seasons of 2010-2012 throughout the WFS. The ultimate aims of the first scientific chapter were: (1) to assess the extent to which

the daytime and nighttime fish communities differed from one another, and (2) to quantitatively define the temporal boundary between these communities, should it exist. Further aims of the study were (3) to determine if it was acceptable to use all three years of data to model one fish community (or pair of diel communities), or if they should be examined on a year-by-year basis.

These simple questions evoke implicit spatial and temporal scales of inquiry that are often assumed in many studies to be of negligible impact. By explicitly examining these, normally implied, lines of questioning, extremely complex multivariate patterns emerged which allowed me to (1) make specific recommendations regarding the timing of diel fish-community compositional changes on the WFS, (2) describe differential responses in these two communities to environmental variability, and (3) provide evidence for a large-scale event that disproportionately affected the nighttime communities, persisted for over one year, and which was coincidentally timed with the *Deepwater Horizon* oil spill.

6.1.2 Chapter Three Summary

Chapter Three used the same dataset as in Chapter Two, but here I explored it from a spatial perspective, using the temporal recommendations from the previous chapter. In this chapter the data were examined independently by year, and by daytime and nighttime surveys within years. Here, the ultimate goal was to partition the variability in groundfish beta-diversity into the (1) pure-spatial, (2) pure-environmental, and (3) mixed, spatial-environmental portions, and to determine their influence on the organization of the groundfishes. This was accomplished using explicit spatial-modeling and variable-selection techniques.

Once again, simple questions regarding the within-shelf spatial variability revealed organizational patterns in the biology of the WFS at scales of inquiry that might normally be

overlooked, particularly at the larger-than-shelf spatial scale. Here I showed that a large-scale event affected the nighttime groundfish communities across the WFS in 2010 and 2011, and that it was operating at a spatial scale greater than the full areal extent of the SEAMAP sampling design. I also show that the daytime SEAMAP sampling survey captured a small amount of spatially-structured abiotic control over groundfish beta-diversity, and a relatively large portion of non-spatial abiotic organization.

6.1.3 Chapter Four Summary

Developing new multivariate clustering techniques has been an active research area for many years, and recently a new method was developed that has gained popularity among ecologists. This method works by employing numerical profiles based on the resemblances between all pairs of objects in a dataset, and uses them in conjunction with more commonly used clustering approaches as a decision criterion. In Chapter Four, we attempted to rigorously scrutinize the results of this new clustering algorithm using a series of unstructured and structured, multivariate data-simulations. The data properties were varied such that we could test for the effects of (1) the probability distribution of the underlying data, (2) the number of groups, (3) the amount of group data cloud overlap in multivariate space, (4) the within group dispersions, and (5) the within group correlation structures among descriptors.

The results from this study showed that the new algorithm had acceptable type-I error rates for $\alpha = 0.05$, which were (1) binomially distributed about ~5%, and (2) resistant to the effects of the dataset dimensionality (both the number of objects and descriptors) as well as to (3) the underlying probability distribution. The power of the method to detect structure was within acceptable limits for datasets with at least ten descriptors if the group centroids were not co-

located in multivariate space. Within these conditions, acceptable clustering returns were found even with (1) group data cloud overlap reaching up to 50%, (2) increasing overdispersion in ecological datasets, (3) and increasing correlation structures. Finally, it was also noted that the power for this test for multivariate structure increases as the number of descriptors increases.

6.1.4 Chapter Five Summary

In Chapter Five, I developed and presented the EL-FISH protocol for investigating large marine ecosystems, and which fits into the integrated ecosystem assessment (IEA) conceptual framework advocated within the United States, at the national fisheries management level. The purpose of the case study presented for the Gulf LME was to determine if it were possible to explicitly model, and account for, the effects of anthropogenic and natural pressures on the valuable living marine resources in the Gulf. More specifically, I was interested in characterizing the structure and function of the fisheries resources from 1980-2011, using indicators of individual and multispecies (1) stock abundance, (2) size structure, (3) diversity and richness, (4) trophic qualities, and (5) revenues. Using these indices, the clustering methods explored in Chapter Four were used to identify groups of years with similar fisheries resource structure and functioning (i.e., long-term regime states). I also developed a new numerical tool to qualitatively describe the differences between any two regime states, in a quantitatively defensible manner, with respect to the underlying response gradients that were used to define them. Finally, using the response-predictor framework, EL-FISH tested for an effect of a set of predictors on the fisheries ecosystem's resources response. The predictors were parameterized to represent the factors that I hypothesized would most affect the Gulf's living marine resources. These indicators were drawn from categories such as: (1) fishing pressures and Gulf LME resource extractions, (2) large-

scale climate variability [e.g., Atlantic Multidecadal Oscillation (AMO)], and (3) small-scale physical-environmental system characteristics (e.g., dissolved nutrient concentrations and/or precipitation levels).

After the imposition of the EL-FISH protocol on the dataset for the Gulf LME, the results highlighted four long-term fisheries regime states, and three phase shifts from 1980-2011. I was able to describe a major resource reorganization that manifested in the system, and which could be described by comparing the regime states from the beginning of the time period, encompassing the years 1980-1986, with that of the final system state during the years 2003-2009, and 2011. The same manifestation in responses was also recorded for the inflection period of this major state-change, which was characterized by examining the phase shift between the 1990-1995 regime state and the 1998-2002 state. This major phase-shift was coincident with the AMO phase change from a cold to a warm regime in 1994/1995, and with a series of capitalization and regulatory changes to the fishing activities in the Gulf over the entire period of the study. In addition to the major phase-shift, I recorded two other phase shifts, previously undescribed, that point to human fishing activities as being major drivers of these changes, and potentially implicate fishing activities as being reductive to the resilience of the fisheries resources in the face of major climate-regime phase changes.

6.2 RESEARCH IMPACTS

6.2.1 Chapter Two Impacts

The results of Chapter Two will help researchers quantitatively define the time of day when groundfish samples collected on the WFS change from being representative of daytime to nighttime communities, by using the local nautical twilight times. This will allow analysts to

retain a greater number of samples for testing hypotheses related to these unique communities, as the method essentially eliminates the crepuscular definition and creates a binary categorization. These results are also impactful because I was able to detect a large-scale temporal signature of a disturbance event that affected the environment in 2010, and which declined rapidly after 2011. This event was noted in a lagged biological-response that began in 2010, peaked in 2011, and subsided in 2012; it was also only detectable in the nighttime communities.

6.2.2 Chapter Three Impacts

The work from Chapter Three, and the previous chapter, affirms the importance of treating the representative assemblage of nighttime groundfishes on the WFS explicitly. This chapter also highlighted the challenges to examining spatially-induced organization of abiotic and biotic resources, given the limitations of the SEAMAP sampling strategy for this unique shelf ecosystem. In short order, increasing the spatial sampling resolution for nighttime operations would increase the ability to detect sub-shelf scale spatial variability within those resources. Additional resolution would benefit daytime survey analyses as well, as it was the case that generally well defined spatial trends in depth, temperature, and salinity gradients were the most well explained patterns in the model results I obtained. This could mean that these are the only variables that require spatial considerations on the WFS, but given the high proportions of unexplained variability in all of the models, it is more likely that either (1) the appropriate variables have not been measured, or (2) the sampling resolution is too poor to capture more subtle spatial trends within the WFS ecosystem.

This chapter outlined potential changes to the sampling protocol that might benefit spatial analyses. It also succeeded in describing the partitioning of the daytime variability while it

highlighted where additional focus could be paid within years, and by survey type (day or nighttime). Finally, Chapter Three's results also provide additional context for researchers who wish to consider more explicitly any of the individual components of organizational control (i.e., pure-spatial, pure-abiotic, or mixed spatial-abiotic) that were identified for any particular sub-division of the survey data in time (e.g., 2010 daytime, or 2012 nighttime).

6.2.3 Chapter Four Impacts

The primary goal of Chapter Four was to determine if clustering with resemblance profiles as decision criteria represented a methodological advancement in clustering ecological datasets, and to define the limits of the algorithm's ability to reliably detect homogeneity. It became apparent that the method, originally developed with species composition and abundance data in mind, is marginally appropriate for such datasets. In fact, the resolution of the clustering solutions (i.e., the number of groups detected) for ecological count data is highly affected by within-group correlation and overdispersion patterns among descriptors. These effects were mitigated when clustering well defined groups with low levels of data cloud overlap, but these structural characteristics are often unknown (hence the need for clustering). Therefore, in the set of recommendations that were produced, we strongly cautioned researchers who intend to use these methods for beta-diversity studies.

A full set of recommendations were presented for the scientific community to consider, when employing these clustering techniques. They were: (1) Excessive group overlap in hyperspace (i.e., greater than 50%) may render these clustering techniques unreliable, therefore it is advisable to utilize data exploration techniques prior to cluster analysis; (2) Medium-to-high correlation structures among descriptors (i.e., greater than 0.6) should be avoided and, therefore,

clustering multispecies composition and abundance data may benefit from employing a data-reduction strategy either to reduce the number of correlates, or to orthogonalize the descriptors; (3) Multivariate datasets subjected to these clustering techniques should contain at least 25 descriptors for maximum efficiency; and (4) Slightly less reliable, but still acceptable, clustering results may be achieved using a minimum of 10 descriptors.

6.2.4 Chapter Five Impacts

The EL-FISH work in Chapter Five highlighted the trade-offs present in a complex and dynamic LME like the Gulf of Mexico, specifically with respect to the fisheries resources structure and function, and to the natural and anthropogenic drivers that affect them. The conceptual framework provided gives researchers and resource managers a new tool that can be utilized to distill large quantities of monitoring data (i.e., indicators) into a format that can be more readily digested, and which highlights and exposes (1) the temporal system-states present for important resources, (2) a defensible description of the differences between those states, (3) the influential drivers affecting those state phase-shifts observed, and (4) the trade-offs between resource states and the pressures that affect them.

The EL-FISH protocol was applied to the Gulf LME, and the results could be immediately applicable to resource managers and stakeholders. I described two new long-term fisheries resource regime states in the period of 1980-2011 that were previously undocumented. I also provide supporting evidence for an already identified phase shift associated with the 1994/1995 AMO phase change. The results provide justification for incorporating the AMO, and/or any other teleconnected processes representing large-scale climate state changes, into any existing models for either (1) the Gulf LME as a whole, (2) single-species stocks, or (3) multi-species

complexes. Evidence was also presented describing the large roles that fishing effort and extractions played in organizing fisheries resources. Regulatory changes and human-usage patterns had profound effects throughout the 30-year period of the study, however, more explicit effort should be undertake to determine the extent to which any particular management action affected any single- or mixed-species responses noted by EL-FISH. Finally, note that the two newly described phase shifts in Chapter Five were almost exclusively the result of fishing activity changes through time.

6.3 CONCLUDING REMARKS

All four of the substantive chapters of this dissertation provided case studies showcasing methods for avoiding particular assumptions and biases associated with temporal, spatial, or methodological analyses or datasets. In the two chapters focusing on the WFS, a framework for analyzing *through* the different influential scales of inquiry was presented. These studies highlighted the complexity of the Gulf LME, and the various temporal and spatial scales that influence the patterns observed within it. It should also be noted that these two analyses were initially based upon simple sets of questions and, by using a hierarchical approach to analysis, I was able to make interpretations well beyond the scope of the initial inquiries.

Chapters Four and Five were both much more technically complex than the previous two chapters. However, once again, they represented departures from the normal operations of researchers, and both attempted to explore new methodologies that could be employed to aid in reducing assumptions, biases, and errors in decision making. The data simulation study in Chapter Four produced tangible recommendations that should be implemented immediately for anyone using those methods. As I described in Chapter Five, EL-FISH is a readily transferrable

method that plugs into the IEA framework and is currently available to resource managers and stakeholders seeking to provide important context to the decision making process.

This dissertation is the culmination of work focused on helping researchers (including the author) to (1) refine their study questions, (2) consider appropriate scales of inquiry, (3) avoid arbitrary decision making, and (4) identify and describe the interconnections and dynamic complexities of large marine ecosystems with respect to their biotic and abiotic descriptors. In developing these tools and frameworks, I have hopefully stumbled upon useful methods that will aid future investigators in their efforts. Specifically, I encourage others to consider the recommendations made here regarding (1) the definition of daytime and nighttime species assemblages on the WFS, (2) the importance of the nighttime communities to the description of marine ecosystem health, (3) the inter-annual variability of fish assemblages on the WFS, (4) the efficacy of clustering with resemblance profiles, and how to avoid potential pitfalls, (5) the identification and description of ecosystem-level resource regime states, and (6) the elucidation of trade-offs and context surrounding potential ecosystem management decisions for large marine environments. Furthermore, the techniques developed and demonstrated here are fully transferrable, and it is my sincere hope that some of these methods will become more widely used by the greater research community.

APPENDIX A:

CHAPTER TWO SUPPLEMENTAL TABLES

A.1 SUPPLEMENTAL TABLES

Table A.1 – Vertebrate species captured in trawl samples. A comprehensive list of all individual vertebrate species captured via groundfish trawl sampling in the SEAMAP operations on the west Florida shelf during the years 2010-2012. Only species that were present in all three years of sampling were retained for analyses and represented here. All names were taken from the American Fisheries Society (AFS) naming guide (Page et al. 2013); scientific and common names in parentheses were drawn directly from the SEAMAP database. Parenthetical family names are the accepted AFS common families.

Family (English)	Scientific Name	Common Name
Antennariidae (frogfishes)	*Fowlerichthys ocellatus* (*Antennarius ocellatus*)	Ocellated Frogfish
Antennariidae (frogfishes)	*Fowlerichthys radiosus*(*Antennarius radiosus*)	Singlespot Frogfish (Big-Eyed Frogfish)
Apogonidae (cardinalfishes)	*Apogon affinis*	Bigtooth Cardinalfish
Apogonidae (cardinalfishes)	*Apogon aurolineatus*	Bridle Cardinalfish
Apogonidae (cardinalfishes)	*Apogon pseudomaculatus*	Twospot Cardinalfish
Apogonidae (cardinalfishes)	*Apogon quadrisquamatus*	Sawcheek Cardinalfish
Apogonidae (cardinalfishes)	*Astrapogon alutus*	Bronze Cardinalfish
Apogonidae (cardinalfishes)	*Phaeoptyx pigmentaria*	Dusky Cardinalfish
Apogonidae (cardinalfishes)	*Phaeoptyx xenus*	Sponge Cardinalfish
Ariommatidae (ariommatids)	*Ariomma regulus*	Spotted Driftfish

Table A.1 (Continued)

Balistidae (triggerfishes)	*Balistes capriscus*	Gray Triggerfish
Batrachoididae (toadfishes)	*Opsanus pardus*	Leopard Toadfish
Batrachoididae (toadfishes)	*Porichthys plectrodon*	Atlantic Midshipman
Blenniidae (combtooth blennies)	*Parablennius marmoreus*	Seaweed Blenny
Bothidae (lefteye flounders)	*Bothus ocellatus*	Eyed Flounder
Bothidae (lefteye flounders)	*Bothus robinsi*	Twospot Flounder
Carangidae (jacks)	*Caranx crysos*	Blue Runner
Carangidae (jacks)	*Chloroscombrus chrysurus*	Atlantic Bumper
Carangidae (jacks)	*Decapterus punctatus*	Round Scad
Carangidae (jacks)	*Selene vomer*	Lookdown
Carangidae (jacks)	*Seriola zonata*	Banded Rudderfish
Carangidae (jacks)	*Trachurus lathami*	Rough Scad
Carcharhinidae (requiem sharks)	*Carcharhinus acronotus*	Blacknose Shark
Carcharhinidae (requiem sharks)	*Rhizoprionodon terraenovae*	Atlantic Sharpnose Shark
Chaetodontidae (butterflyfishes)	*Chaetodon ocellatus*	Spotfin Butterflyfish
Chaetodontidae (butterflyfishes)	*Chaetodon sedentarius*	Reef Butterflyfish
Chaetodontidae (butterflyfishes)	*Prognathodes aya* (*Chaetodon aya*)	Bank Butterflyfish
Clupeidae (herrings)	*Opisthonema oglinum*	Atlantic Thread Herring
Clupeidae (herrings)	*Sardinella aurita*	Spanish Sardine (Round Sardinella)
Congridae (conger eels)	*Paraconger caudilimbatus*	Margintail Conger
Cynoglossidae (tonguefishes)	*Symphurus diomedeanus*	Spottedfin Tonguefish
Cynoglossidae (tonguefishes)	*Symphurus plagiusa*	Blackcheek Tonguefish
Cynoglossidae (tonguefishes)	*Symphurus urospilus*	Spottail Tonguefish
Dasyatidae (whiptail stingrays)	*Dasyatis centroura*	Roughtail Stingray (Clam Cracker)
Diodontidae (porcupinefishes)	*Chilomycterus schoepfi*	Striped Burrfish

Table A.1 (Continued)

Echeneidae (remoras)	*Echeneis naucrates*	Sharksucker
Echeneidae (remoras)	*Echeneis neucratoides*	Whitefin Sharksucker
Ephippidae (spadefishes)	*Chaetodipterus faber*	Atlantic Spadefish
Epinephelidae (groupers)	*Epinephelus morio*	Red Grouper
Epinephelidae (groupers)	*Hyporthodus flavolimbatus* (*Epinephelus flavolimbatus*)	Yellowedge Grouper
Epinephelidae (groupers)	*Mycteroperca microlepis*	Gag
Epinephelidae (groupers)	*Mycteroperca phenax*	Scamp
Gerreidae (mojarras)	*Eucinostomus argenteus*	Spotfin Mojarra
Gerreidae (mojarras)	*Eucinostomus gula*	Silver Jenny
Gerreidae (mojarras)	*Eucinostomus harengulus*	Tidewater Mojarra
Gobiesocidae (clingfishes)	*Gobiesox strumosus*	Skilletfish
Haemulidae (grunts)	*Anisotremus virginicus*	Panamic Porkfish
Haemulidae (grunts)	*Haemulon aurolineatum*	Tomtate
Haemulidae (grunts)	*Haemulon plumieri*	White Grunt
Haemulidae (grunts)	*Haemulon striatum*	Striped Grunt
Haemulidae (grunts)	*Orthopristis chrysoptera*	Pigfish
Holocentridae (squirrelfishes)	*Sargocentron bullisi* (*Holocentrus bullisi*)	Deepwater Squirrelfish
Labridae (wrasses and parrotfishes)	*Lachnolaimus maximus*	Hogfish
Labridae (wrasses and parrotfishes)	*Nicholsina usta*	Emerald Parrotfish
Labridae (wrasses and parrotfishes)	*Xyrichtys novacula* (*Hemipteronotus novacula*)	Pearly Razorfish
Labrisomidae (labrisomid blennies)	*Starksia ocellata*	Checkered Blenny
Lutjanidae (snappers)	*Lutjanus campechanus*	Red Snapper
Lutjanidae (snappers)	*Lutjanus griseus*	Gray Snapper
Lutjanidae (snappers)	*Lutjanus synagris*	Lane Snapper
Lutjanidae (snappers)	*Ocyurus chrysurus*	Yellowtail Snapper

Table A.1 (Continued)

Lutjanidae (snappers)	*Rhomboplites aurorubens*	Vermillion Snapper
Monacanthidae (filefishes)	*Aluterus heudelotii*	Dotterel Filefish
Monacanthidae (filefishes)	*Aluterus schoepfi*	Orange Filefish
Monacanthidae (filefishes)	*Monacanthus ciliatus*	Fringed Filefish
Monacanthidae (filefishes)	*Stephanolepis hispidus*	Planehead Filefish
Mullidae (goatfishes)	*Mullus auratus*	Red Goatfish
Mullidae (goatfishes)	*Pseudupeneus maculatus*	Spotted Goatfish
Mullidae (goatfishes)	*Upeneus parvus*	Dwarf Goatfish
Muraenidae (morays)	*Gymnothorax saxicola*	Honeycomb Moray
Nettastomatidae (duckbill eels)	*Hoplunnis diomediana*	Blacktail Pikeconger
Ogcocephalidae (batfishes)	*Halieutichthys aculeatus*	Pancake Batfish
Ogcocephalidae (batfishes)	*Ogcocephalus corniger*	Longnose Batfish
Ogcocephalidae (batfishes)	*Ogcocephalus cubifrons* (*Ogcocephalus radiatus*)	Polka-dot Batfish
Ogcocephalidae (batfishes)	*Ogcocephalus parvus*	Roughback Batfish
Ophichthidae (snake eels)	*Echiophis intertinctus*	Spotted Spoon-nose Eel
Ophichthidae (snake eels)	*Ophichthus puncticeps*	Palespotted Eel
Ophidiidae (cusk-eels)	*Lepophidium jeannae*	Mottled Cusk-eel
Ophidiidae (cusk-eels)	*Ophidion antipholus* (*Ophidion beani*)	Longnose Cusk-eel
Ophidiidae (cusk-eels)	*Ophidion holbrookii*	Bank Cusk-eel
Ophidiidae (cusk-eels)	*Ophidion selenops*	Mooneye Cusk-eel
Ophidiidae (cusk-eels)	*Otophidium omostigma*	Polka-dot Cusk-eel
Opistognathidae (jawfishes)	*Lonchopisthus micrognathus*	Swordtail Jawfish
Ostraciidae (boxfishes)	*Acanthostracion polygonius* (*Lactophrys polygonius)*	Honeycomb Cowfish
Ostraciidae (boxfishes)	*Acanthostracion quadricornis*	Scrawled Cowfish
Paralichthyidae (sand flounders)	*Ancylopsetta quadrocellata*	Ocellated Flounder

Table A.1 (Continued)

Paralichthyidae (sand flounders)	*Citharichthys gymnorhinus*	Anglefin Whiff
Paralichthyidae (sand flounders)	*Citharichthys macrops*	Spotted Whiff
Paralichthyidae (sand flounders)	*Cyclopsetta fimbriata*	Spotfin Flounder
Paralichthyidae (sand flounders)	*Etropus cyclosquamus*	Shelf Flounder
Paralichthyidae (sand flounders)	*Etropus rimosus*	Gray Flounder
Paralichthyidae (sand flounders)	*Gastropsetta frontalis*	Shrimp Flounder
Paralichthyidae (sand flounders)	*Paralichthys albigutta*	Gulf Flounder
Paralichthyidae (sand flounders)	*Syacium papillosum*	Dusky Flounder
Phycidae (phycid hakes)	*Urophycis earllii*	Carolina Hake
Phycidae (phycid hakes)	*Urophycis regia*	Spotted Hake (Spotted Coddling)
Pomacanthidae (angelfishes)	*Holacanthus bermudensis*	Blue Angelfish
Pomacanthidae (angelfishes)	*Pomacanthus arcuatus*	Gray Angelfish
Pomacentridae (damselfishes)	*Chromis enchrysura*	Yellowtail Reeffish
Pomacentridae (damselfishes)	*Stegastes variabilis* (*Pomacentrus variabilis*)	Cocoa Damselfish
Priacanthidae (bigeyes)	*Priacanthus arenatus*	Bigeye
Priacanthidae (bigeyes)	*Pristigenys alta*	Short Bigeye
Rajidae (skates)	*Raja eglanteria*	Clearnose Skate
Rajidae (skates)	*Raja texana*	Roundel Skate
Rhinobatidae (guitarfishes)	*Rhinobatos lentiginosus*	Atlantic Guitarfish
Sciaenidae (drums & croakers)	*Equetus lanceolatus*	Jackknife-fish
Sciaenidae (drums & croakers)	*Pareques umbrosus* (*Equetus umbrosus*)	Cubbyu
Scombridae (mackerels)	*Scomberomorus maculatus*	Atlantic Spanish Mackerel
Scorpaenidae (scorpionfishes)	*Pterois volitans*	Red Lionfish
Scorpaenidae (scorpionfishes)	*Scorpaena agassizii*	Longfin Scorpionfish
Scorpaenidae (scorpionfishes)	*Scorpaena brasiliensis*	Barbfish

Table A.1 (Continued)

Scorpaenidae (scorpionfishes)	*Scorpaena calcarata*	Smoothhead Scorpionfish
Serranidae (sea basses)	*Centropristis ocyurus*	Bank Sea Bass
Serranidae (sea basses)	*Centropristis philadelphica*	Rock Sea Bass
Serranidae (sea basses)	*Diplectrum formosum*	Highfin Sandperch (Sand Perch)
Serranidae (sea basses)	*Rypticus bistrispinus*	Freckled Soapfish
Serranidae (sea basses)	*Rypticus maculatus*	Whitespotted Soapfish
Serranidae (sea basses)	*Schultzea beta*	School Bass
Serranidae (sea basses)	*Serraniculus pumilio*	Pygmy Sea Bass
Serranidae (sea basses)	*Serranus notospilus*	Saddle Bass
Serranidae (sea basses)	*Serranus phoebe*	Tattler
Serranidae (sea basses)	*Serranus subligarius*	Belted Sandfish
Sparidae (porgies)	*Calamus arctifrons*	Grass Porgy
Sparidae (porgies)	*Calamus bajonado*	Jolthead Porgy
Sparidae (porgies)	*Calamus leucosteus*	Whitebone Porgy
Sparidae (porgies)	*Calamus nodosus*	Knobbed Porgy
Sparidae (porgies)	*Calamus penna*	Sheepshead Porgy
Sparidae (porgies)	*Calamus proridens*	Littlehead Porgy
Sparidae (porgies)	*Lagodon rhomboides*	Pinfish
Sparidae (porgies)	*Pagrus pagrus*	Red Porgy
Sparidae (porgies)	*Stenotomus caprinus*	Longspine Porgy
Sphyrnidae (hammerhead sharks)	*Sphyrna tiburo*	Bonnethead
Sphyraenidae (barracudas)	*Sphyraena borealis*	Sennet (Northern Sennet)
Stromateidae (butterfishes)	*Peprilus burti*	Gulf Butterfish
Syngnathidae (pipefishes & seahorses)	*Cosmocampus albirostris* (*Corythoichthys albirostris*)	Whitenose Pipefish

Table A.1 (Continued)

Syngnathidae (pipefishes & seahorses)	*Hippocampus erectus*	Lined Seahorse
Synodontidae (lizardfishes)	*Saurida brasiliensis*	Largescale Lizardfish
Synodontidae (lizardfishes)	*Saurida normani*	Shortjaw Lizardfish
Synodontidae (lizardfishes)	*Synodus foetens*	Inshore Lizardfish
Synodontidae (lizardfishes)	*Synodus intermedius*	Sand Diver
Synodontidae (lizardfishes)	*Synodus poeyi*	Offshore Lizardfish
Synodontidae (lizardfishes)	*Trachinocephalus myops*	Snakefish (Bluntnose Lizardfish)
Tetraodontidae (puffers)	*Sphoeroides dorsalis*	Marbled Puffer
Tetraodontidae (puffers)	*Sphoeroides nephelus*	Southern Puffer
Tetraodontidae (puffers)	*Sphoeroides spengleri*	Bandtail Puffer
Triglidae (searobins)	*Bellator militaris*	Horned Searobin
Triglidae (searobins)	*Prionotus alatus*	Spiny Searobin
Triglidae (searobins)	*Prionotus longispinosus*	Bigeye Searobin
Triglidae (searobins)	*Prionotus martis*	Barred Searobin
Triglidae (searobins)	*Prionotus ophryas*	Bandtail Searobin
Triglidae (searobins)	*Prionotus roseus*	Bluespotted Searobin
Triglidae (searobins)	*Prionotus rubio*	Blackwing Searobin (Blackfin Searobin)
Triglidae (searobins)	*Prionotus scitulus*	Leopard Searobin
Triglidae (searobins)	*Prionotus tribulus*	Bighead Searobin
Uranoscopidae (stargazers)	*Kathetostoma albigutta*	Lancer Stargazer

Table A.2 – Pairwise MANOVA results for annual response and predictor datasets. A table of results for pairwise-multivariate ANOVA for all $\mathbf{X}_z$ (MANOVA-pw), and the non-parametric version for all $\mathbf{Y}_z$ (np-MANOVA-pw), where z = the year of sampling. All p-values were calculated using 1,000 permutations and significance was assessed with $\alpha = 0.05$. F = the multivariate form of Fisher's F-statistic.

	z_1 vs. z_2	F	p-value
Y	2010 vs. 2011	3.33	0.001
	2010 vs. 2012	5.20	0.001
	2011 vs. 2012	5.94	0.001

	z_1 vs. z_2	F	p-value
X	2010 vs. 2011	16.1886	0.001
	2010 vs. 2012	41.6451	0.001
	2011 vs. 2012	23.1438	0.001

A.2 LITERATURE CITED

Page, L. M., H. Espinosa-Pérez, L. T. Findley, C. R. Gilbert, R. N. Lea, N. E. Mandrak, R. L. Mayden, and J. S. Nelson. 2013. Common and Scientific Names of Fishes From the United States, Canada, and Mexico. 7th edition. American Fisheries Society, Bethesda, Maryland.

APPENDIX B:

CHAPTER THREE SUPPLEMENTAL TABLES

B.1 SUPPLEMENTAL TABLES

Table B.1 – Data transformations and object resemblance measures. Data transformations were undertaken to reduce the influence of overly abundant or rare species. Transformations were performed on the raw data tables standardized by the area trawled for each sampling station. Pairwise resemblance measures were calculated for all pairs of objects within the transformed data tables, resulting in square, symmetric dissimilarity matrices used to investigate beta-diversity patterns.

Transformation	Square-root	$\mathbf{Y}^{1/2}$
	Fourth-root	$\mathbf{Y}^{1/4}$
	Logarithmic	$\log_{10}(\mathbf{Y} + 1)$
	Natural Logarithmic	$\log_e(\mathbf{Y} + 1)$
Resemblance	Bray-Curtis dissimilarity	Eq. 7.58 (Legendre and Legendre 2012)
	Canberra dissimilarity	Eq. 7.49 & Eq. 7.50 (Legendre and Legendre 2012)
	Kulczynski quantitative dissimilarity	Eq. 7.25 (Legendre and Legendre 2012)
	Morisita-Horn dissimilarity	Eq. 5 (Chao et al. 2006)
	Sorensen's dissimilarity	Eq. 7.11 & Eq. 7.57 (Legendre and Legendre 2012)

Table B.2 – Variation partitioning results for 2010-2012 daytime SEAMAP survey. Results of the variation partitioning (VPA) of the detrended response data ($\mathbf{Y}_{DT}$) and two sets of predictors – one environmental and one spatial. Environmental variables used were based on either the subset of non-spatial abiotic predictors ($\mathbf{X}_{SEL}$) or the combination of $\mathbf{X}_{SEL}$ with any spatially structured predictors identified ($[\mathbf{Q}^{I}\ \mathbf{Q}^{II}\ \mathbf{X}_{SEL}]$). All *p*-values are provided, and significance was determined using permutation testing methods (1,000 iterations, $\alpha = 0.05$). The R^2_{adj} term represents the adjusted coefficient of determination, and provides an unbiased estimation of the variability in $\mathbf{Y}_{DT}$ explained by each predictor set listed. The fractions [a]-[d] represent the non-spatial, abiotic [a], spatial abiotic [b], spatial [c], and unexplained [d] portions of the VPA solution. The *p*-values listed as "n/a" were not determined because the associated fractions were partitioned directly.

Variation Partitioning

Daytime				[a]	[b]	[c]	[d]
2010	$\mathbf{Y}_{DT}$	$[\mathbf{Q}^{I}\ \mathbf{Q}^{II}\ \mathbf{X}_{SEL}]$	$\mathbf{MEM}^{+}_{SEL}$				
	R^2_{adj}	0.369	0.105	0.2690	0.1005	0.0043	0.6263
	p-value			0.001	n/a	0.344	n/a
2011	$\mathbf{Y}_{DT}$	$\mathbf{X}_{SEL}$	$\mathbf{MEM}^{+}_{SEL}$				
	R^2_{adj}	0.375	0.048	0.3443	0.0302	0.0178	0.6077
	p-value			0.001	n/a	0.014	n/a
2012	$\mathbf{Y}_{DT}$	$[\mathbf{Q}^{I}\ \mathbf{Q}^{II}\ \mathbf{X}_{SEL}]$	$\mathbf{MEM}^{+}_{SEL}$				
	R^2_{adj}	0.322	0.045	0.2935	0.0283	0.0169	0.6613
	p-value			0.001	n/a	0.008	n/a

B.2 LITERATURE CITED

Chao, A., R. L. Chazdon, R. K. Colwell, and T. J. Shen. 2006. Abundance-based similarity indices and their estimation when there are unseen species in samples. Biometrics **62**:361-371.

Legendre, P., and L. Legendre. 2012. Numerical Ecology. Third English edition edition. Elsevier, Amsterdam, The Netherlands.

APPENDIX C:

RESEMBLANCE PROFILES AS CLUSTERING DECISION CRITERIA: ESTIMATING STATISTICAL POWER, ERROR, AND CORRESPONDENCE FOR A HYPOTHESIS TEST FOR MULTIVARIATE STRUCTURE

Received: 27 April 2016 | Revised: 23 November 2016 | Accepted: 22 December 2016

DOI: 10.1002/ece3.2760

ORIGINAL RESEARCH

WILEY Ecology and Evolution Open Access

Resemblance profiles as clustering decision criteria: Estimating statistical power, error, and correspondence for a hypothesis test for multivariate structure

Joshua P. Kilborn | David L. Jones | Ernst B. Peebles | David F. Naar

College of Marine Science, University of South Florida, Saint Petersburg, FL, USA

Correspondence
Joshua P. Kilborn, College of Marine Science, University of South Florida, Saint Petersburg, FL, USA.
Email: jpk@mail.usf.edu

Funding Information
National Oceanic and Atmospheric Administration, Grant/Award Number: NA10NMF4550468.

Abstract

Clustering data continues to be a highly active area of data analysis, and resemblance profiles are being incorporated into ecological methodologies as a hypothesis testing-based approach to clustering multivariate data. However, these new clustering techniques have not been rigorously tested to determine the performance variability based on the algorithm's assumptions or any underlying data structures. Here, we use simulation studies to estimate the statistical error rates for the hypothesis test for multivariate structure based on dissimilarity profiles (DISPROF). We concurrently tested a widely used algorithm that employs the unweighted pair group method with arithmetic mean (UPGMA) to estimate the proficiency of clustering with DISPROF as a decision criterion. We simulated unstructured multivariate data from different probability distributions with increasing numbers of objects and descriptors, and grouped data with increasing overlap, overdispersion for ecological data, and correlation among descriptors within groups. Using simulated data, we measured the resolution and correspondence of clustering solutions achieved by DISPROF with UPGMA against the reference grouping partitions used to simulate the structured test datasets. Our results highlight the dynamic interactions between dataset dimensionality, group overlap, and the properties of the descriptors within a group (i.e., overdispersion or correlation structure) that are relevant to resemblance profiles as a clustering criterion for multivariate data. These methods are particularly useful for multivariate ecological datasets that benefit from distance-based statistical analyses. We propose guidelines for using DISPROF as a clustering decision tool that will help future users avoid potential pitfalls during the application of methods and the interpretation of results.

KEYWORDS

constrained clustering, data simulation, Monte Carlo, permutation testing, PRIMER-E, SIMPROF

1 | INTRODUCTION

In data-rich scientific studies, it is often necessary to apply a clustering algorithm to detect groups of homogenous objects with respect to a set of descriptors (i.e., measured variables). Detection of groups is useful in ecology, economics, genetics, and other disciplines that analyze large, multidimensional datasets. Clustering techniques for multivariate datasets are diverse and can be drawn from methods derived from

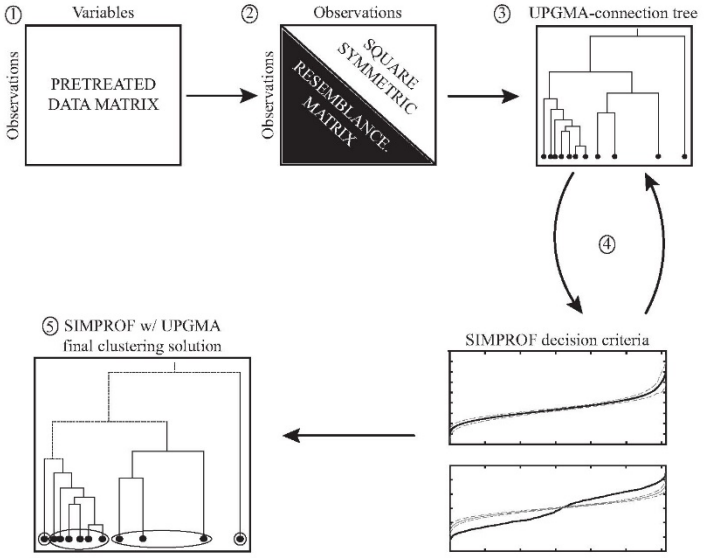

FIGURE 1 Theoretical diagram of the process flow for DISPROF clustering with UPGMA: (1) Data are pretreated and configured. (2) An appropriate resemblance metric is applied to the pretreated dataset. (3) The UPGMA site-connection linkage is assembled. (4) DISPROF is employed in an iterative process to identify the grouping structure in the data and create breaks in the associated linkage tree. (5) DISPROF settles on a final solution, and a two-dimensional dendrogram visualization is created

one or more of the following approaches: sequential versus simultaneous, agglomerative versus divisive, monothetic versus polythetic, hierarchical versus nonhierarchical, probabilistic versus nonprobabilistic, and constrained versus unconstrained (Legendre & Legendre, 2012). In many cases, these methods are sensitive to the sequence of the steps within the algorithm, to random decisions enforced by the algorithm, or to arbitrary assignment of stopping rules, numbers of clusters, or levels of resemblance that define homogeneity.

1.1 | Resemblance profiles and clustering criterion

Multivariate studies of complex datasets are often analyzed statistically using distance-based (db) methods. These db-methods begin with a series of pairwise comparisons between all objects to determine their relative resemblances with respect to a set of descriptors, and these resemblance values can be interpreted as either similarity or dissimilarity. The selection of a resemblance measure is discretionary and varies with the type of data being analyzed as well as the method of analysis (Batagelj & Bren, 1995; Clarke, Somerfield, & Chapman, 2006; Faith, Minchin, & Belbin, 1987). Clarke, Somerfield, and Gorley (2008) developed the SIMPROF routine based on the concept of a "similarity profile," which represents the matrix of pairwise similarity values between any set of objects.

SIMPROF was implemented as a clustering solution in v-6 of the PRIMER software package and was first used to describe community structure in marine nematodes (Liu, Zhang, & Huang, 2007) and larval marine fishes (Muhling, Beckley, Koslow, & Pearce, 2008). Over the last decade, the number of peer-reviewed publications that incorporate SIMPROF in some portion of their methodologies has grown. A search of Web of Science© for the term "SIMPROF" (searched 20 November 2016) returned 32 publications since 2007 and indicated the original Clarke et al. (2008) paper had 279 citations. Publications utilizing SIMPROF tend to come from marine ecology, with studies focusing on beta-diversity in reef corals (Huang et al., 2015), diatoms (Hernandez Almeida & Siqueiros Beltrones, 2012), fishes (Macedo-Soares, Freire, & Muelbert, 2012; Selleslagh et al., 2009), fish gut contents (French, Clarke, Platell, & Potter, 2013), macrofauna (Rehm, Hooke, & Thatje, 2011), and sediment microbes (Gilbert et al., 2009). SIMPROF-based studies have also been conducted on dinoflagellates and ciguatera poisoning (Parsons, Settlemier, & Ballauer, 2011), food webs (Kelly & Scheibling, 2012), habitat classifications (Gonzalez-Mirelis & Buhl-Mortensen, 2015; Valesini, Hourston, Wildsmith, Coen, & Potter, 2010), species/environment relationships (Travers, Potter, Clarke, & Newman, 2012), metagenomics (Khodakova, Smith, Burgoyne, Abarno, & Linacre, 2014), and otolith elemental microchemistry (Moore & Simpfendorfer, 2014). While the preceding literature review reflects the recent use of the algorithm in ecological applications, it is likely that the method has uses in other disciplines as well.

Clarke et al. (2008) demonstrated the use of SIMPROF in conjunction with agglomerative hierarchical clustering via the unweighted pair group method with arithmetic mean (UPGMA; Figure 1), and they also described two theoretical corollaries to the functional dynamics of their algorithm. They proposed that (1) the test for multivariate structure would become more powerful as the number of descriptors increased and (2) that the resolution of any structure identified (i.e., number of groups, G) might be far finer (greater) than is meaningfully interpreted (Clarke et al., 2008). It is our understanding that these corollaries have yet to be tested empirically with numerical simulations, and given recent inconsistencies in the performance of other permutation- and distance-based hypothesis tests (e.g., ANOSIM and MANTEL tests; Anderson & Walsh, 2013; Legendre & Fortin, 2010), we felt this action was warranted.

The present paper intends to improve our understanding of the proposed corollaries to the Clarke et al. (2008) approach, to help users of SIMPROF avoid potential pitfalls during analysis and interpretation, and to encourage use of the method outside of the ecological focus. We tested the SIMPROF method by estimating and describing the type I and type II error rates for the hypothesis test for multivariate structure while varying the datasets' distribution type, dimensionality, data-cloud overlap between adjacent clusters, and data-cloud shape or overdispersion. We also elucidated the effects of dataset configuration variability on the quality of the solution achieved by examining the level of correspondence between the algorithm's clustering solutions and the known grouping partitions for datasets with structure.

1.2 | Review of the SIMPROF approach

For a set of objects, a similarity profile is created by plotting the rank-ordered similarity values versus each value's rank (Figure 2a). This profile is ultimately checked against the mean rank-ordered similarity values for many randomized profiles (i.e., ≥1,000) created via permuting the original descriptor measurements across objects. The π statistic is created by summing the absolute deviations of the observed profile from the mean of the set of permuted profiles. Intuitively, one can see that if an observed profile has many more high and/or low similarity values than would be expected under the null conditions, then multivariate structure would be deemed present (Figure 2b). The null hypothesis (H_o) of "no multivariate structure among objects, with respect to the descriptors" in the original dataset, is formally tested by examining the placement of the observed π statistic relative to the null distribution of all permuted π statistics. To model the null distribution of the π statistic, an additional set of permuted similarity profiles (i.e., ≥1,000 iterations) is created, and their associated π statistics are calculated with respect to the same mean profile used to calculate the original observed π statistic. The *p*-value for the observed π statistic is calculated as the proportion of π statistics that are at least as large as the observed statistic versus the total number of π statistics calculated via permutation (Clarke et al., 2008).

Resemblance profile consideration is inserted into UPGMA clustering as a clustering decision criterion in an iterative process (Figure 1). The data are required to be in [*N* × *P*] matrix format, where the *N* rows represent individual objects (sampling units) and the *P* columns of the matrix represent the descriptors (measured variables). In many real-world, large datasets, there are often some objects where certain descriptor measurements are missing due to either technical failure or human error. When compiling these data, we must remove objects that do not contain an accurate measurement for all descriptors of interest (zero-value measurements may be appropriate, but missing measurements are not). Once the data are assembled and checked for quality, user-defined pretreatments are applied (e.g., standardization and/or normalization) and an appropriate resemblance measure is employed. One advantage to the approach considered here is the use of distribution-free statistics, which releases the analyst from the often-unrealistic assumption of Gaussian data distributions, and decreases the need for data transformations to satisfy those assumptions. Another advantage to using distribution-free significance tests is that they are often generalized to accept any of the potential pool of resemblance measures available to researchers (Legendre & Legendre, 2012).

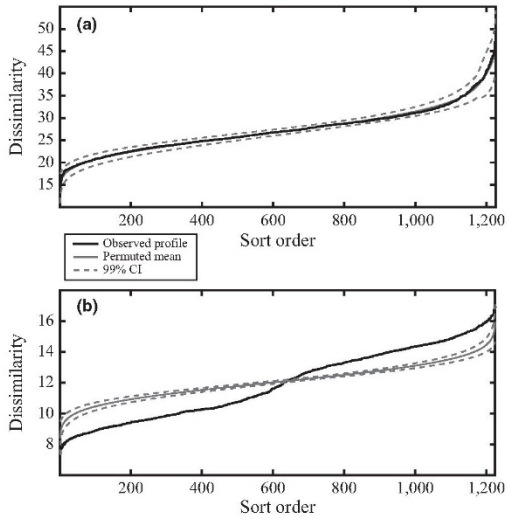

FIGURE 2 Two examples of Euclidean-dissimilarity profiles: Resemblance value sort order is increasing along the *x*-axis, and the sorted pairwise dissimilarity values are increasing along the *y*-axis. (a) A dissimilarity profile for a simulated unstructured dataset drawn from the exponential probability distribution with [*N* × *P*] = [50 × 50]. The observed profile is within the 99% confidence envelope based on 999 permutations of the observed data. (b) A dissimilarity profile for a simulated structured dataset drawn from the normal distribution with two groups having equal variance, [*N* × *P*] = [50 × 50], and *Ov* = 0.01. The observed profile has many dissimilarity values that are above and below the expected mean permuted profile, and its associated 99% confidence envelope, thereby signifying the presence of structure in the dataset

After a square, symmetric distance-matrix is produced, an UPGMA clustering solution is constructed to reflect the magnitude of apparent resemblance between the objects with respect to the descriptors. SIMPROF can be used as an iterative decision criterion to assess each node of the UPGMA dendrogram to determine whether the objects connected by any node are clusters of relative homogeneity, or whether there is additional multivariate structure present in those remaining objects (Clarke et al., 2008).

Recall that the H_o tested by SIMPROF is of "no multivariate structure among objects with respect to the descriptors." When assessing an UPGMA dendrogram, SIMPROF begins hypothesis testing at the node that has the smallest similarity value and that contains all objects. If H_o is rejected and structure is deemed present in the objects connected by the top-level node, the SIMPROF routine repeats independently on the two sets of objects joined at that node. SIMPROF iteratively assesses the presence of structure for all newly identified subsets within the original top-level subsets until a stopping point is

reached and all possible subsets have been identified. The stopping point for the algorithm is when either a nonsignificant p-value (i.e., p-value $\geq \alpha$) for all remaining subsets is obtained (failure to reject H_o), or when the number of objects that remain connected within untested subsets is no greater than two (Clarke et al., 2008). Due to the multiple-testing aspect of the algorithm, a p-value correction method can be employed when determining significance for tests between sets of objects (Clarke et al., 2008). The primary output of UPGMA clustering with SIMPROF is a grouping partition containing a cluster assignment for each object. Using this decision framework creates immediate advantages when interpreting the clustering dendrogram in that (1) the researcher is no longer required to arbitrarily assign a single level of similarity that defines all clusters and (2) the clusters can be defined by varying levels of similarity. To obtain a two-dimensional ordination of the identified groups in hyperdimensional space, a Euclidean embedding can be produced via principle coordinates analysis (PCoA; Gower, 1966). This ordination is based on the same symmetric resemblance matrix used in the clustering process, and the group assignments can be overlain in place of the object labels to present a final clustering diagram.

2 | METHODS

2.1 | Rationale

The only modification we made to the original Clarke et al. (2008) algorithm was to use dissimilarities (or distance) for the computation of the resemblance profile; this convention is consistent with the Fathom Toolbox for MATLAB (Jones, 2015), which was used for our testing and evaluations, and is advantageous because dissimilarity measures span a broad range of types (i.e., metric, nonmetric, or semi-metric) that can be applied to a diversity of potential research disciplines. These types of resemblance measures also allow ordination of the objects via multidimensional methods, which require db-resemblance measures, and are intuitively interpreted with two objects' spatial "closeness" in ordination space as being more similar (i.e., less dissimilar). Because similarity profiles and dissimilarity profiles are analogous, we refer to "DISPROF" hereafter.

To test the effectiveness of DISPROF at detecting the presence of multivariate structure among objects, we used simulated datasets with both unstructured and structured sets of descriptors, under four different simulation scenarios (Table 1). We attempted to simulate data that would be applicable to a range of numerical studies including, but not limited to, the ecological type of data that SIMPROF was initially developed for (Table 2). The unstructured data were simulated with a single grouping structure present and were used for estimating type I error rates for DISPROF; the structured data were simulated with known groups among objects and were used to estimate type II error rates and the power of the hypothesis test. Structured data were also used to examine the effects of descriptor overdispersion in ecological count data, as well as the effects of increasing numbers of descriptors and the type of correlation structure among them. We retained the grouping partitions from the structured data simulations, and doing so allowed us to test the correspondence between the clustering solutions achieved by the UPGMA with DISPROF algorithm and these baseline partitions. The criterion for rejecting H_o in this simulation study was set at $\alpha = .05$, and we opted to use a progressive Bonferroni p-value correction (Legendre & Legendre, 2012) for instances where repeated hypothesis testing was conducted (i.e., simulated structured data testing).

All data simulations were coded in MATLAB using the Fathom Toolbox (Jones, 2015), the OCLUS routine (Steinley & Henson, 2005), and the Darkside Toolbox (Kilborn, 2015). To complete the algorithm testing described below, we used the University of South Florida Research Computing high-performance computing hardware running MATLAB v. 2016 and used an experimental MATLAB module from the Fathom Toolbox called "ClustX."

2.2 | Data simulation methods

In all simulations, varying size conditions for the resultant data matrices were used, and this allowed us to investigate the effects of changing the numbers of objects (N) and dataset dimensionalities (P, number of descriptors) on DISPROF's performance, and also the quality of the clustering solutions achieved by the algorithm. $S = 1{,}000$ datasets were simulated for each combination of $[N \times P]$ under additional simulation scenarios described in Table 1. The simulation scenarios allowed further investigation of DISPROF's performance regarding variation in (1) the underlying probability distribution of the data; (2) the amount of overlap between groups' data clouds; (3) the location and dispersion among groups of objects representing ecological abundance data; and (4) correlation structures among descriptors within groups of objects.

2.2.1 | Unstructured data (Sim 1)

The first set of simulations were used to estimate type I error rates for the DISPROF routine for data drawn from eight different probability distributions (Table 1). Each probability distribution was used to simulate a specific data type, and the properties of the simulated data informed the choice of resemblance measure (Table 2). Each statistical distribution had $S = 40{,}000$ unstructured datasets across all combinations of $[N \times P]$. A total of 320,000 independently generated unstructured datasets were used to complete the type I error rate estimations. Within each of the $S = 1{,}000$ equally sized datasets, the columns were individually parameterized at random from a set range of values specific to the underlying probability distribution (Table 1). The instances where random processes produced objects with all zero-value entries were allowed to persist in the data, and they were treated as a special case during the calculation of Bray–Curtis and Jaccard dissimilarity matrices. In this special case, any comparison of two objects with all zero-value entries would be assigned a dissimilarity value of one (i.e., perfectly dissimilar), as they share no common variability (Anderson & Walsh, 2013; Warton & Hudson, 2004). This convention was upheld for all simulation scenarios where it was appropriate to do so (Sim 1e, 1f, 1h; Sim 3).

TABLE 1 Detail of the simulation scenarios used for the study listed as Sim 1–Sim 4

	Probability distribution	G	Parameter 1	Parameter 2	N	P
Sim 1. Unstructured data						
a.	Binomial	1	$T = 1$	$0 \le q \le 1$	{10, 25, 50, 150, 300}	{2, 3, 10, 25, 50, 150, 225, 300}
b.	Chi-square	1	$1 \le df \le N - 1$	—	{10, 25, 50, 150, 300}	{2, 3, 10, 25, 50, 150, 225, 300}
c.	Exponential	1	$0 \le \mu \le 5$	—	{10, 25, 50, 150, 300}	{2, 3, 10, 25, 50, 150, 225, 300}
d.	Log-normal	1	$0 \le \mu \le 50$	$0 \le \sigma^2 \le 5$	{10, 25, 50, 150, 300}	{2, 3, 10, 25, 50, 150, 225, 300}
e.	Negative binomial	1	$0 \le T \le 10$	$0 \le q \le 1$	{10, 25, 50, 150, 300}	{2, 3, 10, 25, 50, 150, 225, 300}
f.	Negative binomial/ Poisson[a]	1	$1 \le \mu \le 100$	$0 \le \theta \le 1$	{10, 25, 50, 150, 300}	{2, 3, 10, 25, 50, 150, 225, 300}
g.	Normal	1	$-100 \le \mu \le 100$	$0 \le \sigma \le 5$	{10, 25, 50, 150, 300}	{2, 3, 10, 25, 50, 150, 225, 300}
h.	Poisson	1	$0 \le \lambda \le 1{,}000$	—	{10, 25, 50, 150, 300}	{2, 3, 10, 25, 50, 150, 225, 300}
Sim 2. Structured data—overlapping groups						
a.	Normal (OCLUS)	2	$\sigma_1^2 = \sigma_2^2 = 1$	$Ov = \{0.01, 0.02, \ldots 0.49, 0.5\}$	$n_1 = n_2 = 25, N = 50$	{2, 3, 5, 10, 25, 50, 150, 225, 300}
Sim 3. Structured data—Overdispersed descriptors						
a.	Negative binomial/ Poisson[a]	2	$\mu_1 = \mu_2 = 10$	$\theta_1 = 0, \theta_2 = \{0, 0.1, 0.4, 0.9\}$	$n_1 = n_2 = 25, N = 50$	{2, 3, 5, 10, 25, 50, 150, 225, 300}
b.	Negative binomial/ Poisson[a]	2	$\mu_1 = 10, \mu_2 = 30$	$\theta_1 = 0, \theta_2 = \{0, 0.1, 0.4, 0.9\}$	$n_1 = n_2 = 25, N = 50$	{2, 3, 5, 10, 25, 50, 150, 225, 300}
Sim 4. Structured data—correlated descriptors						
a.	Normal	2	$\mu_1 = 10, \mu_2 = 30$	$\Sigma_1 = 0, \Sigma_2 = \{0, 0.6, 0.9\}$	$n_1 = n_2 = 25, N = 50$	{2, 3, 5, 10, 25, 50, 150, 225, 300}
b.	Normal	2	$\mu_1 = 10, \mu_2 = 30$	$\Sigma_1 = \Sigma_2 = \{0.6, 0.9\}$	$n_1 = n_2 = 25, N = 50$	{2, 3, 5, 10, 25, 50, 150, 225, 300}

For each scenario, $S = 1{,}000$ datasets were simulated, and mean dissimilarity profiles (DISPROF) were obtained with 1,000 permutations and the p-values for the test were calculated with 999 permutations ($\alpha = .05$). Variables are as follows: G, total number of groups; N, total number of objects; P, total number of descriptors; T, number of successful trials; df, degrees of freedom; μ_i, mean for all descriptors in group i; λ, Poisson rate parameter; σ_i^2, variance for all descriptors in group i; q, probability of success for a trial; θ_i, overdispersion parameter for all descriptors in group i; Σ_i, correlation among descriptors in group i; Ov, average overlap per axis between data clouds for G_1 and G_2.

[a]Where $\theta = 0$, then $\mu = \sigma^2$, and the negative binomial distribution reduces to the Poisson.

TABLE 2 Probability distributions used in Sim 1–Sim 4: The representative data type and the resemblance measure used to determine the pairwise distance between objects

Probability distribution	Data type	Resemblance
Binomial	Binary, presence/absence	Jaccard
Chi-square	Rational, continuous	Euclidean
Exponential	Rational, continuous	Euclidean
Log-normal	Rational, continuous	Euclidean
Negative binomial	Integer, frequency with many 0's	Bray–Curtis
Negative binomial/Poisson	Overdispersed ecological count data	Bray–Curtis
Normal	Rational, continuous	Euclidean
Poisson	Integer, frequency with many 0's	Bray–Curtis

No data were transformed prior to subjection to the resemblance measure.

Each probability distribution was tested in batches of $S = 1{,}000$ according to their [$N \times P$] configurations. The S independent datasets were each tested with the DISPROF routine one time to determine whether the null was rejected at $\alpha = .05$. The resultant p-value for each DISPROF hypothesis test was collected, and the proportion of all S datasets where the associated p-value was significant was calculated for each [$N \times P$] configuration.

2.2.2 | Structured data—overlapping groups (Sim 2)

The second set of simulations were designed to examine the effects of dataset configuration, as well as the average amount of overlap per dimension between the data clouds that represent grouped objects, on the DISPROF routine and its grouping solutions. We used an established data simulation routine described by Steinley and Henson (2005), called OCLUS, to produce a total of 450,000

datasets with overlapping grouping structures. The OCLUS routine implementation in MATLAB allowed the configuration of the probability distribution type, the number of groups (G) and whether or not they overlap, the number of objects per group (n_i), and the average amount of group overlap across all dimensions (Ov) between groups of objects in hyperdimensional space. Note that Ov for the entire dataset is evenly distributed across all dimensions, and two major assumptions of the OCLUS routine are (1) that all dimensions are independent; and (2) that all groups are independent (Steinley & Henson, 2005). For our purposes, when simulating all structured data with multiple groups (Sim 2–Sim 4), a simple simulation design was employed where two groups ($G = 2$) with $n_1 = n_2 = 25$ ($N = 50$) objects were simulated. In Sim 2, for each [$N \times P$] configuration the average overlap between the two groups was increased progressively from $Ov = 0.01$ to 0.50, in 0.01 increments. $S = 1{,}000$ datasets were simulated for each [$N \times P \times Ov$] configuration. Descriptor data were drawn from the multivariate normal distribution with equal variances ($\sigma_1^2 = \sigma_2^2 = 1$) for both groups (Anderson & Walsh, 2013; Steinley & Henson, 2005). Normally distributed data were used to examine the type II error because the concern that the underlying probability distribution of the data would impart some sort of unknown structure was negligible as the data were simulated in a known grouping configuration. As cluster analysis falls into the category of "exploratory" data analysis, it should be obvious that the amount of overlap between objects in a sampling data set, or any inherent grouping structure, is unknown at the time of testing. Therefore, it is important to understand the empirical effects group location and overlap on clustering solutions if we are to put any faith in the solutions provided by the algorithm.

2.2.3 | Structured data—overdispersed descriptors (Sim 3)

The third simulation scenario also indirectly dealt with group location, but the main focus of these simulations was on determining the effect on DISPROF from increasing the overdispersion of one group while holding the other group constant, and to do so for ecological frequency data (i.e., abundances or counts). We used the Fathom Toolbox for MATLAB to implement ecological-data simulation scenarios similar to those used by Anderson and Walsh (2013), and in Sim 3, we simulated ecological abundance data drawn from the overdispersed negative binomial and/or Poisson distribution (Tables 1 and 2). These data were simulated where the σ^2 >> mean (μ), and the σ^2 parameter is related to μ such that $\sigma^2 = \mu + \theta\mu^2$, where θ is the overdispersion parameter. In cases where $\sigma^2 = \mu$, the data were drawn from the Poisson distribution, and the data were drawn from the negative binomial distribution otherwise. In Sim 3a, we simulated a total of 36,000 datasets with $G = 2$, $\mu_1 = \mu_2 = 10$ (collocated groups), and we induced heterogeneity between the groups by increasing the overdispersion for the descriptors in G_2. In Sim 3b, we maintained the group heterogeneity from increasing θ_2 when we simulated an additional 36,000 datasets with $G = 2$, but in this scenario, we set $\mu_1 = 10$ and $\mu_2 = 30$ (separated groups). For all [$N \times P$] configurations, four different combinations of θ_1 and θ_2 were used to simulate $S = 1{,}000$ datasets for all [$N \times P \times (\theta_1$ and $\theta_2)$] configurations (Table 1). In Sim 3, we simulated ecological count datasets with no overdispersion in G_1 and increasing θ in G_2, and where the groups were collocated in hyperdimensional space (Sim 3a) or where they existed in separate locations (Sim 3b). It should be noted, however, that this method does not account for data-cloud overlap, and is possible that two simulated groups that do not share a mean value could still overlap if the θ parameter were extremely high. We tested values ranging from zero overdispersion, to low ($\theta = 0.1$), to medium ($\theta = 0.4$), to high ($\theta = 0.9$).

2.2.4 | Structured data—increasing correlation (Sim 4)

The fourth set of simulations was used to examine the effects of correlated descriptors within a group of objects on DISPROF and its clustering outputs. We simulated data with different correlation structures (Σ) between descriptors in G_1 and G_2, and where Σ_2 increased in G_2 (Sim 4a), and also with $\Sigma_1 = \Sigma_2$, but still increasing Σ (Sim 4b, Table 1). In both cases, we simulated data drawn from the multivariate normal distribution with $\mu_1 = 10$, $\mu_2 = 30$ and $\sigma_1^2 = \sigma_2^2 = 1$. The square, symmetric correlation-matrices Σ were built such that each descriptor would be correlated with all other descriptors in the dataset by the proportion listed in Σ. Sim 4 examines data with correlated descriptors whose level of correlation varies from no correlation ($\Sigma = 0$), to medium ($\Sigma = 0.6$), to high correlation ($\Sigma = 0.9$).

2.3 | Power, resolution, and correspondence estimation

As all datasets in Sim 2–Sim 4 had $G = 2$, we estimated the proportion of type II errors for each [$N \times P \times$ Ov], [$N \times P \times (\theta_1$ and $\theta_2)$], and [$N \times P \times (\Sigma_1$ and $\Sigma_2)$] configuration by finding the number of instances, per $S = 1{,}000$, where the H_o was retained at $\alpha = .05$ (i.e., no multivariate structure deemed present). Type II error estimates were converted to power, and values ≥0.80 were considered acceptable at our selected confidence level (Cohen, 2013). As our primary interest was in exploring the efficacy of using DISPROF as a clustering criterion, we examined the first iteration of sequential testing of H_o (to record type II error rates), but we also allowed for all subsequent DISPROF iterations to run until the clustering implementation was completed. This unconstrained approach allowed the UPGMA clustering with DISPROF algorithm to settle on complete clustering solutions with the maximum number of groups that could be discovered of $G_{max} = N - 2$.

The final result of each DISPROF clustering attempt was a partition for the simulated objects that identified each object's group membership. In all cases, G and the generated grouping partition were retained for further analysis. The number of groups identified was used to examine the effective resolution of the clustering solution, with larger values of G being indicative of fine resolution and smaller G values being coarse. The grouping partitions were used to compare the computed results against the known reference partition for

TABLE 3 Descriptive statistics for DISPROF type I error based on Sim 1

	Probability distribution	*N*	*P*	Minimum	Mean	Mode	Maximum	σ	*SE*
Sim 1. Type I error – S = 40,000									
a.	Binomial	{10, 25, 50, 150, 300}	{2, 3, 10, 25, 50, 150, 225, 300}	0.008	0.046	0.055	0.068	0.013	.002
b.	Chi-square	{10, 25, 50, 150, 300}	{2, 3, 10, 25, 50, 150, 225, 300}	0.032	0.050	0.050	0.067	0.007	.001
c.	Exponential	{10, 25, 50, 150, 300}	{2, 3, 10, 25, 50, 150, 225, 300}	0.037	0.049	0.049	0.067	0.006	.001
d.	Log-normal	{10, 25, 50, 150, 300}	{2, 3, 10, 25, 50, 150, 225, 300}	0.033	0.050	0.047	0.070	0.008	.001
e.	Negative binomial	{10, 25, 50, 150, 300}	{2, 3, 10, 25, 50, 150, 225, 300}	0.034	0.049	0.050	0.064	0.006	.001
f.	Negative binomial/ Poisson	{10, 25, 50, 150, 300}	{2, 3, 10, 25, 50, 150, 225, 300}	0.028	0.048	0.045	0.063	0.008	.001
g.	Normal	{10, 25, 50, 150, 300}	{2, 3, 10, 25, 50, 150, 225, 300}	0.035	0.051	0.050	0.066	0.008	.001
h.	Poisson	{10, 25, 50, 150, 300}	{2, 3, 10, 25, 50, 150, 225, 300}	0.036	0.049	0.043	0.062	0.007	.001

Unstructured data: Type I error rate estimates and statistics were obtained from $S = 40{,}000$ datasets across all configurations of $[N \times P]$ for each probability distribution simulated. Error rate estimates for each configuration were based on $S = 1{,}000$ datasets, and all p-values were obtained via 999 permutations with significance assessed at $\alpha = .05$. *N*, total number of objects; *P*, total number of descriptors; σ, standard deviation of the mean; *SE*, standard error of the mean.

each structured dataset simulated. The measure of correspondence between the clustering solutions' partitions and their reference partitions was calculated using the Hubert–Arabie adjusted Rand index (ARI_{HA}). This effort was undertaken due to the importance of a clustering algorithm being able to find "correct" structure in the data. The absolute value of ARI_{HA} ranges from 0 to 1, requires a probabilistic interpretation, and measures the likelihood of agreement between one randomly chosen pair of objects represented in both partitions, corrected for chance (Hubert & Arabie, 1985). Negative ARI_{HA} values can be interpreted as a probability of agreement that is less than what would be expected by chance alone. We interpreted ARI_{HA} values ≥0.80 as "good" correspondence with anything above 0.90 being "excellent." Likewise, ARI_{HA} values <0.80 were interpreted as "moderate" correspondence, and values below 0.65 were interpreted as "poor" correspondence (Steinley, 2004).

3 | RESULTS

3.1 | Data simulation scenarios

3.1.1 | Unstructured data (Sim 1)

The mean estimated type I error rates for DISPROF were within the confidence interval that would be expected for the chosen level of $\alpha = .05$ for all simulated unstructured data, regardless of the base probability distribution that the data were drawn from (Table 3). There was also no apparent effect of the number of objects or descriptors on the type I error rates for DISPROF (Figure 3).

3.1.2 | Structured data—overlapping groups (Sim 2)

The mean power values for each *P*-dimension, calculated from the 50 proportions of type II errors, estimated for each $[N \times P \times Ov]$ configuration ($S = 1{,}000$), showed an increase in the power of DISPROF to detect the presence of multivariate structure as the overall dimensionality of the dataset increased (Table 4). A closer look at each *P*-dimension's power values (Figure 4) showed that, for $P \leq 10$, as *Ov* decreased, the statistical power of DISPROF increased asymptotically from unacceptable levels toward 1. For all values of $P \geq 25$, the power was estimated to equal 1 for all *Ov*. Furthermore, for any given *Ov* the power increased as *P* increased. The average number of groups ($\bar{G}$) per $S = 50{,}000$ datasets from all $[N \times P]$ configurations across all 50 *Ov* levels was similar across all *P*, ranging from a minimum $\bar{G} = 1.81$ ($P = 2$) to a maximum $\bar{G} = 2.16$ ($P = 5$; Table 4). Closer inspection of each $[P \times Ov]$ combination ($S = 1{,}000$) revealed that DISPROF clustering solutions where $P \leq 3$ displayed an increase in $\bar{G}$ as *Ov* decreased. $\bar{G}$ increased from a value of $\bar{G} < 2$ and asymptotically approached the mean of $\bar{G}$ for all clustering solutions within a given $[P \times Ov]$ combination. For all $P \geq 5$, $\bar{G}$ values remained above 2 for all *Ov* and were much more tightly bound around their respective means (Figure 5a, Table 4). The mean correspondence values ($\overline{ARI_{HA}}$) for each $S = 50{,}000$ datasets from all $[N \times P]$ configurations across all *Ov* increased as *P* increased (Table 4), and for any single *Ov* level, the $\overline{ARI_{HA}}$ also increased with *P* (Figure 5b). A more detailed view of $\overline{ARI_{HA}}$ within each *P*-dimension (Figure 5b) indicated for $P \leq 5$ the mean ARI_{HA} values persisted below 0.8 for the majority of *Ov* scenarios, but had a generally increasing trend. Eventually, the $\overline{ARI_{HA}}$ had high correspondence values at low levels of *Ov*. All $P \geq 10$

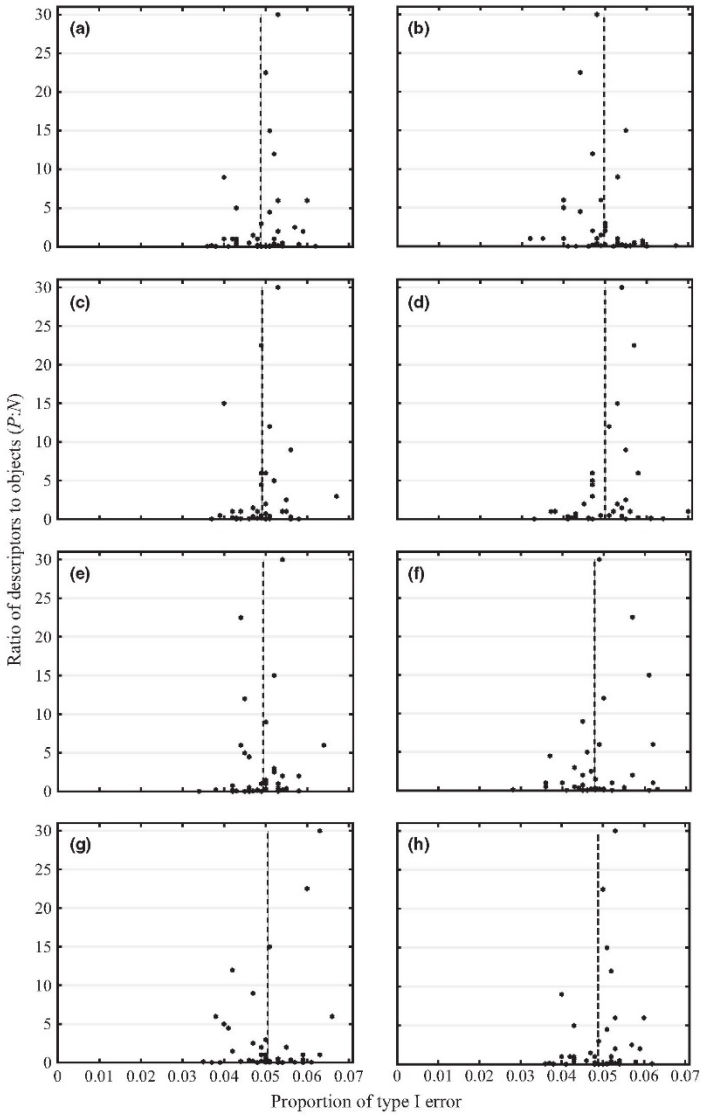

FIGURE 3 Ratio of *P*:*N* versus the proportion of type I error: The type I error rates (α = .05) for the DISPROF hypothesis test for multivariate structure of *S* = 1,000 simulated unstructured datasets from eight different probability distributions simulated in scenario Sim 1. Data points represent each of the 40 different [*N* × *P*] configurations; the dotted vertical line indicates the mean type I error rate for all 40 configurations. All data were randomly parameterized and drawn from the (a) binomial, (b) chi-square, (c) exponential, (d) log-normal, (e) negative binomial, (f) negative binomial/Poisson, (g) normal, and (h) Poisson probability distributions. The σ and standard error for all probability distributions tested were ≤0.01 and .002, respectively

clustering solutions had $\overline{ARI}_{HA}$ values that were considerably less variable across all levels of *Ov* than those for *P* ≤ 5. These solutions' correspondence values were tightly bound around their respective mean $\overline{ARI}_{HA}$ values (Table 4) and displayed good or excellent correspondence (Figure 5b).

3.1.3 | Structured data—overdispersed descriptors (Sim 3)

The performance of DISPROF across all 36 combinations of [*N* × *P* × {θ_1 and θ_2}] {*S* = 1,000} was more consistent when μ_1 = 10, μ_2 = 30 (Sim 3b) than when $\mu_1 = \mu_2$ = 10 (Sim 3a) (Table S1). Sim 3a displayed increasing power to detect groups as the amount of overdispersion in G_2 increased, even when the groups' centroids overlapped and the only distinction between the groups was their respective θ structures. Sim 3b maintained power values of 1 for all configurations except three {*P* = {2, 3}, θ_1 = 0, θ_2 = 0.4; *P* = 3, θ_1 = 0, θ_2 = 0.9}, whose power values were all above 0.85. The power of DISPROF within all [*P* × {θ_1 and θ_2}] configurations where θ_2 > 0 increased with *P* until a threshold value of *P* was met, and for the remaining dimensions where $P \geq P_{threshold}$, the power was 1. The value of $P_{threshold}$ decreased as θ_2 increased and the difference in spread of the two groups became more pronounced (Table S1).

TABLE 4 Descriptive statistics for power, $\bar{G}$, and $\overline{ARI}_{HA}$ for DISPROF based on Sim 2

P	*Ov*	Minimum	Mean	Mode	Maximum	σ	*SE*
Sim 2. Power – $\sigma_1^2 = \sigma_2^2 = 1$, $n_1 = n_2 = 25$, $S = 50{,}000$							
$P = 2$	$Ov = \{0.01, 0.02, \ldots 0.49, 0.5\}$	0.342	0.626	0.476	1.000	0.221	.004
$P = 3$	$Ov = \{0.01, 0.02, \ldots 0.49, 0.5\}$	0.491	0.713	0.629	1.000	0.164	.003
$P = 5$	$Ov = \{0.01, 0.02, \ldots 0.49, 0.5\}$	0.770	0.877	0.760	1.000	0.068	.001
$P = 10$	$Ov = \{0.01, 0.02, \ldots 0.49, 0.5\}$	0.990	0.997	0.999	1.000	0.002	<.001
$P \geq 25$	$Ov = \{0.01, 0.02, \ldots 0.49, 0.5\}$	1.000	1.000	1.000	1.000	0.000	.000
Sim 2. $\bar{G}$ – $\sigma_1^2 = \sigma_2^2 = 1$, $n_1 = n_2 = 25$, $S = 50{,}000$							
$P = 2$	$Ov = \{0.01, 0.02, \ldots 0.49, 0.5\}$	1.46	1.81	1.66	2.14	0.23	<.01
$P = 3$	$Ov = \{0.01, 0.02, \ldots 0.49, 0.5\}$	1.70	1.95	2.16	2.19	0.16	<.01
$P = 5$	$Ov = \{0.01, 0.02, \ldots 0.49, 0.5\}$	2.07	2.16	2.13	2.22	0.03	<.01
$P = 10$	$Ov = \{0.01, 0.02, \ldots 0.49, 0.5\}$	2.08	2.15	2.15	2.21	0.02	<.01
$P = 25$	$Ov = \{0.01, 0.02, \ldots 0.49, 0.5\}$	2.05	2.06	2.06	2.09	0.01	<.01
$P = 50$	$Ov = \{0.01, 0.02, \ldots 0.49, 0.5\}$	2.03	2.06	2.06	2.09	0.01	<.01
$P = 150$	$Ov = \{0.01, 0.02, \ldots 0.49, 0.5\}$	2.03	2.06	2.06	2.09	0.01	<.01
$P = 225$	$Ov = \{0.01, 0.02, \ldots 0.49, 0.5\}$	2.04	2.07	2.06	2.09	0.01	<.01
$P = 300$	$Ov = \{0.01, 0.02, \ldots 0.49, 0.5\}$	2.04	2.06	2.07	2.09	0.01	<.01
Sim 2. $\overline{ARI}_{HA}$ – $\sigma_1^2 = \sigma_2^2 = 1$, $n_1 = n_2 = 25$, $S = 50{,}000$							
$P = 2$	$Ov = \{0.01, 0.02, \ldots 0.49, 0.5\}$	0.116	0.347	0.116	0.927	0.232	.005
$P = 3$	$Ov = \{0.01, 0.02, \ldots 0.49, 0.5\}$	0.198	0.407	0.198	0.897	0.190	.004
$P = 5$	$Ov = \{0.01, 0.02, \ldots 0.49, 0.5\}$	0.447	0.591	0.447	0.883	0.111	.002
$P = 10$	$Ov = \{0.01, 0.02, \ldots 0.49, 0.5\}$	0.846	0.875	0.846	0.934	0.019	<.001
$P = 25$	$Ov = \{0.01, 0.02, \ldots 0.49, 0.5\}$	0.984	0.988	0.984	0.991	0.001	<.001
$P = 50$	$Ov = \{0.01, 0.02, \ldots 0.49, 0.5\}$	0.995	0.997	0.995	0.998	0.001	<.001
$P = 150$	$Ov = \{0.01, 0.02, \ldots 0.49, 0.5\}$	0.995	0.997	0.995	0.998	0.001	<.001
$P = 225$	$Ov = \{0.01, 0.02, \ldots 0.49, 0.5\}$	0.996	0.997	0.996	0.998	0.001	<.001
$P = 300$	$Ov = \{0.01, 0.02, \ldots 0.49, 0.5\}$	0.995	0.997	0.995	0.998	0.001	<.001

Structured data—overlapping groups: Power estimates for each [$N \times P \times Ov$] configuration were based on $S = 1{,}000$ datasets with mean values based on 50 [$P \times Ov$] configurations at each P; all p-values were obtained via 999 permutations with significance assessed at $\alpha = .05$. Mean number of groups ($\bar{G}$) and average clustering solution correspondence ($\overline{ARI}_{HA}$) estimations and statistics were obtained from $S = 50{,}000$ datasets across all Ov for each configuration of [$N \times P$]. N, total number of objects (n_i = number of objects in group i); P, total number of descriptors; Ov, average overlap per axis between data clouds for G_1 and G_2; σ_i^2, variance of group i; σ, standard deviation of the mean; *SE*, standard error of the mean.

The mean number of groups identified in Sim 3b across all [$P \times \{\theta_1$ and $\theta_2\}$] configurations where $\theta_2 < 0.9$ was approximately 2 (the correct number), and there was no apparent effect of increasing P or θ_2 when the two groups were sufficiently separated in hyperdimensional space (Table 5). For simulations where $\theta_2 = 0.9$, $\bar{G}$ increased from ~2.5 groups identified per 1,000 datasets at $P = 2$, to ~4 groups at $P = \{5, 10\}$, after which the value of $\bar{G}$ tapered off to around 2 starting at $P = 150$ (Table 5). The mean correspondence values for scenarios where $\theta_2 = \{0, 0.1\}$ remained excellent for all P; where $\theta_2 \geq 0.4$, the $\overline{ARI}_{HA}$ increased with P (Table 6). In Sim 3a, where $\mu_1 = \mu_2$, DISPROF clustering, on average, never settled on the solution of $G = 2$. When $\theta_1 = \theta_2 = 0$, all P returned $\bar{G} = 1$ (as the two groups were effectively identical), but for all other [$P \times \{\theta_1$ and $\theta_2\}$] configurations where $\theta_2 > 0$, as P increased so did the value of $\bar{G}$ (max $\bar{G} = 28$ groups, Table 5). The same pattern was observed in the $\overline{ARI}_{HA}$ values for Sim 3a as was seen for $\bar{G}$; for all $\theta_1 = \theta_2 = 0$ scenarios, the $\overline{ARI}_{HA} = 0$, and for all other levels of θ_2 the $\overline{ARI}_{HA}$ values increased along with P (Table 6), reaching their maximum values around 1 when $P \geq 25$.

3.1.4 | Structured data—correlated descriptors (Sim 4)

For all P, when both groups had no correlation structure, $\bar{G}$ was consistently ~2, and $\overline{ARI}_{HA}$ values were excellent; where at least one group had no correlation structure, $\bar{G}$ increased and the $\overline{ARI}_{HA}$ decreased as P increased (Table 7). For all P where the correlation structure for either group was $\Sigma \geq 0.6$ (medium to high), DISPROF produced clustering solutions where $\bar{G}$ increased with P (Table 7). However, in those same scenarios, the $\overline{ARI}_{HA}$ decreased as P increased, and it should be noted that none of the simulation scenarios in Sim 4a or 4b that included any amount of within-group descriptor correlation returned clustering solutions with an $\overline{ARI}_{HA} \geq 0.8$ for any $P \geq 5$.

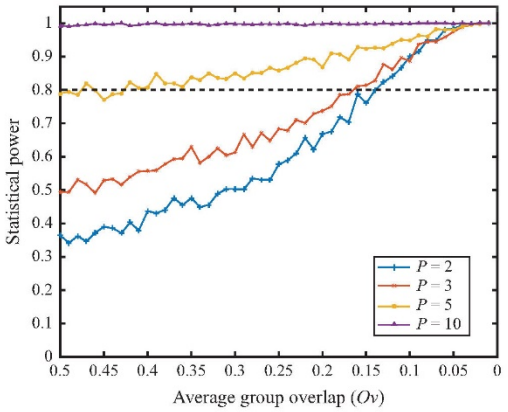

FIGURE 4 Power of the DISPROF test versus the proportion of group overlap: Statistical power of DISPROF versus *Ov* for all *P* tested under Sim 2. Each line plot represents the 50 power values for *S* = 1,000 datasets at each *Ov* level for a given *P*. The horizontal dashed line at power = 0.8 is the lower limit of acceptable power values

4 | DISCUSSION

The DISPROF algorithm is designed to test the H_o that there is "no multivariate structure among objects, with respect to a set of descriptors" in a dataset. The utility of deploying the algorithm with a clustering technique such as UPGMA is in (1) the reduction of arbitrary decision criteria (i.e., dissimilarity thresholds for group identification); (2) the ability to assess multivariate structure at multiple levels of resemblance; (3) the inclusion of the frequentist approach to hypothesis testing; and (4) the application of db multivariate statistical techniques. As such, it is important to determine where UPGMA clustering, with DISPROF implemented as a decision criterion, is affected by changes in data configuration, distribution, dispersion, and correlation. We were particularly interested in statistical error rates associated with DISPROF and the resolution and correspondence of the grouping solutions provided by DISPROF with UPGMA under a variety of potential data scenarios.

4.1 | Type I error and power of DISPROF

4.1.1 | Type I error

When assessing the DISPROF algorithm's H_o, there appears to be no effect of distribution type or [*N* × *P*] configuration on type I error rates. The mean type I error rates for all [*N* × *P*] within each probability distribution type fell within acceptable ranges for the expected number of rejections (α = .05). As DISPROF correctly failed to reject H_o with acceptable levels of type I error, it is, therefore, reasonable to assume that there is a low likelihood that the underlying probability distribution will impart some sort of unknown grouping structure to the dataset (e.g., where some unwanted noise structure might elevate false positives). This is notable given that these techniques were developed for ecological datasets such as those tested in Sim 1f, but they appear to be applicable to many common data types collected by different lines of scientific inquiry (Tables 1 and 2). However, the activity displayed by DISPROF in Sim 3a and Sim 4 leads us to believe that further investigation may be required for datasets with high levels of overdispersion or correlation among descriptors. In these cases, misclassification appears to increase along with both θ and Σ, and is exacerbated by increases in *P* (Tables 6 and 7). These findings are also notable as overdispersion and correlation are two common qualities of ecological datasets.

4.1.2 | Power

The power of DISPROF to detect structure in data is generally poor with low-dimensional ($P \leq 5$) multivariate normal data, and with low-dimensional ($P \leq 10$) ecological count data where $\mu_1 = \mu_2$, the latter being expected as this configuration can be interpreted as $G = 1$. As DISPROF performed decidedly better when $\mu_1 = 10$ and $\mu_2 = 30$, it follows that the hypothesis test relies heavily on the location parameter when assigning group membership, and when heterogeneity of groups is only defined by overdispersion the two are confounded by the algorithm. A similar response to collocated sets of heterogeneous objects was observed during empirical investigation of ANOSIM and the MANTEL test (Anderson & Walsh, 2013). The power of DISPROF improves dramatically once $P \geq 25$, and increases with greater separation between groups in hyperdimensional space. With group separation in hyperspace, the power of DISPROF to evaluate H_o is unaffected by increasing the overdispersion in ecological data, and the test for structure is able to correctly identify the presence of groups in virtually all simulated datasets where $\mu_1 = 10$ and $\mu_2 = 30$. The presence of correlation structure among the descriptors within any group also has no noticeable effect on the power of DISPROF to detect structure.

The power of DISPROF is excellent in most cases and, as Clarke et al. (2008) predicted, its ability to detect structure becomes more powerful as the dimensionality of the predictors increases, and so we have found their corollary (1) to be supported. A potential explanation for the increase in power observed along with the increases in *P* may be related to the idea of a group's identity, or the unique combination of numerical values that quantitatively represent a set of objects (i.e., their "fingerprint"). The more descriptors used to quantify an object, the less likely the unique fingerprint that describes that group of similar objects could be re-created by chance. Therefore, during the randomization process of the DISPROF test, and with a large enough *P*, breaking the structure in the original data is relatively easy to do in order to create the null distribution for the test statistic. This is essentially the overfitting problem in reverse (Babyak, 2004; Hawkins, 2004). This overfitting is appropriate because it essentially creates highly unique observed resemblance profiles to test against for structure, and because no extrapolation or interpolation is based on the overfitted identity. Any unique group identity exposed in the dataset

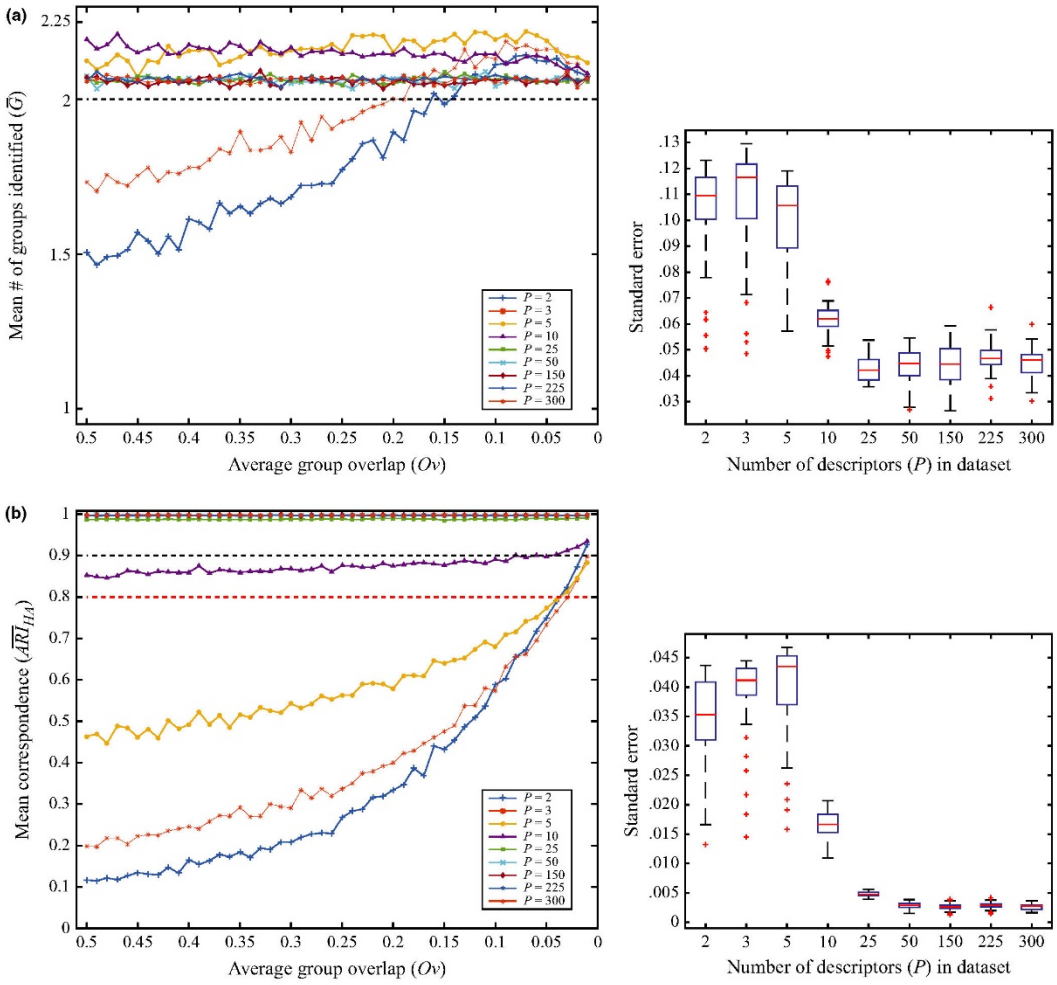

FIGURE 5 The relationship for $\bar{G}$ and $\overline{ARI}_{HA}$ with Ov for DISPROF clustering: (a) The mean number of groups identified ($\bar{G}$) versus the average data cloud overlap (Ov) for all P tested under Sim 2. Each line plot represents the 50 $\bar{G}$ values for S = 1,000 datasets at each Ov level for a given P. The optimal grouping solution (G = 2) is represented by the horizontal dashed line. (b) The mean correspondence of the grouping solution ($\overline{ARI}_{HA}$) versus the average data cloud overlap (Ov) for all P tested under Sim 2. Each line plot is configured as in panel (a), the horizontal black dashed line represents lower bound for excellent correspondence ($\overline{ARI}_{HA}$ = 0.9), and the red dashed line represents lower bound for good correspondence ($\overline{ARI}_{HA}$ = 0.8). Boxplots to the right represent the distribution of standard errors for each estimate of the $\bar{G}$ and $\overline{ARI}_{HA}$ for all Ov within a noted dimensionality for P. The horizontal red line in each boxplot represents the median standard error value in the distribution, with the upper and lower edges of the box being the 25th and 75th percentiles. Whiskers extend to encompass the most extreme data points, and outliers are plotted individually as crosses

will be similarly overfitted because all objects are represented in the same space of descriptors.

4.2 | Resolution and correspondence of DISPROF

If either of the theoretical corollaries presented by Clarke et al. (2008) were to be considered cautionary, it would be corollary (2), which regards the resolution of DISPROF solutions being finer than ecologists (or any professional) utilizing the method could interpret meaningfully. We further contend that the correspondence between these grouping partitions and any known grouping structure in the simulated datasets is informative and is indicative of the DISPROF clustering method's ability to settle on "meaningful" solutions. Therefore, any discussion of the issues surrounding the resolution of the grouping

TABLE 5 Descriptive statistics for $\bar{G}$ for DISPROF based on Sim 3

P	θ_1 and θ_2	Minimum	Mean	Mode	Maximum	σ	*SE*	*P*	θ_1 and θ_2	Minimum	Mean	Mode	Maximum	σ	*SE*
Sim 3a. $\bar{G}$ – $\mu_1 = \mu_2 = 10$, $n_1 = n_2 = 25$, $S = 1{,}000$								Sim 3b. $\bar{G}$ – $\mu_1 = 10$, $\mu_2 = 30$, $n_1 = n_2 = 25$, $S = 1{,}000$							
$P = 2$	$\theta_1 = \theta_2 = 0$	1.00	1.06	1.00	4.00	0.28	.01	$P = 2$	$\theta_1 = \theta_2 = 0$	2.00	2.07	2.00	5.00	0.32	.01
	$\theta_1 = 0, \theta_2 = 0.1$	1.00	1.10	1.00	5.00	0.35	.01		$\theta_1 = 0, \theta_2 = 0.1$	2.00	2.07	2.00	5.00	0.30	.01
	$\theta_1 = 0, \theta_2 = 0.4$	1.00	1.32	1.00	5.00	0.62	.02		$\theta_1 = 0, \theta_2 = 0.4$	1.00	2.16	2.00	5.00	0.62	.02
	$\theta_1 = 0, \theta_2 = 0.9$	1.00	1.75	1.00	6.00	0.86	.03		$\theta_1 = 0, \theta_2 = 0.9$	1.00	2.51	2.00	6.00	0.98	.03
$P = 3$	$\theta_1 = \theta_2 = 0$	1.00	1.07	1.00	4.00	0.30	.01	$P = 3$	$\theta_1 = \theta_2 = 0$	2.00	2.06	2.00	5.00	0.29	.01
	$\theta_1 = 0, \theta_2 = 0.1$	1.00	1.13	1.00	5.00	0.42	.01		$\theta_1 = 0, \theta_2 = 0.1$	2.00	2.05	2.00	5.00	0.27	.01
	$\theta_1 = 0, \theta_2 = 0.4$	1.00	1.84	1.00	6.00	0.99	.03		$\theta_1 = 0, \theta_2 = 0.4$	2.00	2.36	2.00	6.00	0.62	.02
	$\theta_1 = 0, \theta_2 = 0.9$	1.00	3.18	3.00	8.00	1.44	.05		$\theta_1 = 0, \theta_2 = 0.9$	1.00	3.45	3.00	7.00	1.03	.03
$P = 5$	$\theta_1 = \theta_2 = 0$	1.00	1.07	1.00	6.00	0.34	.01	$P = 5$	$\theta_1 = \theta_2 = 0$	2.00	2.05	2.00	4.00	0.24	.01
	$\theta_1 = 0, \theta_2 = 0.1$	1.00	1.25	1.00	6.00	0.58	.02		$\theta_1 = 0, \theta_2 = 0.1$	2.00	2.06	2.00	5.00	0.27	.01
	$\theta_1 = 0, \theta_2 = 0.4$	1.00	3.93	3.00	10.00	1.73	.05		$\theta_1 = 0, \theta_2 = 0.4$	2.00	2.34	2.00	5.00	0.55	.02
	$\theta_1 = 0, \theta_2 = 0.9$	3.00	7.27	7.00	13.00	1.71	.05		$\theta_1 = 0, \theta_2 = 0.9$	2.00	4.23	4.00	8.00	1.23	.04
$P = 10$	$\theta_1 = \theta_2 = 0$	1.00	1.06	1.00	4.00	0.31	.01	$P = 10$	$\theta_1 = \theta_2 = 0$	2.00	2.07	2.00	6.00	0.35	.01
	$\theta_1 = 0, \theta_2 = 0.1$	1.00	1.94	1.00	8.00	1.14	.04		$\theta_1 = 0, \theta_2 = 0.1$	2.00	2.05	2.00	4.00	0.24	.01
	$\theta_1 = 0, \theta_2 = 0.4$	4.00	9.71	10.00	16.00	1.96	.06		$\theta_1 = 0, \theta_2 = 0.4$	2.00	2.24	2.00	6.00	0.50	.02
	$\theta_1 = 0, \theta_2 = 0.9$	8.00	12.91	12.00	18.00	1.65	.05		$\theta_1 = 0, \theta_2 = 0.9$	2.00	3.94	4.00	10.00	1.22	.04
$P = 25$	$\theta_1 = \theta_2 = 0$	1.00	1.11	1.00	7.00	0.57	.02	$P = 25$	$\theta_1 = \theta_2 = 0$	2.00	2.06	2.00	5.00	0.28	.01
	$\theta_1 = 0, \theta_2 = 0.1$	1.00	6.01	6.00	14.00	2.30	.07		$\theta_1 = 0, \theta_2 = 0.1$	2.00	2.06	2.00	6.00	0.32	.01
	$\theta_1 = 0, \theta_2 = 0.4$	12.00	17.93	18.00	23.00	1.66	.05		$\theta_1 = 0, \theta_2 = 0.4$	2.00	2.05	2.00	6.00	0.28	.01
	$\theta_1 = 0, \theta_2 = 0.9$	14.00	19.70	20.00	24.00	1.58	.05		$\theta_1 = 0, \theta_2 = 0.9$	2.00	2.64	2.00	7.00	0.81	.03
$P = 50$	$\theta_1 = \theta_2 = 0$	1.00	1.10	1.00	8.00	0.51	.02	$P = 50$	$\theta_1 = \theta_2 = 0$	2.00	2.09	2.00	6.00	0.41	.01
	$\theta_1 = 0, \theta_2 = 0.1$	5.00	12.73	13.00	20.00	2.37	.08		$\theta_1 = 0, \theta_2 = 0.1$	2.00	2.06	2.00	7.00	0.35	.01
	$\theta_1 = 0, \theta_2 = 0.4$	18.00	23.12	23.00	26.00	1.40	.04		$\theta_1 = 0, \theta_2 = 0.4$	2.00	2.07	2.00	6.00	0.32	.01
	$\theta_1 = 0, \theta_2 = 0.9$	19.00	23.55	24.00	26.00	1.30	.04		$\theta_1 = 0, \theta_2 = 0.9$	2.00	2.17	2.00	6.00	0.45	.01
$P = 150$	$\theta_1 = \theta_2 = 0$	1.00	1.10	1.00	10.00	0.61	.02	$P = 150$	$\theta_1 = \theta_2 = 0$	2.00	2.07	2.00	9.00	0.41	.01
	$\theta_1 = 0, \theta_2 = 0.1$	18.00	22.75	23.00	27.00	1.41	.04		$\theta_1 = 0, \theta_2 = 0.1$	2.00	2.05	2.00	6.00	0.27	.01
	$\theta_1 = 0, \theta_2 = 0.4$	24.00	25.91	26.00	27.00	0.31	.01		$\theta_1 = 0, \theta_2 = 0.4$	2.00	2.05	2.00	7.00	0.28	.01
	$\theta_1 = 0, \theta_2 = 0.9$	24.00	25.92	26.00	27.00	0.29	.01		$\theta_1 = 0, \theta_2 = 0.9$	2.00	2.05	2.00	7.00	0.31	.01
$P = 225$	$\theta_1 = \theta_2 = 0$	1.00	1.11	1.00	9.00	0.67	.02	$P = 225$	$\theta_1 = \theta_2 = 0$	2.00	2.07	2.00	6.00	0.36	.01
	$\theta_1 = 0, \theta_2 = 0.1$	21.00	24.83	25.00	27.00	0.95	.03		$\theta_1 = 0, \theta_2 = 0.1$	2.00	2.07	2.00	5.00	0.32	.01
	$\theta_1 = 0, \theta_2 = 0.4$	25.00	25.99	26.00	27.00	0.12	<.01		$\theta_1 = 0, \theta_2 = 0.4$	2.00	2.09	2.00	7.00	0.40	.01
	$\theta_1 = 0, \theta_2 = 0.9$	25.00	25.99	26.00	28.00	0.12	.00		$\theta_1 = 0, \theta_2 = 0.9$	2.00	2.07	2.00	6.00	0.35	.01
$P = 300$	$\theta_1 = \theta_2 = 0$	1.00	1.10	1.00	10.00	0.60	.02	$P = 300$	$\theta_1 = \theta_2 = 0$	2.00	2.07	2.00	6.00	0.34	.01
	$\theta_1 = 0, \theta_2 = 0.1$	23.00	25.65	26.00	27.00	0.58	.02		$\theta_1 = 0, \theta_2 = 0.1$	2.00	2.06	2.00	6.00	0.32	.01
	$\theta_1 = 0, \theta_2 = 0.4$	25.00	26.00	26.00	27.00	0.05	<.01		$\theta_1 = 0, \theta_2 = 0.4$	2.00	2.08	2.00	6.00	0.37	.01
	$\theta_1 = 0, \theta_2 = 0.9$	25.00	26.00	26.00	27.00	0.07	<.01		$\theta_1 = 0, \theta_2 = 0.9$	2.00	2.08	2.00	8.00	0.41	.01

Structured data—overdispersed descriptors: Estimates of the mean number of groups identified ($\bar{G}$) for each [$N \times P \times (\theta_1, \theta_2)$] configuration were based on $S = 1{,}000$ datasets. *N*, total number of objects (n_i = number of objects in group *i*); *P*, total number of descriptors; θ_i, overdispersion for descriptors in group *i*; μ_i, mean value of descriptors in group *i*; σ, standard deviation of the mean; *SE*, standard error of the mean.

TABLE 6 Descriptive statistics for $\overline{ARI}_{HA}$ for DISPROF based on Sim 3

P	θ_1 and θ_2	Minimum	Mean	Mode	Maximum	σ	SE	P	θ_1 and θ_2	Minimum	Mean	Mode	Maximum	σ	SE
Sim 3a. $\overline{ARI}_{HA}$ ~ $\mu_1 = \mu_2 = 10$, $n_1 = n_2 = 25$, $S = 1{,}000$								Sim 3b. $\overline{ARI}_{HA}$ ~ $\mu_1 = 10$, $\mu_2 = 30$, $n_1 = n_2 = 25$, $S = 1{,}000$						
$P = 2$	$\theta_1 = \theta_2 = 0$	−0.013	0.000	0.000	0.060	0.003	<.001	$P = 2$	$\theta_1 = \theta_2 = 0$	0.676	0.988	1.000	1.000	0.042	.001
	$\theta_1 = 0, \theta_2 = 0.1$	−0.013	0.000	0.000	0.077	0.004	<.001		$\theta_1 = 0, \theta_2 = 0.1$	0.399	0.909	1.000	1.000	0.100	.003
	$\theta_1 = 0, \theta_2 = 0.4$	−0.004	0.004	0.000	0.310	0.019	.001		$\theta_1 = 0, \theta_2 = 0.4$	0.000	0.563	0.000	1.000	0.269	.009
	$\theta_1 = 0, \theta_2 = 0.9$	−0.006	0.014	0.000	0.326	0.035	.001		$\theta_1 = 0, \theta_2 = 0.9$	0.000	0.316	0.000	1.000	0.232	.007
$P = 3$	$\theta_1 = \theta_2 = 0$	−0.021	0.000	0.000	0.021	0.002	<.001	$P = 3$	$\theta_1 = \theta_2 = 0$	0.721	0.994	1.000	1.000	0.030	.001
	$\theta_1 = 0, \theta_2 = 0.1$	−0.007	0.000	0.000	0.038	0.002	<.001		$\theta_1 = 0, \theta_2 = 0.1$	0.615	0.970	1.000	1.000	0.059	.002
	$\theta_1 = 0, \theta_2 = 0.4$	−0.007	0.012	0.000	0.312	0.032	.001		$\theta_1 = 0, \theta_2 = 0.4$	0.000	0.780	0.920	1.000	0.161	.005
	$\theta_1 = 0, \theta_2 = 0.9$	−0.003	0.063	0.000	0.555	0.086	.003		$\theta_1 = 0, \theta_2 = 0.9$	0.000	0.539	0.770	1.000	0.170	.005
$P = 5$	$\theta_1 = \theta_2 = 0$	−0.019	0.000	0.000	0.028	0.002	<.001	$P = 5$	$\theta_1 = \theta_2 = 0$	0.701	0.996	1.000	1.000	0.025	.001
	$\theta_1 = 0, \theta_2 = 0.1$	−0.011	0.001	0.000	0.109	0.006	<.001		$\theta_1 = 0, \theta_2 = 0.1$	0.727	0.992	1.000	1.000	0.029	.001
	$\theta_1 = 0, \theta_2 = 0.4$	0.000	0.065	0.000	0.422	0.075	.002		$\theta_1 = 0, \theta_2 = 0.4$	0.527	0.915	1.000	1.000	0.088	.003
	$\theta_1 = 0, \theta_2 = 0.9$	0.002	0.264	0.151	0.573	0.112	.004		$\theta_1 = 0, \theta_2 = 0.9$	0.256	0.705	0.882	1.000	0.121	.004
$P = 10$	$\theta_1 = \theta_2 = 0$	−0.017	0.000	0.000	0.017	0.001	<.001	$P = 10$	$\theta_1 = \theta_2 = 0$	0.701	0.995	1.000	1.000	0.030	.001
	$\theta_1 = 0, \theta_2 = 0.1$	−0.003	0.005	0.000	0.125	0.014	<.001		$\theta_1 = 0, \theta_2 = 0.1$	0.747	0.997	1.000	1.000	0.018	.001
	$\theta_1 = 0, \theta_2 = 0.4$	0.026	0.260	0.219	0.533	0.097	.003		$\theta_1 = 0, \theta_2 = 0.4$	0.708	0.984	1.000	1.000	0.035	.001
	$\theta_1 = 0, \theta_2 = 0.9$	0.247	0.451	0.452	0.558	0.054	.002		$\theta_1 = 0, \theta_2 = 0.9$	0.589	0.860	0.961	1.000	0.097	.003
$P = 25$	$\theta_1 = \theta_2 = 0$	−0.019	0.000	0.000	0.106	0.004	<.001	$P = 25$	$\theta_1 = \theta_2 = 0$	0.676	0.997	1.000	1.000	0.020	.001
	$\theta_1 = 0, \theta_2 = 0.1$	−0.003	0.059	0.012	0.310	0.056	.002		$\theta_1 = 0, \theta_2 = 0.1$	0.656	0.996	1.000	1.000	0.022	.001
	$\theta_1 = 0, \theta_2 = 0.4$	0.328	0.460	0.476	0.535	0.034	.001		$\theta_1 = 0, \theta_2 = 0.4$	0.626	0.997	1.000	1.000	0.021	.001
	$\theta_1 = 0, \theta_2 = 0.9$	0.467	0.515	0.515	0.533	0.011	<.001		$\theta_1 = 0, \theta_2 = 0.9$	0.673	0.966	1.000	1.000	0.049	.002
$P = 50$	$\theta_1 = \theta_2 = 0$	−0.017	0.000	0.000	0.029	0.002	<.001	$P = 50$	$\theta_1 = \theta_2 = 0$	0.676	0.995	1.000	1.000	0.027	.001
	$\theta_1 = 0, \theta_2 = 0.1$	0.028	0.236	0.266	0.481	0.080	.003		$\theta_1 = 0, \theta_2 = 0.1$	0.626	0.996	1.000	1.000	0.025	.001
	$\theta_1 = 0, \theta_2 = 0.4$	0.430	0.506	0.510	0.523	0.012	<.001		$\theta_1 = 0, \theta_2 = 0.4$	0.665	0.995	1.000	1.000	0.028	.001
	$\theta_1 = 0, \theta_2 = 0.9$	0.430	0.509	0.508	0.520	0.004	<.001		$\theta_1 = 0, \theta_2 = 0.9$	0.727	0.992	1.000	1.000	0.024	.001
$P = 150$	$\theta_1 = \theta_2 = 0$	−0.018	0.000	0.000	0.035	0.002	<.001	$P = 150$	$\theta_1 = \theta_2 = 0$	0.631	0.995	1.000	1.000	0.027	.001
	$\theta_1 = 0, \theta_2 = 0.1$	0.352	0.454	0.468	0.517	0.028	.001		$\theta_1 = 0, \theta_2 = 0.1$	0.792	0.997	1.000	1.000	0.015	<.001
	$\theta_1 = 0, \theta_2 = 0.4$	0.395	0.505	0.505	0.508	0.004	<.001		$\theta_1 = 0, \theta_2 = 0.4$	0.633	0.997	1.000	1.000	0.019	.001
	$\theta_1 = 0, \theta_2 = 0.9$	0.428	0.505	0.505	0.508	0.003	<.001		$\theta_1 = 0, \theta_2 = 0.9$	0.689	0.997	1.000	1.000	0.021	.001
$P = 225$	$\theta_1 = \theta_2 = 0$	−0.010	0.000	0.000	0.013	0.001	<.001	$P = 225$	$\theta_1 = \theta_2 = 0$	0.699	0.996	1.000	1.000	0.026	.001
	$\theta_1 = 0, \theta_2 = 0.1$	0.424	0.484	0.464	0.513	0.021	.001		$\theta_1 = 0, \theta_2 = 0.1$	0.714	0.996	1.000	1.000	0.022	.001
	$\theta_1 = 0, \theta_2 = 0.4$	0.465	0.505	0.505	0.507	0.002	<.001		$\theta_1 = 0, \theta_2 = 0.4$	0.646	0.995	1.000	1.000	0.029	.001
	$\theta_1 = 0, \theta_2 = 0.9$	0.391	0.505	0.505	0.507	0.004	<.001		$\theta_1 = 0, \theta_2 = 0.9$	0.663	0.996	1.000	1.000	0.024	.001

(Continues)

TABLE 6 (Continued)

P	θ_1 and θ_2	Minimum	Mean	Mode	Maximum	σ	SE	P	θ_1 and θ_2	Minimum	Mean	Mode	Maximum	σ	SE
P = 300	$\theta_1 = \theta_2 = 0$	−0.010	0.000	0.000	0.019	0.001	<.001	P = 300	$\theta_1 = \theta_2 = 0$	0.607	0.996	1.000	1.000	0.023	.001
	$\theta_1 = 0, \theta_2 = 0.1$	0.464	0.502	0.505	0.510	0.011	<.001		$\theta_1 = 0, \theta_2 = 0.1$	0.739	0.997	1.000	1.000	0.020	.001
	$\theta_1 = 0, \theta_2 = 0.4$	0.465	0.505	0.505	0.507	0.001	<.001		$\theta_1 = 0, \theta_2 = 0.4$	0.611	0.996	1.000	1.000	0.026	.001
	$\theta_1 = 0, \theta_2 = 0.9$	0.465	0.505	0.505	0.507	0.002	<.001		$\theta_1 = 0, \theta_2 = 0.9$	0.610	0.995	1.000	1.000	0.027	.001

Structured data—overdispersed descriptors: Estimates of mean correspondence ($\overline{ARI}_{HA}$) for each [N × P × (θ_1, θ_2)] configuration were based on S = 1,000 datasets, where correspondence is measured between the clustering solution achieved via DISPROF w/UPGMA and the simulated grouping partition. *N*, total number of objects (n_i = number of objects in group *i*); *P*, total number of descriptors; θ_i, overdispersion for descriptors in group *i*; μ_i, mean value of descriptors in group *i*; σ, standard deviation of the mean; *SE*, standard error of the mean. ARI_{HA} values estimate the likelihood of agreement between one randomly selected pair of objects represented in both partitions, corrected for change, and negative values represent probabilities that are less than would be expected by random chance alone.

solutions is incomplete without also discussing their correspondence with reality (i.e., "correctness").

4.2.1 | Effect of group locations

The structured data were simulated as either two groups whose location in hyperspace was defined by the progressively decreasing amount of average overlap between the groups' data clouds (Sim 2), or as two stationary groups whose location was predefined to be the same (Sim 3a) or different (Sim 3b, Sim 4). In all cases, we have demonstrated that when the two groups have higher overlap in hyperspace, the DISPROF algorithm has a tendency to underestimate the number of groups, and often settles on solutions where only a single large group exists. When clustering multivariate normal data, as in Sim 2, the effects of the amount of overlap are overridden by increases in the dimensionality of the dataset (Figure 5a) and potentially are due to the increase in complexity of the fingerprint for the groups that coincides with the extra dimensions. The result of this override is that even at levels of data overlap that reach as much as 50%, DISPROF clustering is able to detect the correct number of groups in data that have $P \geq 5$. However, the correspondence values for those correct numbers of groups do not reach acceptable levels ($\overline{ARI}_{HA} \geq 0.80$) until $P \geq 10$ (Figure 5b). Therefore, when clustering multivariate normal data with equal variances, the most reliable resolution and correspondence levels will be achieved with $P \geq 10$.

The simulated ecological count data showed a profound effect of group location on the resolution and correspondence of the clustering solutions provided by DISPROF. Particularly in cases where the two sets of objects had the same central tendency but different overdispersion structures, and regardless of the number of descriptors in the dataset, DISPROF either underestimated the number of groups (e.g., $G_{mode} = 1$), or very greatly overestimated it (e.g., $G_{mode} = 26$). This directly contrasts with the performance of DISPROF with ecological count data whose groups are separated in hyperspace. In these cases, once again regardless of the number of descriptors, DISPROF performed optimally and identified the correct number of groups, on average, in ecological data, even with high levels of overdispersion. This finding is consistent with those for the multivariate normal data, in that low *Ov* improved DISPROF's performance as a clustering criterion. High group overlap may negatively affect DISPROF in the same manner as having low numbers of descriptors (*P*), where the high-overlap situation allows for group fingerprints that are not unique enough when compared to one another. In this case, the randomization process is unable to break the structure in the datasets and the differences between the mean resemblance profile (representing H_o) and the observed profile are negligible (i.e., no structure present); thus, the routine returns a solution that identifies the entire data cloud as one group.

4.2.2 | Effects of overdispersion among descriptors within groups

The ecological count data used here were simulated so that we could examine the effects of increasing the overdispersion (θ) of G_2

TABLE 7 Descriptive statistics for $\bar{G}$ and $\overline{ARI}_{HA}$ for DISPROF based on Sim 4

P	Σ_1 and Σ_2	Minimum	Mean	Mode	Maximum	σ	SE	P	Σ_1 and Σ_2	Minimum	Mean	Mode	Maximum	σ	SE
Sim 4. $\bar{G} - \mu_1 = 10, \mu_2 = 30, n_1 = n_2 = 25, S = 1.000$								Sim 4. $\overline{ARI}_{HA} - \mu_1 = 10, \mu_2 = 30, n_1 = n_2 = 25, S = 1.000$							
$P = 2$	$\Sigma_1 = \Sigma_2 = 0$	2.000	2.058	2.000	5.000	0.294	.009	$P = 2$	$\Sigma_1 = \Sigma_2 = 0$	0.691	0.994	1.000	1.000	0.033	.001
	$\Sigma_1 = \Sigma_2 = 0.6$	2.000	3.620	3.000	7.000	0.974	.031		$\Sigma_1 = \Sigma_2 = 0.6$	0.345	0.769	1.000	1.000	0.153	.005
	$\Sigma_1 = \Sigma_2 = 0.9$	4.000	6.515	6.000	10.000	0.986	.031		$\Sigma_1 = \Sigma_2 = 0.9$	0.254	0.411	0.353	0.752	0.071	.002
	$\Sigma_1 = 0, \Sigma_2 = 0.6$	2.000	2.844	3.000	6.000	0.740	.023		$\Sigma_1 = 0, \Sigma_2 = 0.6$	0.413	0.881	1.000	1.000	0.111	.004
	$\Sigma_1 = 0, \Sigma_2 = 0.9$	3.000	4.343	4.000	7.000	0.743	.023		$\Sigma_1 = 0, \Sigma_2 = 0.9$	0.398	0.699	0.684	0.892	0.053	.002
$P = 3$	$\Sigma_1 = \Sigma_2 = 0$	2.000	2.056	2.000	4.000	0.247	.008	$P = 3$	$\Sigma_1 = \Sigma_2 = 0$	0.731	0.995	1.000	1.000	0.027	.001
	$\Sigma_1 = \Sigma_2 = 0.6$	2.000	4.553	4.000	10.000	1.017	.032		$\Sigma_1 = \Sigma_2 = 0.6$	0.326	0.637	0.505	1.000	0.136	.004
	$\Sigma_1 = \Sigma_2 = 0.9$	5.000	7.601	8.000	11.000	1.074	.034		$\Sigma_1 = \Sigma_2 = 0.9$	0.193	0.341	0.306	0.562	0.058	.002
	$\Sigma_1 = 0, \Sigma_2 = 0.6$	2.000	3.349	3.000	6.000	0.744	.024		$\Sigma_1 = 0, \Sigma_2 = 0.6$	0.505	0.812	1.000	1.000	0.096	.003
	$\Sigma_1 = 0, \Sigma_2 = 0.9$	3.000	4.899	5.000	8.000	0.798	.025		$\Sigma_1 = 0, \Sigma_2 = 0.9$	0.381	0.668	0.650	0.830	0.044	.001
$P = 5$	$\Sigma_1 = \Sigma_2 = 0$	2.000	2.064	2.000	5.000	0.307	.010	$P = 5$	$\Sigma_1 = \Sigma_2 = 0$	0.691	0.996	1.000	1.000	0.025	.001
	$\Sigma_1 = \Sigma_2 = 0.6$	3.000	5.335	5.000	10.000	0.988	.031		$\Sigma_1 = \Sigma_2 = 0.6$	0.311	0.537	0.588	0.923	0.101	.003
	$\Sigma_1 = \Sigma_2 = 0.9$	6.000	8.943	9.000	13.000	1.077	.034		$\Sigma_1 = \Sigma_2 = 0.9$	0.168	0.284	0.257	0.473	0.047	.001
	$\Sigma_1 = 0, \Sigma_2 = 0.6$	2.000	3.731	4.000	7.000	0.746	.024		$\Sigma_1 = 0, \Sigma_2 = 0.6$	0.492	0.766	0.777	1.000	0.074	.002
	$\Sigma_1 = 0, \Sigma_2 = 0.9$	4.000	5.535	5.000	9.000	0.823	.026		$\Sigma_1 = 0, \Sigma_2 = 0.9$	0.365	0.640	0.630	0.783	0.036	.001
$P = 10$	$\Sigma_1 = \Sigma_2 = 0$	2.000	2.066	2.000	5.000	0.316	.010	$P = 10$	$\Sigma_1 = \Sigma_2 = 0$	0.709	0.996	1.000	1.000	0.024	.001
	$\Sigma_1 = \Sigma_2 = 0.6$	4.000	6.248	6.000	10.000	1.034	.033		$\Sigma_1 = \Sigma_2 = 0.6$	0.259	0.446	0.482	0.823	0.076	.002
	$\Sigma_1 = \Sigma_2 = 0.9$	8.000	10.540	10.000	15.000	1.221	.039		$\Sigma_1 = \Sigma_2 = 0.9$	0.136	0.234	0.222	0.388	0.036	.001
	$\Sigma_1 = 0, \Sigma_2 = 0.6$	3.000	4.196	4.000	8.000	0.795	.025		$\Sigma_1 = 0, \Sigma_2 = 0.6$	0.462	0.719	0.731	0.925	0.053	.002
	$\Sigma_1 = 0, \Sigma_2 = 0.9$	4.000	6.407	6.000	11.000	0.908	.029		$\Sigma_1 = 0, \Sigma_2 = 0.9$	0.309	0.615	0.616	0.727	0.030	.001
$P = 25$	$\Sigma_1 = \Sigma_2 = 0$	2.000	2.056	2.000	6.000	0.266	.008	$P = 25$	$\Sigma_1 = \Sigma_2 = 0$	0.729	0.997	1.000	1.000	0.014	.000
	$\Sigma_1 = \Sigma_2 = 0.6$	5.000	7.640	7.000	12.000	1.133	.036		$\Sigma_1 = \Sigma_2 = 0.6$	0.205	0.355	0.326	0.588	0.059	.002
	$\Sigma_1 = \Sigma_2 = 0.9$	8.000	12.723	13.000	17.000	1.282	.041		$\Sigma_1 = \Sigma_2 = 0.9$	0.120	0.185	0.161	0.309	0.029	.001
	$\Sigma_1 = 0, \Sigma_2 = 0.6$	3.000	4.911	5.000	9.000	0.788	.025		$\Sigma_1 = 0, \Sigma_2 = 0.6$	0.402	0.676	0.666	0.925	0.042	.001
	$\Sigma_1 = 0, \Sigma_2 = 0.9$	5.000	7.505	7.000	10.000	0.905	.029		$\Sigma_1 = 0, \Sigma_2 = 0.9$	0.455	0.593	0.583	0.679	0.021	.001
$P = 50$	$\Sigma_1 = \Sigma_2 = 0$	2.000	2.068	2.000	5.000	0.302	.010	$P = 50$	$\Sigma_1 = \Sigma_2 = 0$	0.775	0.996	1.000	1.000	0.018	.001
	$\Sigma_1 = \Sigma_2 = 0.6$	6.000	8.792	9.000	12.000	1.197	.038		$\Sigma_1 = \Sigma_2 = 0.6$	0.185	0.303	0.287	0.518	0.052	.002
	$\Sigma_1 = \Sigma_2 = 0.9$	10.000	14.368	14.000	21.000	1.468	.046		$\Sigma_1 = \Sigma_2 = 0.9$	0.098	0.156	0.146	0.264	0.024	.001
	$\Sigma_1 = 0, \Sigma_2 = 0.6$	3.000	5.499	5.000	9.000	0.878	.028		$\Sigma_1 = 0, \Sigma_2 = 0.6$	0.517	0.650	0.626	0.823	0.036	.001
	$\Sigma_1 = 0, \Sigma_2 = 0.9$	5.000	8.405	8.000	14.000	1.078	.034		$\Sigma_1 = 0, \Sigma_2 = 0.9$	0.393	0.578	0.573	0.646	0.021	.001

(Continues)

TABLE 7 (Continued)

P	Σ_1 and Σ_2	Minimum	Mean	Mode	Maximum	σ	SE	P	Σ_1 and Σ_2	Minimum	Mean	Mode	Maximum	σ	SE
$P = 150$	$\Sigma_1 = \Sigma_2 = 0$	2.000	2.054	2.000	4.000	0.247	.008	$P = 150$	$\Sigma_1 = \Sigma_2 = 0$	0.889	0.998	1.000	1.000	0.011	.000
	$\Sigma_1 = \Sigma_2 = 0.6$	7.000	10.652	10.000	16.000	1.316	.042		$\Sigma_1 = \Sigma_2 = 0.6$	0.137	0.235	0.218	0.371	0.038	.001
	$\Sigma_1 = \Sigma_2 = 0.9$	12.000	17.067	17.000	24.000	1.578	.050		$\Sigma_1 = \Sigma_2 = 0.9$	0.073	0.122	0.119	0.237	0.019	.001
	$\Sigma_1 = 0, \Sigma_2 = 0.6$	4.000	6.476	6.000	10.000	0.973	.031		$\Sigma_1 = 0, \Sigma_2 = 0.6$	0.492	0.616	0.616	0.731	0.027	.001
	$\Sigma_1 = 0, \Sigma_2 = 0.9$	6.000	9.766	10.000	14.000	1.166	.037		$\Sigma_1 = 0, \Sigma_2 = 0.9$	0.453	0.562	0.555	0.626	0.015	.000
$P = 225$	$\Sigma_1 = \Sigma_2 = 0$	2.000	2.052	2.000	6.000	0.282	.009	$P = 225$	$\Sigma_1 = \Sigma_2 = 0$	0.716	0.997	1.000	1.000	0.016	.000
	$\Sigma_1 = \Sigma_2 = 0.6$	8.000	11.348	11.000	16.000	1.357	.043		$\Sigma_1 = \Sigma_2 = 0.6$	0.131	0.217	0.208	0.328	0.035	.001
	$\Sigma_1 = \Sigma_2 = 0.9$	14.000	18.052	18.000	23.000	1.550	.049		$\Sigma_1 = \Sigma_2 = 0.9$	0.076	0.112	0.110	0.186	0.017	.001
	$\Sigma_1 = 0, \Sigma_2 = 0.6$	4.000	6.769	7.000	10.000	0.963	.030		$\Sigma_1 = 0, \Sigma_2 = 0.6$	0.443	0.609	0.603	0.712	0.027	.001
	$\Sigma_1 = 0, \Sigma_2 = 0.9$	7.000	10.169	10.000	14.000	1.139	.036		$\Sigma_1 = 0, \Sigma_2 = 0.9$	0.405	0.558	0.552	0.608	0.014	.000
$P = 300$	$\Sigma_1 = \Sigma_2 = 0$	2.000	2.053	2.000	6.000	0.317	.010	$P = 300$	$\Sigma_1 = \Sigma_2 = 0$	0.646	0.997	1.000	1.000	0.018	.001
	$\Sigma_1 = \Sigma_2 = 0.6$	8.000	11.973	12.000	17.000	1.342	.042		$\Sigma_1 = \Sigma_2 = 0.6$	0.124	0.203	0.188	0.321	0.031	.001
	$\Sigma_1 = \Sigma_2 = 0.9$	14.000	18.726	19.000	24.000	1.659	.052		$\Sigma_1 = \Sigma_2 = 0.9$	0.070	0.107	0.104	0.218	0.017	.001
	$\Sigma_1 = 0, \Sigma_2 = 0.6$	4.000	7.107	7.000	10.000	1.001	.032		$\Sigma_1 = 0, \Sigma_2 = 0.6$	0.412	0.602	0.597	0.717	0.026	.001
	$\Sigma_1 = 0, \Sigma_2 = 0.9$	7.000	10.588	11.000	14.000	1.175	.037		$\Sigma_1 = 0, \Sigma_2 = 0.9$	0.378	0.555	0.552	0.616	0.015	.000

Structured data—correlated descriptors: Estimates of the mean number of groups identified ($\bar{G}$) and mean correspondence (ARI_{HA}) for each [$N \times P \times (\Sigma_1, \Sigma_2)$] configuration were based on $S = 1{,}000$ datasets, where correspondence is measured between the clustering solution achieved via DISPROF with UPGMA and the simulated partition. N, total number of objects in group i); P, total number of descriptors; Σ_i, correlation among descriptors in group i; μ_i, mean value of descriptors in group i; σ, standard deviation of the mean; SE, standard error of the mean. ARI_{HA} values estimate the likelihood of agreement between one randomly selected pair of objects represented in both partitions, corrected for chance.

while holding $\theta_1 = 0$. The purpose of this exercise was to increase the relatability of the results to ecological data, as many species composition and abundance datasets are highly overdispersed. Our results indicate that when the groups do not overlap in hyperspace, the effects of the overdispersion of the second group are negligible when considering the resolution of the clustering solutions, but the correspondence of those solutions with reality is unacceptable when $P \leq 10$ for data with high overdispersion ($\theta_2 = 0.9$). When the groups are defined by different levels of overdispersion and share a location, the effects of increasing overdispersion become more pronounced and are seemingly amplified by increasing the dimensionality of the dataset being tested. In these cases, the resolution of the solutions is as described previously, but the correspondence levels for the resultant partitions are all inadequate. The point of interest, however, is that the $\overline{ARI}_{HA}$ values tended to be around 0.5 for clustering scenarios where the overdispersion among descriptors is medium or high (i.e., $\theta_2 = \{0.4, 0.9\}$) and $P \geq 25$ (and for $\theta_2 = 0.1$, the $P_{threshold} = 150$). This indicates that one group is being identified fairly well and the other is being completely misrepresented by the grouping algorithm. We suspect that the increase in θ_2 causes the numerical fingerprint of the objects within the group to be too dissimilar when only compared to one another, and the result is a series of singleton groups, as the clustering algorithm iteratively works through the UPGMA connection of the overdispersed nodes. It seems as though the effects of overdispersion among ecological count data are secondary to the effects of group location in hyperspace, but supersede those of dataset dimensionality (dimension < overdispersion < location).

4.2.3 | Effects of correlation structure among descriptors within groups

Our simulation studies that incorporated different correlation structures among descriptors within groups were also undertaken in an effort to relate our investigations to studies incorporating ecological datasets, which often contain descriptors that are correlated with one another to some degree. We used multivariate normal data in our simulations to ensure that the observed effects of different correlation scenarios were not confounded by some other distributional assumptions. It appears as though medium to high levels of correlation ($\Sigma = \{0.6, 0.9\}$) among descriptors within a group will strongly impact the number of groups identified, and it tends to increase $\bar{G}$ as Σ increases. Drawing inferences from these clustering results may be dubious, however, because for virtually all clustering solutions that had medium or high correlation among descriptors, regardless of dimension, the mean correspondence was well below acceptable limits.

Correlation structure among groups affects the shape of the data cloud in hyperspace. It is interesting to note that DISPROF seems to have an improved ability to detect more "correct" structure in data where the shapes (i.e., correlation structures) of the groups are the same ($\Sigma_1 = \Sigma_2$), as opposed to one group having no correlation structure (i.e., spherical data cloud) and the second group having medium-to-large correlations among descriptors (i.e., data cloud distortion). As our simulations only explore medium-to-high correlation among all descriptors, it would be of interest to examine low, negative, and mixed correlation structures to describe DISPROF's performance variability under a full range of correlation conditions. The control scenarios, where $\Sigma_1 = \Sigma_2 = 0$, were among the only scenarios that returned reasonable $\bar{G}$ or $\overline{ARI}_{HA}$ results; however, these scenarios effectively recreate a simplified version of those data simulated under Sim 2. The overall $\overline{ARI}_{HA}$ results suggest that increasing the correlation between descriptors in one group and not the other tends to produce increasingly unreliable grouping partitions, and these results are in line with those from Sim 2, where low P results in low $\overline{ARI}_{HA}$. One explanation for this might be that as the level of correlation between descriptors increases the effective size of P decreases, and when considering the pairwise dissimilarity between objects, because the variability across all correlated descriptors in a group is essentially the same, datasets with high P and Σ tend to have similar DISPROF clustering dynamics as datasets with low P and no correlation structure.

5 | CONCLUSIONS

5.1 | DISPROF as a clustering decision criterion

Strengths of using resemblance profiles as a hypothesis test for multivariate structure are that the type I error rates (1) are within the range of acceptability for $\alpha = .05$, (2) tend to be binomially distributed around 5%, and (3) are resistant to the effects of both the underlying probability density function and (4) the $[N \times P]$ configuration of the data. Additional strengths include the facts that, when $\mu_1 \neq \mu_2$, the power of DISPROF (5) is within the acceptable range for $P \geq 10$ and is unaffected (6) by up to 50% average group overlap, (7) by increasing overdispersion among ecological count data, and (8) by increasing correlation structures among descriptors. Finally, (9) the first theoretical corollary proposed by Clarke et al. (2008), that the power of the test for multivariate structure increases as P increases, was confirmed.

From a traditional statistical error perspective, it appears that using resemblance profiles is a very effective method for identifying multivariate structure; it rarely identifies structure that is not present and it almost always identifies structure that is present. The weaknesses of using this hypothesis test are mostly related to the second Clarke et al. (2008) corollary, where the resolution of any grouping structure identified may be too fine to interpret meaningfully. The realized power of the resemblance profile hypothesis test comes when it is implemented as a clustering criterion, and success is based upon the partition returned by the algorithm. The resolution of the partition and the solution's correspondence with interpretable multivariate structure in the dataset are ultimately what the researchers will use to explain their theories. The second Clarke et al. (2008) corollary appears to be valid, but it manifests differently depending on the type, configuration, and hyperdimensional structure of the dataset being considered. However, if we constrain

our analysis to relatively high-dimensional, low-correlation datasets where the group locations are separated, then the resolution-versus-interpretability concern wanes greatly. The power to detect structure is very high, even with P as low as 10 descriptors, and so it follows that any additional resolution imparted on the solution (which may account for any reduction in correspondence) is likely the result of an actual numerical signal in the dataset, and can be manifest from random (or unmeasured) processes, or error. An alternative explanation may be related to the construction of the null distribution for the test statistic π, where group properties such as location and hyperdimensional shape may preclude the permutation procedure from accurately depicting the null scenario.

5.2 | Recommendations for using DISPROF (SIMPROF)

The results presented for type I error, power, resolution, and correspondence suggest that using resemblance profiles as a test for multivariate structure, and as a clustering decision criterion, has strengths and weaknesses. The results also highlight pitfalls that can be avoided if particular care is taken prior to implementation of these clustering techniques. The complex interactions between the data type/configuration and the hyperdimensional structure and overlap between groups strongly affect the results achieved when clustering with DISPROF. The method is nonetheless an improvement over traditional UPGMA clustering, most notably due to the removal of the arbitrary and static assignments of resemblance thresholds that define groups of objects. Because the realized power of using resemblance profiles as clustering decision criteria cannot be maximized without making tradeoffs between resolution and correspondence with interpretable structure, we make the following recommendations.

1. Exploratory analysis, such as principle coordinates analysis (PCoA), should be performed to determine, at a minimum, if any hypothesized grouping structures might have high amounts of overlap (i.e., $Ov > 50\%$) in hyperdimensional space, and DISPROF should be avoided in high-overlap situations. Data clouds that appear to overlap greatly could produce unreliable results and should not be clustered using these methods.
2. Medium-to-high correlation (i.e., ≥0.6) among all descriptors should be avoided, and efforts should be made to either reduce or remove the correlated descriptors in a dataset. In an effort to create more parsimonious models, priority should be given to descriptors that are indicative of independent processes, whenever possible. In the case of ecological abundance data, where many species are often both of interest and are highly correlated, it may be of benefit to use a dimension reduction technique (e.g., PCoA) that produces new orthogonal descriptors, with no correlation structures, prior to clustering with DISPROF.
3. The data dimensionality should be restricted to $P \geq 25$ descriptors in order to achieve solutions with ideal resolution and "excellent" correspondence ($\overline{ARI}_{HA} \geq 0.90$) to meaningfully interpretable structure.
4. A less conservative guideline would be to restrict the number of descriptors to $P \geq 10$. This new limit retains power, increases the potential for higher resolution solutions, and reduces correspondence from "excellent" to "good" ($0.80 \leq \overline{ARI}_{HA} < 0.90$).

Since its initial development and addition to PRIMER-E (Clarke & Gorley, 2015), the use of resemblance profiles has been gaining traction as a clustering criterion, mostly in the ecological literature. Our results provide recommendations for ecologists to use when applying these methods, and demonstrate the methods' transferability to other numerical analyses, data types, and disciplines. With a better understanding of the dynamic performance of resemblance profiles as clustering criteria and the potential variability in the results they produce, researchers can more confidently deploy SIMPROF and interpret the results with respect to beta-diversity, species/environment relationships, or any other complex multivariate model and/or associated hypotheses. While there appear to be clear advantages imparted by the use of resemblance profiles as clustering criteria, there are still many questions that deserve additional attention that were beyond the scope of this evaluation.

ACKNOWLEDGMENTS

This work was completed in partial fulfillment of the requirements for JPK's doctoral degree. JPK was supported by NOAA-National Marine Fisheries Service grant NA10NMF4550468. The authors would like to acknowledge the use of the services provided by Research Computing at the University of South Florida for algorithm testing. We thank Dr. D. Steinley and Dr. R. Henson for generously providing the OCLUS MATLAB code for simulation of overlapping clustered datasets.

CONFLICT OF INTEREST

None declared.

DATA AVAILABILITY

All simulated datasets and analyses performed in MATLAB are publicly available upon request.

REFERENCES

Anderson, M. J., & Walsh, D. C. I. (2013). PERMANOVA, ANOSIM, and the Mantel test in the face of heterogeneous dispersions: What null hypothesis are you testing? *Ecological Monographs*, *83*, 557–574.

Babyak, M. A. (2004). What you see may not be what you get: A brief, nontechnical introduction to overfitting in regression-type models. *Psychosomatic Medicine*, *66*, 411–421.

Batagelj, V., & Bren, M. (1995). Comparing resemblance measures. *Journal of Classification*, *12*, 73–90.

Clarke, K. R., & Gorley, R. N. (2015). *User manual/tutorial*. Plymouth, UK: PRIMER-E.

Clarke, K. R., Somerfield, P. J., & Chapman, M. G. (2006). On resemblance measures for ecological studies, including taxonomic dissimilarities and a zero-adjusted Bray-Curtis coefficient for denuded assemblages. *Journal of Experimental Marine Biology and Ecology*, *330*, 55–80.

Clarke, K. R., Somerfield, P. J., & Gorley, R. N. (2008). Testing of null hypotheses in exploratory community analyses: Similarity profiles and biota-environment linkage. *Journal of Experimental Marine Biology and Ecology*, *366*, 56–69.

Cohen, J. (2013). *Statistical power analysis for the behavioral sciences*. Burlington, VT: Elsevier Science.

Faith, D. P., Minchin, P. R., & Belbin, L. (1987). Compositional dissimilarity as a robust measure of ecological distance. *Vegetatio*, *69*, 57–68.

French, B., Clarke, K. R., Platell, M. E., & Potter, I. C. (2013). An innovative statistical approach to constructing a readily comprehensible food web for a demersal fish community. *Estuarine Coastal and Shelf Science*, *125*, 43–56.

Gilbert, J. A., Field, D., Swift, P., Newbold, L., Oliver, A., Smyth, T., … Joint, I. (2009). The seasonal structure of microbial communities in the western English channel. *Environmental Microbiology*, *11*, 3132–3139.

Gonzalez-Mirelis, G., & Buhl-Mortensen, P. (2015). Modelling benthic habitats and biotopes off the coast of Norway to support spatial management. *Ecological Informatics*, *30*, 284–292.

Gower, J. C. (1966). Some distance properties of latent root and vector methods used in multivariate analysis. *Biometrika*, *53*, 325–338.

Hawkins, D. M. (2004). The problem of overfitting. *Journal of Chemical Information and Computer Sciences*, *44*, 1–12.

Hernandez Almeida, O. U., & Siqueiros Beltrones, D. A. (2012). Substrate-dependent differences between the structures of epiphytic and epilithic diatom assemblages off the southwestern coast of the Gulf of California. *Botanica Marina*, *55*, 149–159.

Huang, D. W., Licuanan, W. Y., Hoeksema, B. W., Chen, C. A., Ang, P. O., Huang, H., … Chou, L. M. (2015). Extraordinary diversity of reef corals in the south China sea. *Marine Biodiversity*, *45*, 157–168.

Hubert, L., & Arabie, P. (1985). Comparing partitions. *Journal of Classification*, *2*, 193–218.

Jones, D. L. (2015). *The Fathom toolbox for MATLAB*. St. Petersburg, FL: University of South Florida, College of Marine Science.

Kelly, J. R., & Scheibling, R. E. (2012). Fatty acids as dietary tracers in benthic food webs. *Marine Ecology Progress Series*, *446*, 1–22.

Khodakova, A. S., Smith, R. J., Burgoyne, L., Abarno, D., & Linacre, A. (2014). Random whole metagenomic sequencing for forensic discrimination of soils. *PLoS ONE*, *9*, e104996. doi: 10.1371/journal.pone.0104996.

Kilborn, J. P. (2015). *The Darkside toolbox for MATLAB*. St. Petersburg, FL: University of South Florida, College of Marine Science.

Legendre, P., & Fortin, M. J. (2010). Comparison of the Mantel test and alternative approaches for detecting complex multivariate relationships in the spatial analysis of genetic data. *Molecular Ecology Resources*, *10*, 831–844.

Legendre, P., & Legendre, L. (2012). *Numerical ecology* (3rd English ed.). Amsterdam, the Netherlands: Elsevier.

Liu, X. S., Zhang, Z. N., & Huang, Y. (2007). Sublittoral meiofauna with particular reference to nematodes in the southern Yellow Sea, China. *Estuarine Coastal and Shelf Science*, *71*, 616–628.

Macedo-Soares, L. C. P., Freire, A. S., & Muelbert, J. H. (2012). Small-scale spatial and temporal variability of larval fish assemblages at an isolated oceanic island. *Marine Ecology Progress Series*, *444*, 207–222.

MATLAB and Statistics Toolbox Release (2016a). The MathWorks, Inc.. Natick, Massachusetts: United States.

Moore, B. R., & Simpfendorfer, C. A. (2014). Assessing connectivity of a tropical estuarine teleost through otolith elemental profiles. *Marine Ecology Progress Series*, *501*, 225–238.

Muhling, B. A., Beckley, L. E., Koslow, J. A., & Pearce, A. F. (2008). Larval fish assemblages and water mass structure off the oligotrophic south-western Australian coast. *Fisheries Oceanography*, *17*, 16–31.

Parsons, M. L., Settlemier, C. J., & Ballauer, J. M. (2011). An examination of the epiphytic nature of *Gambierdiscus toxicus*, a dinoflagellate involved in ciguatera fish poisoning. *Harmful Algae*, *10*, 598–605.

Rehm, P., Hooke, R. A., & Thatje, S. (2011). Macrofaunal communities on the continental shelf off Victoria Land, Ross Sea, Antarctica. *Antarctic Science*, *23*, 449–455.

Selleslagh, J., Amara, R., Laffargue, P., Lesourd, S., Lepage, M., & Girardin, M. (2009). Fish composition and assemblage structure in three Eastern English Channel macrotidal estuaries: A comparison with other French estuaries. *Estuarine Coastal and Shelf Science*, *81*, 149–159.

Steinley, D. (2004). Properties of the Hubert-Arabie adjusted rand index. *Psychological Methods*, *9*, 386–396.

Steinley, D., & Henson, R. (2005). OCLUS: An analytic method for generating clusters with known overlap. *Journal of Classification*, *22*, 221–250.

Travers, M. J., Potter, I. C., Clarke, K. R., & Newman, S. J. (2012). Relationships between latitude and environmental conditions and the species richness, abundance and composition of tropical fish assemblages over soft substrata. *Marine Ecology Progress Series*, *446*, 221–241.

Valesini, F. J., Hourston, M., Wildsmith, M. D., Coen, N. J., & Potter, I. C. (2010). New quantitative approaches for classifying and predicting local-scale habitats in estuaries. *Estuarine Coastal and Shelf Science*, *86*, 645–664.

Warton, D. I., & Hudson, H. M. (2004). A MANOVA statistic is just as powerful as distance-based statistics, for multivariate abundances. *Ecology*, *85*, 858–874.

SUPPORTING INFORMATION

Additional Supporting Information may be found online in the supporting information tab for this article.

How to cite this article: Kilborn JP, Jones DL, Peebles EB, Naar DF. Resemblance profiles as clustering decision criteria: Estimating statistical power, error, and correspondence for a hypothesis test for multivariate structure. *Ecol Evol*. 2017;7:2039–2057. https://doi.org/10.1002/ece3.2760

APPENDIX D:

CHAPTER FIVE SUMMPLEMENTAL TABLES AND FIGURES

D.1 SUPPLEMENTAL TABLES

Table D.1 – RDA results. Full table of results from the redundancy analysis based on the Gulf LME EL-FISH response indicators **Y** and predictors **X**. Where, F = canonical test statistic; R^2 = fraction of explained variation; R^2_{adj} = the unbiased estimator of R^2; and m = the canonical axes produced by the RDA algorithm. Corresponding eigenvalues and proportions of variance explained are given for all m and residual axes.

F = 3.71
R^2 = 0.9913
R^2_{adj} = 0.7290
p-value = 0.003
iterations = 1,000

			Fraction of variance explained		
m	Eigenvalues	Resid. Eigenval.	Axis	Cumulative	Residual
1	15.66	0.43	0.3196	0.3196	0.0087
2	7.93		0.1618	0.4814	
3	3.93		0.0802	0.5616	
4	3.62		0.0738	0.6354	
5	2.83		0.0578	0.6932	
6	1.78		0.0362	0.7295	
7	1.59		0.0325	0.7620	
8	1.49		0.0304	0.7924	
9	1.30		0.0266	0.8190	
10	1.19		0.0243	0.8433	
11	1.11		0.0226	0.8659	
12	0.97		0.0198	0.8858	
13	0.70		0.0143	0.9000	
14	0.64		0.0130	0.9131	
15	0.58		0.0119	0.9250	
16	0.52		0.0106	0.9356	
17	0.50		0.0102	0.9458	
18	0.44		0.0090	0.9547	
19	0.35		0.0071	0.9619	

Table D.1 (Continued)

20	0.28	0.0058	0.9677
21	0.24	0.0049	0.9725
22	0.21	0.0043	0.9768
23	0.17	0.0035	0.9803
24	0.13	0.0027	0.9830
25	0.13	0.0026	0.9856
26	0.09	0.0018	0.9874
27	0.06	0.0013	0.9887
28	0.05	0.0011	0.9898
29	0.05	0.0010	0.9907
30	0.03	0.0005	0.9913

Table D.2 – SIMPROF clustering results. Full table of clustering outputs from SIMPROF clustering of the standardized **Y** matrix converted to Euclidean dissimilarity. The π-statistic and p-value for each clustering attempt, along with the number of groups being evaluated, are presented. The final clustering solution is given in Figure 5.4b.

Evaluation of…	π-statistic	p-value
2 groups	461.148	0.001
3 groups	215.888	0.002
4 groups	78.856	0.003
5 groups	4.234	1.000
5 groups	18.084	0.005
6 groups	71.076	0.006
7 groups	7.345	0.231
7 groups	12.355	0.016
8 groups	1.938	0.099
8 groups	2.838	0.340
8 groups	7.219	0.055
9 groups	0.966	1.000
9 groups	0.000	1.000

Number of groups identified:	8
Permutations:	1,000
α-level :	0.05
Bonferoni progressive correction:	yes
Dissimilarity metric:	Euclidean

Table D.3 (Part 1) – Table of all $\lambda_{ab}(Y)$. Table of proportional contributions to the difference observed between regime states for each response indicator in **Y** (rows) for all possible pairs of *RS*s (columns). Indicators are organized according to the subcategories assigned in Table 5.1. Each column is color coded where warm colors represent low $\lambda_{ab}(\mathbf{y}_i)$ and cool colors are for high values. Each column's colors are scaled to the minimum and maximum $\lambda_{ab}(\mathbf{y}_i)$ values, and the color white represents the median value. All summary statistics are provided in the last six rows, including the total proportion of the difference retained when only examining the indicators that passed the threshold requirement (bold values) set in EL-FISH step 4 of the text.

		RS_1 v RS_2	RS_1 v RS_3	RS_1 v RS_4	RS_1 v RS_5	RS_1 v RS_6	RS_1 v RS_7	RS_1 v RS_8	RS_2 v RS_3	RS_2 v RS_4	RS_2 v RS_5	RS_2 v RS_6	RS_2 v RS_7	RS_2 v RS_8	RS_3 v RS_4
Lower - TL	MENHADEN	0.002	0.001	0.004	0.009	0.009	0.014	0.015	0.000	0.007	0.014	0.013	0.018	0.020	0.011
	N SHRMP	0.006	0.006	0.011	0.015	0.015	0.019	0.020	0.007	0.013	0.019	0.018	0.022	0.024	0.017
	S SHR 1	**0.031**	**0.031**	**0.029**	0.027	0.027	0.023	0.022	**0.030**	**0.028**	0.024	0.024	0.019	0.018	0.025
	S SHR 5	**0.030**	**0.030**	**0.029**	0.027	0.027	0.024	0.023	**0.030**	**0.028**	0.024	0.025	0.021	0.019	0.026
Upper - TL	BRD BP BBS	**0.031**	**0.031**	**0.029**	0.026	0.026	0.023	0.021	**0.030**	0.028	0.023	0.023	0.019	0.017	0.025
	BRD BP CBC	0.025	0.025	0.027	0.027	0.027	**0.026**	**0.026**	0.026	0.027	**0.026**	**0.027**	**0.025**	0.025	**0.027**
	BRD RS BBS	0.017	0.017	0.020	0.023	0.023	0.024	0.025	0.018	0.022	0.024	0.024	**0.026**	**0.026**	0.024
	BRD RS CBC	0.021	0.022	0.024	0.026	0.026	**0.026**	**0.026**	0.022	0.025	0.026	0.026	**0.026**	**0.026**	0.026
	N BN SHARK	0.024	0.025	0.026	0.027	0.027	**0.026**	**0.026**	0.025	0.027	**0.026**	**0.026**	**0.026**	0.025	0.027
	N BT SHARK	0.029	0.029	**0.029**	**0.028**	**0.028**	0.026	0.025	**0.029**	**0.028**	0.026	**0.026**	0.023	0.022	**0.027**
	N COBIA	0.026	0.025	0.021	0.016	0.016	0.010	0.008	0.024	0.018	0.010	0.010	0.004	0.001	0.013
	N GAG GR	**0.030**	**0.030**	**0.029**	**0.028**	**0.028**	0.025	0.024	**0.030**	**0.028**	0.025	0.025	0.022	0.021	0.027
	N KING MAC	0.025	0.025	0.026	0.027	0.027	**0.026**	**0.026**	0.026	0.027	**0.026**	**0.026**	**0.025**	0.025	0.027
	N MUTTON	0.020	0.020	0.023	0.025	0.025	0.025	**0.026**	0.021	0.024	0.025	0.025	**0.026**	**0.026**	0.025
	N SPAN MAC	0.013	0.012	0.006	0.000	0.000	0.005	0.007	0.010	0.003	0.005	0.004	0.011	0.013	0.002
	N TILE E	0.027	0.027	0.028	**0.028**	**0.028**	**0.026**	**0.026**	0.027	**0.028**	**0.026**	**0.026**	0.025	0.024	**0.027**
	N TILE W	**0.031**	**0.031**	**0.029**	0.026	0.026	0.022	0.021	**0.030**	0.028	0.023	0.023	0.018	0.016	0.025
	N TRIGGER	0.019	0.019	0.022	0.024	0.024	0.025	0.025	0.020	0.023	0.025	0.025	**0.026**	**0.026**	0.025
	N YE GR E	0.023	0.023	0.025	0.026	0.026	**0.026**	**0.026**	0.024	0.026	**0.026**	**0.026**	**0.026**	**0.025**	0.026
	N YE GR W	**0.030**	**0.029**	0.026	0.022	0.022	0.017	0.015	0.029	0.024	0.017	0.017	0.011	0.009	0.019

Table D.3 – Part 1 (Continued)

		RS1 v RS2	RS1 v RS3	RS1 v RS4	RS1 v RS5	RS1 v RS6	RS1 v RS7	RS1 v RS8	RS2 v RS3	RS2 v RS4	RS2 v RS5	RS2 v RS6	RS2 v RS7	RS2 v RS8	RS3 v RS4
Rev.	REV MEX	0.006	0.005	0.000	0.006	0.006	0.011	0.012	0.004	0.003	0.010	0.010	0.016	0.018	0.008
	REV US	**0.031**	**0.031**	0.028	0.025	0.025	0.021	0.019	**0.030**	0.027	0.021	0.021	0.016	0.014	0.023
Structure & Function	DIV LA	0.010	0.011	0.015	0.019	0.019	0.021	0.022	0.012	0.017	0.021	0.021	0.024	0.025	0.020
	DIV TX	0.011	0.010	0.005	0.001	0.001	0.006	0.008	0.009	0.002	0.006	0.006	0.012	0.014	0.003
	EVEN LA	0.014	0.015	0.018	0.022	0.022	0.024	0.024	0.016	0.020	0.023	0.023	0.025	**0.026**	0.023
	EVEN TX	0.009	0.010	0.014	0.018	0.018	0.021	0.022	0.011	0.016	0.021	0.020	0.024	0.025	0.019
	MTL SURV	0.004	0.005	0.010	0.014	0.014	0.018	0.019	0.006	0.012	0.018	0.018	0.022	0.023	0.016
	PD RATIO	0.007	0.006	0.001	0.005	0.005	0.010	0.012	0.005	0.003	0.010	0.009	0.015	0.017	0.007
	RICH LA	0.024	0.023	0.018	0.013	0.013	0.007	0.005	0.022	0.015	0.007	0.008	0.000	0.002	0.010
	RICH TX	0.011	0.010	0.004	0.001	0.001	0.007	0.009	0.008	0.001	0.007	0.006	0.013	0.015	0.004
	MTL COM	0.007	0.008	0.012	0.016	0.016	0.020	0.021	0.009	0.015	0.019	0.019	0.023	0.024	0.018
	MTL COM2	0.023	0.024	0.025	0.027	0.027	**0.026**	**0.026**	0.024	0.026	**0.026**	**0.026**	**0.026**	**0.025**	0.026
	MTL MEX	**0.029**	**0.029**	**0.029**	**0.028**	**0.028**	0.026	0.025	**0.029**	**0.028**	0.026	0.026	0.023	0.022	**0.027**
	PRED COM	0.020	0.019	0.015	0.009	0.009	0.003	0.001	0.018	0.011	0.003	0.003	0.004	0.006	0.006
	PRED COM2	0.027	0.027	0.028	**0.028**	**0.028**	**0.026**	**0.026**	0.027	0.028	**0.026**	**0.026**	0.025	0.024	**0.027**
	PRED MEX	**0.029**	**0.029**	**0.029**	**0.028**	**0.028**	0.026	0.025	**0.029**	**0.028**	0.026	0.026	0.023	0.022	**0.027**
	MTL REC	0.028	0.028	0.028	**0.028**	**0.028**	**0.026**	0.025	0.028	**0.028**	**0.026**	**0.026**	0.024	0.023	**0.027**
	PRED REC	**0.029**	**0.029**	**0.029**	**0.028**	**0.028**	0.026	0.025	**0.029**	**0.028**	0.026	0.026	0.023	0.022	**0.027**
	ATL CROK	0.011	0.010	0.005	0.001	0.001	0.006	0.008	0.009	0.002	0.006	0.005	0.012	0.014	0.003
	GROW GRA	0.011	0.012	0.016	0.019	0.019	0.022	0.023	0.013	0.018	0.022	0.022	0.024	**0.025**	0.021
	KINGFSH	0.026	0.026	0.027	**0.028**	**0.028**	**0.026**	**0.026**	0.027	0.028	**0.026**	**0.027**	0.025	0.024	**0.027**
	MAMM STR	0.013	0.012	0.007	0.001	0.001	0.005	0.007	0.011	0.003	0.004	0.004	0.011	0.013	0.002
	RED DRUM	**0.029**	**0.029**	**0.029**	**0.028**	**0.028**	0.026	0.025	**0.029**	**0.028**	0.026	0.026	0.023	0.022	**0.027**
	RED SNAP	0.023	0.024	0.025	0.026	0.026	**0.026**	**0.026**	0.024	0.026	**0.026**	**0.026**	**0.026**	**0.025**	0.026
	S FLOUND	0.022	0.022	0.024	0.026	0.026	**0.026**	**0.026**	0.023	0.025	**0.026**	0.026	**0.026**	**0.026**	0.026

Table D.3 – Part 1 (Continued)

		RS_1 v RS_2	RS_1 v RS_3	RS_1 v RS_4	RS_1 v RS_5	RS_1 v RS_6	RS_1 v RS_7	RS_1 v RS_8	RS_2 v RS_3	RS_2 v $RS4$	RS_2 v RS_5	RS_2 v RS_6	RS_2 v RS_7	RS_2 v RS_8	RS_3 v RS_4
Struct. & Funct.	SEATRT	**0.029**	**0.029**	**0.029**	**0.028**	**0.028**	0.026	0.025	**0.029**	**0.028**	0.026	0.026	0.023	0.022	**0.027**
	SHEEPHD	0.016	0.016	0.020	0.022	0.022	0.024	0.025	0.017	0.021	0.024	0.024	**0.026**	**0.026**	0.023
	SPAN MAC	0.028	0.028	**0.029**	**0.028**	**0.028**	0.026	0.025	0.029	**0.028**	**0.026**	**0.026**	0.024	0.022	**0.027**
	TUR NEST	0.014	0.015	0.018	0.021	0.021	0.023	0.024	0.016	0.020	0.023	0.023	0.025	**0.026**	0.022
	Minimum	0.002	0.001	0.000	0.000	0.000	0.003	0.001	0.000	0.001	0.003	0.003	0.000	0.001	0.002
	Median	0.023	0.023	0.024	0.025	0.025	0.024	0.024	0.024	0.025	0.024	0.024	0.023	0.022	0.025
	Maximum	0.031	0.031	0.029	0.028	0.028	0.026	0.026	0.030	0.028	0.026	0.027	0.026	0.026	0.027
	Stnd Dev	0.009	0.009	0.009	0.009	0.009	0.007	0.007	0.009	0.009	0.008	0.008	0.007	0.006	0.008
	Stnd Err	0.002	0.002	0.002	0.002	0.002	0.001	0.001	0.002	0.002	0.001	0.001	0.001	0.001	0.001
	Total Retained	**0.358**	**0.356**	**0.347**	**0.334**	**0.334**	**0.315**	**0.312**	**0.354**	**0.339**	**0.315**	**0.316**	**0.308**	**0.309**	**0.324**

Table D.3 (Part 2) – Table of all $\lambda_{ab}(Y)$. See Table D.3 (Part 1) for full description of details of this continuation of that table.

		RS_5 v RS_5	RS_5 v RS_6	RS_5 v RS_7	RS_5 v RS_8	RS_4 v RS_5	RS_4 v RS_6	RS_4 v RS_7	RS_4 v RS_8	RS_5 v RS_6	RS_5 v RS_6	RS_5 v RS_8	RS_6 v RS_7	RS_6 v RS_8	RS_7 v RS_8
Lower - TL	MENHADEN	0.019	0.018	0.023	0.025	**0.033**	**0.028**	**0.032**	**0.035**	0.009	**0.032**	**0.036**	**0.037**	**0.039**	0.028
	N SHRMP	0.023	0.022	**0.026**	**0.027**	**0.032**	**0.029**	**0.032**	**0.033**	0.015	**0.031**	**0.034**	**0.034**	0.035	0.019
	S SHR 1	0.019	0.020	0.014	0.012	0.002	0.009	0.003	0.001	0.027	0.004	0.003	0.004	0.012	0.029
	S SHR 5	0.020	0.021	0.016	0.014	0.005	0.011	0.006	0.002	0.027	0.007	0.000	0.001	0.008	0.026
Upper - TL	BRD BP BBS	0.018	0.019	0.013	0.011	0.000	0.008	0.002	0.003	0.026	0.003	0.005	0.006	0.014	0.030
	BRD BP CBC	0.025	**0.025**	0.023	0.022	0.018	0.021	0.018	0.016	0.027	0.019	0.015	0.014	0.009	0.011
	BRD RS BBS	**0.026**	**0.026**	**0.026**	**0.027**	0.027	**0.027**	0.027	0.026	0.023	0.027	0.026	0.026	0.023	0.004
	BRD RS CBC	**0.026**	**0.026**	0.025	0.025	0.022	0.024	0.023	0.021	0.026	0.023	0.021	0.020	0.016	0.004
	N BN SHARK	**0.025**	**0.026**	0.024	0.023	0.019	0.022	0.020	0.017	0.027	0.020	0.016	0.016	0.011	0.009

Table D.3 – Part 2 (Continued)

		RS3 v RS5	RS3 v RS6	RS3 v RS7	RS3 v RS8	RS4 v RS5	RS4 v RS6	RS4 v RS7	RS4 v RS8	RS5 v RS6	RS5 v RS6	RS5 v RS8	RS6 v RS7	RS6 v RS8	RS7 v RS8
Upper - TL	N BT SHARK	0.023	0.024	0.020	0.018	0.011	0.016	0.012	0.009	**0.028**	0.013	0.007	0.006	0.000	0.020
	N COBIA	0.002	0.004	0.004	0.007	0.020	0.011	0.019	0.024	0.016	0.017	0.026	0.027	**0.035**	**0.041**
	N GAG GR	0.022	0.022	0.018	0.016	0.008	0.014	0.009	0.005	**0.028**	0.010	0.004	0.002	0.004	0.023
	N KING MAC	0.025	**0.025**	0.024	0.023	0.018	0.021	0.019	0.016	0.027	0.019	0.015	0.015	0.010	0.011
	N MUTTON	**0.026**	**0.026**	**0.026**	**0.026**	0.024	0.025	0.024	0.023	0.025	0.025	0.023	0.022	0.019	0.001
	N SPAN MAC	0.012	0.011	0.017	0.020	**0.032**	0.024	**0.030**	**0.034**	0.000	0.029	**0.036**	**0.037**	**0.042**	**0.037**
	N TILE E	0.024	0.025	0.022	0.021	0.014	0.019	0.015	0.013	**0.028**	0.016	0.011	0.010	0.005	0.015
	N TILE W	0.017	0.019	0.013	0.010	0.000	0.007	0.001	0.003	0.026	0.002	0.005	0.006	0.014	0.031
	N TRIGGER	**0.026**	**0.026**	**0.026**	**0.026**	0.025	0.026	0.025	0.024	0.024	0.025	0.024	0.024	0.020	0.001
	N YE GR E	**0.026**	**0.026**	0.025	0.024	0.021	0.023	0.021	0.020	0.026	0.022	0.019	0.018	0.014	0.007
	N YE GR W	0.010	0.011	0.004	0.001	0.012	0.002	0.010	0.015	0.022	0.008	0.017	0.018	0.026	**0.038**
Rev.	REV MEX	0.017	0.016	0.021	0.024	**0.033**	**0.027**	**0.032**	**0.035**	0.006	**0.031**	**0.036**	**0.037**	**0.041**	**0.031**
	REV US	0.015	0.016	0.010	0.007	0.005	0.004	0.003	0.008	0.025	0.002	0.010	0.011	0.019	**0.034**
Structure & Function	DIV LA	0.024	0.024	**0.026**	**0.027**	0.031	**0.029**	**0.030**	0.031	0.019	**0.030**	0.031	0.031	0.031	0.014
	DIV TX	0.013	0.012	0.018	0.021	**0.032**	0.024	**0.031**	**0.034**	0.001	**0.029**	**0.036**	**0.037**	**0.042**	**0.036**
	EVEN LA	**0.026**	0.025	**0.027**	**0.027**	0.028	**0.028**	0.028	0.028	0.022	0.028	0.028	0.028	0.026	0.008
	EVEN TX	0.024	0.023	**0.026**	**0.027**	**0.031**	**0.029**	**0.031**	**0.032**	0.018	**0.030**	**0.032**	0.032	0.032	0.015
	MTL SURV	0.022	0.022	**0.025**	**0.027**	**0.033**	**0.029**	**0.032**	**0.034**	0.014	**0.031**	**0.034**	**0.035**	**0.036**	0.021
	PD RATIO	0.016	0.015	0.021	0.024	**0.033**	0.026	**0.032**	**0.035**	0.005	**0.031**	**0.036**	**0.037**	**0.041**	**0.032**
	RICH LA	0.001	0.001	0.007	0.010	0.023	0.014	0.022	0.027	0.013	0.020	0.029	0.030	**0.037**	**0.041**
	RICH TX	0.014	0.012	0.019	0.022	**0.032**	0.025	**0.031**	**0.035**	0.001	**0.030**	**0.036**	**0.037**	**0.042**	**0.035**
	MTL COM	0.023	0.023	**0.026**	**0.027**	**0.032**	**0.029**	**0.031**	**0.033**	0.016	**0.031**	**0.033**	**0.033**	0.034	0.018
	MTL COM2	**0.026**	**0.026**	0.024	0.024	0.020	0.023	0.021	0.019	0.027	0.021	0.018	0.017	0.013	0.008
	MTL MEX	0.023	0.024	0.020	0.018	0.011	0.016	0.012	0.009	**0.028**	0.013	0.007	0.006	0.000	0.020
	PRED COM	0.005	0.003	0.011	0.014	0.027	0.018	0.025	0.030	0.009	0.024	0.032	**0.033**	**0.040**	**0.041**
	PRED COM2	0.024	0.025	0.022	0.021	0.015	0.019	0.016	0.013	**0.028**	0.016	0.012	0.011	0.005	0.015

Table D.3 – Part 2 (Continued)

		RS_3 v RS_5	RS_3 v RS_6	RS_3 v RS_7	RS_3 v RS_8	RS_4 v RS_5	RS_4 v RS_6	RS_4 v RS_7	RS_4 v RS_8	RS_5 v RS_6	RS_5 v RS_6	RS_5 v RS_8	RS_6 v RS_7	RS_6 v RS_8	RS_7 v RS_8
Structure & Function	PRED MEX	0.023	0.023	0.019	0.018	0.010	0.016	0.011	0.008	**0.028**	0.012	0.006	0.005	0.001	0.021
	MTL REC	0.024	0.024	0.021	0.020	0.013	0.018	0.014	0.011	**0.028**	0.015	0.009	0.008	0.002	0.018
	PRED REC	0.022	0.023	0.019	0.017	0.009	0.015	0.011	0.007	**0.028**	0.011	0.005	0.004	0.002	0.021
	ATL CROK	0.013	0.011	0.018	0.021	**0.032**	0.024	**0.030**	**0.034**	0.001	**0.029**	**0.036**	**0.037**	**0.042**	**0.036**
	GROW GRA	0.025	0.024	**0.027**	**0.027**	0.030	**0.028**	0.030	0.031	0.019	**0.030**	0.031	0.031	0.030	0.012
	KINGFSH	0.025	0.025	0.023	0.021	0.016	0.020	0.017	0.014	**0.028**	0.017	0.013	0.012	0.006	0.014
	MAMM STR	0.012	0.010	0.017	0.020	**0.031**	0.023	0.030	**0.034**	0.001	0.029	**0.036**	**0.036**	**0.042**	**0.037**
	RED DRUM	0.022	0.023	0.019	0.017	0.010	0.015	0.011	0.007	**0.028**	0.012	0.006	0.005	0.002	0.021
	RED SNAP	**0.026**	**0.026**	0.024	0.024	0.020	0.023	0.021	0.019	0.026	0.021	0.018	0.017	0.013	0.007
	S FLOUND	**0.026**	**0.026**	0.025	0.025	0.022	0.024	0.022	0.021	0.026	0.023	0.020	0.019	0.015	0.005
	SEATRT	0.023	0.023	0.020	0.018	0.010	0.016	0.011	0.008	**0.028**	0.012	0.007	0.006	0.001	0.020
	SHEEPHD	**0.026**	**0.025**	**0.027**	**0.027**	0.027	**0.027**	0.027	0.027	0.022	0.027	0.027	0.027	0.024	0.006
	SPAN MAC	0.023	0.024	0.020	0.019	0.011	0.017	0.012	0.009	**0.028**	0.013	0.008	0.007	0.000	0.019
	TUR NEST	**0.025**	0.025	**0.027**	**0.027**	0.029	**0.028**	0.028	0.028	0.021	0.028	0.028	0.028	0.026	0.008
	Minimum	0.001	0.001	0.004	0.001	0.000	0.002	0.001	0.001	0.000	0.002	0.000	0.001	0.000	0.001
	Median	0.023	0.023	0.021	0.021	0.021	0.023	0.021	0.021	0.025	0.021	0.020	0.019	0.019	0.020
	Maximum	0.026	0.026	0.027	0.027	0.033	0.029	0.032	0.035	0.028	0.032	0.036	0.037	0.042	0.041
	Stnd Dev	0.006	0.007	0.006	0.006	0.010	0.007	0.010	0.011	0.009	0.009	0.012	0.012	0.015	0.012
	Stnd Err	0.001	0.001	0.001	0.001	0.002	0.001	0.002	0.002	0.002	0.002	0.002	0.002	0.003	0.002
	Total Retained	**0.308**	**0.309**	**0.315**	**0.324**	**0.387**	**0.336**	**0.374**	**0.408**	**0.334**	**0.366**	**0.421**	**0.429**	**0.477**	**0.440**

D.2 SUPPLEMENTAL FIGURES

Figure D.1 – Frequency of $\lambda_{ab}(\mathbf{Y})$ for all pairwise comparisons of group centroids. Frequency histograms for all possible pairwise comparisons of group centroids' $\lambda_{ab}(\mathbf{Y})$ values. The x-axes represent the $\lambda_{ab}(\mathbf{y}_i)$ values for all indicators in **Y** (scaled to the global maximum value), and the y-axis represents their frequencies of occurrence (also scaled to the global maximum).

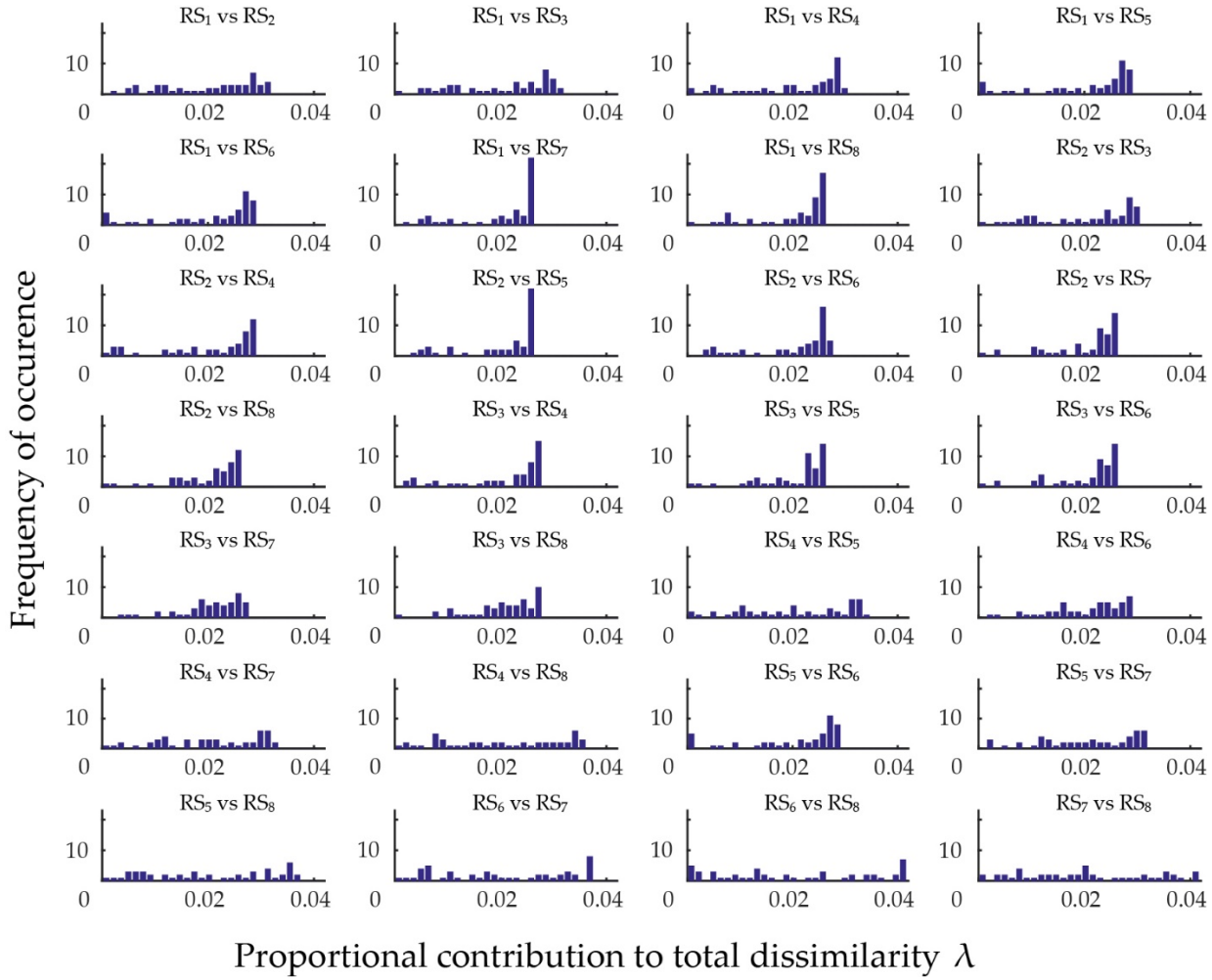

Figure D.2 – Time-series plots for all X. The time-series plots for all **X** indicators, where values are standardized via z-score translation. Independent axes are years and dependent axes are the standardized index values, scaled to the global minimum and maximum values. For details of each indicator, including trend lines, see (Karnauskas et al. 2013, Karnauskas et al. 2015).

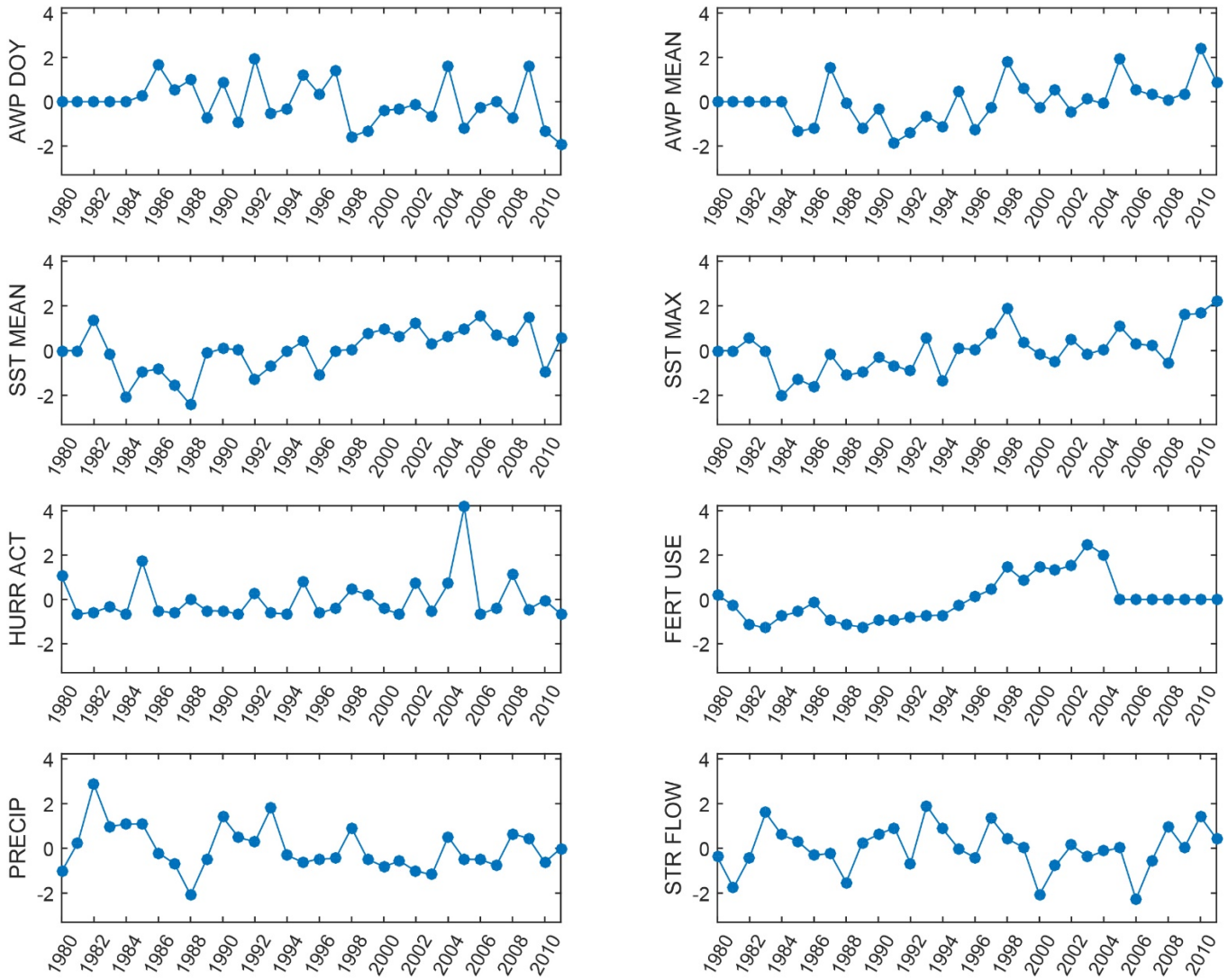

Figure D.2 (Continued)

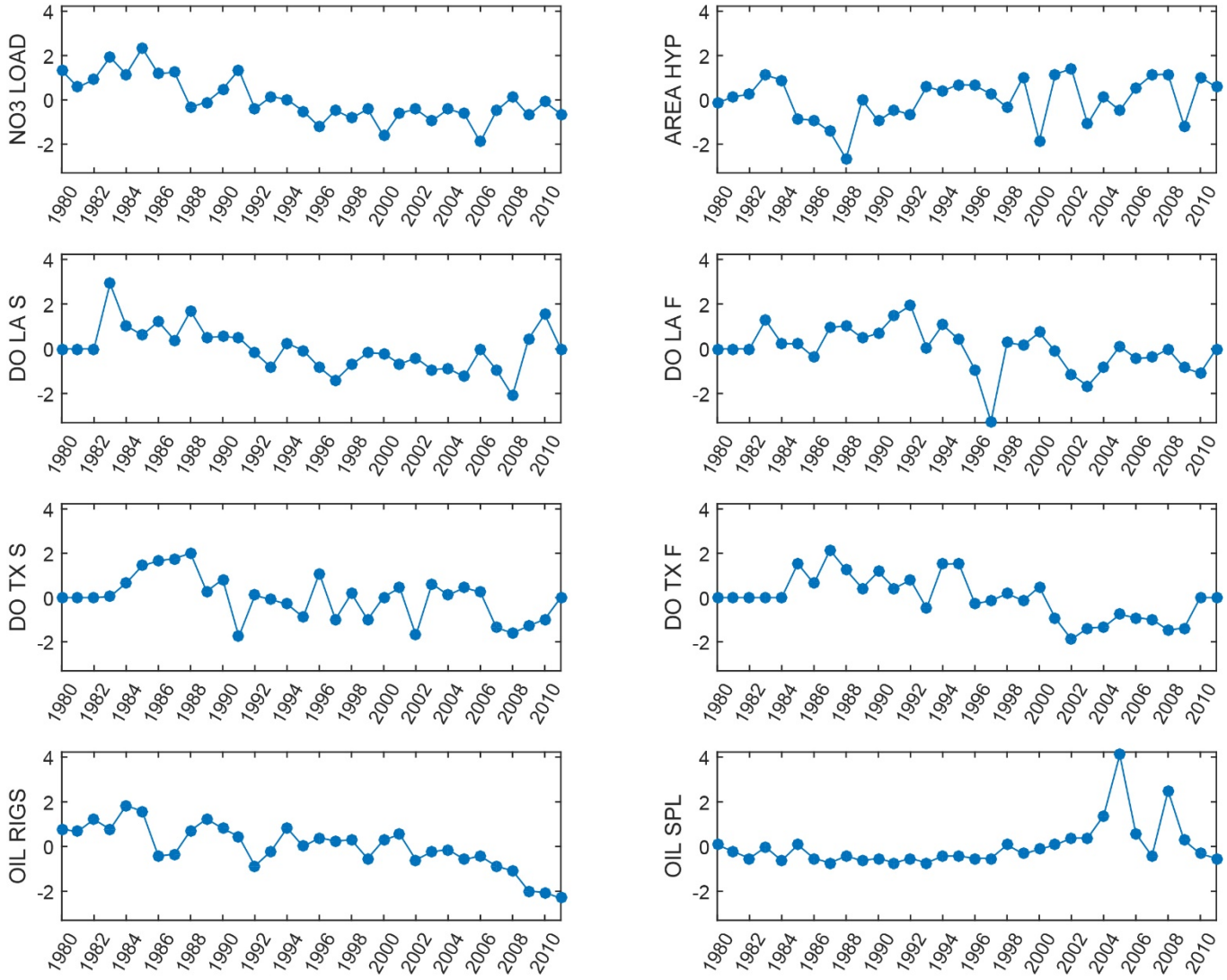

Figure D.2 (Continued)

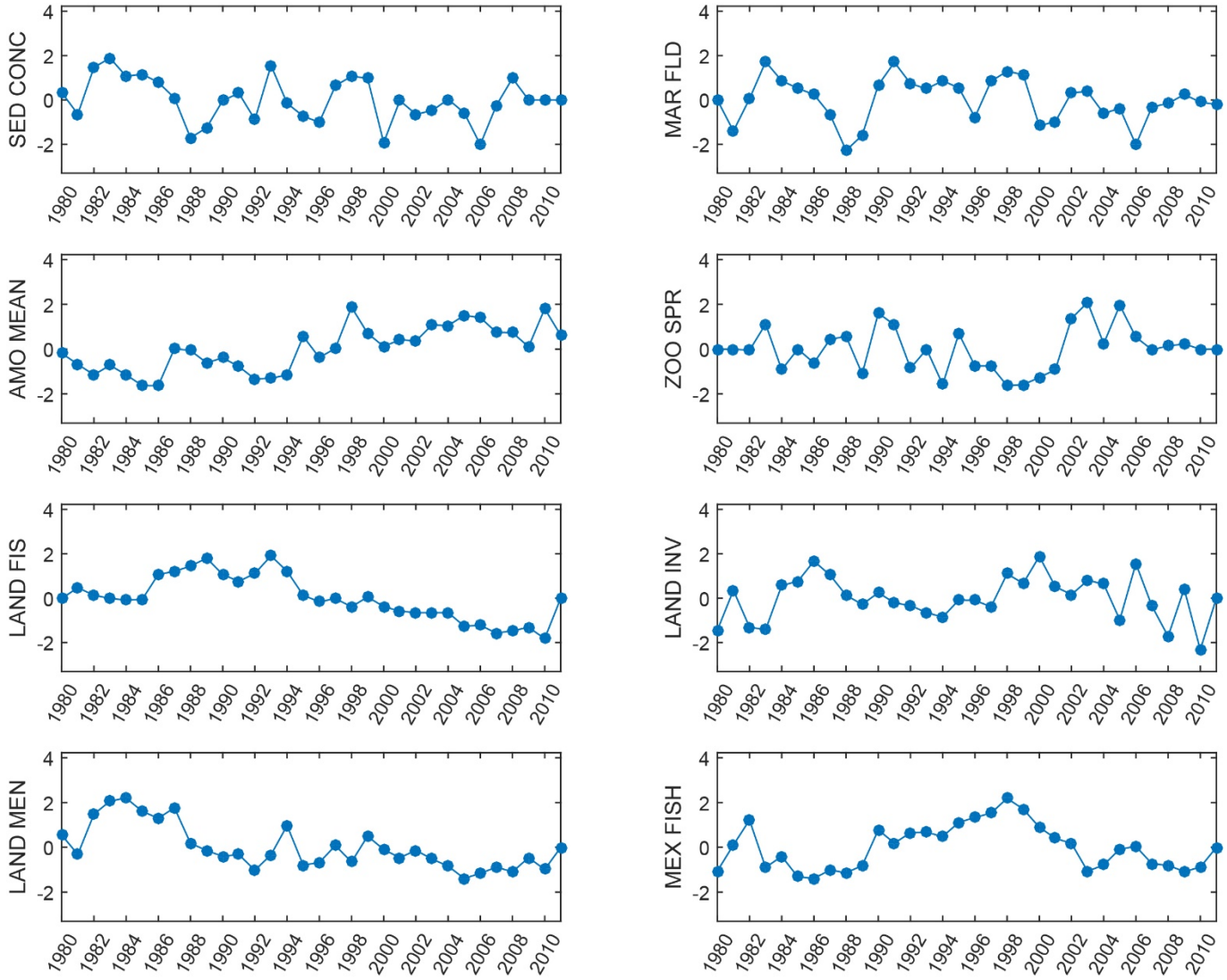

Figure D.2 (Continued)

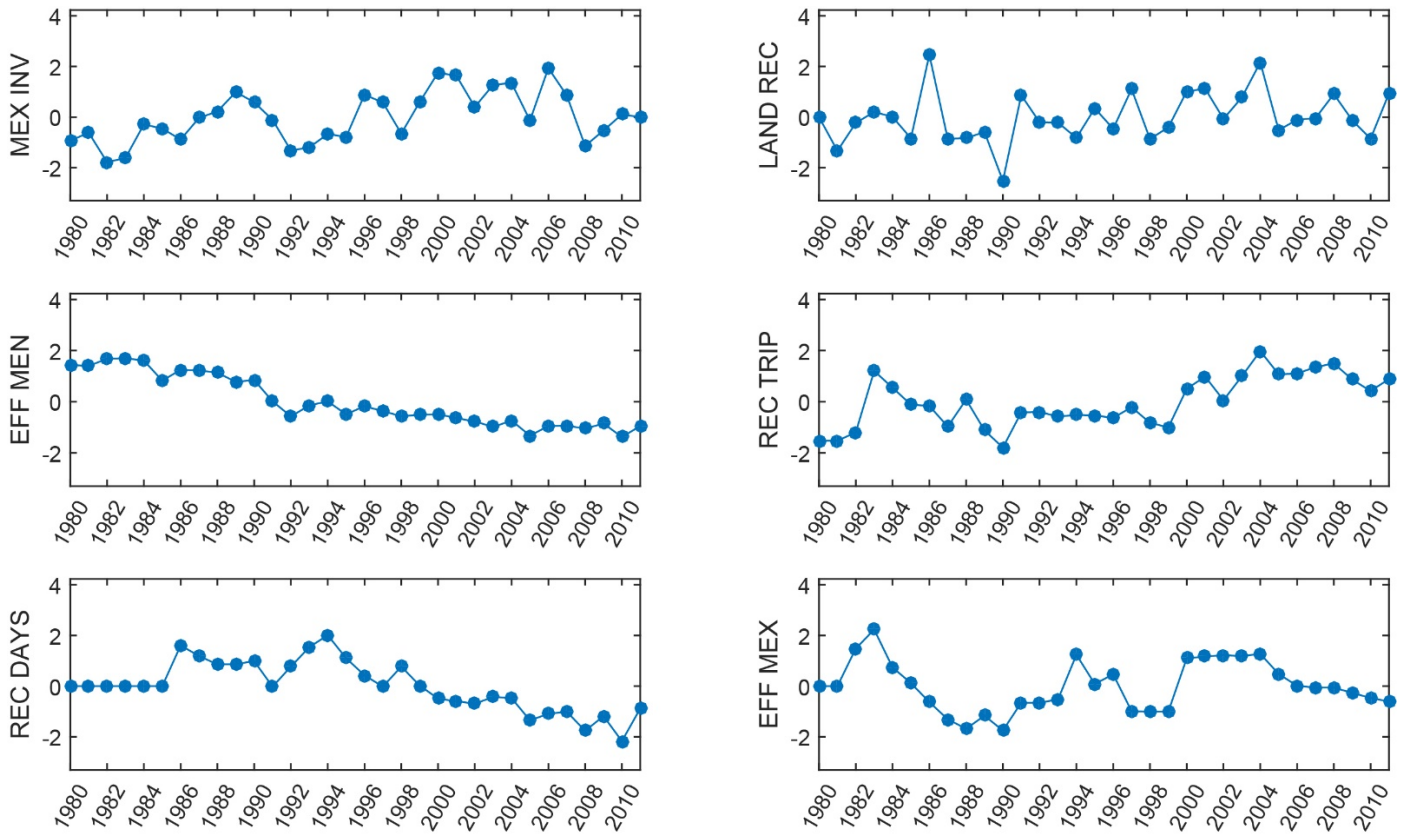

Figure D.3 – Time-series plots for all Y. Time-series plots for all **Y** indicators, where values are standardized via z-score translation. Independent axes are years and dependent axes are the standardized index values, scaled to the global minimum and maximum. For details of each indicator, including trend lines, see (Karnauskas et al. 2013, Karnauskas et al. 2015).

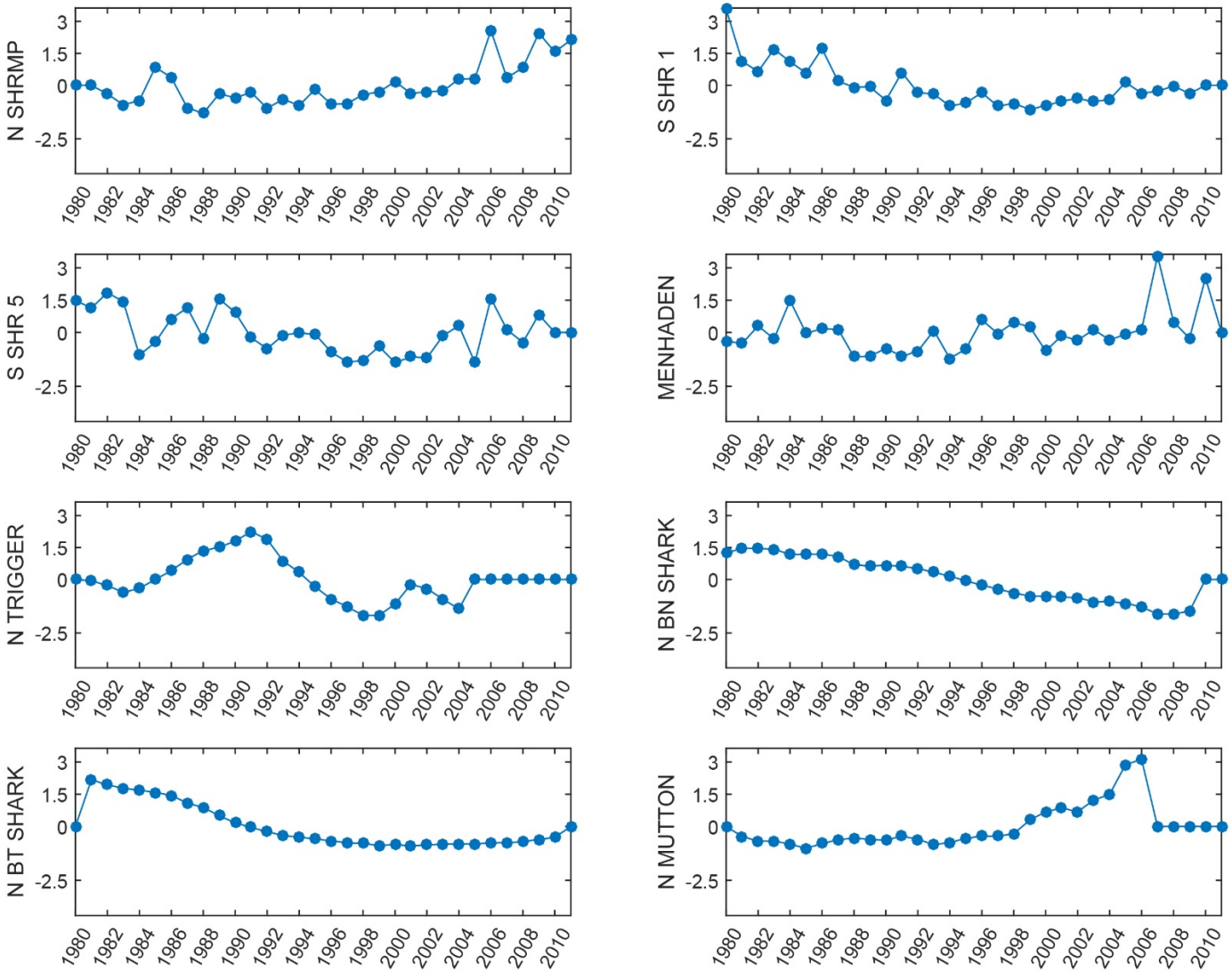

Figure D.3 (Continued)

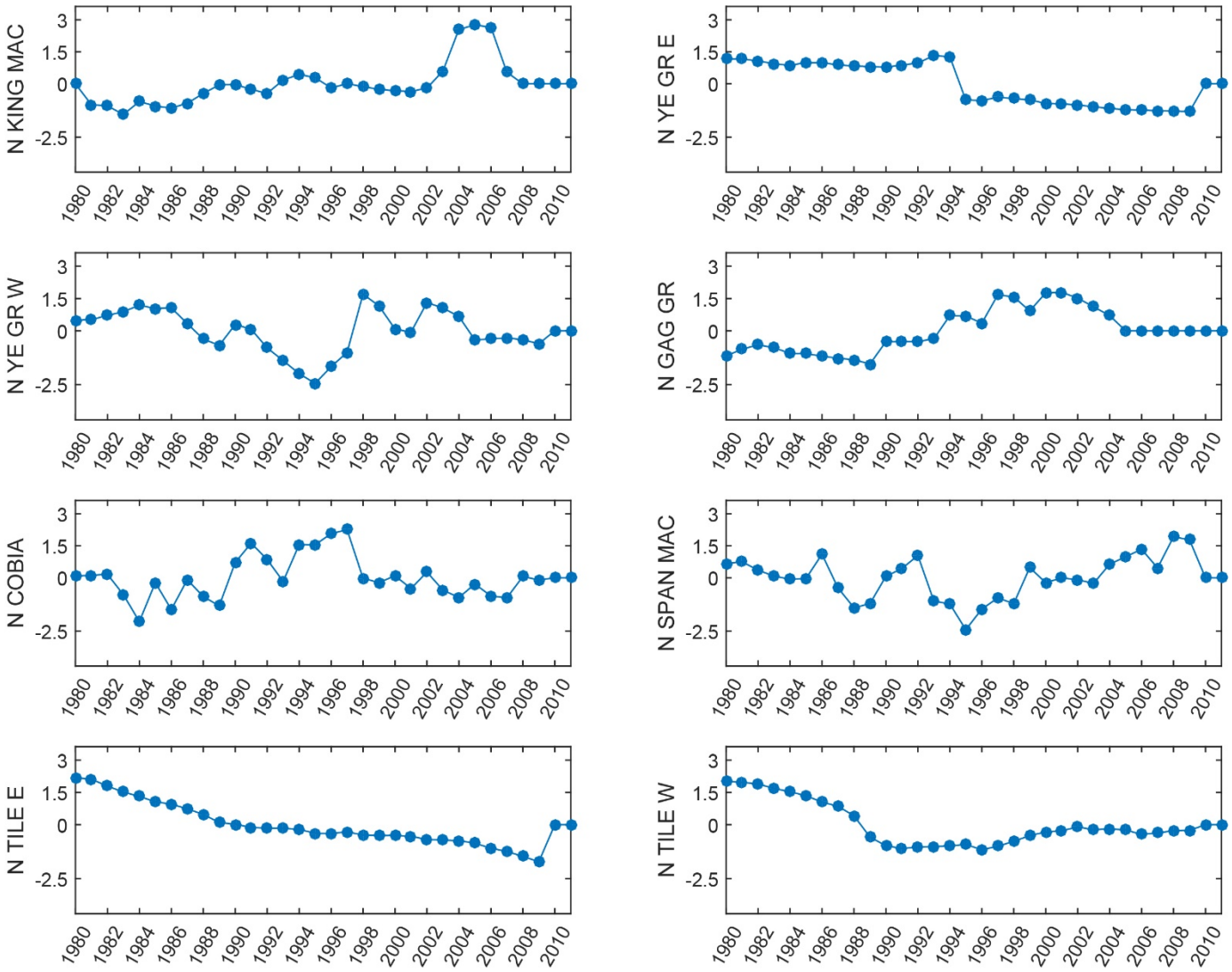

Figure D.3 (Continued)

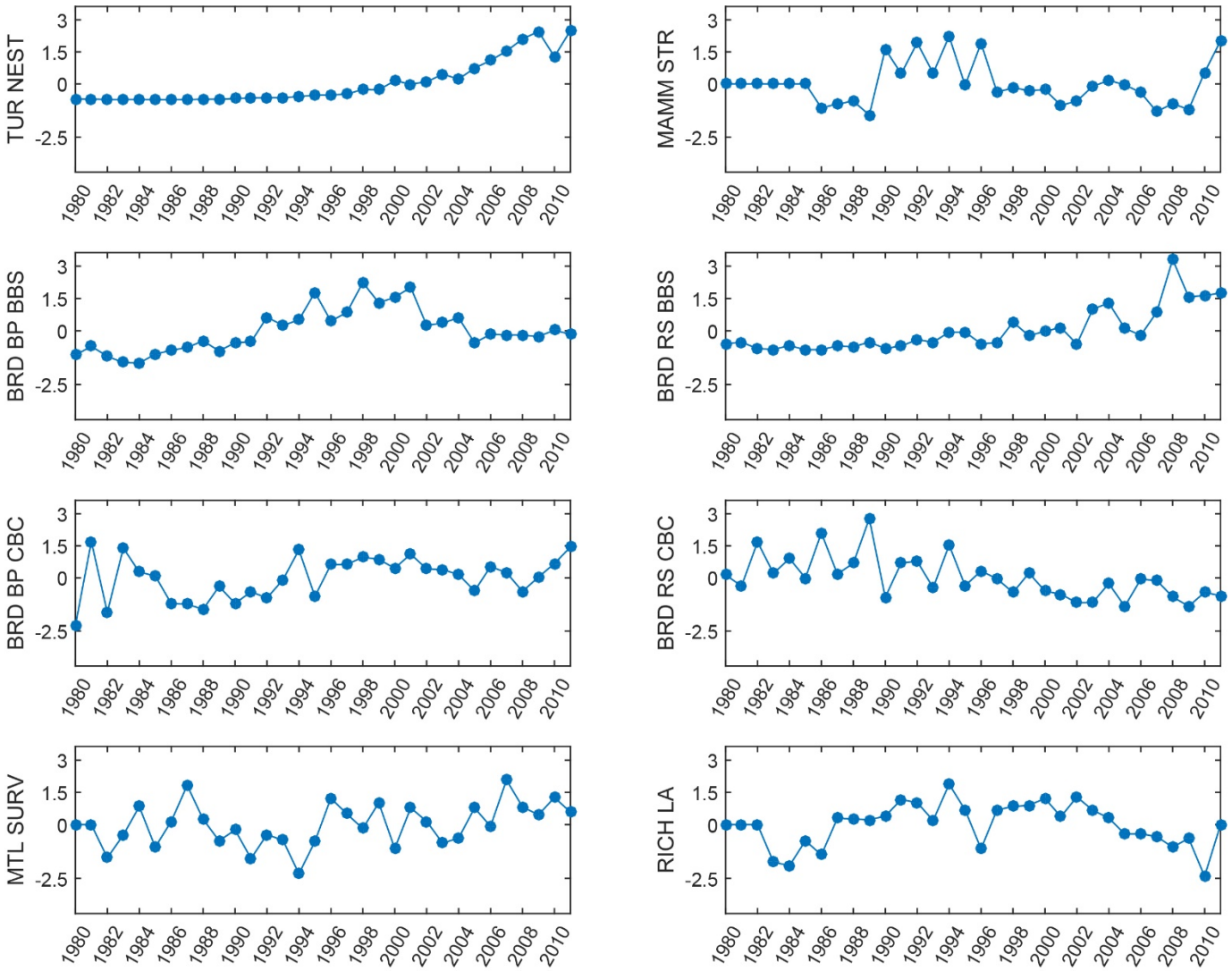

Figure D.3 (Continued)

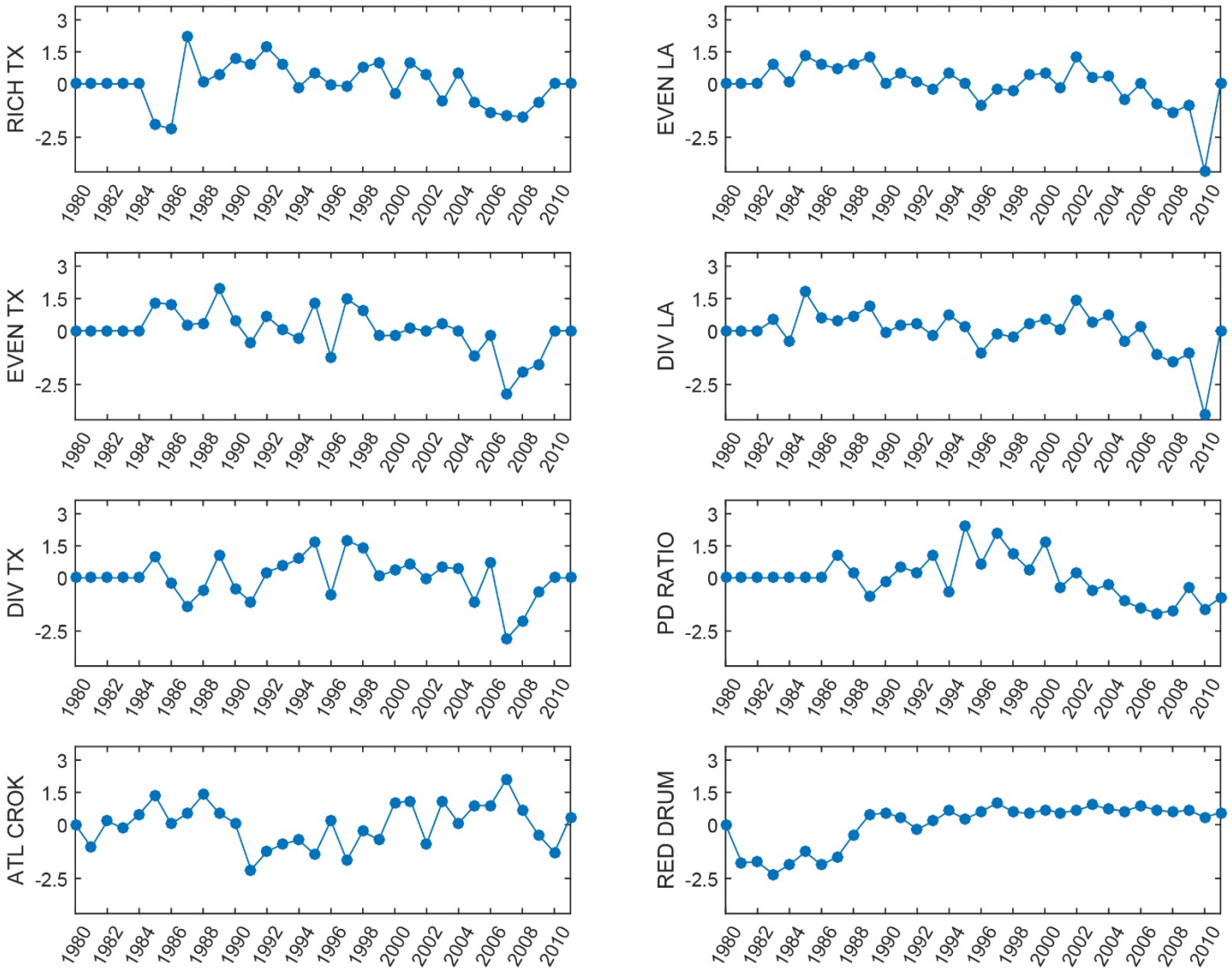

Figure D.3 (Continued)

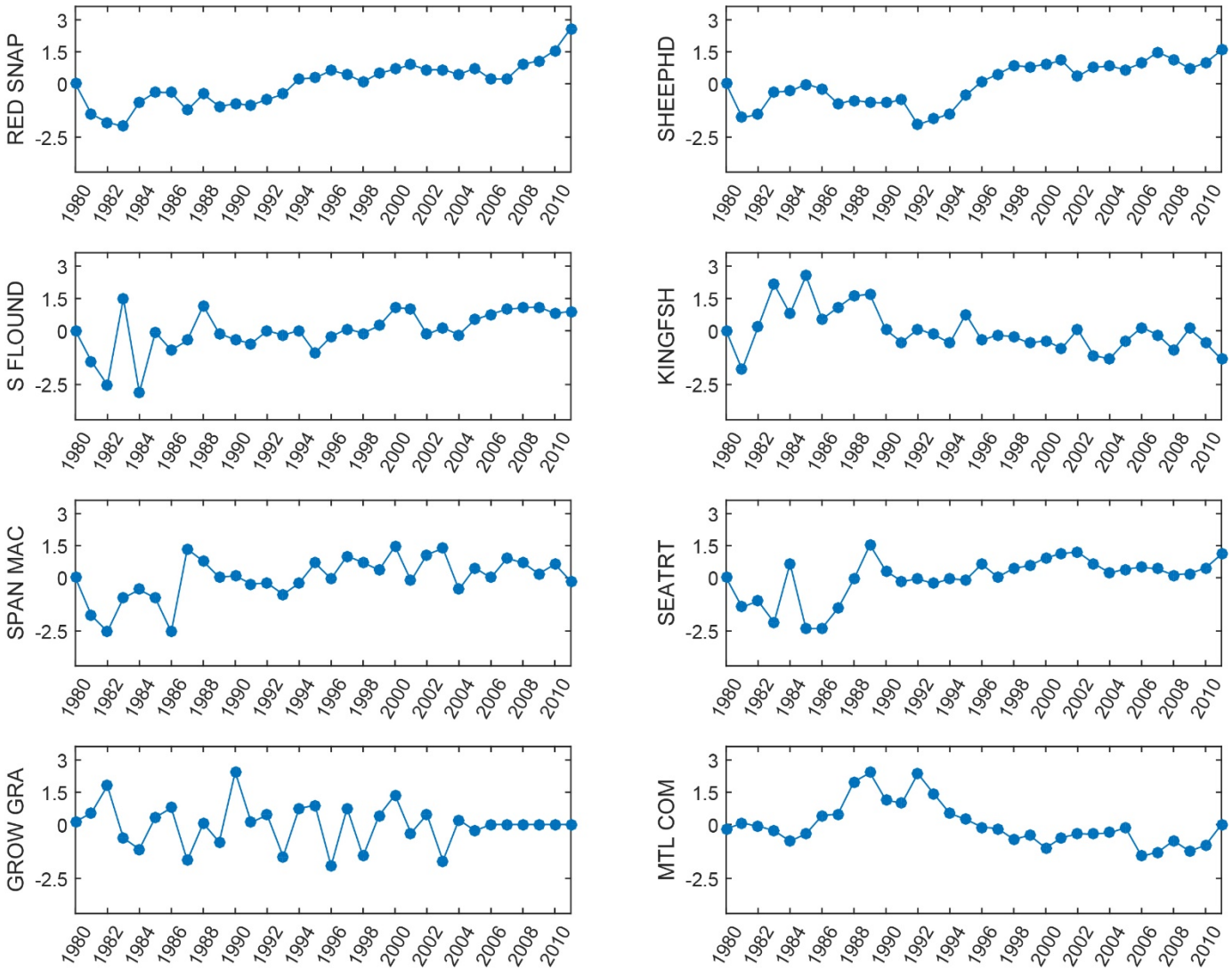

Figure D.3 (Continued)

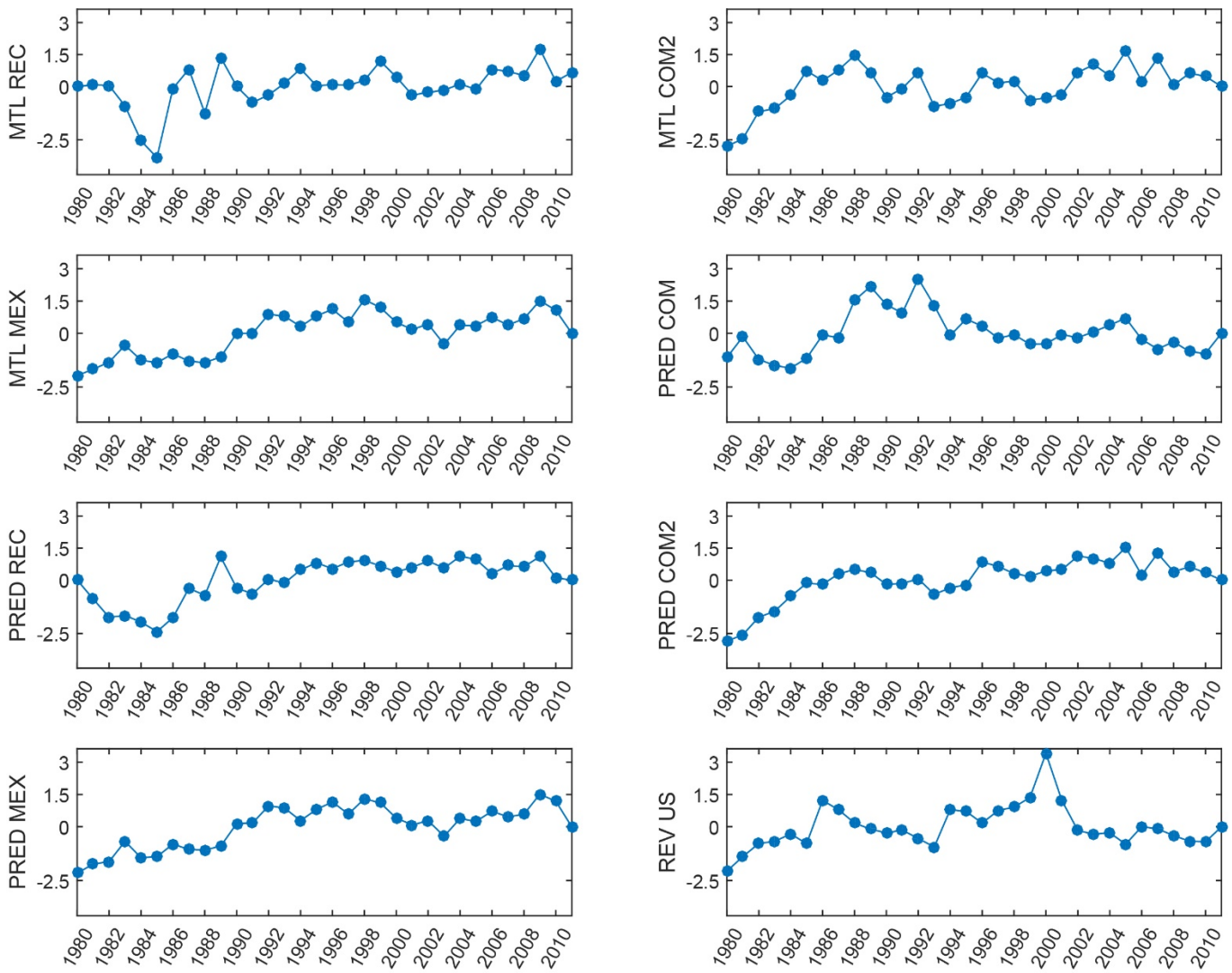

Figure D.3 (Continued)

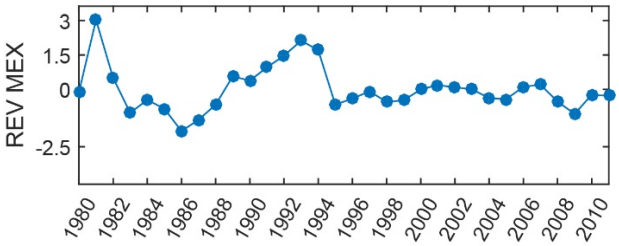

D.3 LITERATURE CITED

Karnauskas, M., M. J. Schirripa, J. K. Craig, G. S. Cook, C. R. Kelble, J. J. Agar, B. A. Black, D. B. Enfield, D. Lindo-Atichati, B. A. Muhling, K. M. Purcell, P. M. Richards, and C. Z. Wang. 2015. Evidence of climate-driven ecosystem reorganization in the Gulf of Mexico. Global Change Biology **21**:2554-2568.

Karnauskas, M., M. J. Schirripa, C. R. Kelble, G. S. Cook, and J. K. Craig. 2013. Ecosystem status report for the Gulf of Mexico. Pages 1-52 *in* N. U.S. Department of Commerce, editor.